Biochemical Treatment of Acid Mine Drainage by Constructed Wetlands in Northeast India

A Thesis

Submitted in partial fulfilment of the requirements

for the degree of

Doctor of Philosophy

by

Shweta Singh

Department of Civil Engineering
Indian Institute of Technology Guwahati
Guwahati – 781039, Assam, India

November 2022

Dedicated

to

My Family

भारतीय प्रौद्योगिकी संस्थान गुवाहाटी
INDIAN INSTITUTE OF TECHNOLOGY GUWAHATI
DEPARTMENT OF CIVIL ENGINEERING

Statement

I hereby declare that the content embodied in this thesis entitled **Biochemical Treatment of Acid Mine Drainage by Constructed Wetlands in Northeast India** is the outcome of investigations carried out by me in the Department of Civil Engineering, Indian Institute of Technology Guwahati, Guwahati, Assam, India under the supervision of **Prof. Saswati Chakraborty**. In keeping with the general practice of reporting scientific observations, due acknowledgments have been made wherever the work described is based on the findings of other investigators.

Date: 10th November 2022
Place: Guwahati

Shweta Singh
Roll No. 166104009
Department of Civil Engineering
Indian Institute of Technology Guwahati
Guwahati – 781039, Assam, India

भारतीय प्रौद्योगिकी संस्थान गुवाहाटी
INDIAN INSTITUTE OF TECHNOLOGY GUWAHATI
DEPARTMENT OF CIVIL ENGINEERING

Certificate

It is certified that the work described in this thesis entitled **Biochemical Treatment of Acid Mine Drainage by Constructed Wetlands in Northeast India** by **Ms. Shweta Singh** (Roll No. 166104009) for the award of degree of Doctor of Philosophy is an authentic record of the results obtained from the research work carried out under my supervision in the Department of Civil Engineering, Indian Institute of Technology Guwahati, Assam, India. I certify that she has fulfilled all the requirements according to the rules of this institute regarding the investigations embodied in her thesis and this work has not been submitted elsewhere for a degree.

Date: 10th November 2022
Place: Guwahati

Dr. Saswati Chakraborty
Professor
Department of Civil Engineering
Indian Institute of Technology Guwahati
Guwahati – 781039, Assam, India

Acknowledgements

My sincere appreciation to everyone who helped me through their best of knowledge, capabilities and resources during my research work and made it possible to achieve momentous accomplishment extends beyond sheer expression of words.

I would like to begin with my cordial acknowledgement and paramount gratitude to my thesis supervisor, **Prof. Saswati Chakraborty** for her incredible guidance and placing her complete trust on me and finally granting me the opportunity to work under her excellence. Her compassion, dedication, patience, empathy and down-to-earth nature have always motivated me to triumph over several hurdles encountered during the course of my doctorate journey. She is one of the best teacher with profound knowledge of subjects and her moral principles on research ethics is extremely admirable. Her pragmatic approach and perceptive vision have significantly enlightened my perspective and knowledge. She has been truly a blessing and I feel very privileged to work under her mentorship as an independent researcher.

I would like to express my sincere acknowledgement to the Chairman of my Doctoral Committee, **Prof. Mohammad Jawed** and members, **Prof. Sharad Bhaurao Gokhale** and **Prof. Prabirkumar Saha** for their critical scrutiny, close examination and valuable suggestions to improvise the quality of my research work and worth of my thesis. I thank current departmental head, **Prof. Sharad Bhaurao Gokhale** and former heads, **Prof. Chandan Mahanta** and **Prof. Subashisa Dutta** of Department of Civil Engineering, IIT Guwahati for providing amenities and support during my research tenure. I would like to extend my sincere regards to current Lab Incharge, **Prof. Saswati Chakraborty** and former Lab Incharges, **Prof. Pranab Kumar Ghosh**, **Dr. Sri Harsha Kota** and **Prof. Ajay Kalamdhad** of Environmental Engineering Laboratory, Department of Civil Engineering, IIT Guwahati for providing decent lab facilities with all-time access to instruments and equipments. I owe my deep sense of gratefulness to my course work instructors, **Prof. Mohammad Jawed**, **Prof. Saswati Chakraborty**, **Prof. Pranab Kumar Ghosh**, **Prof. Bishnupada Mandal** and **Prof. Kaustuba Mohanty** for teaching and sharing knowledge on various subjects.

I am truly obliged to **Ms. Jonali Saikia** (Scientific Officer, Department of Civil Engineering, IIT Guwahati), **Mr. Payodhar Pathak** and **Mr. Chittaranjan Medhi** (Technical Superintendents, Environmental Engineering Lab, IIT Guwahati) for their amenable help with instruments. I express heartily thanks to the current departmental office staff members, **Mr. Susanta Kr. Sarma**, **Ms. Juri J. Hazarika**, **Mr. Bhrigu Kalita** and **Ms. Archana Rajbongshi** for their kind co-operation in the matter of official requests.

I acknowledge **Central Instrument Facility (CIF)** and **Centre for the Environment**, IIT Guwahati for sample analysis in sophisticated instruments. I would like to gratefully acknowledge **Indian Institute of Technology Guwahati** and **Ministry of Education (MoE),**

India for providing financial assistance as research fellowship, which made this study possible.

I owe my deep appreciation to the **Department of Mechanical Engineering** and **Central Workshop**, IIT Guwahati for the kind help received in reactor fabrication. I would like to extend my sincere esteems to Assistant Workshop Superintendent, **Mr. Nandan Kanan Das** and technical staffs, including **Mr. Jiten Basumatary**, **Mr. Dulumoni Das**, **Mr. Gakul Das** and **Mr. Gautam Gogoi** for their timely help. I am thankful to **Prof. Sharad Bhaurao Gokhale** and his research group (Air Pollution Lab, IIT Guwahati) for facilitating meteorological data.

I sincerely acknowledge **North Eastern Coalfield (NEC)**, Margherita, Assam and General Manager, **Shri S. P. Dutta** for granting permission to coal mine visits. I would like to encompass my vote of thanks to all managers and agents, **Shri. Rupjyoti Boruah**, **Shri. Sanjay Kumar Singh**, **Shri. T. K. Baitha**, **Shri. P. Patil**, **Shri. Saurabh Ch. Mukherjii**, **Shri. M. S. Singh** and **Shri. Md. Murtaza Ali** as well as many other employees, **Mr. Debol Chakraborty**, **Mr. Tapan Kumar Baitra**, **Mr. M. K. Das**, **Mr. B. R. Das**, **Mr. C. Appaya** and **Mr. Jata Rao** for their efforts and cooperation during minewater sampling from different collieries.

I am very thankful to the Editors and anonymous Reviewers of all published articles in the respective Journals for thoroughly scrutinizing our manuscripts with their valuable insights and finally for their recommendation of acceptance.

The moment my doctorate journey began, I started to comprehend the importance of having good companionship of true friends and motivating colleagues. I was extremely fortunate to meet some incredibly talented and inspiring people who have left unforgettable impression on my heart and this acknowledgement would be incomplete without mentioning their names. I am indebted to my amazing seniors, especially, **Dr. Sachin Kumar Tomar**, **Dr. Subrat Kumar Mallick**, **Dr. Rajneesh Kumar** and **Mr. Chandra Bhanu Gupt** for their selfless love, care and guidance when I was going through the most perplexing time of research. I extend my regards to my lab group members, **Dr. Praisy Terangpi**, **Dr. Sayanti Ghosh**, **Dr. Jinat Aktar**, **Mr. Christy K. Benny**, **Mr. Anjishnu Biswas** and **Ms. Akhiladas E. K.** for their help, care and lessons during different phases of my research work. I thank my seniors, **Dr. Arvind Kumar Shakya**, **Dr. Mayur Shirish Jain**, **Dr. Veluchamy C.**, **Dr. Kunwar Raghvendra Singh**, **Dr. Vihangraj Vijaykumar Kulkarni**, **Dr. Rakhee Das** and **Dr. Gaurav Goel** for their general advice and suggestions.

It was a pleasure to work with enthusiastic juniors, **Mr. Bhupendra Nautiyal**, **Mr. Barun Kanoo**, **Mr. Neeldip Barman**, **Mr. Gajala Rajshekar**, **Ms. Vipasha Maholia**, **Ms. Shinjini Paul Choudhury**, **Ms. S. Sethulekshmi**, **Mr. Rejil R. Nath**, **Ms. Tympangika C. Sungoh**, **Ms. T. Snehasree**, **Mr. Saleeq V. P.**, **Mr. Smitom S. Borah**, **Mr. Sanjib Das**, **Mr. M. Krishna Chaitanya**, **Mr. Chakka Nagendra Subrahmanyam**, **Mr. Promit Kumar Bhaumik**, **Mr. Prabhakar Choudhary**, **Mr. Anirban Das**, **Mr. Hriten Ghosh**, **Mr. Agnibha Maity**, **Mr. Vaibhav Khandelwal**, **Mr. Subham Meher**, **Mr. Sreekant Yadav**, **Mr. Himanshu Kumar** and **Mr. Punyamurthy Tarakesh**. I would like to thank all of them for their valuable suggestions, rendered helps, sleepless late night company and making my PhD a cherish-able experience.

I lay my unfathomable regards to my closest school friend, **Mr. Avinash Sinha**, who supported and motivated me through all phases and for being always there, just a call away. I place my warm regards to my college buddies, **Ms. Leichombam Menan Devi**, **Ms. Ketho Kezo**, **Ms. Ninsana Marak**, **Ms. Juribha Mawlong**, **Ms. Bonita Yurembam** and **Ms. Athira Sreenivasan** for their immense love and cheer at all times. I am also thankful to my enduring friendly colleagues, **Dr. Senjuti Halder**, **Dr. Ande Bhuvaneswari Devi**, **Dr. Venkatesh Reddy**, **Dr. Monica Naorem**, **Ms. Kasturi Gogoi**, **Ms. Neelam Dutta**, **Ms. Sophia Leimapokpam**, **Ms. N. Debeni Devi**, **Ms. Darshana Baruah**, **Mr. Rajhans Negi**, **Mr. Ankit P. Goswami**, **Mr. Argha K. Guha** and **Mr. Sameer Singh** for their encouragement and support.

My utmost admiration goes to my support system and backbone, my family, **Papa**, **Mummy**, **Didi**, **Grandparents**, **Sanjay Mama**, **Meera Mausi**, **Urmila Mausi** and youngest cousin brother **Aditya** for their constant unconditional love, blessings, encouragement and showing me the dreams and making me the person that I am today.

Finally, I wish to express my heartedly gratitude to the **Almighty God** for giving me this beautiful life and listening to my prayers.

Date: 10th November 2022 **Shweta Singh**

Abstract

India is one of the largest producers of coal and coal mines are the major backbone of India's economy. Amongst various pollution concerns of coal mining, the incidence of water pollution in the form of acidic metal-rich discharge, called acid mine drainage (AMD), is widespread and globally regarded as the most challenging wastewater with large environmental impacts. The acidic nature of AMD (pH < 3.0) resulting from the oxidation of sulfide-rich mineral ores and the release of sulfate ions further intensify the degree of complexity of mine wastewater. Till date, the management of AMD remains a great challenge as many remediation measures fail to attain a satisfactory economical and sustainable approach. AMD from the North Eastern Coalfield (NEC), Assam, India, is highly polluted and unregulated without any control measures. The impending effects of AMD pollution from Indian coalfields are often overlooked and critical investigation for the potential remedial measures is scarce. The present study is the first research attempt to demonstrate a passive treatment strategy for AMD from the NEC using constructed wetlands (CWs). In this context, the development of lab-scale CWs and factors governing the biochemical mechanisms of pollutant removal were considered.

The influence of climatic variables on the characteristics of AMD from the NEC, Assam, and its deleterious impact on the surrounding soil was investigated. Elevated concentration (in mg L^{-1}) of Fe (0.12–302), Al (6.73–32) and Mn (0.10–16), as well as the presence of toxic metals such as Co (< 1.47), Ni (< 5.24) and Cr (< 0.54) were found in the coal mine discharge. The release of pollutants, particularly sulfate and metals, increased in the monsoon season, followed by highly concentrated pollutants in the post-monsoon season. The change in the season had a predominant effect on the oxidative leaching of sulfide minerals, which indicated a strong control of local climatic conditions on AMD chemistry.

Horizontal subsurface flow CWs (HSSF-CWs) were designed to treat simulated AMD and acclimatized with the diluted concentration of pollutants followed by full-strength AMD under continuous mode. The treatment performance of HSSF-CWs (A and C) utilizing various organic wastes as the wetland media were compared. CWs demonstrated significant improvement in the water quality and partial to complete removal of metals with negligible manganese removal. The biological removal of manganese by sulfate-reducing bacteria (SRB) was difficult due to the slower precipitation rate in anaerobic CWs. Complete elimination of acidity (alkalinity generation of 600–1300 mg L^{-1} as $CaCO_3$; effluent pH 6.3–7.4) and partial removal of sulfate (57–62%) were obtained. Media accounted major retention (58–95%) for all metals, and plants (*Typha latifolia*) exhibited poor bioaccumulation and translocation for all heavy metals except for Mn and Co. Toxicity Characteristic Leaching Procedure (TCLP) test suggested very negligible leachability of chromium for safe disposal. However, the potential release of weakly bound Mn, Al, Co and Ni associated with exchangeable and carbonate-bound fractions was indicated under adverse environmental conditions.

The role of plants and the impact of hydraulic loading rates (HLRs) in the remediation of AMD and metal attenuation were studied in planted (PCW) and unplanted (CCW) CWs. Significant impairment of sulfate reduction was observed in PCW (24–90%) than CCW (37–93%), suggesting the suppression of microbial-assisted sulfate reduction due to the formation of micro-aerobic zones by the oxygen release from wetland plants. Both CWs exhibited excellent metal removal: Fe (78–100%), Al (40–85%), Zn (93–98%), Co (92–96%), Ni (89–96%) and Cr (95–99%), except Mn. Effluent water quality deteriorated and metal removal efficiency reduced drastically on increasing HLR. HLR has an important role in the passive treatment of AMD than the presence of plants in CWs. The application of a chelating agent and organic acids revealed resource value by metal extraction and recovery from wetland media. Ethylenediaminetetraacetic acid (EDTA) achieved higher metal extraction efficiency for Fe, Zn and Cr; nevertheless, organic acids (acetic and ascorbic acid) achieved comparable extraction efficiency. Good metal recovery values were obtained in the order: Fe (49–98%) > Zn (57–95%) > Ni (67–87%) > Cr (68–84%) > Co (50–74%) > Al (30–48%).

Furthermore, the influence of seasonality on the efficacy of CW microcosms was studied. Rainfall has a stronger influence in the northeastern region of India during monsoon. The experimental period was restricted from January to August, and the effect of rainfall events on sheltered (SCW) and unsheltered (UCW) CWs was investigated under natural conditions. Findings revealed a significant difference in the sulfate reduction efficiency of SCW (60%) and UCW (51%). Heavy rainfall imposed a highly sensitive and poor treatment response in UCW, resulting in a significantly lower treatment efficiency for all constituents due to possible shortening of hydraulic retention time (HRT) in UCW with minimal or insignificant dilution effect. This study highlights the limitations of CWs in the rainfall-affected region and recommends necessary design control measures to manage the effects of rainfall.

In addition, the long-term treatment appraisal of HSSF-CW (B) comprising gravel media was evaluated under varying COD/SO_4^{2-} ratios using lactate as a carbon source. Moderate alkalinity generation (63–191 mg L^{-1} as $CaCO_3$) and pH improvement of AMD from 2.2 to 5.6 was achieved. High average metal removal efficiency was attained for Fe (73%), Al (79%), Zn (98%), Co (95%), Ni (99%) and Cr (100%), but Mn (21%). As COD/SO_4^{2-} reduced from 0.67 to 0.33, sulfate reduction decreased significantly from 74% to 44% and metal removal efficiency subsided. Dissimilatory sulfate reduction was identified as the major biological pathway assisting sulfate removal, bicarbonate alkalinity generation and metal sulfide precipitation. The formation of insoluble metal precipitates (oxides, hydroxides and sulfides) accounted for about 32–76% metal removal. Major SRB genera identified were *Desulfosporosinus meridiei*, *Desulfotomaculum*, *Thermodesulfobium* and *Desulfovibrio*. Further, iron-metabolizing microbial groups (*Geobacter lovleyi*, *Acidiphilium* and *Halothiobacillus*) controlled the biochemical cycling of iron (oxidation or reduction) and its bioavailability.

***Keywords*:** Acid mine drainage, Constructed wetlands, Heavy metals, Sulfate pollution, Phytoremediation, Metal recovery, Microbial metagenomics.

Contents

List of Figures

List of Tables

Abbreviations

AAS	Atomic absorption spectrometer
AR	Analytical grade
ARD	Acid rock drainage
ATP	Adenosine triphosphate
BCF	Bio-concentration factor
BDL	Below detectable limit
BT	Billion tons
CEQG	Canadian Environmental Quality Guideline
CIL	Coal India Limited
COD	Chemical oxygen demand
CPCB	Central Pollution Control Board
CSG	Chinese Soil Guideline
CW	Constructed wetland
DNA	Deoxyribonucleic acid
DO	Dissolved oxygen
DW	Dry weight
e.g.	For example
EC	Electrical conductivity
EDX	Energy dispersive X-ray spectrometer
EPA	Environmental Protection Agency
FESEM	Field emission electron microscope
Fig.	Figure
FW	Fresh weight
FWS	Free-water surface
HDPE	High density polyethylene
HF	Horizontal flow
HLR	Hydraulic loading rate
HRT	Hydraulic retention time
HSSF	Horizontal sub-surface flow
i.e.	That is
IS	Indian Standard
JCPDS	Joint Committee on Powder Diffraction Standards
LR	Laboratory grade
Ltd.	Limited
MLD	Million litres per day
MT	Million tons
NCBI	National Center for Biotechnology Information
NCL	Northern Coalfield
NEC	North Eastern Coalfield
No.	Number
NTU	Nephelometric turbidity unit
ORP	Oxidation-reduction potential
PDF	Powder Diffraction File
PDL	Permissible discharge limit
PRB	Permeable reactive barrier

RAPS	Reducing and alkalinity producing system
RNA	Ribonucleic acid
ROL	Radial oxygen loss
rpm	Revolution per minute
SAPS	Successive alkalinity producing systems
SF	Surface flow
sp.	Specie
spp.	Species
SQG	Sediment Quality Guideline
SRA	Sequence Read Archive
SRB	Sulfate-reducing bacteria
SSF	Sub-surface flow
TCA	Tricarboxylic acid
TCLP	Toxicity Characteristic Leaching Procedure
TDS	Total dissolved solids
TEL	Threshold effects level
TF	Translocation factor
TH	Total hardness
TSS	Total suspended solids
TVS	Total volatile solids
UM	Underground mine
VF	Vertical flow
VFW	Vertical flow wetland
VSSF	Vertical sub-surface flow
WCL	Western Coalfield
WHO	World Health Organization
XRD	X-ray powder diffraction

Notations

$\%$	Percentage
$^{\circ}C$	Degree Celsius
μg	Microgram
μm	Micrometre
atm	Atmospheric pressure
cm	Centimetre
d	Day
g	Gram
h	Hour
ha	Hectare
kg	Kilogram
K_H	Hydrolysis constant
km	Kilometre
K_{sp}	Solubility product constant
KV	Kilovolt
L	Litre
m	Metre
M	Molar
mA	Milliampere
meq	Milliequivalent
mg	Milligram
min	Minute
mL	Millilitre
mm	Millimetre
mM	Millimolar
mS	Millisiemens
mV	Millivolt
N	Normality
ng	Nanogram
nm	Nanometre
s	Second
v/v	Volume/volume
w/v	Weight/volume

1

Introduction and Literature Review

This chapter entails a brief discussion about the occurrence of acid mine drainage (AMD) and describes different prevention and treatment techniques practiced globally. An extensive literature survey on the bioremediation of AMD using constructed wetlands (CWs) – a passive treatment approach, is presented. This chapter also focuses on the different mechanisms involved in the attenuation process of pollutants and highlights the objectives of the current study articulated to bridge the literature gaps.

1.1 Introduction

The discovery and utilization of fossil fuel reserves have been the greatest benison to human prosperity; though limited in nature, the demand is endlessly increasing. Currently, fossil fuels account for about 86% of the global primary energy demand, representing oil, gas, coal, renewable and alternative energy resources share of 36, 27, 23 and 14%, respectively, in the global energy mix (Abas et al., 2015). Worldwide coal reserves are estimated to be about 1054 billion tons (BT) (Choudhury et al., 2021). Since 1971, coal consumption and production have increased by more than 150% (Liu and Liu, 2020), which are further expected to increase many folds due to the faster depletion of oil and gas in the future. As global coal energy demand grows, operations such as coal mining, extraction, beneficiation and processing will exacerbate many environmental concerns.

Acid mine drainage (AMD) or acidic ferruginous mine discharge, also known as acid rock drainage (ARD), is one such challenging source of environmental contamination due to extensive mining activity, which poses an ecological threat and remains a perpetual environmental issue. The process of AMD generation is rather continuous in active as well as in abandoned mines even after years of closure, with high flow rates of about 5–50 L s^{-1} (Bálintová et al., 2018; Chon and Hwang, 2000; Singh, 1987; Taylor et al., 2005). AMD emanation from various sources includes beneficiation processes, mine dewatering, intersection of the water table, rock fissures, heavy rainfall, seepage from tailings and waste rock piles. AMD from coal mines has been a global nuisance and is typically identified by the

presence of low pH (2.4–3.9), high sulfate (1500–7599 mg L^{-1}), low organics (10–25 mg L^{-1}), rich in iron (4.60–1472 mg L^{-1}) and many other heavy metals (Caraballo et al., 2011; Clyde et al., 2016; Equeenuddin et al., 2010; Tao et al., 2012).

The generation of sulfate and metal-rich AMD in the northeastern parts of India due to several anthropogenic and coal mining activities has been long discussed (Chabukdhara and Singh, 2016; Singh, 1987). Many studies have underlined the deleterious impact of untreated AMD disposal on soil, groundwater and surface streams (Dutta et al., 2018, 2017; Equeenuddin et al., 2010). Dutta et al. (2019) investigated the remediation strategy for AMD generated in the North Eastern Coalfield (NEC) region using limestone, which revealed quite a large amount of the lime requirement (107–640 g for 1 L AMD) for neutralization and thereby potential hazardous nature of the discarded limestone.

AMD is considered the most severe form of water pollution and is regarded as "second only to global warming and ozone depletion" by the USA Environmental Protection Agency (USEPA) in terms of ecological threat (Moodley et al., 2018). The untreated AMD is often discharged into the rivers or streams and deteriorates the water quality, affecting the aquatic habitat and ultimately collapsing the food chain and ecosystems at much higher levels. AMD is not compliant with drinking water standards and must be discharged after treatment to acceptable levels complying with regulatory agencies like USEPA and Central Pollution Control Board (CPCB). The latest findings by Zhou et al. (2020) revealed a greater number of heavy metals in the aquatic environment of developing regions (Africa, Asia and South America) have exceeded the threshold concentration values of the World Health Organization (WHO) and USEPA standards than compared to developed regions (Europe and North America).

To address this issue of AMD, various control measures at the mine source have been proposed and implemented (Johnson and Hallberg, 2005; Park et al., 2019). However, complete mitigation of AMD formation at a mine site is often infeasible. Therefore, utilization of best-suited treatment strategies becomes imperative (Kefeni et al., 2017; Skousen et al., 2019). The most conventional physicochemical treatment includes chemical precipitation, coagulation-flocculation, flotation, adsorption, ion exchange and membrane filtration (Kurniawan et al., 2006). Voluminous sludge generation, energy intensiveness, membrane fouling, high labour and maintenance requirements are the major limitations encountered in conventional treatment (Kurniawan et al., 2006). Lately, many advanced technologies such as bio-electrochemical systems (Pozo et al., 2017), electrodialysis (Aydin et al., 2019) and electrochemical techniques (Brewster et al., 2020) have gained considerable popularity due to their advantages over conventional techniques. However, advanced techniques lack field applications, require a substantial initial investment and high electrical supply (Kiran et al., 2017; Rambabu et al., 2020). Biological treatment systems rely on microbial processes to remediate acidity and dissolved metals, including wetlands, permeable reactive barriers (PRBs), successive alkalinity producing systems (SAPS) and bioreactors.

CWs are artificial wetlands engineered to provide a biological treatment approach

for AMD, where microbially mediated bio-chemical transformations assist the reduction of sulfate to sulfide and biogenic sulfide further precipitates dissolved metals as insoluble solids (Johnson and Hallberg, 2005). CWs can potentially remove trace amounts of metals with stable metal precipitates and less sludge production, which even conventional techniques fail to remove and thus offer a long-term treatment outlook. CWs operate with minimal maintenance and offer a cost-effective and environmental friendly approach. It appears to be a striking alternative, particularly in India, due to its prevailing warm subtropical climate conditions (Zhang et al., 2014).

Therefore, in the present study, CW was adopted to treat mine wastewater (containing pollutants such as acidity, sulfate and metals) representing AMD from the North Eastern Coalfield (Makum collieries), Assam, India. This study highlighted a holistic approach for the bioremediation of AMD in CWs using different wetland media and potential post-treatment metal recovery options from the media deposits were considered. Intensive investigation on the role of vegetation, effect of hydraulic loading rates (HLRs), seasonality and carbon addition at varying COD/SO_4^{2-} ratios on sulfate reduction and metal attenuation were studied.

1.2 Thesis organization

This thesis is structured into six chapters. The ongoing **Chapter 1** bestows light on the fundamentals of the present study with a brief introduction, encompassing scientific findings, gaps in the literature and research objectives. **Chapter 2** details the hydrochemistry of AMD from various collieries of the NEC during different seasons. **Chapter 3** gives a comparative perspective on the performance of CWs amended with different organic media. In addition, heavy metal accumulation within wetland components and metal mobilization are accounted. **Chapter 4** discusses the aspect of vegetation (*Typha latifolia*) and the effect of HLRs and rainfall on AMD treatment. Furthermore, the prospects of metal recovery from wetland media are highlighted. **Chapter 5** deals with the performance evaluation of CW consisting of gravel media under varying COD/SO_4^{2-} ratios. **Chapter 6** concludes the key findings from the present study and suggests a scope for future research.

1.3 Literature background

1.3.1 Generation of acid mine drainage (AMD) in coal mines

Metal-bearing sulfide-rich minerals undergo rapid oxidation on exposure to air (or oxygen) and water (Akcil and Koldas, 2006; Johnson and Hallberg, 2005). This weathering process results in the dissolution of metal ions from its mineral component (e.g., pyrite, FeS_2) due to excessive release of H^+ ions, as represented in equation (1.1), which further lower down pH (or increases acidity) of the water as the time progresses. The ferrous iron (Fe^{2+}) produced gets readily oxidized to ferric iron (Fe^{3+}) under oxygenated conditions, as given by equation (1.2) (Akcil and Koldas, 2006). The generated ferric iron gets easily precipitated as $Fe(OH)_3$ and jarosite ($2.3 < pH < 3.5$) (Equation 1.3), while some Fe^{3+} further oxidizes pyrite at a much faster rate (17–180 times faster) even under anoxic conditions according to equation (1.4)

(Zheng et al., 1986). These reactions form a chain sequence and continue until all minerals are depleted. In a similar way, a variety of other metal sulfides such as arsenopyrite (FeAsS), chalcopyrite ($CuFeS_2$), chalcocite (Cu_2S), millerite (NiS), molybdenite (MoS_2), sphalerite (ZnS) and galena (PbS) can be oxidized in the presence of oxygen and water or through another pathway (polysulfide mechanism).

$$FeS_2 + 3.5O_2 + H_2O \longrightarrow Fe^{2+} + 2SO_4^{2-} + 2H^+ \tag{1.1}$$

$$Fe^{2+} + H^+ + \frac{1}{4}O_2 \longrightarrow Fe^{3+} + \frac{1}{2}H_2O \tag{1.2}$$

$$Fe^{3+} + 3H_2O \longrightarrow Fe(OH)_3 + 3H^+ \tag{1.3}$$

$$FeS_2 + 14Fe^{3+} + 8H_2O \longrightarrow 15Fe^{2+} + 2SO_4^{2-} + 16H^+ \tag{1.4}$$

However, the oxidation of sulfides of the type MS (M stands for metal) does not release acid, e.g., sphalerite oxidation, according to equation (1.5) (Kaksonen and Puhakka, 2007).

$$ZnS + 2O_2 \longrightarrow Zn^{2+} + SO_4^{2-} \tag{1.5}$$

In addition to the above-mentioned abiotic mechanisms, biological microbial-assisted oxidation plays a significant role in AMD formation, particularly at pH < 4.0. Several iron-oxidizing acidophilic bacteria such as *Acidithiobacillus ferrooxidans*, *Leptospirillum ferrooxidans*, *Ferrimicrobium acidiphilium* and *Halothiobacillus neapolitanus* have been isolated from AMD impacted sediments and found to accelerate pyrite oxidation under given favorable conditions (Hallberg and Johnson, 2003; Johnson, 1995). The primary factors that determine the rate of acid generation are pH, temperature, oxygen content of the gas phase, oxygen concentration in water phase, degree of saturation with water, chemical activity of Fe^{3+}, surface area of exposed metal sulfide, chemical activation energy required to initiate acid generation and bacterial activity (Akcil and Koldas, 2006).

1.3.2 AMD scenario in India

The inevitable occurrence of AMD has been reported across the globe. Some major coal mining countries are China, India, the USA, Australia and South Africa, where about 40–70% of electricity supply is met by coal fuels (Li et al., 2015). Approximately 19,300 km of streams and rivers and 72,000 ha of lakes and reservoirs worldwide have been contaminated by mine effluents (Johnson and Hallberg, 2005), among which about 8000–23,000 km of streams are reported in the USA alone (Cravotta III and Trahan, 1996; Johnson, 1995). Global heavy metal concentrations in rivers and lakes have substantially increased over the last five decades (1970–2017) due to mining and other secondary metal waste discharge (Zhou et al., 2020).

India being the second-largest producer of coal in the world, million litres of coal mine drainage are daily disposed to the natural water sources without any treatment (Mittal et al., 2021; Ray and Dey, 2020). Table 1.1 depicts AMD characteristics from different Indian coal mines. The major polluting coal mines due to AMD are Western Coalfield (WCL), Northern

Coalfield (NCL), North Eastern Coalfield and coal-producing zones (Khasi, Garo and Jaintia hills) of Meghalaya. Most of the coal mines from Raniganj, Jharia and Korba Coalfields are not generating acidic drainage due to the dearth of pyrites in the seams (Ray and Dey, 2020). Despite the non-acidic mine drainage, Indian coal mine water comprises high heavy metal contaminants and thus, requires immediate attention. About 206–400 million litres per day (MLD) of mine water is reported to be discharged into the rivers (Tiwary and Dhar, 1994). For instance, Neogi et al. (2017) reported an annual discharge 22.35 × 10^6 m^3 of mine water and 18.50 × 10^3 tonnes of solute loads into nearby waterways from North Karanpura Coalfield.

1.3.3 Environmental implications

AMD is a multifarious pollutant consisting of toxic metals, high sulfate concentration (high salinity), total dissolved solids (TDS) and high acidity, all of which negatively affect the environment (Fig. 1.1). The most significant and visible impact of AMD is the smothering of metal precipitates on the surface of water bodies and sediment, limiting light penetration, oxygen diffusion and vegetation speciation (Sheridan et al., 2018). Higher sulfate concentration could accelerate eutrophication and sulfide toxicity (Geurts et al., 2009). Due to high acidity, the mobility of the metals in the environment increases significantly and the toxicity impact of metals on marine life is very evident (Gao et al., 2021). Heavy metal toxicity at high concentrations occurs through ligand interactions or the displacement of essential metal ions via (i) impairment of cell membrane, (ii) shift of enzyme specificity, (iii) disruption of cellular functions and (iv) mutilation of deoxyribonucleic acid (DNA) structure (Bruins et al., 2000).

Plant-metal uptake, translocation, sequestration and storage pose a serious danger to the growth of the plants by inducing oxidative and genotoxic stress, especially in agriculture crops that become the source of metal pollution and raise a risk to human health. Heavy metal accumulation in plants beyond the permissible limits inhibits electron transport, reduces CO_2 fixation, and causes chloroplast disorganization depending upon the type of plant species, metal element and metal bioavailability in soil (Table 1.2). Metal toxicity may also induce reduced plant growth by amplifying the generation of free radicals and reactive oxygen species. The excess amount of Fe generates the free radicals, which irreversibly weaken the cell structure and harm the membrane, proteins and DNA (Vardhan et al., 2019).

The exposure of metals to human beings at a concentration higher than the critical values can produce serious health issues, damaging the lungs, liver, kidneys, blood compositions and other fundamental organs (Table 1.3). Some heavy metals are carcinogenic, like As, Pb, Hg, Ni, Cd and Cr, which can cause muscular dystrophy, Alzheimer's disease, different types of cancers and multiple sclerosis under a long period of exposure (Vardhan et al., 2019). These metals primarily target proteins involved in signaling or cellular regulatory processes such as apoptosis, cell cycle regulation, cell growth, DNA repair and methylation. Additionally, heavy metals also target the nervous system by causing inhibition of neurotransmitter and neuron damage leading to neurotoxicity (Engwa et al., 2019).

Table 1.1 AMD characteristics from Indian coal mines (national scenario).

Coal mine	Location	pH	EC (mS m^{-1})	TDS (mg L^{-1})	SO_4^{2-} (mg L^{-1})	TH (mg L^{-1} as $CaCO_3$)	Major metals present (mg L^{-1})	References
North Karanpura Coalfield	Hazaribagh, Chatra, Palamu and Ranchi districts of Jharkhand	6.4–8.8	25–187	185–1343	3.20–931	57–965	Fe (0.36–3.26), Mn (0.00–7.23), Al (0.00–0.21), Zn (0.00–0.62)	Neogi et al. (2017)
Korba Coalfield	Korba district of Chattisgarh	6.7–8.5	13–105	97–785	6.10–226	37–466	Fe (0.09–4.51), Mn 0.01–1.53), Al (0.01–0.54)	Singh et al. (2016)
Bapung and Lumshnong Coalfields	Jaintia hills of Meghalaya	1.6–4.8	60–586	423–4469	457–4489	–	Fe (38.50–290), Al (15.20–118), Mn (0.27–11.70), Zn (0.26–15.50), Ni (0.02–5.15)	Sahoo et al. (2012)
Raniganj Coalfield	Parts of West Bengal and Jharkhand	6.5–8.8	40–200	171–1626	3.90–586	48–863	Fe (0.07–0.97), Mn (0.00–0.14), Zn (0.02–0.20)	Singh et al. (2010)
Western Coalfield (WCL)	Parts of Madhya Pradesh and Maharashtra	2.8–6.0	–	700–3300	400–1950	–	Fe (2–51), Mn (0.03–3.06), Cu (0.01–0.04)	Tiwary (2001)
Northern Coalfield (NCL)	Singrauli, Madhya Pradesh	1.5–6.7	–	380–2324	498–1678	–	Fe (33–84), Mn (0.02–0.40), Cu (0.00–0.02)	Tiwary (2001)
North Eastern Coalfield (NEC)	Tinsukia district of Assam	2.3–7.6	79–676	1068–1339	176–3615	460–5720	Fe (2.10–256), Al (0.07–35), Mn (0.53–25), Zn (0.02–5), Ni (0.00–11), Co (0.00–1.62), Cr (0.00–0.13)	Dutta et al. (2018, 2019); Equeenuddin et al. (2010)

EC: electrical conductivity; TDS: total dissolved solids; TH: total hardness.

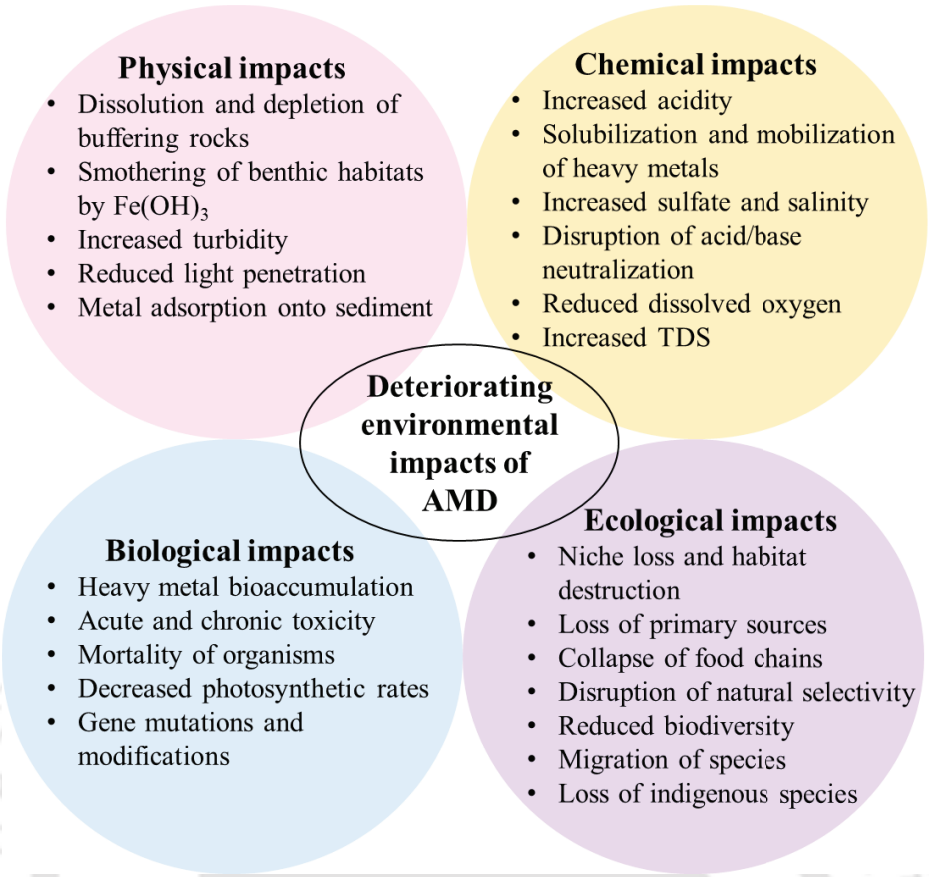

Fig. 1.1 Environmental impacts of AMD [adopted from Sheridan et al. (2018)].

Table 1.2 Effects of heavy metals on plants (Simate and Ndlovu, 2014).

Heavy metal	Effects
Cadmium	Decreases seed germination, lipid content and plant growth; induces phytochelatins production
Lead	Reduces chlorophyll production and plant growth; increases superoxide dismutase
Nickel	Reduces seed germination, dry mass accumulation, protein production, chlorophylls and enzymes; increases free amino acids
Mercury	Decreases photosynthetic activity, water uptake and antioxidant enzymes; accumulates phenol and proline
Zinc	Reduces Ni toxicity and seed germination; increases plant growth and adenosine triphosphate (ATP)/chlorophyll ratio
Chromium	Decreases enzyme activity and plant growth; produces membrane damage, chlorosis and root damage
Copper	Inhibits photosynthesis, plant growth and reproductive process; decreases thylakoid surface area

1.3.4 Preventive and remediation options

The preventive or source control measures limit the contact of pyrite (or sulfidic minerals) with environmental components such as oxygen, water and microorganisms, thus dismissing the treatment and disposal requirement of pollutants. Many prevention strategies involve either isolation of sulfidic minerals, exclusion of air and water inflow, or controlling the activity of AMD-forming bacteria (Fig. 1.2). Preventive methods are best suited for abandoned mines, while others are only practical for active operations (Skousen et al., 2019).

Table 1.3 Effects of heavy metals on human health and their permissible limits in inland surface water discharge (Crisponi et al., 2013; Leyssens et al., 2017; Puntarulo, 2005; Rambabu et al., 2020; Simate and Ndlovu, 2014).

Heavy metal	Effects	CPCB (1993)*	EPA (2002)*
Arsenic	Bronchitis, dermatitis, poisoning	0.20	0.10
Cadmium	Renal dysfunction, lung disease, lung cancer, bone defects, increased blood pressure, kidney damage, bronchitis, bone marrow cancer and gastrointestinal disorder	2.00	0.01
Lead	Mental retardation in children, developmental delay, fatal infant encephalopathy, congenital paralysis, sensor neural deafness, liver, kidney, and gastrointestinal damage, acute or chronic damage to the nervous system and epilepticus	0.10	0.05
Manganese	Damage to the central nervous system	2.00	0.20
Mercury	Damage to the nervous system, protoplasm poisoning, spontaneous abortion, minor physiological changes, tremors, gingivitis and acrodynia characterized by pink hands and feet	0.01	0.005
Zinc	Damage to the nervous membrane	5.00	2.00
Chromium	Damage to the nervous system, fatigue and irritability	2.00	0.05
Copper	Anaemia, liver and kidney damage, stomach and intestinal irritation	3.00	0.50
Iron	Enhances microbial infection, advanced hepatic fibrosis, Neoplasia, Cardiomyopathy, Atherosclerosis and leads to chronic diseases	3.00	2.00
Aluminium	Dialysis dementia, osteomalacia and microcytic anaemia without iron deficiency	–	5.00
Cobalt	Lipid peroxidation, interruption of the mitochondrial function, alteration of Ca and Fe homeostasis, trigger erythropoiesis, interruption of thyroid iodine uptake and induction of genotoxic effects	–	0.05
Nickel	Allergic contact dermatitis, chronic bronchitis, lung and nasal cancer	3.00	0.10

*Permissible levels are in mg L^{-1}.

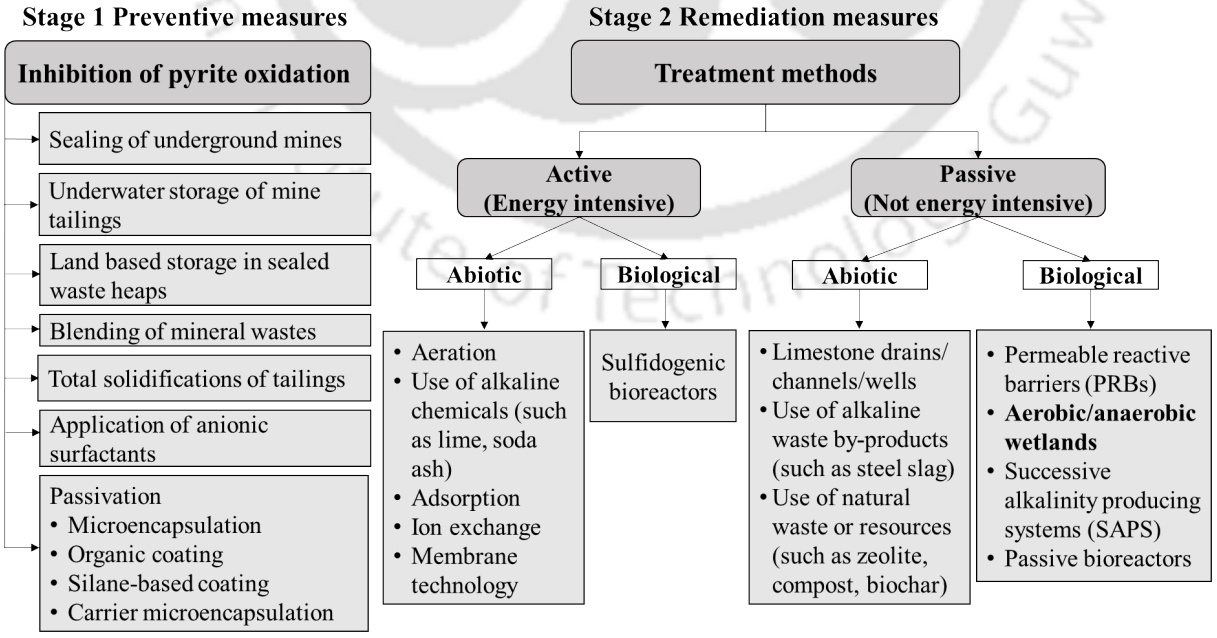

Fig. 1.2 Preventive control and remediation measures for AMD [adapted and modified from Johnson and Hallberg (2005); Park et al. (2019)].

However, the prevention techniques are not always pragmatic to preclude the formation of AMD. Therefore, once AMD is formed, immediate remediation and a rehabilitation paradigm shift become imperative (Kefeni et al., 2017). Remediation measures have been divided into "active" (involving constant resource and energy input) and "passive" (involving relatively low resource and energy input) processes (Johnson and Hallberg, 2005). These methods can be further distinguished based on either biological (biotic) or chemical (abiotic) mechanisms for eliminating pollutants (Fig. 1.2).

1.3.4.1 Preventive source control measures

Proper prevention of AMD generation should be a crucial precondition to preserve and protect the environment and enhance ecological sustainability (Kefeni et al., 2017). Among the available management techniques, dry barriers, wet covers, bactericides, microencapsulation and seals are commonly employed. For dry covers, various materials like non-reactive fine mine residue, combination of clay/ash and sludge/natural soil, industrial alkaline wastes and organic materials are used as an effective isolation layer to contain mine tailing (Park et al., 2019). The low permeable cover (e.g., clayey silty soil) limits oxygen diffusion into the pyritic wastes, reducing the oxidation rate. Decomposition of organic material by aerobic bacteria takes oxygen trapped within the organic layer and prevents further oxidation of sulfide minerals. Inundation of sulfide-bearing waste with water is widely used because of very slow oxygen diffusion (1.90×10^{-9} m^2 s^{-1}); however, complete prevention of AMD is impractical as 100% elimination of dissolved oxygen (DO) is very difficult and Fe^{3+} acts as an alternate oxidizer (Choudhury et al., 2021). Further, alkaline cover may enhance the solubility of some heavy metals, whereas organic cover can cause reductive dissolution of Fe^{3+}. Moreover, water cover is not applicable in arid and semi-arid regions (Park et al., 2019).

Bactericides such as anionic surfactants, organic acids and food preservatives have been used to inhibit the growth of microorganisms involved in AMD formation. Acidophilic iron- and sulfur-oxidizing bacteria maintain a near-neutral pH within their cell membrane by preventing proton entry into the cell through a cytoplasmic membrane (Baker-Austin and Dopson, 2007). But bactericides promote the entry of protons within the cell membrane, which causes disruptions of enzymatic functions and eventual death of the cell at high concentrations (Park et al., 2019). However, bactericides cannot permanently inhibit microbial activity, so repetitive addition is required. Co-disposal or blending of reactive mine tailings with either potentially acid consuming or alkaline-producing materials (such as lime, limestone and phosphate minerals) has been considered a promising approach. Limestone blending involves four mechanisms to control pyrite oxidation. Firstly, the precipitation of Fe^{3+} in the hydroxide form limits its further participation as an oxidizing agent in pyrite dissolution. Secondly, pH increase (6.1–8.4) impairs the activity of oxidizing bacteria (*Acidithiobacillus ferrooxidans*). Other mechanisms include the coating of oxidized compounds on the reactive surface of sulfide minerals and the formation of a protective layer consisting of ferric oxy-hydroxide and gypsum with very low permeability that acts as an oxygen and water diffusion barrier (Mylona et al., 2000).

The application of organic coatings (like sodium oleate, humic acid and lignin) makes the mineral surface hydrophobic, limiting water-mineral interactions and providing physical protection. Microencapsulation technique acts on particle level where each sulfide mineral grain is coated with a chemically inert material. Carrier-microencapsulation is a modified version of microencapsulation that targets sulfide minerals specifically (Satur et al., 2007). However, the long-term stability of these coatings is unknown.

1.3.4.2 Active remediation measures

The active treatment methods include the application of neutralizing chemicals (such as lime, limestone and quick lime) and aeration (particularly for iron and manganese oxidation) for acidity and metal removal and to some extent, sulfate removal in the form of gypsum ($CaSO_4.2H_2O$) sludge (Skousen et al., 2019; Tchobanoglous et al., 2003). Other sophisticated active treatment options include adsorption, ion exchange and membrane process (reverse osmosis and nanofiltration) (Naidu et al., 2019). Overall, the active remediation methods are very effective and quick; however, the associated cost of chemical reagent, capital investment, maintenance and disposal of hazardous voluminous sludge (or floc) sabotage its long-term sustainable feasibility.

A promising active biological treatment option is the sulfidogenic bioreactor, which offers a simultaneous reduction of metals and sulfate below the desired limits with the viable potential of metal recovery as metal sulfides (Altun et al., 2014). Bekmezci et al. (2011) reported higher sulfate reduction (88%) and metal removal efficiencies (99%) for metals like Co, Cu, Fe, Ni and Zn, except for Mn (25–77%) from synthetic AMD in an ethanol-fed sulfate-reducing anaerobic bioreactor. Sahinkaya et al. (2019) employed a sulfidogenic anaerobic membrane bioreactor, which reported exceptionally higher sulfate reduction (95%) on doubling metal concentrations in the feed and obtained > 99% metal removal (Fe, Cu, Zn, Co and Ni) with partial removal of Mn (76–91%) and As (41–67%). On the downside, sulfidogenic bioreactors face major scale-up challenges from lab to the field-scale applications due to their high cost, skilled labor requirement and high operational and maintenance expenditures (Kiran et al., 2017). Therefore, researchers have inclined their keen interest in utilizing passive treatment strategies for AMD treatment.

1.3.4.3 Passive remediation

Passive treatment systems are mostly recommended for post-closure treatment scenarios and are best suited for AMD with low acidity (< 800 mg L^{-1} as $CaCO_3$) and low flow rates (< 50 L s^{-1}) (Taylor et al., 2005). The passive treatment system includes limestone drains (LDs) (Cravotta III and Trahan, 1996), PRBs (Gibert et al., 2011), SAPS (Yim et al., 2015), passive bioreactors (Neculita et al., 2007), CWs (Lizama-Allende et al., 2021) and utilization of alkalinity generating natural and industrial waste by-products (Kaur et al., 2018). However, the application of passive systems also encounters many downfalls such as large area footprint, performance is less predictable, difficult process control and inefficiency in handling seasonal flow fluxes (Johnson and Hallberg, 2005).

(a) Limestone based systems

These are passive geochemical systems primarily employed as a pretreatment step to CWs or anoxic ponds for acidity and metal removal. The treatment principle involves metal reduction (or oxidation) under reducing (or oxidizing) conditions by raising the pH of net acidic mine discharge using inorganic reactive materials, such as limestone. However, the removal of sulfate is considerably low in these systems. These systems are generally classified as anoxic limestone drains, open or oxic limestone drains, limestone diversion wells and limestone leach beds.

Anoxic limestone drains consist of underground trenches (or capped channels) preferably laid in the direction of the topographical slope and filled with limestone. These systems are strictly impervious to air and operate under high partial CO_2 pressure ($> 10^{-1}$ atm), thereby instigating limestone dissolution rate and high alkalinity production (up to 320 mg L^{-1} as $CaCO_3$) (Watzlaf et al., 2000). However, these systems are best suited to treat net acidic mine drainage with a low concentration of Fe^{3+} (< 2 mg L^{-1}), Al and DO (< 1 mg L^{-1}). Lower DO in mine drainage prevents oxidation of Fe^{2+} as ferrous hydroxide ($Fe(OH)_2$) precipitation occurs at pH > 8.0, which is usually not attained or reported in any anoxic limestone drains. Otherwise, ferric hydroxide ($Fe(OH)_3$) precipitation can cause 'armouring' and prevent any further reaction by reducing the flow permeability, causing immediate failure (Skousen et al., 2017; Watzlaf et al., 2000). Oxic limestone drains are analogous to anoxic limestone drains, where AMD flows through open conduits filled with larger crushed limestone (> 30 cm) and thereby, removal occurs via oxidative precipitation with moderate alkalinity production (55–136 mg L^{-1}) (Cravotta III and Trahan, 1996). These systems are employed for AMD having high concentrations of Fe^{3+}, Al and DO. Oxic limestone drains are expected to operate for several years as armored limestone and have shown only 2–45% reduction in acid neutralization capacity than unarmored limestone (Ziemkiewicz et al., 1997).

Limestone diversion wells typically comprise of a cylindrical concrete (or metal container) (1.50–1.80 m in diameter and 2–2.50 m in depth) filled with limestone particles and a large metallic pipeline for AMD conveyance at the center of the well (Skousen et al., 2017). Diversion wells are usually constructed downstream of acidic flow, where a part of diverted AMD flow surges into the bottom of the well at high hydraulic pressure and then flows back upwards, creating high turbulence and mixing with the limestone. This process aids in metal removal via hydrolysis and precipitation, where metal flocs remain suspended and flushed out with the outflow. The stirring action of water helps in scouring the precipitate layer, which ensures the continuous dissolution of limestone (Taylor et al., 2005).

Limestone leach beds are small open pond structures lined or filled with crushed limestone (2–10 cm), where AMD is retained for a designed residence time (> 30 min) (Black et al., 1999). Schueck et al. (2004) recommended the installation of up-flow daily flushing to overcome the armoring of the limestone bed. Nevertheless, periodic maintenance

and consistent replacement of exhausted bed would be needed. Steel-slag leach beds are an extensive modification, consisting of steel slag (a by-product of steel manufacturing) as the acidity neutralizing alternative, often designed for a residence time of 1–4 h (Simmons et al., 2002). The major potential risks associated with the steel-slag beds are: (i) leaching of toxic metals from slag matrix such as Pb, Ni, Cr, Cd, V and fluoride, (ii) potential remobilization of slag metal sludge during the exhaustion of slag's alkalinity and (iii) disposal of metal-laden slag sludge after failures (lifespan of about 6.20 years) (Kruse et al., 2012).

(b) Alkaline natural resources and industrial by-products

Realizing the repercussions of lime neutralization, many researchers have deliberately shifted their interest to utilize alternative waste materials for a sustainable AMD treatment. Waste materials arising from different industrial processes or naturally occurring resources are thus, now identified as suitable candidates based on their neutralizing and metal sorption capacity. Neutralizing materials derived in the form of industrial byproducts such as coal fly ash (Gitari et al., 2018), Bayer precipitates from alumina industries (Kaur et al., 2018), metallurgical slags (iron slag, basic oxygen slag and stainless steel slag) from iron and steel making industries (Name and Sheridan, 2014), Portland cement from cement industries (Sephton and Webb, 2019) and green liquor dregs from Kraft process in paper mill industries (Sebogodi et al., 2020) have been comprehensively studied in the AMD remediation. In addition, various alkaline natural materials such as natural zeolite (Motsi et al., 2009), calcareous rocks (García-Valero et al., 2020) and activated mineral adsorbents (e.g., attapulgite, bentonite clay and schwertmannite) (Falayi and Ntuli, 2015; Masindi et al., 2015; Zhang et al., 2018) have shown promising results in AMD neutralization and metal removal. Thus, it was very evident from the previous results that hydroxyl and carbonate groups present in different proportions and compositions of an alkaline material played a substantial role in buffering pH. Metal(loid)s encapsulation in the precipitates and co-precipitates formed at higher pH constituted the primary metal removal pathway. The metal sorption property of metallurgical slags was found to be the function of its high surface area, porosity and ion-exchange ability. However, further intensive investigation on sludge stability and metal leachability after treatment to meet disposal compliance is indispensable.

The mechanism of heavy metal biosorption on agricultural and animal residues has been long recognized owing to the material's intrinsic property and the presence of various functional groups that assist in metal sequestration and complexation (Sud et al., 2008). Earlier research works have suggested the potential application of bio-materials derived from plant and animal wastes such as dairy manure compost (Zhang, 2011), shrimp shells (Núñez-Gómez et al., 2019), spent coffee grounds (Ayala and Fernandez, 2019) and bone meal (Payus et al., 2014). Most studies have reported batch processes and further research innovation for designing continuous reactors to scale up in industrial applications would provide commercial viability and validation. Furthermore, investigation on the reversibility of the process and re-availability of binding sites would govern the effectiveness of such treatment at large-scale applications.

(c) Permeable reactive barriers (PRBs)

PRBs are in-situ passive biological remediation, where major principle governing processes are adsorption, ion exchange, precipitation and dissimilatory sulfate reduction facilitated by sulfate-reducing bacteria (SRB). PRBs are buried intercepting sections in the flow path of groundwater AMD plumes, which consist of organic-based reactive materials such as a mixture of gravel, limestone and organic media (Gibert et al., 2011). The choice of reactive mixture composition depends on AMD inflow characteristics and hydraulic permeability of the media to ensure designed residence time (usually 1–6 d). PRBs are very effective when treating AMD contaminated groundwater flow having low DO and Fe^{3+}, as precipitation of metal sulfides results from the sulfate reduction in the reactive zone of the barrier (Benner et al., 1999). PRBs have low operational cost with no land requirement. However, prior to PRB construction, rigorous site investigation, surface mapping and geophysical exploration are necessary to prevent cross-contamination with any nearby aquifer and thus, its implementation cost is relatively high. Besides, exhaustion of reactive media mass, clogging of the pores and reduced permeability of the barrier often limits the lifespan of a PRB (Taylor et al., 2005).

(d) Successive alkalinity producing systems (SAPS)

SAPS are modified submerged vertical flow wetlands devised particularly to treat low flow (< 15 L s^{-1}) and low acidity (< 100 kg $CaCO_3$ d^{-1}) mine discharge (Taylor et al., 2005). These are also collectively referred to as reducing and alkalinity producing systems (RAPS) or vertical flow wetlands (VFWs) (Skousen et al., 2017). SAPS incorporate both anoxic limestone drain technology and sulfate reduction mechanisms by SRB within one unit. It essentially consists of a submerged vertical flow basin (1.70–2.60 m), filled with organic compost (0.20–0.60 m), followed by a limestone bed at the bottom (0.50–1 m). The idea is to produce reducing conditions in the first organic layer as mine wastewater percolates down such that all iron is reduced to Fe^{2+} with simultaneous sulfate reduction (Yim et al., 2015). Thus, low DO mine drainage containing mostly Fe^{2+} reacts with limestone to increase pH and metal precipitation without causing any coating or armouring of the limestone bed. However, SAPS involve high money expenditure in construction and require consistent monitoring and flushing of the accumulated metal precipitates to prevent clogging and compaction of the media.

(e) Passive bioreactors

Passive bioreactors are modified sulfidogenic bioreactors, defined distinctively as a simple flow-through design reactor with a solid reactive organic mixture that acts as a carbon source and physical support for microbial attachment for SRB assisting metal sulfide precipitation (Neculita et al., 2007). The choice of suitable organic media plays a vital role in determining the process efficiency and economic feasibility of bioreactors. Choudhary and Sheoran (2011) investigated comparative performance between different single media derived from cellulosic waste and organic waste in lab-scale passive bioreactors, among which organic waste (goat manure) indicated excellent acidity reduction (1030 mg L^{-1} as $CaCO_3$), sulfate removal (54%) and metal removal efficiencies > 99% for Fe, Zn, Cu, Ni, Co and about 74% for Mn. However,

the use of a single organic media might promote short-circuiting in on-site bioreactors by limiting the permeability of the compacted media bed. Therefore, generally, a mixture of organic media containing easily biodegradable simple organics (such as cow manure, compost) and complex recalcitrant organics (such as alfalfa, sawdust, woodchips) have been most widely adopted in pilot-scale studies (Song et al., 2012). Metal removal mechanisms outlined in passive bioreactors include adsorption on the media surface, complexation and precipitation of metals as hydroxides and carbonates during the start-up of bioreactors, whereas sulfide precipitation becomes the predominant mechanism once the steady-state condition is achieved (Neculita et al., 2007).

(f) Constructed wetlands

CWs are designed to simulate the natural process existing in natural wetlands and ecosystems. Traditionally, CWs are broadly distinguished into two groups based on water depth with respect to the media bed: surface flow (SF) or free-water surface (FWS) and sub-surface flow (SSF). In SF CWs, the water surface is above the media and completely flooded. In contrast, in SSF CWs, the water level is maintained below the media layer and forms interaction with different microorganisms. SSF CWs can be further categorized depending on the flow path as horizontal flow (HF) or vertical flow (VF). Hybrid systems incorporate both SF and SSF CWs. In general, CW involves a complex network of bio-chemical interactions between its various components (such as media, vegetation and microbes) that play a vital role in water quality improvement. Depending upon the mine water characteristics and remediative reactions (oxidation or reduction), CWs are classified as aerobic and anaerobic (Fig. 1.3).

Aerobic constructed wetlands are surface flow, shallow depth (10–30 cm) and narrow channels such that length to width ratio is usually more than 10 (Gazea et al., 1996) [Fig. 1.3 (a)]. Typically, aerobic CWs are employed as the final 'polishing unit' that are designed to treat net alkaline mine discharge (pH > 5.0) under oxidizing conditions (Skousen et al., 2017). The primary processes involved are ion-exchange, adsorption, oxidation and hydrolysis of ferrous iron, which results in the production of H^+ ions. This drop in pH limits the rate of ferrous iron oxidation, which is controlled by pH and oxygen concentration as per the equation (1.6) (Stumm and Morgan, 1981).

$$\frac{d[Fe^{2+}]}{dt} = k.\frac{[O_2][Fe^{2+}]}{[H^+]^2} \tag{1.6}$$

where $k = 8.0 \times 10^{13}$ litre^2 mole^{-2} atm^{-1} min^{-1} at 25°C. At low pH (< 3.0), the reaction proceeds at a rate independent of pH. Thus, neutrophilic iron-oxidizing bacteria (such as *Gallionella ferruginea*) present near the oxic pockets (preferably roots of plants) control the ferrous iron oxidation, which is a relatively slow process (Johnson and Hallberg, 2005). Therefore, it is desirable to introduce alkalinity by providing an anoxic limestone drain system prior to aerobic CWs, which would promote the effective removal of metals, including Mn and Al.

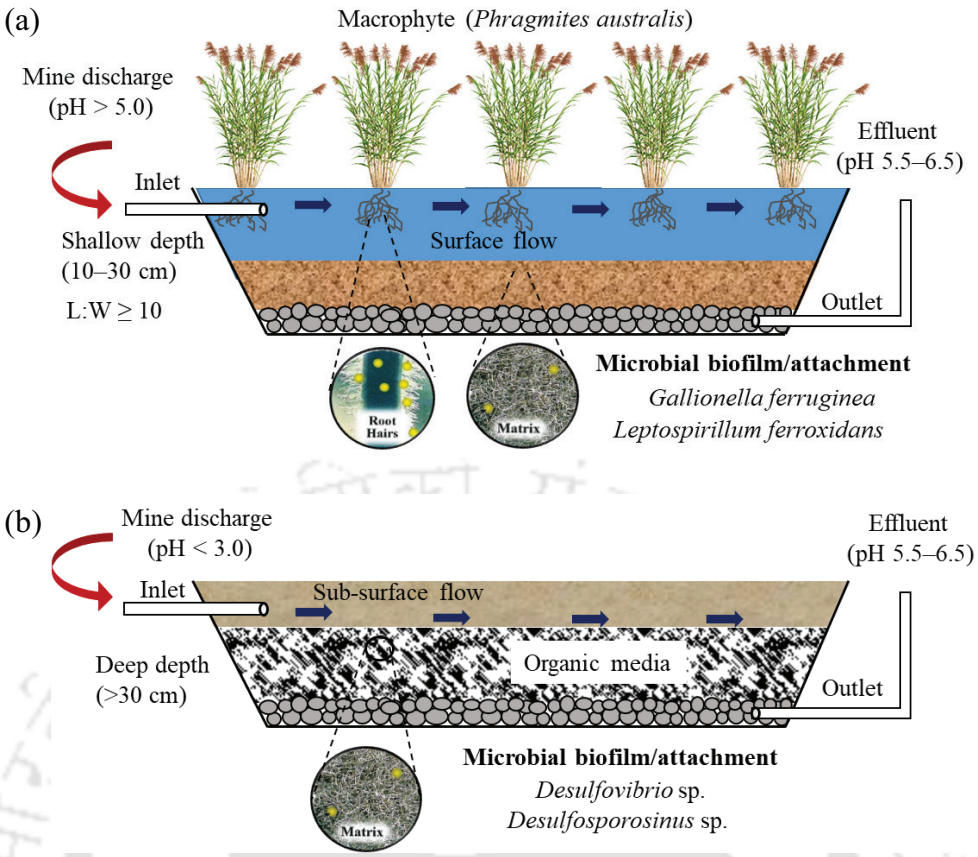

Fig. 1.3 Schematic representation of (a) surface flow aerobic wetland and (b) sub-surface flow anaerobic wetland with remediative functions.

Anaerobic/compost constructed wetlands are quite opposite of aerobic CWs [Fig. 1.3 (b)], designed strictly to treat net acidic (pH < 3.0, acidity > 300 mg L^{-1} as $CaCO_3$) metal-rich mine discharge and operate under reducing conditions (Gazea et al., 1996). Anaerobic CWs are deep sub-surface flow (> 30 cm) basins, which are typically filled with a mixture of limestone and organic waste materials (e.g., manure, wood chips, peat, husk, straw) or compost (e.g., mushroom spent compost) (Gazea et al., 1996; Younger, 1998). Rapid depletion of oxygen due to the biodegradation of organic carbon present in organic media provides a suitable anaerobic condition for SRB growth (such as *Desulfovibrio* sp.) and acts as biocatalysts in the dissimilatory sulfate reduction as given in equation (1.7). The bicarbonate alkalinity and limestone dissolution (if provided) essentially raise the pH of the mine water (acidity removal rate 3.5 g m^{-2} d^{-1}). The liberated H_2S further reacts with metal ions (represented by M^{2+}) to precipitate biogenic metal sulfides (represented by MS) as described by equation (1.8), which is more stable over a wide pH range (Kaksonen and Puhakka, 2007; Skousen et al., 2017). The metal precipitation reaction releases protons, thus adding to the acidity of the water. Therefore, excess sulfate needs to be reduced to compensate for the acidity. However, depletion of organics over time and replacement with fresh media adds to the maintenance. Furthermore, the disposal of exhausted media needs careful handling, as sulfide-bearing flocs in media could oxidize to sulfate and release acidity. Despite the outlined bio-chemical reactions, the overtime changes in the microbial diversity and media composition in anaerobic CWs are still lacking and offers future research scope.

$$2CH_2O + SO_4^{2-} \longrightarrow 2HCO_3^- + H_2S \quad (1.7)$$

where CH_2O denotes the electron donor.

$$M^{2+} + H_2S \longrightarrow MS\,(\downarrow) + 2H^+ \quad (1.8)$$

CWs are cost-effective, technically feasible, require low operation and maintenance, offer aesthetic enhancement, environmentally friendly, low volume of sludge generation, high long-term performance, ability to remove metal and sulfates and metal precipitates formed are stable and thus provide lasting retention. However, like any other biological systems, CWs also encounter problems such as large area requirement, media clogging, less-predictable performance, longer retention time and uncertainty about long-term fate and stability of the accumulated deposits. Table 1.4 gives a brief comparison of AMD treatment in CWs as reported in the literature.

1.3.5 Wetland mechanism in metal attenuation and sulfate removal

CWs employ a multifaceted network of biotic and abiotic routes (or mechanisms) for metal attenuation. The underlying metal removal mechanisms in CW involve physical (settling, sedimentation and filtration), chemical (sorption, oxidation, hydrolysis, precipitation and co-precipitation reactions) and biological (plant uptake and bacterial metabolism) processes (Sheoran and Sheoran, 2006). The entire process of metal attenuation is inter-dependent and co-existing, and therefore it is very complex to decipher the level of individual involvement of different wetland mechanisms.

1.3.5.1 Physico-chemical mechanisms

(a) Filtration and sedimentation

Filtration and sedimentation play a major part in retaining metals once metal form precipitates or in the colloidal state. Settling and interception of metal particulates primarily occurs in sand/gravel media (in the case of HF and VF wetlands), where metals get trapped and strongly bound with other incoming organic and suspended matter, which affects the hydraulic conductivity and wetland performance over time. In the case of FWS, low inflow velocity accompanied by plant litter presence promotes settling and interception of metal solids (Kadlec and Wallace, 2008). Particulates denser than water can be readily settled out under relatively low-velocity flow conditions, whereas floc-formation is essential for sedimentation for lighter particles. The formation of floc is improved by increasing pH, suspended solids concentration, algal densities and ionic strength of wastewater (Matagi et al., 1998). Flocs tend to settle rapidly and may result in the adsorption of other suspended particles and heavy metals (Sheoran and Sheoran, 2006). Lim et al. (2001) demonstrated the importance of sedimentation and filtration in laboratory-scale FWS and HSSF CWs that were either planted with *Typha angustifolia* or left unplanted. Systems received primary treated sewage spiked with high Cu levels. As the dissolved Cu fractions accounted for only 3 to 6% of the influent Cu load, sedimentation and filtration were the major removal mechanisms.

Table 1.4 Application of CWs for the treatment of AMD.

Type of CW	Media	Plant species	Pollutants present*	Performance efficiency (%)			Remarks	Reference
				Metal removal	Sulfate removal	Final pH		
HSSF (lab-scale)	Limestone or zeolite	*Phragmites australis*	pH (2.0), Fe (49–57), Pb (0.88–0.90), Zn (10–12), As (2.10–3.70) and SO_4^{2-} (2044)	Fe (> 96), Pb (> 94), Zn (> 40) and As (> 96)	13–29	3.5–6.7	Metal sulfide precipitation was not observed as the major removal route	Lizama-Allende et al. (2021)
VSSF (lab-scale)	Pumice stones, limestone and loamy soil	*Phragmites australis*	pH (4.0), Cu (20), Zn (30), Cd (0.30), Mn (0.50), Pb (2.50), Fe (4.50) and SO_4^{2-} (174)	Cu (99), Zn (21), Cd (40) and Pb (90)	59	–	Higher metal reduction in planted CWs than unplanted and sulfate removal was due to neutralization	Blesson et al. (2021)
HSSF (pilot-scale)	Sand and gravel	*Scirpus grossus*	pH (2.0), Fe (10) and Al (3.30)	Fe (33) and Al (100)	–	5.0–8.0	Rhizobacteria enhanced plant growth and metal accumulation	Ismail et al. (2020)
Settling tank + adsorbent tank + HSSF (pilot-scale)	Limestone/ laterite	*Phragmites australis*	pH (7.3), As (0.22–0.30), Mn (2.56–3.75), Cd (0.33–0.63), Zn (0.81–1.33) and Pb (0.37–0.65)	As (89.90), Mn (99.50), Cd (93.30), Zn (80.10) and Pb (66.80)	–	–	Importance of media selection for targeted metals; laterite was more efficient for As removal	Nguyen et al. (2019)
FWS (lab-scale)	Hydroponic	*Chrysopogon zizanioides*	pH (2.5), Fe (81), Al (70), Mn (22), Zn (1.40), Ni (0.70), Cu (0.20), Pb (0.08), Cr (0.01) and SO_4^{2-} (502)	Fe (81), Al (11), Mn (27), Zn (35), Ni (38), Cu (8), Pb (81) and Cr (21)	28	3.5	Primary localization of metals on the root surface as Fe plaques	Kiiskila et al. (2019)
VF + HF (lab-scale)	Crushed sea shell grits	*Typha domingensis*	pH (2.6), Fe (200), Mn (18), Cu (4), Pb (2) and Zn (12)	Fe (99.20), Mn (100), Cu (99.80), Pb (100) and Zn (99.90)	–	8.1	Metal removal occurred mainly via abiotic routes as the pH increased	Bavandpour et al. (2018)
VF (lab-scale)	Pea gravel (80% limestone)	*Phragmites australis*	pH (2.5–3.0) and Fe (50–100)	Fe (∼100)	–	7.0	Microbial activity significantly improved iron removal	Weber et al. (2010)
SSF (lab-scale)	Sand and gravel	*Juncus effuses*	pH (3.3), Fe (12), Zn (1.20) and SO_4^{2-} (2000–3000)	Fe (17–97) and Zn (20–77)	–	4.8	Sensitive to heavy rainfall causing remobilization of iron	Wiessner et al. (2006)
FWS (field-scale)	–	*Typha latifolia*	pH (8.2), Cd (0.05), Pb (11.50) and Zn (14.50)	Cd (94), Pb (99) and Zn (97)	–	7.7	Settling and increased storage were the most prominent removal mechanism	Yang et al. (2006)

*Units are in mg L^{-1}, except for pH.

(b) Sorption

The sorption mechanism of media (particularly SSF CWs) plays a dynamic role in removing metals and metalloids from wastewater. It may be identified either as short-term accumulation or long-term stabilization. Sorption defines a range of processes such as adsorption (surface phenomena where ions get attached to the surface of the adsorbent), absorption (bulk phenomena) and precipitation reactions. The former is further classified as physisorption (physical processes with weak Van der Waals interactions) and chemisorption (chemical processes with strong covalent bonds). The adsorption process is predominant during the initial period of operation when the sorption sites of media are unsaturated. The surface of organic media contains many polar functional groups (such as acids and phenolics), which are exchanged with the metal ions present in AMD to form more stable chelate complexes, as represented in equation (1.9) (Kadlec and Wallace, 2008). This form of chemical binding increases with the organic matter content of media, whereas it declines with decreasing pH.

$$2HP + M^{2+} \leftrightarrow MP_2 + 2H^+ \tag{1.9}$$

where 'P' denotes the organic material (peat) and M^{2+} is a divalent metal ion.

(c) Precipitation and co-precipitation

Precipitation and co-precipitation reactions are major driving mechanisms for metal removal. Precipitation of metals is facilitated when the solubility product (K_{sp}) of the concerned metal is exceeded, which is determined by pH and the initial concentration of metal ions. The nature of the insoluble precipitate formed governs the stability and bioavailability of the precipitated metal ions in the aquatic environment. Secondary minerals, including (oxy-) hydroxides of metals such as Fe, Al and Mn, assist the co-precipitation of other metals. Cu, Co, Ni, Pb and Zn are very often co-precipitated in the oxides of Fe and Mn (Sheoran and Sheoran, 2006). The formation of iron oxyhydroxides requires high pH and DO conditions, whereas aluminium oxyhydroxides flocs may form under circumneutral pH conditions and do not require oxygen, as represented by equations (1.10–1.11) and (1.12), respectively (Kadlec and Wallace, 2008). Additionally, radial oxygen loss (ROL) from roots and the formation of iron plaque on the surface of roots are reported to retain Zn and As (Kiiskila et al., 2017). In a reducing environment, pH controls the precipitation of metals as carbonates, hydroxides and sulfides.

$$Fe^{2+} + H^+ + 2.5O_2 \longrightarrow Fe^{3+} + 0.5H_2O \tag{1.10}$$

$$Fe^{3+} + 2H_2O \longrightarrow FeOOH + 3H^+ \tag{1.11}$$

$$Al^{3+} + H_2O \longrightarrow Al(OH)_3\ (\downarrow) + 3H^+ \tag{1.12}$$

The abiotic sulfate removal route includes mineral precipitations (such as gypsum, $CaSO_4$). However, the solubility of gypsum is influenced by the presence of other pollutants present in wastewater, ion-pairing and ion activity (Wu et al., 2013).

(d) Association of metals with oxides (oxidation) and hydroxides (hydrolysis)

Many metals may undergo oxidation or hydrolysis depending on pH, oxidation-reduction potential (ORP) and various anions present. The oxidation or hydrolysis of Fe and Al are described in equations (1.10–1.12). However, the abiotic oxidation of Mn is remarkably slow (Equation 1.13) and oxidation starts only at pH > 8 making it the most difficult to remove (Sheoran and Sheoran, 2006).

$$Mn^{2+} + 0.25O_2 + 1.5H_2O \longrightarrow MnOOH + 2H^+ \tag{1.13}$$

The redox potential of media decides the stability of metal oxides and (oxy-) hydroxides as under a reducing environment (below –100 mV), metals bound to Fe, Al and Mn flocs tend to remobilize and release back rapidly. Because oxidized iron acts as an electron acceptor, it can also inhibit bacterial sulfate reduction by outcompeting SRB for electron donors.

(e) Precipitation as metal carbonates

The occurrence of metal carbonate precipitation is primarily governed by the water pH, partial pressure of CO_2 and dissolved carbonate concentration. It is an important mechanism in wetlands that drain limestone catchment areas (Matagi et al., 1998). The CO_2 utilization by plants and algal biomass may also increase pH via periphyton photosynthesis, leading to $CaCO_3$ supersaturation and facilitating the precipitation of calcitic minerals (Kadlec and Wallace, 2008). In wetlands, carbonate precipitation of metals like Zn, Cu, Pb and Ni is well documented in many studies (Kröpfelová et al., 2009) (Equation 1.14).

$$M^{2+}\begin{Bmatrix} SO_4 \\ Cl_2 \end{Bmatrix} + Na_2CO_3 \longrightarrow MCO_3\,(\downarrow) + Na_2\begin{Bmatrix} SO_4 \\ Cl_2 \end{Bmatrix} \tag{1.14}$$

(f) Precipitation as metal sulfides

Metal sulfide precipitation via biological reduction of sulfate by SRB under anaerobic conditions is the most desired route for metal removal (Equation 1.7–1.8). The key requirements for sulfide precipitation are anaerobic conditions (ORP below –100 mV), presence of electron donors and microbial consortia (such as *Desulfovibrio* and *Desulfotomaculum*) capable of utilizing dissolved sulfate as electron acceptors (Kadlec and Wallace, 2008; Kaksonen and Puhakka, 2007). However, excessive generation of H_2S (or HS^-) can adversely cause toxicity to SRB and may increase metal mobility (Sánchez-Andrea et al., 2014). O'Sullivan et al. (2004) reported efficient removal of Fe, Pb and Zn from an active lead-zinc mine by bacterial sulfate reduction in FWS CWs planted with *Typha latifolia*. The sequential extraction of the sediment revealed that metals were mainly in the residual form (e.g., sulfide bound). Machemer et al. (1993) demonstrated that metal sulfide precipitation as acid volatile sulfides was the major metal removal process in pilot-scale CW treating AMD in Idaho Springs, Colorado. Similarly Stein et al. (2007) emphasized consistent removal of Zn with sulfate and presumably reflected zinc-sulfide precipitation in SSF treatment wetland receiving mine-impacted water.

Overall, it is concluded that the removal of metals in CWs occurs through a complex array of physicochemical processes such as sorption and precipitation as oxides, hydroxides and sulfides (Lesage, 2006). Thus, elucidation of these processes is a difficult task.

1.3.5.2 Biological mechanisms

(a) Microbial metabolism

Microbial processes involved directly or indirectly in metal attenuation are classified into (i) metal assimilation into their cells, (ii) biosorption, (iii) microbial oxidation-reduction of metals, (iv) methylation and (v) biogeochemical cycle-assisted metal removal (Kosolapov et al., 2004). Biosorption comprises several mechanisms like adsorption, ion exchange, chelation and entrapment interactions involving many functional groups, including carboxyl, sulfonate, phosphate, hydroxyl and amino moieties. Anaerobic metal-reducing bacteria are accomplished to receive metals as terminal electron acceptors via respiration, and the resulting reduced metals may be less or more soluble, depending on the specific elemental chemistry. The immobilization of metals like Cr, Se and U is reported through reduction processes bio-catalyzed by microorganisms (Green, 2011; Kosolapov et al., 2004). The reduction of Cr(VI) to Cr(III) leads to its effective immobilization and retention in the media of CWs, whereas the reduction of other metals, including Hg, Fe and Mn, enhances their mobility and release from CWs (Lesage, 2006). Organic matter provides the methyl-donor source for the methylation mechanism, which involves the conversion of toxic metal(loid)s (e.g., Hg, As and Se) into methyl derivatives and its subsequent removal by volatilization (Bolan et al., 2014).

Biotic transformations of sulfur include biologically catalyzed redox reactions such as assimilatory and dissimilatory sulfate reduction (Wu et al., 2013). In assimilatory sulfate reduction, sulfate is taken up by most bacterial species and it undergoes reduction prior to incorporation into biological compounds (cysteine, methionine, co-enzyme A, etc.) (Rinzema et al., 1988). Assimilatory sulfate uptake into organic S by plants or microorganisms is relatively minor compared to organic S formation via dissimilatory reduction of sulfate to H_2S (Wu et al., 2013). Under anaerobic conditions, a group of bacteria couples the oxidation of reduced organic or inorganic compounds to the reduction of sulfate for bioenergetics purposes. This process is known as dissimilatory sulfate reduction. However, the problems associated with dissimilatory sulfate reduction are primarily linked to sulfide production. Toxicity of sulfide is pH dependent since only the unionized hydrogen sulfide form is able to pass through the cell membrane (Kaksonen and Puhakka, 2007). Above pH 8.0–9.0, virtually all dissolved sulfide is present in the ionized form (Fig. 1.4). Knowledge of the complex microbiology and biochemistry of dissimilatory sulfate reduction is essential to understand the factors that control sulfidogenesis (Rinzema et al., 1988). pH, type of inoculum and substrate have a major effect on the microbial community composition. In the case of complex media, the major biological conversion processes are sulfate reduction, acetogenesis and methanogenesis, together with hydrolytic- and fermentative bacteria. Fig. 1.5 illustrates the possible metabolic pathways of organic compound degradation under anaerobic conditions.

The complex biopolymers are first degraded by anaerobic hydrolytic- and fermentative-bacteria. Clostridia are well-known sugar and protein fermenters using different fermentation pathways depending on the strain and the substrate. SRB catalyze the final reaction of the digestion process. Acetogens assimilate carbon into cell material through the acetyl-coA pathway and involve in the syntrophic degradation of fermentation intermediates. Competition between SRB and methane-producing bacteria (MPB) can occur, however, at an excess of sulfate, according to the Gibbs energy yield, SRB generally should outcompete methanogens. Methanogens are sensitive to low pH and therefore, acidophilic SRB outcompete methanogens at low pH (Sánchez-Andrea et al., 2014).

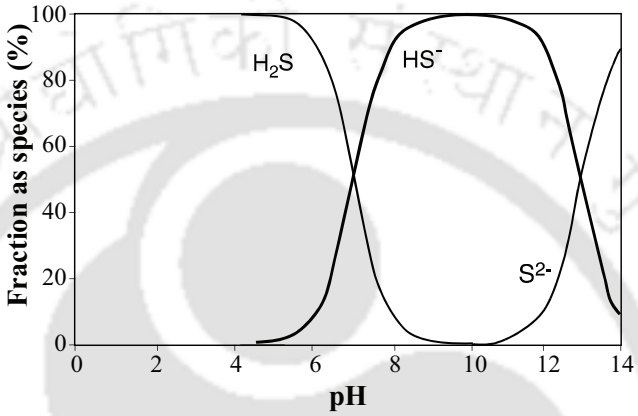

Fig. 1.4 Effect of pH on relative distribution of sulfide species in water [adopted from Sawyer et al. (2003)].

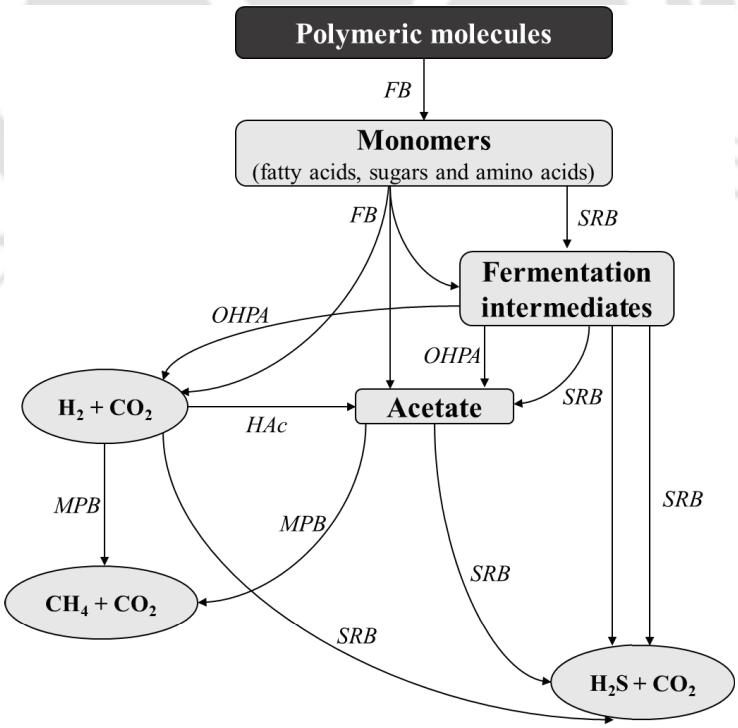

Fig. 1.5 Pathways of organic compound degradation under anaerobic conditions [modified and adopted from Rinzema et al. (1988)]. (FB – fermentative bacteria; OHPA – obligate hydrogen-producing acetogens; HAc – homoacetogenic bacteria; MPB – methane-producing bacteria; SRB – sulfate-reducing bacteria).

(b) Plant uptake

Metal accumulation in plants is an important biological process by phytostabilization, phytoaccumulation, and phytovolatilization that may or may not contribute significantly to metal removal. Wetland plants can be generally divided into four groups: Emergent macrophytes (e.g., *Carex rostrata*, *Phragmites australis*, *Scirpus lacustris* and *Typha latifolia*), floating leaved macrophytes (e.g., *Nymphaea odorata* and *Nuphar lutea*), submerged macrophytes (e.g., *Myriophyllum spicatum*, *Ceratophyllum demersum* and *Rhodophyceae*) and free-floating macrophytes (e.g., *Lemna minor*, *Spirodela polyrhiza* and *Eichhornia crassipes*) (Butt et al., 2021).

The uptake rate and uptake routes of the metal vary largely depending on the type of plants, growth rate and initial metal concentration in plant tissue, e.g., metal uptake in emergent and surface-floating plants takes place through roots, whereas roots, as well as leaves, are involved in the case of floating and submerged plants (Matagi et al., 1998). Plants may also contribute to metal trapping into the media via rhizodeposition and catalyze biochemical reactions (chelation) involving organic acids from root exudates such as citrate, oxalate, malate, malonate, fumarate, and acetate (Ryan et al., 2001). Metal immobilization in the rhizosphere and storage in the belowground biomass (roots) is usually higher than its translocation to the aboveground biomass (shoots), indicating the potential phytostabilization ability of the plants (Batool and Saleh, 2020). Apart from direct metal uptake in plant tissues, the indirect assistance is provided by means of ROL in the root zone, which results in iron plaque formation, where concentrations can reach 5–10 times the concentrations seen in the surrounding sediments (Sundby et al., 1998). However, there have been contradictory reports about whether plaque formation reduces or increases the metal-plant uptake. Lai et al. (2012) estimated ROL (ng cm^{-2} min^{-1}) from 35 wetland plants, among which thirteen species exceeded 100, while some species ranged between 50–100 and for few species below 50. In CWs, metal sulfide precipitation is an important removal mechanism and the ROL from plants can negatively affect the metal removal efficiency due to the presence of more oxidized conditions, evidenced by a higher redox potential, limited sulfate reduction and metal-sulfide precipitation (O'Sullivan et al., 2004; Stein et al., 2007). Leaf and stem litter also participate in metal accumulation and possibly, over time, it may become enriched with metals due to cation adsorption or amalgamation of fine particles with adsorbed metals (Weis and Weis, 2004). The decomposing plant litter also acts as a carbon source for microbial functions. The decomposition of biomass may release or sink metals.

Previous researchers presented conflicting results, expressing the insignificant to a considerably significant role of plants in metal elimination. Lee and Scholz (2007) reported the negative impact of *P. australis* in the removal of Ni and Cu, most likely by lowering of pH due to enhanced nitrification. Mays and Edwards (2001) reported negligible contribution of plants in metal uptake (1–3%), while Liu et al. (2007) presented high uptake of metals (19.90% Cd, 22.60% Pb and 23.80% Zn) in wetland plants (*Alternanthera philoxeroides*, *Zizania latifolia*, *Echinochloa crus-galli* and *Polygonum hydropiper*) from artificial wastewater.

Rahman et al. (2011) reported very high As retention (44–49%) in the roots of *Juncus effusus*, indicating remarkable efficiency of As retention capacity in planted CW (59–61%) than unplanted wetlands (44%).

Plants adapt different mechanisms to tolerate metal toxicity by (i) metal sequestration in cellular sections, which are insensitive or tolerant to metals, (ii) restricting metal translocation into shoots, (iii) metal translocation to old leaves, (iv) synthesis of biochemical biomarker chelators (phytochelatins, peptides) in plant tissues for metal chelation, (v) biomineralization of metals and (vi) prompting the function of antioxidant enzymes (like glutathione peroxidase and reductase) (Weis and Weis, 2004).

1.3.6 Factors governing treatment efficacy of mine wastewater

Various factors govern the performance of a wetland system, which includes design parameters, operational and environmental conditions. These factors are discussed below.

1.3.6.1 AMD characteristics

Mine water characteristics vary from site to site and may exhibit a range of pollutant concentrations, primarily a function of the mineralogy of the underlying rocks, geological strata and availability of oxygen and water. This implies that the proposal and implementation of any passive treatment system would depend on the strength and characteristics of a mine discharge originating from a particular region. Table 1.5 depicts wide variations in the characteristics of AMD produced globally. Aerobic wetlands promote the oxidation of ferrous iron and subsequent hydrolysis of the ferric iron; thus majorly employed for net alkaline mine waters (Johnson and Hallberg, 2005). These remediative reactions result in acidity generation [Equations (1.2) and (1.3)] and necessitate the sufficient availability of alkalinity in mine waters to prevent a significant fall in pH. The chemical oxidation of ferrous iron proceeds rapidly as most aerobic wetlands operate at near-neutral pH. Further, neutrophilic iron-oxidizing bacteria (e.g., *Gallionella ferruginea*) and iron-metabolizing bacteria (e.g., *Leptothrix* spp.) contribute to iron oxidation. Opitz et al. (2022) demonstrated passive aerobic treatment as the suitable and more sustainable alternative for long-term treatment of circumneutral, ferruginous seepage at an opencast lignite mine in southeast Germany. The surface-flow wetlands enhanced Fe removal and stimulated biogeochemical processes that contributed to removing secondary contaminants such as Mn and NH_4.

Anaerobic wetlands are typically used to treat high-strength net acidic and metal-rich mine waters (Johnson and Hallberg, 2005). Electron donors (as organic matrix/media) drive the reductive reactions within anaerobic wetlands. Sobolewski et al. (2022) designed a pilot-scale horizontal wetlands passive treatment train comprising a settling basin, surface flow wetland, horizontal-flow anaerobic wetland, aeration channel and rock drain for treating mine drainage from the St Louis Tunnel (located at the Rico-Argentine Site). The study revealed effective removal of total Zn, Cd and Mn, which attributed to sulfide precipitation in the anaerobic cell and filtration of suspended ZnS particles in the anaerobic wetland whereas Mn attenuated in the aerobic portion of the anaerobic cell as Mn oxides and carbonates.

Table 1.5 Global scenario of the AMD generation and its characteristics from different mines.

Active/abandoned mine (ore–type)	Location	AMD characteristics			References
		pH	Metal concentration (mg L^{-1})	Sulfate (mg L^{-1})	
Witwatersrand (Au)	Johannesburg, South Africa	2.3–6.9	Fe(0.05–1010), Al (0.03–629), Mn (0.01–169), Zn (0.01–108), Cr (1.70–17.30), Cd (0.01–10.10), Pb (0.10–3.15), Cu (0.03–11.40), Co (0.03–29.80) and Ni (0.13–71.10)	109–7571	Naicker et al. (2003), Tutu et al. (2008)
Mount Morgan mine (polymetallic)	Queensland, Australia	2.6–3.7	Fe (13–1487), Al (209–3074), Mn (51.10–355), Co (0.44–6.55), Cu (3.10–138), Ni (0.24–1.54) and Zn (7.11–81.40)	8390–56240	Edraki et al. (2005), Kaur et al. (2018)
Friendship Hill (coal)	Pennsylvania, USA	2.9	Fe (167), Al (56) and Mn (9.80)	2200	Hammarstrom et al. (2003)
Iron Mountain mine (polymetallic)	California, USA	0.8–3.1	Fe (30–12600), Al (36.40–772), Mn (1.60–10.20), As (0.04–4.90), Cd (0.03–9.10), Co (0.07–0.81), Cr (0.004–0.19), Cu (12–158) and Zn (3.90–1030)	511–49400	Campbell et al. (2020)
Rio Tinto mine (polymetallic)	SW Spain	1.4–7.6	Fe (1.10–4300), Mn (4.04–78.40), As (0–25), Co (2.58–26.70), Cd (0.08–4.29), Cu (0.01–623), Ni (0.28–1.98), Pb (0–2.40) and Zn (0.04–420)	37–16000	Hudson-Edwards et al. (1999), Valente et al. (2015)
Almagrera complex (polymetallic)	SW Spain	3.0–3.6	Fe (13.70–2231), Al (15.30–628), Mn (113–881), Cu (0.50–398) and Zn (38–2075)	1403–6625	Macías et al. (2017)
Ilgwang (Cu)	Busan, South Korea	2.5–6.5	Fe (0.05–148), Al (0.01–32), Mn (0.10–6.66), As (0.01–0.78), Cu (0.99–15.63) and Zn (0.07–13.30)	2–920	Han et al. (2017)
Gangreung (coal)	South Korea	2.4–4.2	Fe (0.50–1033), Al (0.30–338) and Mn (0–20.60)	279–5046	Kim and Chon (2001)
Dabaoshan Mine (polymetallic)	Guangdong, China	2.6–7.0	Fe (0.02–116), Al (0–62.60), Mn (0–29.30), Cu (0–7.67), Pb (0.02–0.70), Cd (0–0.25), Zn (0–34.60) and As (0–0.03)	2.89–2108	Zhao et al. (2012)
Xingren Coalfield (coal)	Guizhou, China	2.5–8.4	Fe (0.01–1472), Al (0.01–180), Mn (0–26.30) and As (0.002–0.06)	18–7599	Wu et al. (2009), Tao et al. (2012)

1.3.6.2 *Nature of media matrix and availability of carbon source*

The choice of media material is a critical parameter in CWs (in particular SSF CWs) because it provides a suitable growing medium for plants and plays a vital role in removing pollutants from wastewater through a sorption mechanism. Traditional wetland media are soil, sand and gravel. However, the quality of a media is defined by its hydraulic permeability, pH, EC and cation exchange capacity. The redox potential of media is also an important factor and determines the metal removal (such as Fe and Mn) by providing reducing conditions.

Various readily available organic and waste materials have been used for AMD treatment in CWs. The exploration of suitable media alternatives for passive AMD remediation forms a part of the circular economy by providing a long-lasting, inexpensive and easily obtainable organic carbon source, which can sustain the various anaerobic microorganisms responsible for reducing the sulfate concentrations. Oberholzer et al. (2022) showed chicken feathers as a potential substrate enhancer by boosting organic carbon availability to SRB and achieving pH elevation, sulfate and metal reductions in AMD water for reuse. Oil palm empty fruit bunches have shown its ability to increase the pH of AMD (∼ 4) to 6–9 as an excellent organic media in forest CW for managing mine waste water (Noor et al., 2020). Additionally, organic solids can be converted into biochar by pyrolysis as biochar provides an attractive biofilter (or CW media) for AMD treatment due to its alkaline nature and high adsorption capacity for dissolved metals (Chang et al., 2022). The supplementation of external carbon sources such as sucrose, plant broth and domestic wastewater has been shown to fuel sulfate reduction bioprocess in CWs (Chang et al., 2022; Chen et al., 2021; Wang et al., 2021). Table 1.6 provides a list of different wetland media employed for AMD treatment.

Table 1.6 Various wetland media applied for AMD treatment.

Type of CW	Influent characteristics (mg L^{-1}), except pH	Wetland media	Removal efficiency (%), except pH	Reference
VSSF (lab-scale)	pH (4.0), Cu (5), Cd (5.20), Zn (5.10), Cr (6.20), Fe (56) and SO_4^{2-} (920)	Walnut shell and its biochar[a]	pH (4.0–6.5), Cu (99), Cd (97), Zn (94), Cr (93), Fe (76) and SO_4^{2-} (40)	Chang et al. (2022)
VFCW (lab-scale)	pH (4.1), Zn (20), Cd (0.30), Cu (20), Pb (1.10) and Mn (0.60)	Clamshells	pH (6.9–7.2), Zn (85–93), Cd (84–98), Cu (97–99), Pb (98–99) and Mn (64–84)	Nguyen et al. (2022)
MS + VFCW + SFCW (lab-scale)	pH (2.5), Mn (25), Fe (250), Zn (50), Cd (10), Cu (10) and SO_4^{2-} (1500)	Straw and cow manure[b]	pH (8.1), Mn (89), Fe (99), Zn (99), Cd (99), Cu (99) and SO_4^{2-} (52)	Wang et al. (2021)
HSSF (bench-scale)	pH (8.1), B (23), As (0.10), Al (5), Fe (5), Pb (1.50) and SO_4^{2-} (420)	Rice husk	pH (8.2), B (36) and SO_4^{2-} (44)	San Miguel-Espinosa et al. (2019)
HSSF (small-scale)	pH (1.4–4), Fe (2000) and SO_4^{2-} (6000)	Basic oxygen furnace slag	pH (6.5–7.0), Fe (∼ 100) and SO_4^{2-} (75)	Sheridan et al. (2013)
VSSF (lab-scale)	pH (5.8), As (0.89), B (24), Cu (1.43), Fe (21), Mn (2.38), Zn (1.25) and SO_4^{2-} (75)	Cocopeat	pH (5.7), As (99), B (8.8), Cu (99), Fe (99), Mn (98), Zn (99) and SO_4^{2-} (12)	Lizama-Allende et al. (2011)

[a]Supplemented with sucrose and plant straw broth; MS: mixing and sedimentation pond; [b]co-treatment with domestic wastewater.

1.3.6.3 Loading rate

HLR is a critical factor in controlling the efficiency of the SSF CWs. The nominal hydraulic retention time (HRT) depends on the applied HLR. Higher HLR means the faster passage of wastewater through the media and thus lesser contact time, which in turn affects treatment efficiency. Longer HRTs (lower HLRs) have shown a positive effect on the treatment efficiency of CW by facilitating longer contact period with microorganisms, which results in the design of larger wetland areas. HF systems are generally more vulnerable to HLR increase than VF systems due to water logging conditions, which induce flow short-circuiting at higher loadings. A maximum hydraulic loading may be applied to wetlands, which is a function of the pressure differential and hydraulic conductivity of the wetlands. If the hydraulic loading of wetlands is greater than the maximum flow rate, the surface flow will occur (Song et al., 2001). Table 1.7 summarizes the the impact of different HRTs on wetland systems.

1.3.6.4 Seasonal variation

The effects of temperature and season significantly impact the treatment performance of CWs. It is usually documented that microbial growth rates and rates of treatment processes assayed in vitro decrease sharply with decreasing temperature (Kadlec and Wallace, 2008; Zhang et al., 2014); whereas other studies suggest that CW performance does not respond to temperature or change in season as expected. Seasonal characteristics vary regionally, and relevant climatic conditions should be considered to identify the specific treatment response. The wetland design must account for the seasonality of the local environment as an essential factor, particularly in areas where climate fluctuations are significant. The plant-mediated oxygen transfer is affected by cold temperatures during winter, which results in a greater net effect of seasonal variation on water treatment in temperate regions (Stein et al., 2007).

Table 1.7 Effect of different HRTs on the treatment efficacy of CWs.

Type of CW	Wastewater composition (mg L^{-1}), except pH	HRT (d)	Results/observations	Reference
VSF-VSF (pilot-scale)	pH (6.7–7.3), Cd (0.02–0.11) and Zn (0.63–2)	3.8, 2.4, 1.7 and 1.2	Shortening of HRT had no significant effect on Cd (69–91%) and Zn (73–92%) removal	Nguyen et al. (2021)
SSF CW (small-scale)	Single metal solution of Cd, Cr, Cu, Ni and Zn concentration (5–100)	2, 4, 6, 8, 10 and 12	Highest metal removal rate was recorded on day 12 while the lowest was observed on day 2	Thani et al. (2019)
Column CW (small-scale)	Pb (1), Cu (1–5), Ni (1–5), Zn (1–5) and SO_4^{2-} (850)	1.6–3.4	No significant difference was observed in metal removal, except Pb at various HRTs. Cu, Ni and Zn removal increased with increasing metal concentration and HLR	Sochacki et al. (2014)
VF CW (pilot-scale)	Pb (1.30–2.98) and Cu (0.98–1.93)	0.018–0.042[a]	No reduction in the removal of Pb (98–100) and Cu (83–97)	Scholz et al. (2002)

[a]Applied HLR in $m^3\ m^{-2}\ d^{-1}$.

However, less temperature variability occurs in tropical and subtropical areas, and all seasons remain similar in temperature. Xu and Mills (2018) observed a major shift in sulfur cycling from sulfate reduction during warm months to sulfide oxidation as the dominant reaction during cool months in a wetland treating storm runoff from the Tritium Processing Facility (Aiken, South Carolina).

The bioavailability of toxic metals in an anoxic environment is governed by the coupling and biogeochemical cycling of Fe, S and carbon. Karimian et al. (2018) explained that the stability of Fe^{2+} (more stable under reducing conditions) or Fe^{3+} (thermodynamically stable under oxidizing conditions) precipitate minerals is dependent on pH and periodic redox oscillations, particularly in regions prone to extreme variations in seasonal rainfall. Albalawneh et al. (2016) detected lower metal removal (13–54% Co, 9–48% Cd) in HSSF CW due to evaporative concentration and mineral dissolution in an arid climate. Similarly, Sheoran (2005) investigated the performance of a natural wetland for treating discharge from a copper mine tailing impoundment in Rajasthan, India, under arid conditions. Better treatment performance was found in the post-monsoon season with only a 10% reduction in sulfate levels due to dilution and was considered insignificant. On the contrary, another study by Aregu (2022) evaluated the effect of seasonal variation on the treatment performance of high-strength tannery wastewater in HSSF CW. Results showed no significant difference in chromium removal between the dry (97.65–99.24%) and rainy (97.38–99.49%) seasons.

1.4 Summary of the literature review and research challenges

The coal mine wastewater consists of high acidity, toxic heavy metals and elevated sulfate concentration. AMD minimization and prevention at the site remain the best choice for AMD management strategies. However, due to practical difficulties encountered in preventing the formation of AMD at the source, treatment techniques have been the major counteracting measures for AMD (Simate and Ndlovu, 2014). Several environmental, AMD composition, pH and economic factors dictate the choice of AMD treatment options. Active treatment requires continuous chemical inputs and is prone to the high cost of sludge disposal (Johnson and Hallberg, 2005), but usually more effective and requires a shorter process time. Passive treatment options are relatively cheaper and viewed as an economical alternative. The waste produced is denser, less voluminous, and more stable than the sludge produced during chemical treatment. In addition, passive treatment has lower overall environmental impacts and provides ecological restoration (Kefeni et al., 2017). The detailed life cycle assessment (LCA) analysis of various five passive and two active AMD treatment approaches confirmed that the active treatment option has greater LCA impacts than the passive treatment approaches (Hengen et al., 2014; Martínez et al., 2019).

The perpetual history of acidic mine discharge rich in sulfate and metals in the northeastern parts of India due to coal mining activities is terribly evident (Chabukdhara and Singh, 2016; Dutta et al., 2018; Equeenuddin et al., 2010). Yet, there has been no scrutiny for the possible mitigation and treatment strategies for such wastewater. Most of the previous

literature on the bioremediation of AMD in CWs were carried out for various mine wastewater (real or synthetic) originating from different coal mines or polymetallic mines, particularly from the USA, UK and other European countries. Severe environmental impacts of AMD generation from the NEC, Assam, India, are prevalent due to its specific geographical location (high stripping ratio), extremes of climatic variables (heavy rainfall) and presence of high sulfur coal with pyrite (Choudhury et al., 2021). Despite these facts, little emphasis has been given to the biological treatment approach for AMD produced in the NEC using CWs and research on its remedial measures is scarce.

CW is a complex system and combination of various components such as media, plants and microbes, which actively participate in pollutant removal. Vegetation forms one of the principal components of CWs and takes part in metal removal by phytostabilization, phytoaccumulation and phytovolatilization. Most of the literature reports presented a controversial aspect of wetland plants involved in the remediation of AMD, when the results of similar studies performed under different experimental conditions are explored. Some studies suggested a significant difference between planted and unplanted systems, while some results indicated insignificant and even negative impacts of plants in metal removal. Wetland media is the major metal retention sink; therefore, many researchers have raised concern regarding the leaching of metals from wetland bed after long-term use of CWs due to the increased metal bioavailability. However, no studies have reported the prospects of metals recovery from wetland media deposits.

Environmental factors (such as temperature, evapotranspiration and rainfall) play a significant role in the efficacy of the CWs. However, only a few studies have considered the role of climatic variations and seasonality on the treatment performance of AMD. Seasonal variation affects the stability of retained metal complexes, flow fluxes and water chemistry (pH and redox potential). Increased HLR due to heavy rainfall has been linked to the remobilization of Fe in CWs (Wiessner et al., 2006). Further, metal-removal processes are seasonally regulated by sulfate oxidation/reduction mechanisms. Rainfall is predominant in the northeast region of India. AMD chemistry and treatment function of CWs is strongly regulated by local climatic conditions, yet the prospects of AMD treatment from NEC, pertinent to Indian subtropics, are not addressed. The information about the performance of CWs for AMD remediation in a subtropical Indian climate, considering the influence of season is not available.

Sulfate reduction and metal sequestration in CWs is controlled by the presence and nature of organic carbon matrix, which initiates the biological coupling of oxidation/reduction reactions. Most studies explored the application of organic-based wastes (with or without modifications/pre-treatments) for the remediation of AMD in CWs. On the contrary, in many sulfidogenic bioreactors, where processes are regulated in a closed reactor and hence extremely sophisticated, the use of simple organic carbon sources and the importance of management of COD/SO_4^{2-} ratio for the effective AMD treatment is widely reported. However, the treatment prospects of AMD with a simple carbon for long-term operational optimization in CWs are scarce.

1.5 Objectives of the study and research methodology

The prime focus of this study was to propose a treatment strategy for highly acidic synthetic mine wastewater, simulated to represent AMD from the NEC, Assam, using HSSF-CWs with potential resource recovery, and to develop the biochemical mechanisms involved. The role of various environmental and operational parameters was studied. In addition, the aspect of metal recovery from wetland media and identification of microbial community structure were examined. The flow diagram of the research methodology is illustrated in Fig. 1.6.

The following sequence of studies were carried out to achieve the objectives.

- Seasonal characterization of AMD from various collieries of the North Eastern Coalfield in the northeastern state (Assam), India.
- Performance evaluation of HSSF-CWs consisting of different organic mixtures as wetland media and identification of microbial composition and diversity.
- Role of vegetation, effect of HLRs and influence of rainfall on AMD remediation using small-scale CWs with potential post-treatment metal recovery prospects.
- Long-term treatment performance of gravel-based HSSF-CW in response to different COD/SO_4^{2-} ratios for elucidating the biochemical mechanisms involved in sulfate reduction and metal removal.

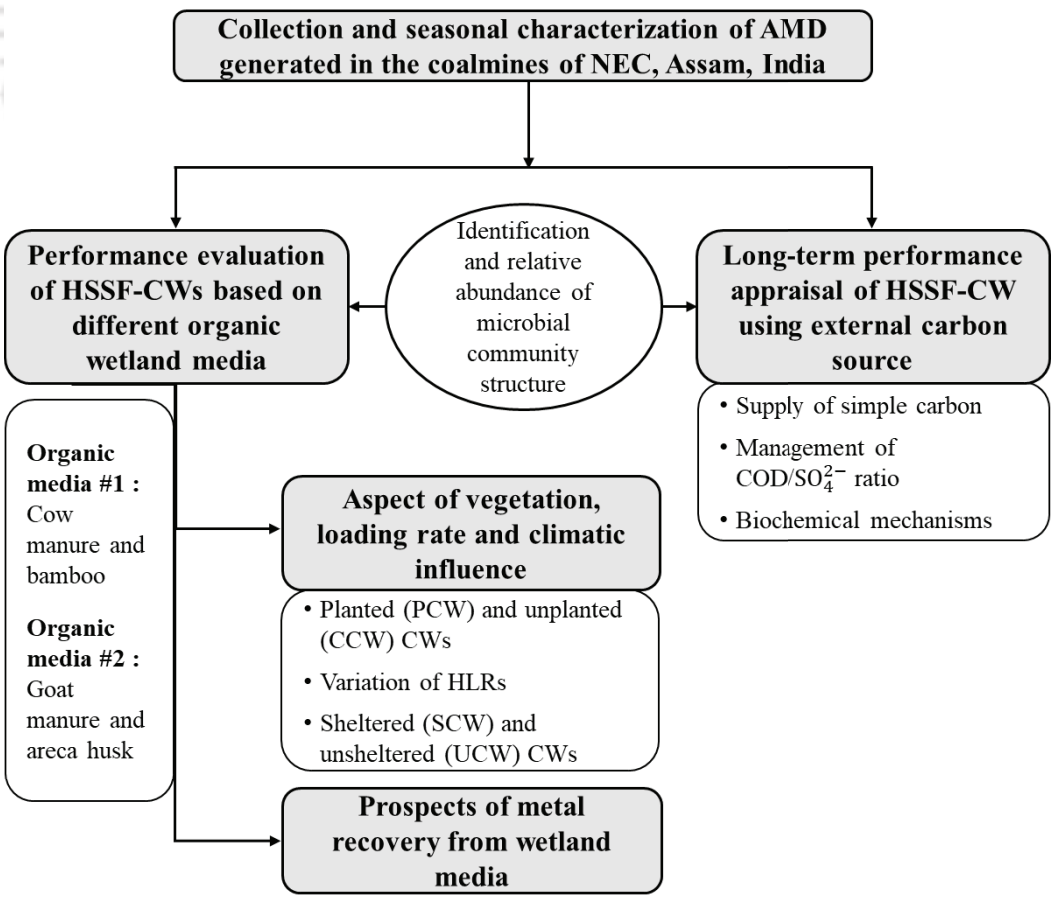

Fig. 1.6 Flow diagram of research methodology.

References

Abas, N., Kalair, A., and Khan, N. (2015). Review of fossil fuels and future energy technologies. *Futures*, 69:31–49.

Akcil, A. and Koldas, S. (2006). Acid mine drainage (AMD): Causes, treatment and case studies. *Journal of Cleaner Production*, 14(12-13):1139–1145.

Albalawneh, A., Chang, T. K., Chou, C. S., and Naoum, S. (2016). Efficiency of a horizontal sub-surface flow constructed wetland treatment system in an arid area. *Water*, 8(2):51.

Altun, M., Sahinkaya, E., Durukan, I., Bektas, S., and Komnitsas, K. (2014). Arsenic removal in a sulfidogenic fixed-bed column bioreactor. *Journal of Hazardous Materials*, 269:31–37.

Aregu, M. B. (2022). Industrial wastewater treatment efficiency of mixed substrate (pumice and scoria) in horizontal subsurface flow constructed wetland: Comparative experimental study design. *Air, Soil and Water Research*, 15.

Ayala, J. and Fernandez, B. (2019). Treatment of mining waste leachate by the adsorption process using spent coffee grounds. *Environmental Technology*, 40(15):2037–2051.

Aydin, M., Yuzer, B., Hasancebi, B., and Selcuk, H. (2019). Application of electrodialysis membrane process to recovery sulfuric acid and wastewater in the chalcopyrite mining industry. *Desalination and Water Treatment*, 172:206–211.

Baker-Austin, C. and Dopson, M. (2007). Life in acid: pH homeostasis in acidophiles. *Trends in Microbiology*, 15(4):165–171.

Batool, A. and Saleh, T. A. (2020). Removal of toxic metals from wastewater in constructed wetlands as a green technology; catalyst role of substrates and chelators. *Ecotoxicology and Environmental Safety*, 189:109924.

Bavandpour, F., Zou, Y. C., He, Y. H., Saeed, T., Sun, Y., and Sun, G. Z. (2018). Removal of dissolved metals in wetland columns filled with shell grits and plant biomass. *Chemical Engineering Journal*, 331:234–241.

Bekmezci, O. K., Ucar, D., Kaksonen, A. H., and Sahinkaya, E. (2011). Sulfidogenic biotreatment of synthetic acid mine drainage and sulfide oxidation in anaerobic baffled reactor. *Journal of Hazardous Materials*, 189(3):670–676.

Benner, S. G., Blowes, D. W., Gould, W. D., Herbert, R. B., and Ptacek, C. J. (1999). Geochemistry of a permeable reactive barrier for metals and acid mine drainage. *Environmental Science & Technology*, 33(16):2793–2799.

Black, C., Ziemkiewicz, P., and Skousen, J. (1999). Construction of a limestone leach bed and preliminary water quality results in Beaver Creek. In *Proceedings of 20th WV surface mine drainage task force symposium*, Morgantown , West Virginia.

Blesson, S., Pushparaj, A. N., and Soda, S. (2021). Removal of heavy metals from synthetic mine drainage in laboratory scale constructed wetlands. In *Trends in Civil Engineering and Challenges for Sustainability*, pages 507–523. Springer, Singapore.

Bálintová, M., Singovszká, E., Holub, M., and Demčák, Š. (2018). Influence of acid mine drainage on surface water quality. In *Water Resources in Slovakia: Part I*, The Handbook of Environmental Chemistry, pages 239–258. Springer, Cham, Switzerland.

Bolan, N., Kunhikrishnan, A., Thangarajan, R., Kumpiene, J., Park, J., Makino, T., Kirkham, M. B., and Scheckel, K. (2014). Remediation of heavy metal(loid)s contaminated soils – to mobilize or to immobilize? *Journal of Hazardous Materials*, 266:141–166.

Brewster, E. T., Freguia, S., Edraki, M., Berry, L., and Ledezma, P. (2020). Staged electrochemical treatment guided by modelling allows for targeted recovery of metals and rare earth elements from acid mine drainage. *Journal of Environmental Management*,

275:111266.

Bruins, M. R., Kapil, S., and Oehme, F. W. (2000). Microbial resistance to metals in the environment. *Ecotoxicology and Environmental Safety*, 45(3):198–207.

Butt, M. A., Zafar, M., Ahmed, M., Shaheen, S., and Sultana, S. (2021). Types of wetland and wetland plants. In *Wetland Plants*, pages 35–54. Springer, Cham.

Campbell, K. M., Alpers, C. N., and Nordstrom, D. K. (2020). Formation and prevention of pipe scale from acid mine drainage at iron mountain and Leviathan Mines, California, USA. *Applied Geochemistry*, 115:104521.

Caraballo, M. A., Macías, F., Rötting, T. S., Nieto, J. M., and Ayora, C. (2011). Long term remediation of highly polluted acid mine drainage: A sustainable approach to restore the environmental quality of the Odiel river basin. *Environmental Pollution*, 159(12):3613–3619.

Chabukdhara, M. and Singh, O. P. (2016). Coal mining in northeast India: An overview of environmental issues and treatment approaches. *International Journal of Coal Science & Technology*, 3(2):87–96.

Chang, J., Deng, S., Li, X., Li, Y., Chen, J., and Duan, C. (2022). Effective treatment of acid mine drainage by constructed wetland column: Coupling walnut shell and its biochar product as the substrates. *Journal of Water Process Engineering*, 49:103116.

Chen, J., Li, X., Jia, W., Shen, S., Deng, S., Ji, B., and Chang, J. (2021). Promotion of bioremediation performance in constructed wetland microcosms for acid mine drainage treatment by using organic substrates and supplementing domestic wastewater and plant litter broth. *Journal of Hazardous Materials*, 404:124125.

Chon, H.-T. and Hwang, J.-H. (2000). Geochemical characteristics of the acid mine drainage in the water system in the vicinity of the Dogye coal mine in Korea. *Environmental Geochemistry and Health*, 22(2):155–172.

Choudhary, R. P. and Sheoran, A. S. (2011). Comparative study of cellulose waste versus organic waste as substrate in a sulfate reducing bioreactor. *Bioresource Technology*, 102(6):4319–4324.

Choudhury, A., Lahkar, J., Saikia, B. K., Singh, A. K. A., Chikkaputtaiah, C., and Boruah, H. P. D. (2021). Strategies to address coal mine-created environmental issues and their feasibility study on northeastern coalfields of Assam, India: A review. *Environment, Development and Sustainability*, 23:9667–9709.

Clyde, E. J., Champagne, P., Jamieson, H. E., Gorman, C., and Sourial, J. (2016). The use of a passive treatment system for the mitigation of acid mine drainage at the Williams Brothers Mine (California): Pilot-scale study. *Journal of Cleaner Production*, 130:116–125.

CPCB (1993). *General Standards for Discharge of Environmental Pollutants Part-A: Effluents, Schedule - VI (Rule 3A)*. Central Pollution Control Board, New Delhi, India.

Cravotta III, C. A. and Trahan, M. K. (1996). Limestone drains to increase pH and remove dissolved metals from an acidic coal-mine discharge in Pennsylvania. In *13th annual meeting of the American Society for Surface Mining and Reclamation*, pages 836–840, Princeton, United States.

Crisponi, G., Fanni, D., Gerosa, C., Nemolato, S., Nurchi, V. M., Crespo-Alonso, M., Lachowicz, J. I., and Faa, G. (2013). The meaning of aluminium exposure on human health and aluminium-related diseases. *BioMolecular Concepts*, 4:77–87.

Dutta, M., Islam, N., Rabha, S., Narzary, B., Bordoloi, M., Saikia, D., Silva, L. F. O., and Saikia, B. K. (2019). Acid mine drainage in an Indian high-sulfur coal mining area: Cytotoxicity assay and remediation study. *Journal of Hazardous Materials*, 389:121851.

Dutta, M., Khare, P., Chakravarty, S., Saikia, D., and Saikia, B. K. (2018). Physico-chemical and elemental investigation of aqueous leaching of high sulfur coal and mine overburden from Ledo coalfield of Northeast India. *International Journal of Coal Science & Technology*, 5:265–281.

Dutta, M., Saikia, J., Taffarel, S. R., Waanders, F. B., de Medeiros, D., Cutruneo, C. M. N. L., Silva, L. F. O., and Saikia, B. K. (2017). Environmental assessment and nano-mineralogical characterization of coal, overburden and sediment from Indian coal mining acid drainage. *Geoscience Frontiers*, 8(6):1285–1297.

Edraki, M., Golding, S. D., Baublys, K. A., and Lawrence, M. G. (2005). Hydrochemistry, mineralogy and sulfur isotope geochemistry of acid mine drainage at the Mt. Morgan mine environment, Queensland, Australia. *Applied Geochemistry*, 20(4):789–805.

Engwa, G. A., Ferdinand, P. U., Nwalo, F. N., and Unachukwu, M. N. (2019). Mechanism and health effects of heavy metal toxicity in humans. In *Poisoning in the Modern World*. IntechOpen, London, UK.

EPA (2002). *Standards for Effluent Discharge Regulations. General Notice No. 44. of 2003*. Environmental Protection Agency. (accessed on 17.04.19).

Equeenuddin, S. M., Tripathy, S., Sahoo, P. K., and Panigrahi, M. K. (2010). Hydrogeochemical characteristics of acid mine drainage and water pollution at Makum Coalfield, India. *Journal of Geochemical Exploration*, 105(3):75–82.

Falayi, T. and Ntuli, F. (2015). Effect of attapulgite calcination on heavy metal adsorption from acid mine drainage. *Korean Journal of Chemical Engineering*, 32(4):707–716.

Gao, Y., Qiao, Y., Xu, Y., Zhu, L., and Feng, J. (2021). Assessment of the transfer of heavy metals in seawater, sediment, biota samples and determination the baseline tissue concentrations of metals in marine organisms. *Environmental Science and Pollution Research*, 28(22):1–13.

García-Valero, A., Martínez-Martínez, S., Faz, A., Rivera, J., and Acosta, J. A. (2020). Environmentally sustainable acid mine drainage remediation: Use of natural alkaline material. *Journal of Water Process Engineering*, 33:101064.

Gazea, B., Adam, K., and Kontopoulos, A. (1996). A review of passive systems for the treatment of acid mine drainage. *Minerals Engineering*, 9(1):23–42.

Geurts, J. J. M., Sarneel, J. M., Willers, B. J. C., Roelofs, J. G. M., Verhoeven, J. T. A., and Lamers, L. P. M. (2009). Interacting effects of sulphate pollution, sulphide toxicity and eutrophication on vegetation development in fens: A mesocosm experiment. *Environmental Pollution*, 157(7):2072–2081.

Gibert, O., Rötting, T., Cortina, J. L., de Pablo, J., Ayora, C., Carrera, J., and Bolzicco, J. (2011). In-situ remediation of acid mine drainage using a permeable reactive barrier in Aznalcóllar (Sw Spain). *Journal of Hazardous Materials*, 191(1-3):287–295.

Gitari, W. M., Petrik, L. F., and Akinyemi, S. A. (2018). Treatment of acid mine drainage with coal fly ash: Exploring the solution chemistry and product water quality. In *Coal Fly Ash Beneficiation-Treatment of Acid Mine Drainage with Coal Fly Ash*, pages 79–99. InTech, Rijeka, Croatia.

Green, S. J. (2011). Microorganisms and processes linked to uranium reduction and immobilization. In *Microbial Metal and Metalloid Metabolism: Advances and Applications*, pages 117–138. ASM Press, United Kingdom.

Hallberg, K. B. and Johnson, D. B. (2003). Novel acidophiles isolated from moderately acidic mine drainage waters. *Hydrometallurgy*, 71(1-2):139–148.

Hammarstrom, J. M., Sibrell, P. L., and Belkin, H. E. (2003). Characterization of limestone reacted with acid-mine drainage in a pulsed limestone bed treatment system at the

Friendship Hill National Historical Site, Pennsylvania, USA. *Applied Geochemistry*, 18(11):1705–1721.

Han, Y.-S., Youm, S.-J., Oh, C., Cho, Y.-C., and Ahn, J. S. (2017). Geochemical and eco-toxicological characteristics of stream water and its sediments affected by acid mine drainage. *Catena*, 148:52–59.

Hengen, T. J., Squillace, M. K., O'Sullivan, A. D., and Stone, J. J. (2014). Life cycle assessment analysis of active and passive acid mine drainage treatment technologies. *Resources, Conservation and Recycling*, 86:160–167.

Hudson-Edwards, K. A., Schell, C., and Macklin, M. G. (1999). Mineralogy and geochemistry of alluvium contaminated by metal mining in the Rio Tinto area, southwest Spain. *Applied Geochemistry*, 14(8):1015–1030.

Ismail, N., Abdullah, S. R. S., Idris, M., Kurniawan, S. B., Halmi, M. I. E., Sbani, N. H. A., Jehawi, O. H., and Hasan, H. A. (2020). Applying rhizobacteria consortium for the enhancement of *Scirpus grossus* growth and phytoaccumulation of Fe and Al in pilot constructed wetlands. *Journal of Environmental Management*, 267:110643.

Johnson, D. B. (1995). Acidophilic microbial communities: Candidates for bioremediation of acidic mine effluents. *International Biodeterioration & Biodegradation*, 35(1-3):41–58.

Johnson, D. B. and Hallberg, K. B. (2005). Acid mine drainage remediation options: A review. *Science of the Total Environment*, 338(1-2):3–14.

Kadlec, R. H. and Wallace, S. D. (2008). *Treatment Wetlands*. CRC press, Boca Raton, FL.

Kaksonen, A. H. and Puhakka, J. A. (2007). Sulfate reduction based bioprocesses for the treatment of acid mine drainage and the recovery of metals. *Engineering in Life Sciences*, 7(6):541–564.

Karimian, N., Johnston, S. G., and Burton, E. D. (2018). Iron and sulfur cycling in acid sulfate soil wetlands under dynamic redox conditions: A review. *Chemosphere*, 197:803–816.

Kaur, G., Couperthwaite, S. J., and Millar, G. J. (2018). Performance of bauxite refinery residues for treating acid mine drainage. *Journal of Water Process Engineering*, 26:28–37.

Kefeni, K. K., Msagati, T. A. M., and Mamba, B. B. (2017). Acid mine drainage: prevention, treatment options, and resource recovery: A review. *Journal of Cleaner Production*, 151:475–493.

Kiiskila, J. D., Sarkar, D., Feuerstein, K. A., and Datta, R. (2017). A preliminary study to design a floating treatment wetland for remediating acid mine drainage-impacted water using vetiver grass (*Chrysopogon zizanioides*). *Environmental Science and Pollution Research*, 24(36):27985–27993.

Kiiskila, J. D., Sarkar, D., Panja, S., Sahi, S. V., and Datta, R. (2019). Remediation of acid mine drainage-impacted water by vetiver grass (*Chrysopogon zizanioides*): A multiscale long-term study. *Ecological Engineering*, 129:97–108.

Kim, J.-Y. and Chon, H.-T. (2001). Pollution of a water course impacted by acid mine drainage in the Imgok creek of the Gangreung coal field, Korea. *Applied Geochemistry*, 16(11-12):1387–1396.

Kiran, M. G., Pakshirajan, K., and Das, G. (2017). An overview of sulfidogenic biological reactors for the simultaneous treatment of sulfate and heavy metal rich wastewater. *Chemical Engineering Science*, 158:606–620.

Kosolapov, D. B., Kuschk, P., Vainshtein, M. B., Vatsourina, A. V., Wiessner, A., Kästner, M., and Müller, R. A. (2004). Microbial processes of heavy metal removal from carbon-deficient effluents in constructed wetlands. *Engineering in Life Sciences*, 4(5):403–411.

Kröpfelová, L., Vymazal, J., Švehla, J., and Štíchová, J. (2009). Removal of trace

elements in three horizontal sub-surface flow constructed wetlands in the Czech Republic. *Environmental Pollution*, 157(4):1186–1194.

Kruse, N. A., Mackey, A. L., Bowman, J. R., Brewster, K., and Riefler, R. G. (2012). Alkalinity production as an indicator of failure in steel slag leach beds treating acid mine drainage. *Environmental Earth Sciences*, 67(5):1389–1395.

Kurniawan, T. A., Chan, G. Y. S., Lo, W.-H., and Babel, S. (2006). Physico-chemical treatment techniques for wastewater laden with heavy metals. *Chemical Engineering Journal*, 118(1-2):83–98.

Lai, W.-L., Zhang, Y., and Chen, Z.-H. (2012). Radial oxygen loss, photosynthesis, and nutrient removal of 35 wetland plants. *Ecological Engineering*, 39:24–30.

Lee, B.-H. and Scholz, M. (2007). What is the role of *Phragmites australis* in experimental constructed wetland filters treating urban runoff? *Ecological Engineering*, 29(1):87–95.

Lesage, E. (2006). *Behaviour of heavy metals in constructed treatment wetlands*. PhD Thesis, Faculty of Bioscience Engineering, Ghent University, Ghent, Belgium.

Leyssens, L., Vinck, B., Van Der Straeten, C., Wuyts, F., and Maes, L. (2017). Cobalt toxicity in humans–A review of the potential sources and systemic health effects. *Toxicology*, 387:43–56.

Li, W., Younger, P. L., Cheng, Y., Zhang, B., Zhou, H., Liu, Q., Dai, T., Kong, S., Jin, K., and Yang, Q. (2015). Addressing the CO_2 emissions of the world's largest coal producer and consumer: Lessons from the Haishiwan Coalfield, China. *Energy*, 80:400–413.

Lim, P. E., Wong, T. F., and Lim, D. V. (2001). Oxygen demand, nitrogen and copper removal by free-water-surface and subsurface-flow constructed wetlands under tropical conditions. *Environment International*, 26(5-6):425–431.

Liu, J., Dong, Y., Xu, H., Wang, D., and Xu, J. (2007). Accumulation of Cd, Pb and Zn by 19 wetland plant species in constructed wetland. *Journal of Hazardous Materials*, 147(3):947–53.

Liu, T. and Liu, S. (2020). The impacts of coal dust on miners' health: A review. *Environmental Research*, 190:109849.

Lizama-Allende, K., Ayala, J., Jaque, I., and Echeverría, P. (2021). The removal of arsenic and metals from highly acidic water in horizontal subsurface flow constructed wetlands with alternative supporting media. *Journal of Hazardous Materials*, 408:124832.

Lizama-Allende, K., Fletcher, T. D., and Sun, G. (2011). Enhancing the removal of arsenic, boron and heavy metals in subsurface flow constructed wetlands using different supporting media. *Water Science & Technology*, 63(11):2612–2618.

Machemer, S. D., Reynolds, J. S., Laudon, L. S., and Wildeman, T. R. (1993). Balance of S in a constructed wetland built to treat acid-mine drainage, Idaho-springs, Colorado, USA. *Applied Geochemistry*, 8(6):587–603.

Macías, F., Pérez-López, R., Caraballo, M. A., Cánovas, C. R., and Nieto, J. M. (2017). Management strategies and valorization for waste sludge from active treatment of extremely metal-polluted acid mine drainage: A contribution for sustainable mining. *Journal of Cleaner Production*, 141:1057–1066.

Martínez, N. M., Basallote, M. D., Meyer, A., Cánovas, C. R., Macías, F., and Schneider, P. (2019). Life cycle assessment of a passive remediation system for acid mine drainage: Towards more sustainable mining activity. *Journal of Cleaner Production*, 211:1100–1111.

Masindi, V., Gitari, M. W., Tutu, H., and DeBeer, M. (2015). Efficiency of ball milled South African bentonite clay for remediation of acid mine drainage. *Journal of Water Process Engineering*, 8:227–240.

Matagi, S. V., Swai, D., and Mugabe, R. (1998). A review of heavy metal removal mechanisms in wetlands. *African Journal for Tropical Hydrobiology and Fisheries*, 8:23–35.

Mays, P. A. and Edwards, G. S. (2001). Comparison of heavy metal accumulation in a natural wetland and constructed wetlands receiving acid mine drainage. *Ecological Engineering*, 16(4):487–500.

Mittal, S., Pathak, S., Dhawan, H., and Upadhyayula, S. (2021). A machine learning approach to improve ignition properties of high-ash Indian coals by solvent extraction and coal blending. *Chemical Engineering Journal*, 413:127385.

Moodley, I., Sheridan, C. M., Kappelmeyer, U., and Akcil, A. (2018). Environmentally sustainable acid mine drainage remediation: Research developments with a focus on waste/by-products. *Minerals Engineering*, 126:207–220.

Motsi, T., Rowson, N. A., and Simmons, M. J. H. (2009). Adsorption of heavy metals from acid mine drainage by natural zeolite. *International Journal of Mineral Processing*, 92(1-2):42–48.

Mylona, E., Xenidis, A., and Paspaliaris, I. (2000). Inhibition of acid generation from sulphidic wastes by the addition of small amounts of limestone. *Minerals Engineering*, 13(10-11):1161–1175.

Naicker, K., Cukrowska, E., and McCarthy, T. S. (2003). Acid mine drainage arising from gold mining activity in Johannesburg, South Africa and environs. *Environmental Pollution*, 122(1):29–40.

Naidu, G., Ryu, S., Thiruvenkatachari, R., Choi, Y., Jeong, S., and Vigneswaran, S. (2019). A critical review on remediation, reuse, and resource recovery from acid mine drainage. *Environmental Pollution*, 247:1110–1124.

Name, T. and Sheridan, C. (2014). Remediation of acid mine drainage using metallurgical slags. *Minerals Engineering*, 64:15–22.

Neculita, C., Zagury, G. J., and Bussière, B. (2007). Passive treatment of acid mine drainage in bioreactors using sulfate-reducing bacteria: Critical review and research needs. *Journal of Environmental Quality*, 36(1):1–16.

Neogi, B., Singh, A. K., Pathak, D. D., and Chaturvedi, A. (2017). Hydrogeochemistry of coal mine water of North Karanpura coalfields, India: Implication for solute acquisition processes, dissolved fluxes and water quality assessment. *Environmental Earth Sciences*, 76(14):1–17.

Núñez-Gómez, D., Rodrigues, C., Lapolli, F. R., and Lobo-Recio, M. A. (2019). Adsorption of heavy metals from coal acid mine drainage by shrimp shell waste: Isotherm and continuous-flow studies. *Journal of Environmental Chemical Engineering*, 7(1):102787.

Nguyen, H. T. H., Nguyen, B. Q., Duong, T. T., Bui, A. T. K., Nguyen, H. T. A., Cao, H. T., Mai, N. T., Nguyen, K. M., Pham, T. T., and Kim, K.-W. (2019). Pilot-scale removal of arsenic and heavy metals from mining wastewater using adsorption combined with constructed wetland. *Minerals*, 9(6):379.

Nguyen, T. T., Huang, H., Nguyen, T. A. H., and Soda, S. (2022). Recycling clamshell as substrate in lab-scale constructed wetlands for heavy metal removal from simulated acid mine drainage. *Process Safety and Environmental Protection*, 165:950–958.

Nguyen, T. T., Soda, S., Kanayama, A., and Hamai, T. (2021). Effects of cattails and hydraulic loading on heavy metal removal from closed mine drainage by pilot-scale constructed wetlands. *Water*, 13:1937.

Noor, I., Arifin, Y. F., Priatmadi, B. J., and Saidy, A. R. (2020). Oil palm empty fruit bunch as the selected organic matter in developing the swampy forest system for passive treatment

of acid mine drainage. *Ecology, Environment and Conservation*, 26(3):1424–1431.

Oberholzer, M. M., Oberholster, P. J., Ndlela, L. L., Botha, A.-M., and Truter, J. C. (2022). Assessing alternative supporting organic materials for the enhancement of water reuse in subsurface constructed wetlands receiving acid mine drainage. *Recycling*, 7(3):41.

Opitz, J., Bauer, M., Eckert, J., Peiffer, S., and Alte, M. (2022). Optimising operational reliability and performance in aerobic passive mine water treatment: The multistage westfield pilot plant. *Water, Air, & Soil Pollution*, 233(2):1–16.

O'Sullivan, A. D., Moran, B. M., and Otte, M. L. (2004). Accumulation and fate of contaminants (Zn, Pb, Fe and S) in substrates of wetlands constructed for treating mine wastewater. *Water, Air, and Soil Pollution*, 157(1-4):345–364.

Park, I., Tabelin, C. B., Jeon, S., Li, X., Seno, K., Ito, M., and Hiroyoshi, N. (2019). A review of recent strategies for acid mine drainage prevention and mine tailings recycling. *Chemosphere*, 219:588–606.

Payus, C., David, O., and Yan, M. (2014). Bone meal as alternative treatment for acidic and metal contaminated acid mine drainage water effluent: Lab scale. *American Journal of Environmental Sciences*, 10(1):61–73.

Pozo, G., Pongy, S., Keller, J., Ledezma, P., and Freguia, S. (2017). A novel bioelectrochemical system for chemical-free permanent treatment of acid mine drainage. *Water Research*, 126:411–420.

Puntarulo, S. (2005). Iron, oxidative stress and human health. *Molecular Aspects of Medicine*, 26:299–312.

Rahman, K. Z., Wiessner, A., Kuschk, P., van Afferden, M., Mattusch, J., and Müller, R. A. (2011). Fate and distribution of arsenic in laboratory-scale subsurface horizontal-flow constructed wetlands treating an artificial wastewater. *Ecological Engineering*, 37(8):1214–1224.

Rambabu, K., Banat, F., Pham, Q. M., Ho, S.-H., Ren, N.-Q., and Show, P. L. (2020). Biological remediation of acid mine drainage: Review of past trends and current outlook. *Environmental Science and Ecotechnology*, 2:100024.

Ray, S. and Dey, K. (2020). Coal mine water drainage: The current status and challenges. *Journal of the Institution of Engineers (India): Series D*, 101:165–172.

Rinzema, A., Lettinga, G., et al. (1988). Anaerobic treatment of sulfate-containing waste water. *Biotreatment Systems*, 3:65–109.

Ryan, P. R., Delhaize, E., and Jones, D. L. (2001). Function and mechanism of organic anion exudation from plant roots. *Annual Review of Plant Biology*, 52(1):527–560.

Sahinkaya, E., Isler, E., Yurtsever, A., and Coban, I. (2019). Sulfidogenic treatment of acid mine drainage using anaerobic membrane bioreactor. *Journal of Water Process Engineering*, 31:100816.

Sahoo, P. K., Tripathy, S., Equeenuddin, S. M., and Panigrahi, M. K. (2012). Geochemical characteristics of coal mine discharge vis-à-vis behavior of rare earth elements at Jaintia Hills coalfield, northeastern India. *Journal of Geochemical Exploration*, 112:235–243.

San Miguel-Espinosa, C., Ramila, C., Leiva, E., and Lizama-Allende, K. (2019). Boron and sulfate removal using rice husk as filtration material in horizontal flow constructed wetlands microcosms. *BioResources*, 14(1):363–375.

Satur, J., Hiroyoshi, N., Tsunekawa, M., Ito, M., and Okamoto, H. (2007). Carrier-microencapsulation for preventing pyrite oxidation. *International Journal of Mineral Processing*, 83(3-4):116–124.

Sawyer, C. N., McCarty, P. L., and Parkin, G. F. (2003). *Chemistry for Environmental Engineering and Science*. McGraw Hill, New Delhi, India.

Scholz, M., Höhn, P., and Minall, R. (2002). Mature experimental constructed wetlands treating urban water receiving high metal loads. *Biotechnology Progress*, 18(6):1257–1264.

Schueck, J. H., Helfrich, D. R., and Fromell, D. J. (2004). Limestone upflow pond with siphon discharge design considerations: A simple solution to high volume, high metals amd discharges. In *Proceedings of the 6th annual statewide conference on abandoned mine reclamation, Indiana PA, Western PA Coalition for Abandoned Mine Reclamation*, Bedford, PA, USA.

Sebogodi, K. R., Johakimu, J. K., and Sithole, B. B. (2020). Beneficiation of pulp mill waste green liquor dregs: Applications in treatment of acid mine drainage as new disposal solution in South Africa. *Journal of Cleaner Production*, 246:118979.

Sephton, M. G. and Webb, J. A. (2019). The role of secondary minerals in remediation of acid mine drainage by Portland cement. *Journal of Hazardous Materials*, 367:267–276.

Sheoran, A. S. (2005). Performance of a natural wetland treating acid mine drainage in arid conditions. *Mine Water and the Environment*, 24:150–154.

Sheoran, A. S. and Sheoran, V. (2006). Heavy metal removal mechanism of acid mine drainage in wetlands: A critical review. *Minerals Engineering*, 19(2):105–116.

Sheridan, C., Akcil, A., Kappelmeyer, U., and Moodley, I. (2018). A review on the use of constructed wetlands for the treatment of acid mine drainage. In *Constructed Wetlands for Industrial Wastewater Treatment*, pages 249–262. John Wiley & Sons, Hoboken, NJ.

Sheridan, C., Harding, K., Koller, E., and De Pretto, A. (2013). A comparison of charcoal- and slag-based constructed wetlands for acid mine drainage remediation. *Water SA*, 39(3):369–373.

Simate, G. S. and Ndlovu, S. (2014). Acid mine drainage: Challenges and opportunities. *Journal of Environmental Chemical Engineering*, 2(3):1785–1803.

Simmons, J., Ziemkiewicz, P., and Black, D. C. (2002). Use of steel slag leach beds for the treatment of acid mine drainage. *Mine Water and the Environment*, 21(2):91–99.

Singh, A. K., Mahato, M. K., Neogi, B., and Singh, K. K. (2010). Quality assessment of mine water in the Raniganj coalfield area, India. *Mine Water and the Environment*, 29(4):248–262.

Singh, A. K., Varma, N. P., and Mondal, G. C. (2016). Hydrogeochemical investigation and quality assessment of mine water resources in the Korba coalfield, India. *Arabian Journal of Geosciences*, 9(4):278.

Singh, G. (1987). Mine water quality deterioration due to acid mine drainage. *International Journal of Mine Water*, 6(1):49–61.

Skousen, J., Zipper, C. E., Rose, A., Ziemkiewicz, P. F., Nairn, R., McDonald, L. M., and Kleinmann, R. L. (2017). Review of passive systems for acid mine drainage treatment. *Mine Water and the Environment*, 36(1):133–153.

Skousen, J. G., Ziemkiewicz, P. F., and McDonald, L. M. (2019). Acid mine drainage formation, control and treatment: Approaches and strategies. *The Extractive Industries and Society*, 6(1):241–249.

Sánchez-Andrea, I., Sanz, J. L., Bijmans, M. F. M., and Stams, A. J. M. (2014). Sulfate reduction at low pH to remediate acid mine drainage. *Journal of Hazardous Materials*, 269:98–109.

Sobolewski, A. B., Riese, A. C., Moore, T. J., and Brown, A. R. (2022). Passive treatment of circumneutral mine drainage from the St. Louis Mine Tunnel, Rico CO: Part 3–Horizontal wetlands treatment train pilot study. *Mine Water and the Environment*, pages 1–20.

Sochacki, A., Surmacz-Gorska, J., Faure, O., and Guy, B. (2014). Polishing of synthetic electroplating wastewater in microcosm upflow constructed wetlands: Effect of operating

conditions. *Chemical Engineering Journal*, 237:250–258.

Song, H., Yim, G.-J., Ji, S.-W., Neculita, C. M., and Hwang, T. (2012). Pilot-scale passive bioreactors for the treatment of acid mine drainage: Efficiency of mushroom compost vs. mixed substrates for metal removal. *Journal of Environmental Management*, 111:150–158.

Song, Y., Fitch, M., Burken, J., Nass, L., Chilukiri, S., Gale, N., and Ross, C. (2001). Lead and zinc removal by laboratory-scale constructed wetlands. *Water Environment Research*, 73:37–44.

Stein, O. R., Borden-Stewart, D. J., Hook, P. B., and Jones, W. L. (2007). Seasonal influence on sulfate reduction and zinc sequestration in subsurface treatment wetlands. *Water Research*, 41(15):3440–3448.

Stumm, W. and Morgan, J. J. (1981). *Aquatic chemistry: an introduction emphasizing chemical equilibria in natural waters*. Wiley, New York.

Sud, D., Mahajan, G., and Kaur, M. P. (2008). Agricultural waste material as potential adsorbent for sequestering heavy metal ions from aqueous solutions–A review. *Bioresource Technology*, 99(14):6017–6027.

Sundby, B., Vale, C., Caçador, Z., Catarino, F., Madureira, M.-J., and Caetano, M. (1998). Metal-rich concretions on the roots of salt marsh plants: Mechanism and rate of formation. *Limnology and Oceanography*, 43(2):245–252.

Tao, X., Wu, P., Tang, C., Liu, H., and Sun, J. (2012). Effect of acid mine drainage on a karst basin: A case study on the high-As coal mining area in Guizhou province, China. *Environmental Earth Sciences*, 65(3):631–638.

Taylor, J., Pape, S., and Murphy, N. (2005). A summary of passive and active treatment technologies for acid and metalliferous drainage (AMD). In *5th Australian Workshop on Acid Mine Drainage*, Fremantle, Australia.

Tchobanoglous, G., Burton, F. L., Stensel, H. D., Metcalf, and Eddy (2003). *Wastewater Engineering: Treatment and Reuse*. McGraw Hill Education, India.

Thani, N. S. M., Ghazi, R. M., Amin, M. F. M., and Hamzah, Z. (2019). Phytoremediaton of heavy metals from wastewater by constructed wetland microcosm planted with *Alocasia puber*. *Jurnal Teknologi*, 81(5).

Tiwary, R. K. (2001). Environmental impact of coal mining on water regime and its management. *Water, Air, and Soil Pollution*, 132:185–199.

Tiwary, R. K. and Dhar, B. B. (1994). Environmental pollution from coal mining activities in Damodar river basin, India. *Mine Water and the Environment*, 13(1):1–10.

Tutu, H., McCarthy, T. S., and Cukrowska, E. (2008). The chemical characteristics of acid mine drainage with particular reference to sources, distribution and remediation: The Witwatersrand Basin, South Africa as a case study. *Applied Geochemistry*, 23(12):3666–3684.

Valente, T., Grande, J. A., De la Torre, M. L., Gomes, P., Santisteban, M., Borrego, J., and Braga, M. A. S. (2015). Mineralogy and geochemistry of a clogged mining reservoir affected by historical acid mine drainage in an abandoned mining area. *Journal of Geochemical Exploration*, 157:66–76.

Vardhan, K. H., Kumar, P. S., and Panda, R. C. (2019). A review on heavy metal pollution, toxicity and remedial measures: Current trends and future perspectives. *Journal of Molecular Liquids*, 290:111197.

Wang, H., Zhang, M., Xue, J., Lv, Q., Yang, J., and Han, X. (2021). Performance and microbial response in a multi-stage constructed wetland microcosm co-treating acid mine drainage and domestic wastewater. *Journal of Environmental Chemical Engineering*, 9(6):106786.

Watzlaf, G. R., Schroeder, K. T., and Kairies, C. L. (2000). Long-term performance of anoxic limestone drains. *Mine Water and the Environment*, 19:98–110.

Weber, K. P., Werker, A., Gehder, M., Senger, T., and Legge, R. L. (2010). Influence of the microbial community in the treatment of acidic iron-rich water in aerobic wetland mesocosms. *Bioremediation Journal*, 14(1):28–37.

Weis, J. S. and Weis, P. (2004). Metal uptake, transport and release by wetland plants: Implications for phytoremediation and restoration. *Environment International*, 30(5):685–700.

Wiessner, A., Kuschk, P., Buddhawong, S., Stottmeister, U., Mattusch, J., and Kastner, M. (2006). Effectiveness of various small-scale constructed wetland designs for the removal of iron and zinc from acid mine drainage under field conditions. *Engineering in Life Sciences*, 6(6):584–592.

Wu, P., Tang, C., Liu, C., Zhu, L., Pei, T. Q., and Feng, L. (2009). Geochemical distribution and removal of As, Fe, Mn and Al in a surface water system affected by acid mine drainage at a coalfield in Southwestern China. *Environmental Geology*, 57(7):1457–1467.

Wu, S. B., Kuschk, P., Wiessner, A., Müller, J., Saad, R. A. B., and Dong, R. J. (2013). Sulphur transformations in constructed wetlands for wastewater treatment: A review. *Ecological Engineering*, 52:278–289.

Xu, X. and Mills, G. L. (2018). Do constructed wetlands remove metals or increase metal bioavailability? *Journal of Environmental Management*, 218:245–255.

Yang, B., Lan, C. Y., Yang, C. S., Liao, W. B., Chang, H., and Shu, W. S. (2006). Long-term efficiency and stability of wetlands for treating wastewater of a lead/zinc mine and the concurrent ecosystem development. *Environmental Pollution*, 143(3):499–512.

Yim, G., Ji, S., Cheong, Y., Neculita, C. M., and Song, H. (2015). The influences of the amount of organic substrate on the performance of pilot-scale passive bioreactors for acid mine drainage treatment. *Environmental Earth Sciences*, 73(8):4717–4727.

Younger, P. L. (1998). Design, construction and initial operation of full-scale compost-based passive systems for treatment of coal mine drainage and spoil leachate in the UK. In *Proceedings of the International Mine Water Association Symposium*, pages 413–424, Johannesburg, South Africa.

Zhang, D. Q., Jinadasa, K. B. S. N., Gersberg, R. M., Liu, Y., Ng, W. J., and Tan, S. K. (2014). Application of constructed wetlands for wastewater treatment in developing countries – A review of recent developments (2000–2013). *Journal of Environmental Management*, 141:116–131.

Zhang, M. (2011). Adsorption study of Pb (II), Cu (II) and Zn (II) from simulated acid mine drainage using dairy manure compost. *Chemical Engineering Journal*, 172(1):361–368.

Zhang, Z., Bi, X., Li, X., Zhao, Q., and Chen, H. (2018). Schwertmannite: Occurrence, properties, synthesis and application in environmental remediation. *RSC Advances*, 8(59):33583–33599.

Zhao, H., Xia, B., Qin, J., and Zhang, J. (2012). Hydrogeochemical and mineralogical characteristics related to heavy metal attenuation in a stream polluted by acid mine drainage: A case study in Dabaoshan Mine, China. *Journal of Environmental Sciences*, 24(6):979–989.

Zheng, C. Q., Allen, C. C., and Bautista, R. G. (1986). Kinetic study of the oxidation of pyrite in aqueous ferric sulfate. *Industrial & Engineering Chemistry Process Design and Development*, 25(1):308–317.

Zhou, Q., Yang, N., Li, Y., Ren, B., Ding, X., Bian, H., and Yao, X. (2020). Total concentrations

and sources of heavy metal pollution in global river and lake water bodies from 1972 to 2017. *Global Ecology and Conservation*, 22:e00925.

Ziemkiewicz, P. F., Skousen, J. G., Brant, D. L., Sterner, P. L., and Lovett, R. J. (1997). Acid mine drainage treatment with armored limestone in open limestone channels. *Journal of Environmental Quality*, 26(4):1017–1024.

2

Hydrochemistry of Acid Mine Drainage at the North Eastern Coalfield, Assam, India

This chapter deals with the seasonal variations of the physicochemical characteristics and metal concentrations of AMD from the collieries of North Eastern Coalfield (known as Makum Coalfield, a subsidiary of Coal India Ltd.), Assam, India.

2.1 Introduction

Indian coal reserves account for 319,020 million tons (MT), out of which 1702 MT is deposited in Northeast India and Assam alone contributes 525 MT (Choudhury et al., 2021). Considerable coal deposit is restricted to the eastern part of the state, but several small coal reserves occur in the Karbi Anglong and North Cachar districts of Assam. The majority of Assam coal is of Tertiary origin, confined mainly to the Makum, Dilli-Jaypore and Mikir Hills of Assam (Chattaraj et al., 2016). In 2013–2014, about 91% of the coal production was recovered from open cast mines, exhibiting high coal recovery from open cast mines than underground mines (Choudhury et al., 2021). However, open cast mining has a relatively larger environmental footprint than underground mining.

The environmental impacts of coal mining in the North Eastern Coalfield (NEC) of Assam are very severe due to its specific geographical location, extremes of climatic variables (especially heavy rainfall of about 1606 mm during monsoon) (Jhajharia et al., 2012) and distinct coal characteristics. AMD production is significant due to high sulfur coal with framboidal pyrite and heavy rain (Chabukdhara and Singh, 2016). Due to the folded mountainous landscape of the NEC, the stripping ratio and subsequent generation of overburden materials are also very high (Barooah and Baruah, 1996). Bhagabati and Borkotoki (2014) reported severe deterioration of water and sediment quality of Patkai Lake situated near Tikak opencast mine, Margherita. The study reported high heavy metal content (Pb, Fe and As) and low dissolved oxygen in Patkai Lake, causing low phytoplankton and zooplankton community and fish diversity. Similarly, Equeenuddin et al. (2010) observed

the impacts of AMD on the water quality of surface and groundwater of Makum Coalfield, Assam, and revealed a higher concentration of Pb, Mn and Fe in the groundwater beyond the maximum permissible limit. Besides, high metal contamination and mobilization of metals (Fe, Cd, Cr, Cu, Mn, Ni, Pb and Zn) in stream sediment due to AMD are also reported (Equeenuddin et al., 2013). Dutta et al. (2020) discussed the seasonal influence on the AMD from Ledo colliery; however, further investigation on the seasonal variation of the coal mine discharge from the other collieries of NEC is unknown. Recent literature on the seasonal characteristics of coal mine drainage from different NEC collieries (underground and opencast) is limited.

The prime objective of the current chapter was to characterize the mine wastewater generated in the coal mines of NEC, Assam in different seasons to understand the hydrochemistry of the AMD formation. In addition, the heavy input of metals from the AMD formation and overburden spoil leachate severely affect the sediments in the vicinity of the collieries. Therefore, the assessment of metal mobilization and contamination of the surrounding soil around Makum Coalfield was quantified.

2.2 Study area – geological setting

The Makum Coalfield is situated in the Tinsukia district and extends over an area 30 km long and 5 km wide, bounded by latitude 27°15'N to 27°25'N and longitude 95°40'E to 96°55'E. It has three open cast mines at Tikak, Ledo and Tirap; and underground mines (UMs) at Tipong (Dip mine–UM1, Agragati Khani–UM2 and Pragati Khani–UM3). Very recently, Ledo colliery has been declared abandoned (Table 2.1). All of these coal-bearing beds are disposed along the "belt of Schuppen", which are associated with the Baragolai Tikak Parbat formation of the Barail Group (Oligocene), comprising alternations of sandstone, siltstone, mudstone, carbonaceous shales and coal seams (Misra, 1992). Mostly quartz, kaolinite, illite, feldspar and chlorite make up the major mineral assemblages of the coal seams besides calcite, pyrite, marcasite, gypsum and melanterite (Mukherjee and Srivastava, 2006). The coals are of sub-bituminous rank, high in sulfur (2–11%) with low ash content (3–15%), high content of volatile matter (28–44%) and vitrinite (83–87%), calorific value with strong caking index, while moisture rarely exceeds 5% (Chabukdhara and Singh, 2016; Mukherjee and Srivastava, 2006; Rajarathnam et al., 1996). The coal-bearing strata of Makum Coalfield are bounded by Margherita thrust in the north and Haflong–Disang thrust in the south. Parallel to these major thrusts, several minor thrusts are within this coal belt (Singh, 1987). Fig. 2.1 shows the location of the sampling stations.

2.3 Materials and methods

All the instruments used in the entire research work are given in Appendix–I.

2.3.1 Collection of coal mine drainage

The coal mine discharge was collected directly from the coal mine pit of the open cast mines and storage sump inside underground mines. Soil samples were collected from the nearby coal mines (Fig. 2.1). Periodical sampling was carried out once in each season, i.e., pre-monsoon

(February to May), monsoon (June to September) and post-monsoon (October to January) from 2018 to 2019. Prior to each sampling, the polyethylene bottles were cleaned and rinsed twice with milli-Q water (Merck Millipore, Germany). To measure cations, 250 mL samples were acidified with nitiric acid (HNO_3) to bring the pH < 2.0 and preserved separately. The non-acidified samples were stored for the analysis of anions and non-ionic parameters. The soil samples were collected in clear zip-lock plastic bags and later analyzed for the total metal concentration. The photographic images of coal mines and field sampling are provided in Fig. 2.2.

Table 2.1 Details of the NEC collieries selected for the collection of AMD.

Name of the colliery	Location		Type	Geological reserve (in MT)	Mineable reserve (in MT)
	Latitude	Longitude			
Tirap	27°17'41.9"N	95°46'38.7"E	Open cast	29.20	15.70
Ledo	27°20'59.3"N	95°46'53.4"E	Open cast	6.22	1.68
Tikak	27°17'22.2"N	95°43'51.2"E	Open cast	121	23.70
Tipong	27°18'14"N	95°53'53"E	Underground	69.50	–

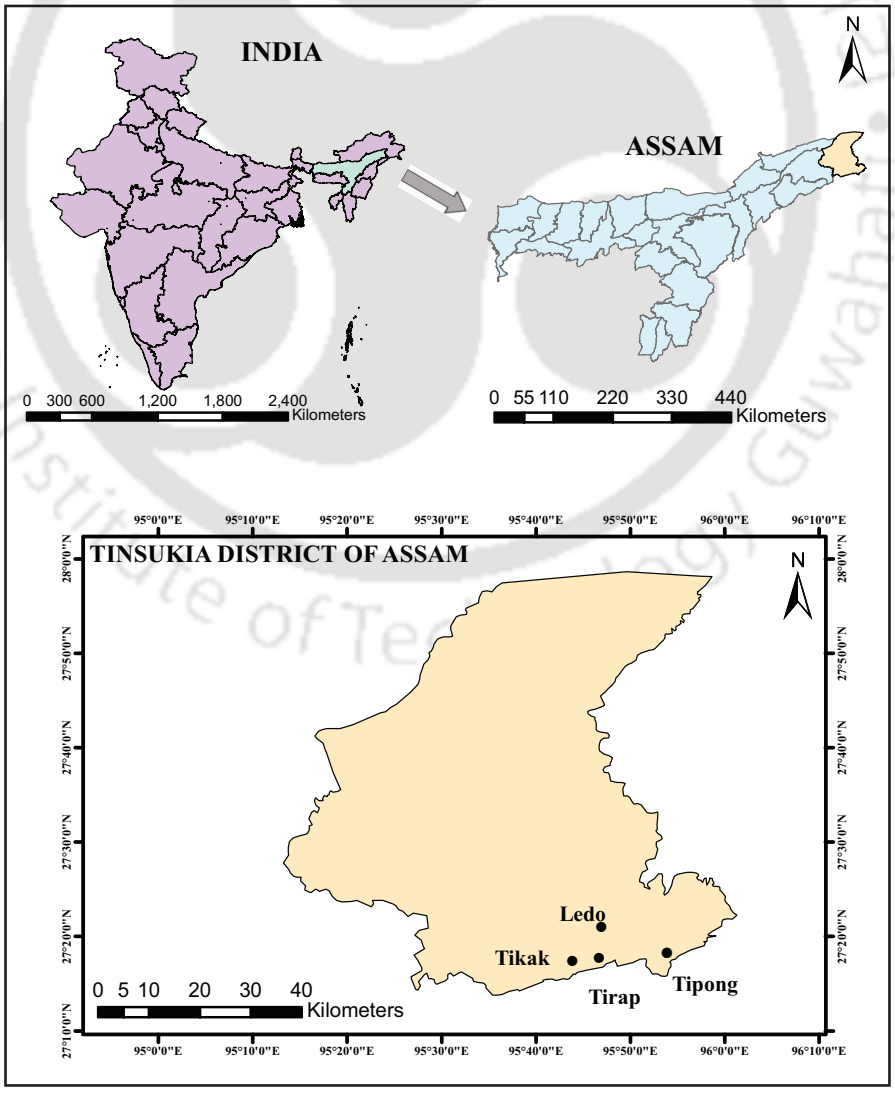

Fig. 2.1 Geographical map of the coal mines from the Makum Coalfield.

Fig. 2.2 Photographic image of mine wastewater collection from (a) Tirap, (b) Ledo, (c) Tikak, (d) Dip mine–UM1, (e) Agragati Khani–UM2 and (f) Pragati Khani–UM3 collieries of the NEC, Assam.

2.3.2 Chemicals and reagents

All the chemicals and reagents used in this study were analytical grade (AR) or laboratory grade (LR). Ferrous ammonium sulfate, potassium dichromate, mercuric sulfate, silver sulfate, sulfuric acid, ferroin indicator, sodium nitroprusside, tri-sodium citrate, ethanol, sodium hypochlorite, sodium nitrite, phosphoric acid, sulfanilamide, *N*-(1-naphthyl)-ethylenediamine dihydrochloride, ammonium hydroxide, nitric acid, manganous sulfate, sodium azide, sodium iodide, sodium thiosulfate, potassium fluoride, potassium permanganate, potassium oxalate, anhydrous sodium sulfate, sodium carbonate, potassium chloride, sodium hydroxide, glacial acetic acid, sodium acetate, potassium nitrate, magnesium chloride, hydrogen peroxide and barium chloride were purchased either from Merck, India, Himedia, India or SRL, India. All the reagents and stock/standard solutions were prepared with milli-Q water.

2.3.3 Analytical methods

Standard sampling techniques, as detailed in Standard Methods (APHA, 2012), have been followed to collect and store samples. All samples were collected in triplicates and measurements of pH, electrical conductivity (EC) and temperature were recorded in-situ using a multi-parameter kit (HI98194, Hanna Instruments, Romania).

Concentrations of metals were determined using Flame Atomic Absorption Spectrometer (FAAS) (Thermo Scientific^{TM} iCE^{TM} 3000 Series, USA) after filtering the samples with a 0.45 μm filter. The detection limits for various elements are indicated in Appendix–I. The concentration of cations such as sodium (Na^+), potassium (K^+) and calcium (Ca^{2+}) was measured using Flame Photometer (Systronics 128, India). DO concentration was measured using modified Winkler's method (APHA, 2012). Total hardness (TH) was directly computed from the separate determinations of calcium and magnesium (APHA, 2012). Total solids and its fractions (total suspended solids–TSS, total dissolved solids–TDS) were obtained after drying the samples at 103–105°C in a hot air oven (ICT, India), whereas further ignition at 550°C in a muffle furnace (Multispan, India) provided respective fixed and volatile solids (APHA, 2012). Chemical oxygen demand (COD) was analyzed by the closed reflux titrimetric method, using ferrous ammonium sulfate as a titrant (APHA, 2012). Ammonia-nitrogen (NH_4^+–N) was measured at a wavelength of 640 nm by phenate method using sodium nitroprusside, phenol and sodium hypochlorite (APHA, 2012). Nitrite-nitrogen (NO_2^-–N) was measured by colorimetric method using phosphoric acid, sulphanilamide and *N*-(1-naphthyl)-ethylenediamine dihydrochloride at a wavelength of 543 nm (APHA, 2012). Nitrate-nitrogen (NO_3^-–N) was analyzed by ion chromatography (792 Basic IC, Metrohm, Switzerland) using an anion column (Metrosep ASupp 5–250/4.0) and carbonate eluent (3.2 mM of sodium carbonate, 1 mM of sodium bicarbonate and 50 mM sulfuric acid). Sulfate (SO_4^{2-}) concentration was measured using the turbidimetric procedure, where light absorbance of the barium sulfate suspension was measured by a photometer (Systronics, India). The standard curves prepared for NH_4^+–N, NO_2^-–N and SO_4^{2-} are given in Appendix–II.

The estimation of total metal concentration in soil samples was determined by acid

digestion. Samples were air-dried and well homogenized (passing through a 2 mm sieve). 1 g (dry weight) of soil was digested with repeated addition of concentrated HNO_3 and hydrogen peroxide (30%, H_2O_2) as per method 3050 B in USEPA (1996). Concentrated hydrochloric acid (HCl) was then added to the initial digestate and the sample was refluxed at 95 ± 5°C without boiling for the next 15 min. After cooling, the sample was diluted to 100 mL and filtered through Whatman No. 41 filter paper. The samples were stored at 4°C until further analysis for the concentration of metals in FAAS.

For elemental composition and distribution, field emission scanning electron microscopy (FESEM) coupled with energy dispersive X-ray spectrometer (EDX) (Zeiss Sigma, Germany) was employed on samples double-coated with gold using a sputter coater (Quorum, SC7620, Quorum Technologies, UK and Edwards, RV3, Czech Republic).

2.3.4 Statistical analysis

The relationships among different physicochemical variables such as pH, EC, TH, TDS, sulfate and total metal concentration (Fe, Al, Mn, Zn, Co, Ni and Cr) and geochemical processes were applied by using the statistical tool (Pearson's correlation) in Microsoft Excel (2016).

2.4 Results and discussions

2.4.1 Seasonal characteristics of coal mine discharge

2.4.1.1 Coal mine discharge in pre-monsoon

The water quality of the coal mine water during the pre-monsoon season is presented in Table 2.2 and Table 2.3. The overall pH of mine discharge from different collieries ranged from 3.0 to 6.5. Coalmine discharge from Tirap and Tikak colliery was extremely acidic (pH < 4.0), whereas the pH of the water from other mines was greater than 5.0. CPCB (1993) recommends pH in the range 5.5–9.0 for safe disposal on inland surface water. EC varied from 88 to 439 mS m^{-1} and all mine discharges were highly polluted with a higher concentration of sulfate, as high as 3212 mg L^{-1}. Thus, sulfate was the major dominating anion in all mine discharges and exceeded recommended discharge criteria of 750 mg L^{-1} as per EPA (2002). A higher amount of sulfate content is a common characteristic of any coal mine water because of the oxidative leaching of sulfide-bearing minerals usually present in coals, mostly pyrite. The mine water was devoid of any organics and therefore, COD was very low, about 5.58 to 22.33 mg L^{-1}. Higher TH values were obtained in all mine water samples, ranging from 391 to 2577 mg L^{-1} as $CaCO_3$, due to a higher concentration of contributing cations Ca^{2+} and Mg^{2+}. The DO level was moderately low in all mine discharges except for Tipong collieries (2–2.80 mg L^{-1}), majorly due to oxygen consumption during the oxidation process of various sulfide minerals. EPA (2002) suggests DO of treated effluent > 5 mg L^{-1}. TDS represents the sum total concentration of all dissolved ions (884 to 5052 mg L^{-1}) and EPA (2002) recommends TDS value < 500 mg L^{-1}. Major dominating cations in mine water were Ca^{2+} (26.20–121 mg L^{-1}) and Mg^{2+} (40.70–554 mg L^{-1}). Relatively lower concentrations of other cations such as Na^+ and K^+ ranging from 3.50 to 197 mg L^{-1} and 3 to 15.60 mg L^{-1} were present.

Table 2.2 Physicochemical characteristics of coal mine drainage from NEC in the pre-monsoon season.

Coal mine	pH	EC (mS m^{-1})	Turbidity (NTU)	TH (mg L^{-1} as $CaCO_3$)	TDS (mg L^{-1})	COD (mg L^{-1})	DO (mg L^{-1})	SO_4^{2-} (mg L^{-1})
Tirap	3.0	434 ± 5.69	18.43 ± 4.25	2552 ± 25	5019 ± 29	8.37 ± 3.95	5.35 ± 0.07	3170 ± 61
Ledo	6.4 ± 0.1	143 ± 3.51	6.27 ± 1.46	755 ± 7.95	1517 ± 96	8.37 ± 3.95	6.25 ± 0.21	756 ± 13
Tikak	3.5 ± 0.2	161 ± 3.61	5.40 ± 0.50	455 ± 16	1380 ± 35	19.53 ± 3.95	5.20 ± 0.14	845 ± 48
Tipong UM1	6.5	132 ± 2	202 ± 3.79	819 ± 3.92	1304 ± 49	16.74	2.80 ± 0.07	656 ± 26
Tipong UM2	5.4	90.33 ± 2.08	158 ± 3.79	394 ± 3.23	891 ± 6.11	22.33	2.60 ± 0.07	502 ± 26
Tipong UM3	6.0	123 ± 4.36	800 ± 4.51	800 ± 8.95	1281 ± 127	22.33	2.00 ± 0.07	788 ± 87

Table 2.3 Concentration of metals (in mg L^{-1}) present in coal mine drainage from NEC in the pre-monsoon season.

Metals	Tirap	Ledo	Tikak	Tipong UM1	Tipong UM2	Tipong UM3
Ca	119 ± 2	43.43 ± 0.06	108 ± 0.20	54.33 ± 0.15	26.27 ± 0.06	48.67 ± 0.06
Na	195 ± 3.22	29.13 ± 0.38	11.20 ± 0.10	41.17 ± 0.49	3.50 ± 0.24	71.53 ± 0.21
K	15.27 ± 0.42	5.83 ± 0.06	5.37 ± 0.25	5.77 ± 0.06	3.07 ± 0.06	5.23 ± 0.21
Mg	548 ± 6.62	157 ± 1.89	44.76 ± 4.06	166 ± 0.97	79.76 ± 0.81	165 ± 2.15
Cd	0.01	BDL	BDL	BDL	0.01	BDL
Cu	0.10 ± 0.01	0.01	BDL	BDL	BDL	BDL
Co	1.44 ± 0.05	BDL	0.05 ± 0.01	0.21 ± 0.03	BDL	BDL
Pb	0.09 ± 0.01	0.04	BDL	0.03	0.02	0.02
Zn	1.48 ± 0.04	0.09	0.18	0.12	0.09 ± 0.01	0.11 ± 0.01
Fe	9.17 ± 0.08	0.13 ± 0.02	121 ± 0.38	37.89 ± 0.34	85 ± 0.25	48.56 ± 0.07
Al	28.86 ± 3.65	22.44 ± 1.18	13.22 ± 0.34	20.14 ± 0.10	28.11 ± 0.12	24.37 ± 0.42
Mn	13.57 ± 1.44	0.40 ± 0.07	1.98 ± 0.10	0.12 ± 0.05	1.45 ± 0.16	0.39 ± 0.02
Ni	2.62 ± 0.04	BDL	0.13 ± 0.04	BDL	BDL	BDL
Cr	0.05	BDL	0.04 ± 0.01	BDL	BDL	BDL

[The data is presented in the 'xx' or 'xx ± yy' format, where 'xx' is the average of three independent values and 'yy' is the standard deviation]

BDL: below detectable limit. Values exceeding the discharge limits as recommended by CPCB (1993) and EPA (2002) are marked in red.

Heavy metals contamination is another serious concern posed by AMD, where many metal ions are often present in the dissolved state at lower pH (Table 2.3). Iron was the most abundant metal ion present in all mine discharges, ranging from 0.12 to 121 mg L^{-1}, thus surfeiting the desirable limit of 3 mg L^{-1}. Aluminium (ranged from 12.83 to 32 mg L^{-1}) was the second most available metal ion exceeding the permissible discharge limit of 5 mg L^{-1} (Table 1.3). Manganese was also found to exceed the permissible limit of 2 mg L^{-1} in all coalmine discharges except Ledo and Tipong. Zinc was detected to be present in the range of 0.09 to 1.52 mg L^{-1} and well below the discharge limits. The amount of cobalt and nickel detected in all mine water samples except Ledo and Tipong exceeded the permissible discharge limit, ranging from 0.06 to 1.48 mg L^{-1} and 0.11 to 2.67 mg L^{-1}, respectively. In general, the concentration of other toxic metals such as cadmium and lead was below 0.01 and 0.05 mg L^{-1}, respectively, in all mine discharges except Tirap, which marginally exceeded the permissible discharge limit (PDL).

To ensure the complete analysis of water samples, an ion balance check was performed, such that the sum of anions should equal the sum of cations to preserve electroneutrality. A significant imbalance (> 5%) would indicate that additional constituents were present or that an error occurred in analyzing one or more of the ions. An error of 2.52, 10.07, 0.89, 15.35, 5.16 and 14.03% have been made in the water sample analysis of Tirap, Ledo, Tikak, Tipong (UM1), Tipong (UM2) and Tipong (UM3), respectively. Fig. 2.3 depicts the bar diagram representation of ion balance.

2.4.1.2 Coal mine discharge in monsoon

The physicochemical characteristics of the coal mine discharge sampled during the monsoon season are presented in Table 2.4. Mine water samples collected from Tirap and Ledo collieries during the monsoon season exhibited similar pH values as obtained in the pre-monsoon season. In contrast, the pH of the mine discharge from Tikak and Tipong (UM1) collieries is lower than the pre-monsoon season, which could be due to a higher rate of pyrite oxidation in summer (monsoon) because of higher temperature (Dutta et al., 2020; Equeenuddin et al., 2010). On the contrary, mine water from Tipong (UM2 and UM3) collieries exhibited higher pH during monsoon than during the pre-monsoon. This indicates that the rate of pyrite oxidation and acid generation is inter-dependent and determined by other abiotic factors such as oxygen content in the gas (or water) phase and degree of saturation (Akcil and Koldas, 2006; Hammack and Watzlaf, 1990). Mine water samples showed a significant drop in DO (1.10–4.80 mg L^{-1}) during the monsoon season due to temperature rise. EC values increase with low and high values of pH due to the presence of more ions in AMD (Dutta et al., 2020); therefore, higher EC values (120–516 mS m^{-1}) were observed for all samples. Higher EC in the monsoon season was substantiated by the concurrent increase in TDS (968–4848 mg L^{-1}), mostly consisting of sulfate (787–4094 mg L^{-1}) and cations like Ca^{2+} (36.20–572 mg L^{-1}), Mg^{2+} (177–328 mg L^{-1}), Na^{+} (31.10–147 mg L^{-1}) and K^{+} (1–32.10 mg L^{-1}).

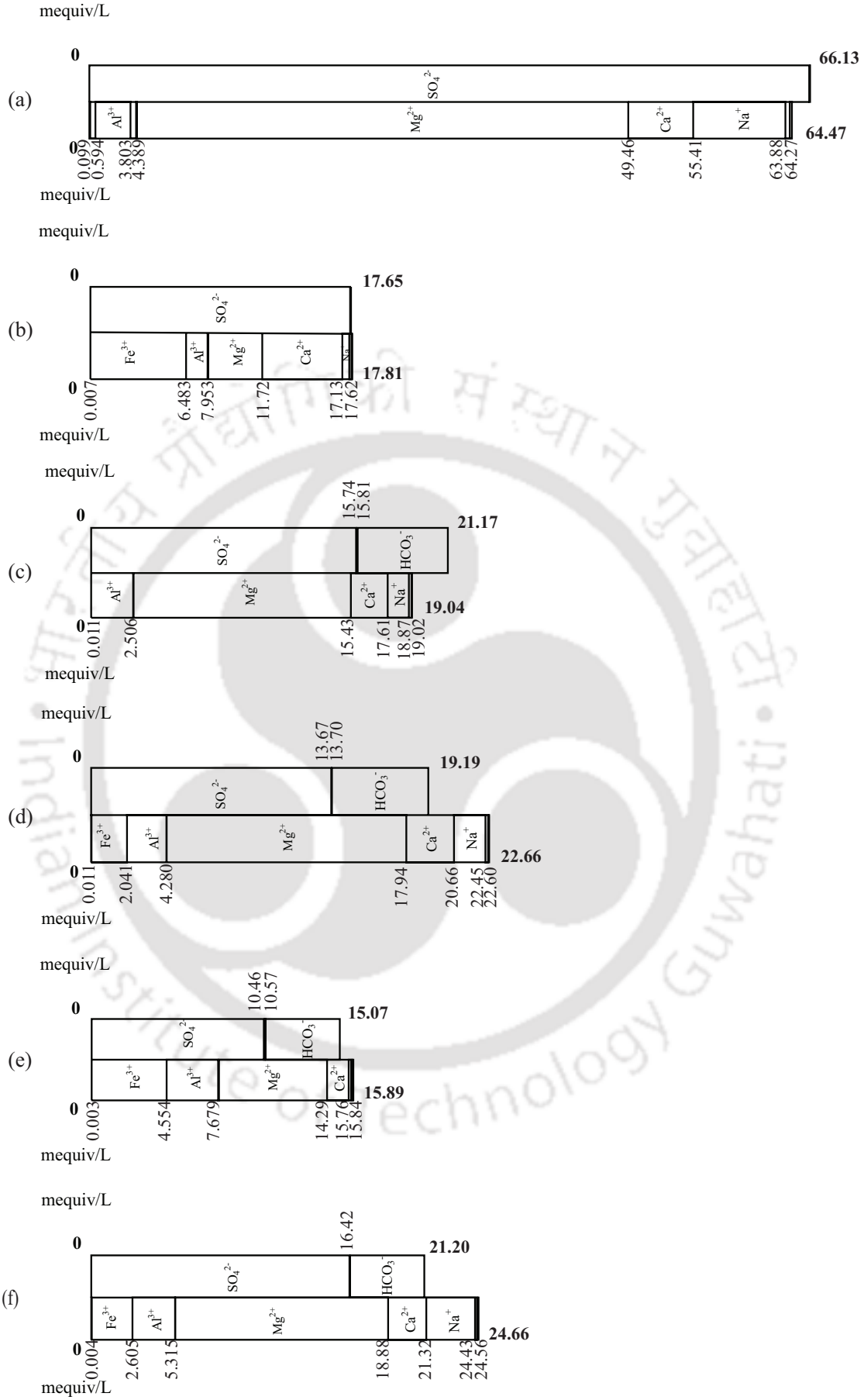

Fig. 2.3 Bar diagram representation of ion balance for (a) Tirap, (b) Tikak, (c) Ledo, (d) Tipong (UM1), (e) Tipong (UM2) and (f) Tipong (UM3) in the pre-monsoon season.

The sulfate concentration apparently increased due to high sulfur deposition at low pH in the monsoon season (Guttikunda et al., 2001). The release of sulfates followed the subsequent release of metals (Table 2.5), especially iron from pyritic seams (1.63–302 mg L^{-1}), aluminium (15.90–30.11 mg L^{-1}) and manganese (0.56–19 mg L^{-1}). The heavy metal contamination of water bodies and AMD itself is directly associated with coal, overburden and sediment in coal mining areas (Dutta et al., 2017; Saikia et al., 2016). Tirap is the most active and industrially important coal mine of the Makum Coalfield, where the concentration of iron in the monsoon season increased by ten folds whereas mine water discharge from the Tikak coal mine exhibited the highest iron concentration. The closure of coal extraction activities at the Ledo coal mine demonstrated exceptionally lower levels of toxic heavy metals such as lead, copper and cadmium, whereas the concentration of metals like iron and zinc remained fairly low (below PDL) at circumneutral pH. On the other hand, the Tikak coal mine exhibited an extremely elevated concentration of heavy metals (Cd, Co, Fe, Al, Ni and Cr) exceeding EPA (2002) discharge limits, where cobalt, aluminium, nickel and chromium concentration increased to about 2–10 times in the monsoon season. Underground coal mines at Tipong are only partially operational. However, despite non-acidic discharge from Tipong collieries, the concentration of metals like iron (33.90–63 mg L^{-1}), aluminium (15.90–30.11 mg L^{-1}) manganese (0.56–1.89 mg L^{-1}), zinc (0.98–4.90 mg L^{-1}), cobalt (0.12–0.63 mg L^{-1}) and chromium (0.17–0.55 mg L^{-1}) was present in excess of admissible limits. Metal loading is usually higher after a rainfall, particularly during the first flush events of monsoon, due to the rapid dissolution of efflorescent salts formed during the dry season (Aykol et al., 2003).

Fig. 2.4 illustrates the bar diagram representation of ion balance for water samples during the monsoon season. Ion balance check indicated 17.29, 6.81, 8.91, 10.60, 12.07 and 9.84% error in the water sample analysis of Tirap, Ledo, Tikak, Tipong (UM1), Tipong (UM2) and Tipong (UM3), respectively. The major contributing cations and anions are indicated in ion balance diagrams, whereas other cations (such as H^+, Cd^{2+}, Co^{2+}, Cu^{2+}, Zn^{2+}, Mn^{2+}, Pb^{2+}, Ni^{2+}, Cr^{3+} and NH_4^+) and other anions (such as Cl^-, F^- and HCO_3^-) had minor contributions.

2.4.1.3 Coal mine discharge in post-monsoon

Table 2.6 presents the water quality parameters of coal mine discharge from different collieries during the post-monsoon season. The pH values observed in the post-monsoon season were similar or relatively higher than the monsoon season except for Tirap and Tipong (UM2 and UM3). In the post-monsoon season, when the temperature was low, the DO concentration increased in all mine discharges (3.70–6.80 mg L^{-1}), whereas the DO concentration of mine water from the Tirap mine was recorded as the lowest. Of all the seasons, highest EC was recorded in the post-monsoon season from all the collieries (97–897 mS m^{-1}), indicating a higher rate of oxidative sulfate leaching (765–7433 mg L^{-1}) and release of metals (Table 2.7). Coal mine discharge from Tirap, Ledo and Tikak showed the highest TDS values (1976–9844 mg L^{-1}), while Tipong collieries exhibited the lowest TDS values (812–1116 mg L^{-1}) in the post-monsoon season. Open cast mines, especially Tirap and Tikak, were found to generate highly acidic and most toxic mine discharge, primarily due to a large amount of mine spoil

Table 2.4 Physicochemical characteristics of coal mine drainage from NEC in the monsoon season.

Coal mine	pH	EC (mS m^{-1})	Turbidity (NTU)	TH (mg L^{-1} as $CaCO_3$)	TDS (mg L^{-1})	COD (mg L^{-1})	DO (mg L^{-1})	SO_4^{2-} (mg L^{-1})
Tirap	3.0	513 ± 4.16	6.77 ± 1.45	2704 ± 87	4803 ± 44	36.36 ± 10	2.90 ± 0.14	4067 ± 27
Ledo	6.5 ± 0.1	179 ± 19	2.47 ± 0.12	1154 ± 105	1376 ± 18	36.36 ± 10	4.60 ± 0.28	966 ± 3.93
Tikak	2.9	426 ± 2.24	129 ± 0.92	2213 ± 199	2860 ± 58	80 ± 10	3.10 ± 0.99	3434 ± 54
Tipong UM1	5.9	146 ± 1.90	152 ± 3.78	1019 ± 16	1288 ± 26	102 ± 21	1.70 ± 0.14	1171 ± 19
Tipong UM2	6.8 ± 0.1	121 ± 0.76	189 ± 1.40	859 ± 25	993 ± 26	36.36 ± 10	1.20 ± 0.14	888 ± 91
Tipong UM3	6.6	133 ± 0.26	918 ± 4.75	1048 ± 7.70	1511 ± 23	50.91 ± 10	1.55 ± 0.07	1131 ± 76

Table 2.5 Concentration of metals (in mg L^{-1}) present in coal mine drainage from NEC in the monsoon season.

Metals	Tirap	Ledo	Tikak	Tipong UM1	Tipong UM2	Tipong UM3
Ca	554 ± 29	65.63 ± 13	445 ± 29	66.77 ± 1.33	45.57 ± 11	56.50 ± 1.64
Na	147 ± 21	33.17 ± 2.54	39.33 ± 4.35	125 ± 60	97.43 ± 43	101 ± 0.46
K	31.57 ± 0.55	5.97 ± 1.79	1.67 ± 0.61	20.93 ± 0.25	14.17 ± 1.07	16.07 ± 0.35
Mg	327 ± 4.99	240 ± 20	268 ± 35	207 ± 3.70	180 ± 3.34	220 ± 1.03
Cd	0.01	0.01	0.07	0.01	BDL	0.01
Cu	0.10 ± 0.01	0.01	0.10 ± 0.01	BDL	BDL	BDL
Co	0.66 ± 0.03	0.13	0.17	0.62	0.12	0.31
Pb	0.02	0.04 ± 0.01	0.03	0.06	0.09	0.06
Zn	2.76 ± 0.60	0.72 ± 0.44	1.64 ± 0.31	4.89 ± 0.01	1.65 ± 0.38	1.02 ± 0.04
Fe	91.59 ± 0.56	1.73 ± 0.09	301 ± 0.54	34.96 ± 0.99	56.54 ± 7.85	52.34 ± 2.35
Al	24.95 ± 0.93	21.38 ± 3.09	26.51 ± 1.47	17.89 ± 1.72	26.13 ± 1.61	29.26 ± 0.74
Mn	17.77 ± 1.16	5.72 ± 1.11	1.13 ± 0.18	0.59 ± 0.02	1.58 ± 0.27	1.03 ± 0.06
Ni	1.59 ± 0.07	0.22 ± 0.01	0.47 ± 0.05	0.01	0.06 ± 0.01	0.07 ± 0.01
Cr	0.48 ± 0.07	0.18 ± 0.01	0.16	0.54	0.19 ± 0.02	0.19 ± 0.02

[The data is presented in the 'xx' or 'xx ± yy' format, where 'xx' is the average of three independent values and 'yy' is the standard deviation]

BDL: below detectable limit. Values exceeding the discharge limits as recommended by CPCB (1993) and EPA (2002) are marked in red.

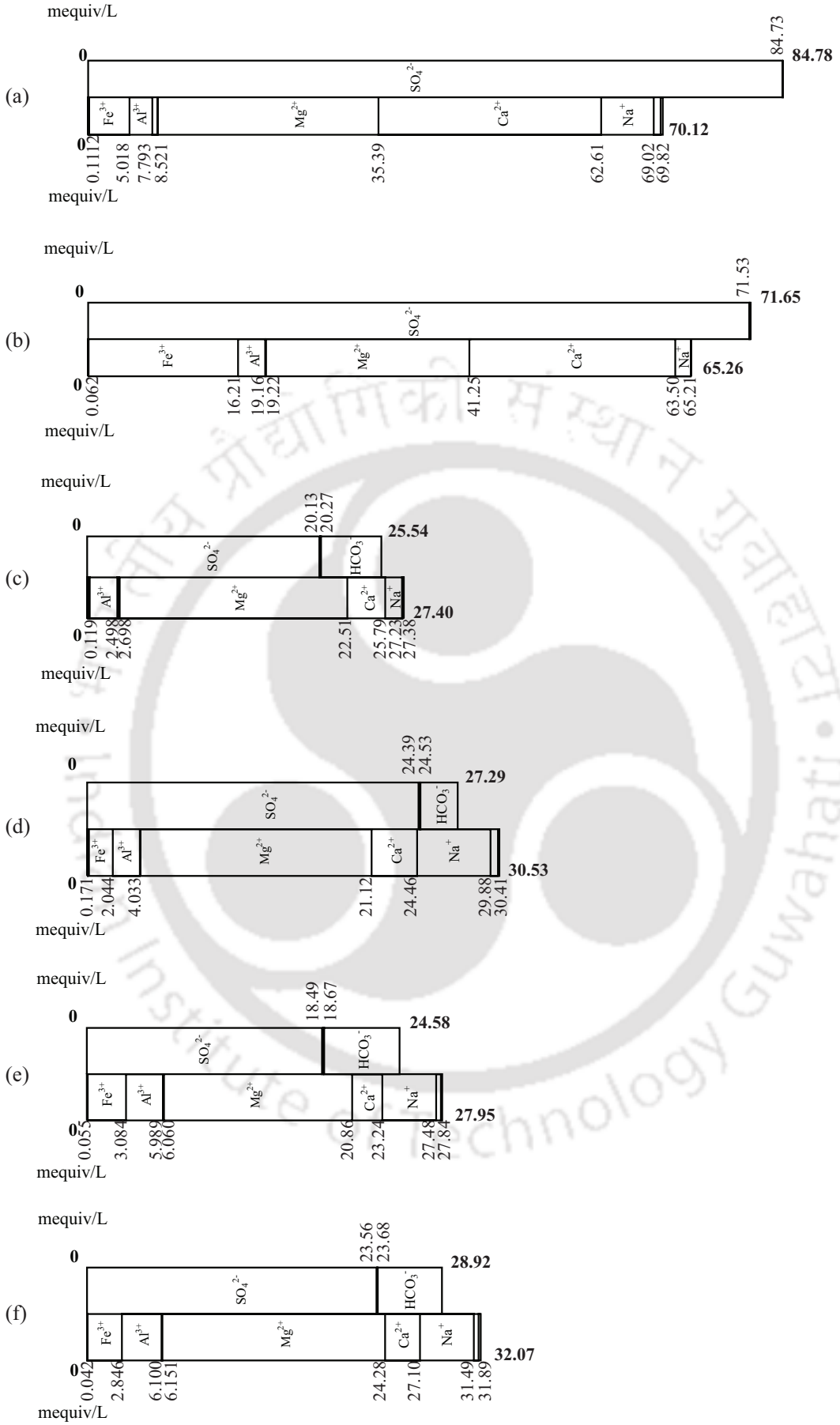

Fig. 2.4 Bar diagram representation of ion balance for (a) Tirap, (b) Tikak, (c) Ledo, (d) Tipong (UM1), (e) Tipong (UM2) and (f) Tipong (UM3) in the monsoon season.

over the coal seam, which is susceptible to abrasion and leaching pollutants. The dissolution of sulfate salts and release of hazardous elements during the monsoon season (wet period of summer) is followed by the surface evaporation in the post-monsoon season (dry period), causing concentration of all solutes and hence higher EC and lower pH (Tutu et al., 2008). This suggests a strong control of climatic conditions on AMD chemistry (Sahoo et al., 2014).

The metal content in coal mine discharge during the post-monsoon season, particularly iron (0.29–102 mg L^{-1}) and aluminium (6.73–31.33 mg L^{-1}), was reasonably lower than the monsoon season. However, the highest manganese and chromium concentration was observed from Tikak and Tirap colliery, respectively, during post-monsoon. Interestingly, the zinc concentration in Tirap and Tikak colliery increased about 2–2.5 times the concentration of monsoon season, exceeding EPA (2002) and CPCB (1993) discharge limits. The concentration of toxic metals such as lead, copper and cadmium consistently persisted below the PDL. In Tirap and Tikak colliery, the cobalt and nickel concentration increased drastically to about 1.5–6 and 2.5–11 times the concentration of monsoon season, respectively, surpassing the discharge limits by a substantial margin. Murray et al. (2021) reported the influence of strong evaporation (dry season) on the geochemistry of AMD in a semi-arid Puna region, resulting in seepages with low pH (1.9–2.2) and high concentrations of metals.

Fig. 2.5 illustrates the bar diagram representation of ion balance for water samples during the post-monsoon season. Ion balance check indicated an error of about 7.56, 10.81, 14.70, 16.77, 9.77 and 7.43% in the water sample analysis of Tirap, Ledo, Tikak, Tipong (UM1), Tipong (UM2) and Tipong (UM3), respectively.

2.4.2 Geochemistry of dissolved ions

The geochemistry of AMD formation is controlled by various geological factors such as the content of acid-generating pyrite (or other iron sulfides), other sulfides, carbonate and other acid-consuming minerals, rock type, nature of ores, reactivity of acid-generating and acid-consuming minerals, trace elements present and extent of pre-mining oxidation (Plumlee et al., 1999). An increase in metal content with lower pH of the coal mine discharge is related to pyrite and other sulfide minerals present in the deposit. Table 2.8 shows the relationship among various physicochemical parameters using Pearson's correlation coefficient matrix.

pH was found to be strongly negatively correlated with all other parameters, especially EC and sulfate, indicating the dissolution of all elements and release of sulfate at lower pH (< 5.0) due to the oxidation of sulfide minerals (Olıas et al., 2004). The leaching of metal ions is associated with low pH, indicated by the high negative correlation of pH with all metals (Table 2.8). However, EC showed a high positive correlation with TDS ($r = 0.92$) and sulfate ($r = 0.98$). Further, it was observed that all metals were strongly positively correlated with the sulfate ($r = 0.37–0.93$), which reveals the existence of some of these metals as sulfate in AMD formation (Equeenuddin et al., 2010). All metals were found to positively correlate with each other (except the correlation of iron with sodium and potassium), suggesting its release from similar mineral deposits or the same origin.

Table 2.6 Physicochemical characteristics of coal mine drainage from NEC in the post-monsoon season.

Coal mine	pH	EC (mS m^{-1})	Turbidity (NTU)	TH (mg L^{-1} as $CaCO_3$)	TDS (mg L^{-1})	COD (mg L^{-1})	DO (mg L^{-1})	SO_4^{2-} (mg L^{-1})
Tirap	2.7	877 ± 23	842 ± 35	6084 ± 107	9088 ± 80	12.39 ± 4.38	0.45 ± 0.07	7231 ± 187
Ledo	6.4 ± 0.1	287 ± 7.09	4.20 ± 0.26	1582 ± 9.55	2079 ± 89	3.10	6.65 ± 0.21	1776 ± 17
Tikak	3.5 ± 0.1	544 ± 26	4.53 ± 0.21	4573 ± 20	9769 ± 63	3.10	4.05 ± 0.50	5766 ± 144
Tipong UM1	6.4 ± 0.2	102 ± 6.43	9.35 ± 0.21	1246 ± 18	1031 ± 33	27.87	4.10 ± 0.14	987 ± 22
Tipong UM2	5.6 ± 0.1	144 ± 7.81	410 ± 1.80	791 ± 17	823 ± 15	24.77 ± 4.38	4.60 ± 0.14	774 ± 13
Tipong UM3	6.2 ± 0.1	150 ± 16	841 ± 14	1141 ± 17	1064 ± 45	18.58 ± 4.38	4.65 ± 0.07	1015 ± 48

Table 2.7 Concentration of metals (in mg L^{-1}) present in coal mine drainage from NEC in the post-monsoon season.

Metals	Tirap	Ledo	Tikak	Tipong UM1	Tipong UM2	Tipong UM3
Ca	1100 ± 30	271 ± 0.87	890 ± 5.50	306 ± 2.08	142 ± 2.08	305 ± 0.58
Na	133 ± 1	70.83 ± 2.14	39.90 ± 0.56	66.57 ± 1.16	10.77 ± 0.15	47.60 ± 0.44
K	59.60 ± 0.44	18.87 ± 0.35	20.53 ± 0.50	14.40 ± 0.36	6.03 ± 0.15	8.93 ± 0.23
Mg	811 ± 8.08	220 ± 2.85	571 ± 2.52	117 ± 3.60	106 ± 5.35	91.92 ± 4.24
Cd	0.01	BDL	0.01	BDL	BDL	BDL
Cu	0.10	0.01	0.08	BDL	BDL	BDL
Co	1.02 ± 0.01	BDL	1.04 ± 0.01	BDL	BDL	BDL
Pb	0.04	BDL	0.03	0.03	0.01	0.01
Zn	7.01 ± 0.11	0.62 ± 0.07	3.44 ± 0.28	1.81 ± 0.06	0.92 ± 0.01	1.41 ± 0.03
Fe	102 ± 0.43	0.31 ± 0.02	91.64 ± 1.83	16.38 ± 0.41	66.32 ± 0.36	33.32 ± 0.36
Al	30.65 ± 0.77	14.44 ± 1.03	22.47 ± 0.64	17.44 ± 0.49	22.59 ± 1.19	7.92 ± 1.11
Mn	15.56 ± 0.61	3.84 ± 0.07	25.82 ± 0.24	1.51 ± 0.01	2.28 ± 0.02	1.95 ± 0.01
Ni	4.39 ± 0.01	0.86 ± 0.01	5.21 ± 0.03	BDL	BDL	BDL
Cr	0.51 ± 0.01	0.22 ± 0.01	0.19 ± 0.01	0.11 ± 0.01	0.06	0.09 ± 0.01

[The data is presented in the 'xx' or 'xx ± yy' format, where 'xx' is the average of three independent values and 'yy' is the standard deviation]
BDL: below detectable limit. Values exceeding the discharge limits as recommended by CPCB (1993) and EPA (2002) are marked in red.

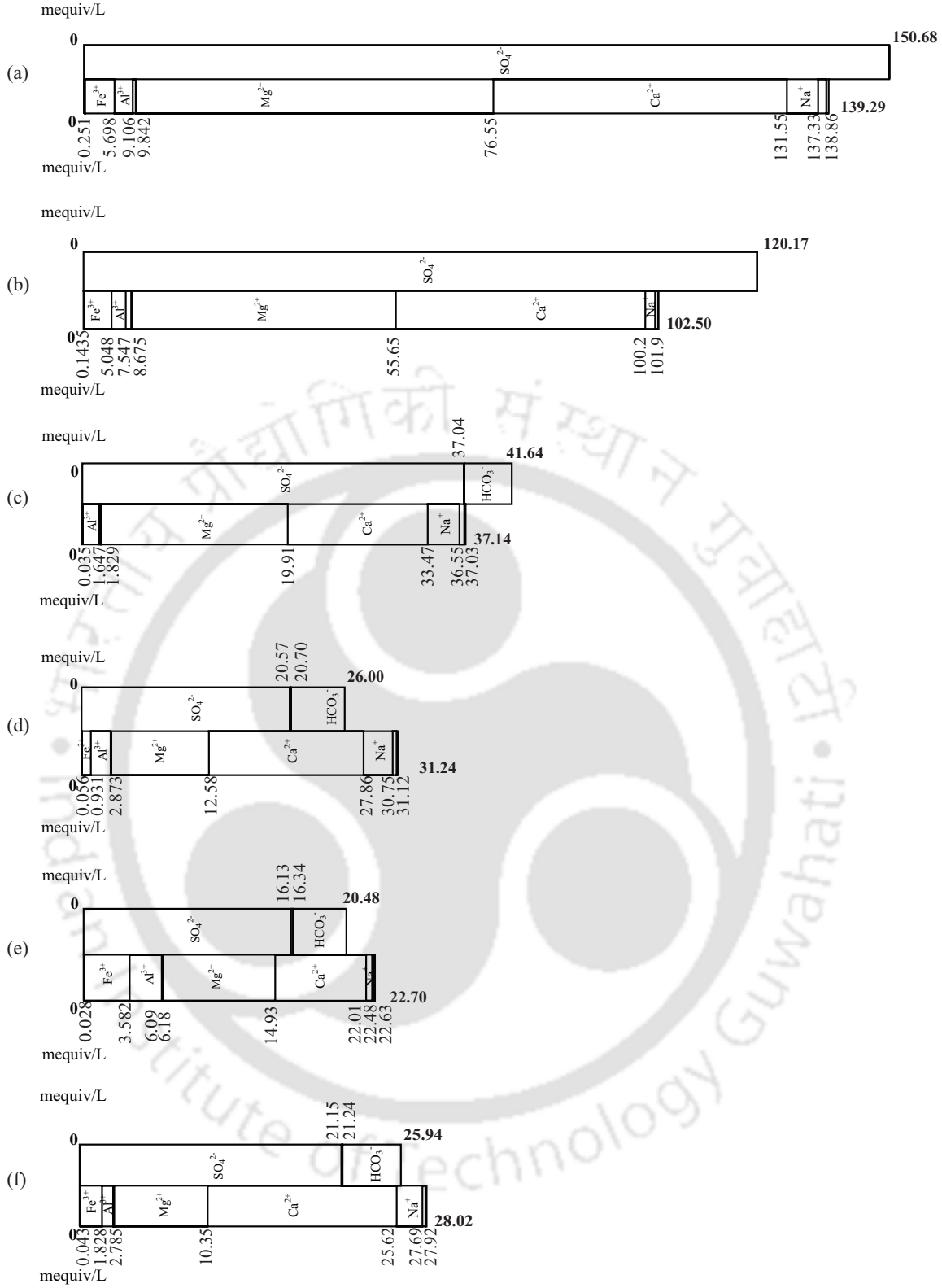

Fig. 2.5 Bar diagram representation of ion balance for (a) Tirap, (b) Tikak, (c) Ledo, (d) Tipong (UM1), (e) Tipong (UM2) and (f) Tipong (UM3) in the post-monsoon season.

The interpretation of geological constraints on the chemistry of AMD formation is presented in the form of the Ficklin diagram (Fig. 2.6), where the range of a sum of metal concentrations (such as Zn, Cu, Cd, Pb, Co and Ni) is constrained against the potential ranges in pH (Plumlee et al., 1999). The grouping of the coal mine drainage is based on pyrite content, base-metal sulfide content and carbonate content of the mineral deposits. The mine

Table 2.8 Pearson's correlation coefficient matrix between various physicochemical parameters in coal mine discharge (n=18).

	pH	EC	TH	TDS	Sulfate	Na	K	Ca	Mg	Fe	Mn	Al	Zn	Co	Ni	Cr
pH	1.0															
EC	**–0.80**	1.0														
TH	**–0.69**	**0.96**	1.0													
TDS	**–0.73**	**0.92**	**0.96**	1.0												
Sulfate	**–0.78**	**0.98**	**0.98**	**0.96**	1.0											
Na	–0.32	0.47	0.43	0.39	0.44	1.0										
K	–0.43	**0.79**	**0.81**	**0.71**	**0.78**	**0.62**	1.0									
Ca	**–0.65**	**0.89**	**0.94**	**0.88**	**0.93**	0.22	**0.76**	1.0								
Mg	**–0.64**	**0.92**	**0.95**	**0.92**	**0.92**	**0.58**	**0.78**	**0.78**	1.0							
Fe	**–0.61**	0.36	0.26	0.23	0.37	–0.18	–0.02	0.37	0.13	1.0						
Mn	**–0.68**	**0.80**	**0.83**	**0.92**	**0.85**	0.41	**0.61**	**0.77**	**0.80**	0.08	1.0					
Al	–0.33	0.40	0.37	0.37	0.40	0.37	0.30	0.17	**0.51**	0.26	0.28	1.0				
Zn	–0.47	**0.73**	**0.79**	**0.69**	**0.76**	**0.53**	**0.86**	**0.75**	**0.74**	0.17	**0.55**	0.23	1.0			
Co	**–0.66**	**0.74**	**0.75**	**0.81**	**0.76**	**0.72**	**0.61**	**0.54**	**0.87**	0.03	**0.79**	0.44	**0.64**	1.0		
Ni	**–0.68**	**0.88**	**0.94**	**0.99**	**0.92**	0.38	**0.68**	**0.84**	**0.92**	0.14	**0.92**	0.34	**0.65**	**0.82**	1.0	
Cr	–0.32	**0.57**	**0.55**	0.45	**0.57**	**0.56**	**0.79**	**0.54**	**0.51**	0.11	**0.41**	0.14	**0.85**	0.46	0.39	1.0

Bold numbers indicate statistically significant correlation ($p < 0.05$).

discharges during the pre-monsoon season are classified as Acid Low-metal and Near-neutral Low-metal; while mine discharges from monsoon and post-monsoon are classified as High-acid High-metal, Acid High-metal and Near-neutral High-metal.

The hydrochemical characteristic of the coal mine drainage is illustrated in the Piper trilinear diagram (Fig. 2.7), plotting the relative concentration of the major ions to depict the dominance of various hydrochemical facies (Piper, 1944). In the Piper diagram, cations (or anions) expressed as percentages of total cations (or total anions) (in meq L^{-1}) are plotted as a single point on the left triangle (or right triangle for anions) and these two points then projected into the central diamond, where a circle drawn at this point with its area proportional to the TDS (Todd and Mays, 2004). In all mine water samples, sulfate is the dominant anion, whereas calcium and magnesium are the major cations. From Fig. 2.7, it can be seen that the composition of coal mine discharge is represented by the dominance of hydrochemical facies of Ca–Mg–SO_4^{2-} type.

2.4.3 Impact of coal mine drainage on soil

The direct discharge of AMD onto the land surface due to excessive overflow or runoff during rainfall contaminates the surrounding soil and acts as a major metal retention sink, which plays a major role in controlling the mobility of metal ions into the aquatic environment (Equeenuddin et al., 2013). Coal mining is one of the main causes of soil and sediment pollution worldwide, essentially associated with coal mine drainage (Liu et al., 2019; Sahoo et al., 2017).

The elemental composition of the metals present in the soil is depicted in Fig. 2.8. Soils were highly enriched with iron, aluminium and lead (Tirap and Tikak). Tikak and Tipong soils showed the presence of arsenic; however, arsenic was not detected in the coal mine discharge from various collieries during any season. These results indicated that the polluted soil could act as a secondary pollution source and further damage vegetation cover and biodiversity of the region.

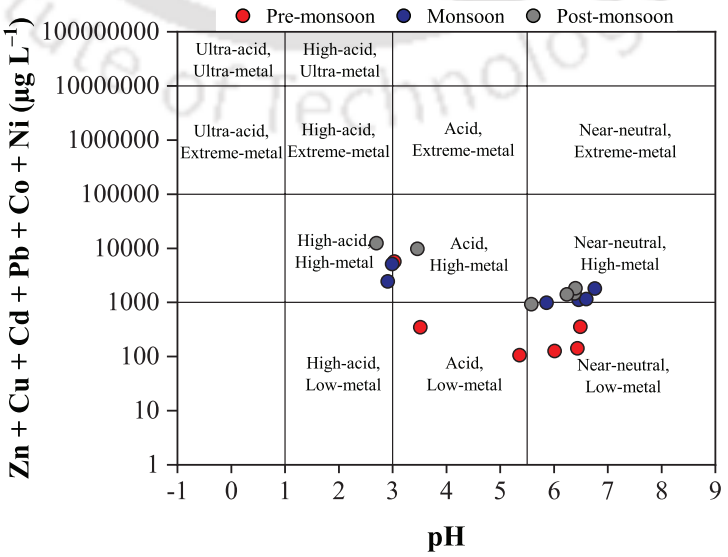

Fig. 2.6 Ficklin diagram coal mine discharge from the NEC during different seasons.

Table 2.9 shows the amount of metal contamination in the surrounding soil of various collieries. Soil obtained from all collieries was highly enriched with iron (21,266–27,105 mg kg^{-1}) and aluminium (4013–14,298 mg kg^{-1}), followed by magnesium (379–1462 mg kg^{-1}), manganese (80.70–676 mg kg^{-1}), cobalt (426–535 mg kg^{-1}), copper (1.76–306 mg kg^{-1}), cadmium (238–268 mg kg^{-1}) and zinc (35.24–144 mg kg^{-1}). Noticeable amounts of chromium (32.76–138 mg kg^{-1}), nickel (46.63–105 mg kg^{-1}) and lead (1.64–9.46 mg kg^{-1}) were also present. Compared with other standard reference values, the average concentrations of Cd, Cu, Co, Zn, Mn and Cr exceeded the world average non-polluted soil. Only the average concentration of Mn, Pb, Zn (except at Ledo) and Cr (except at Tipong) did not exceed the sediment quality guideline (SQG) of WHO (2004). Most of the studied metals exceeded the

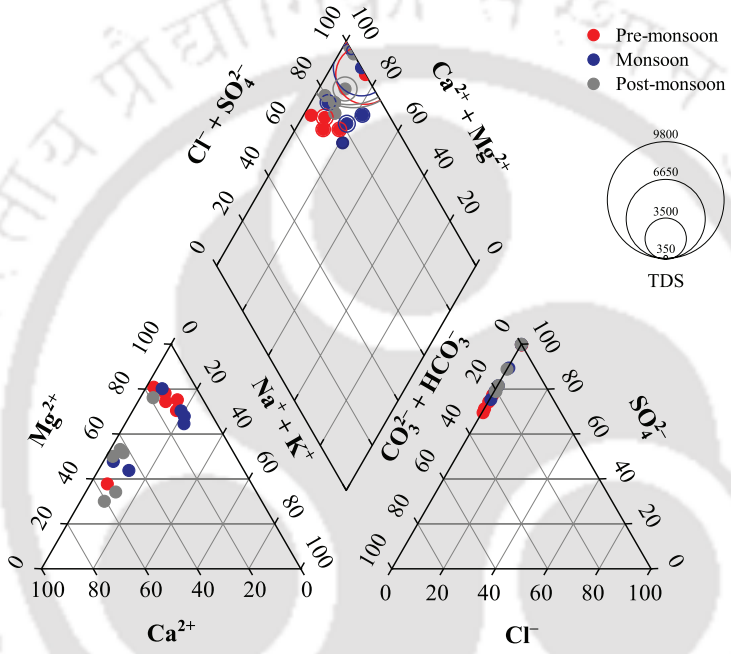

Fig. 2.7 Piper trilinear diagram representing various hydrochemical facies.

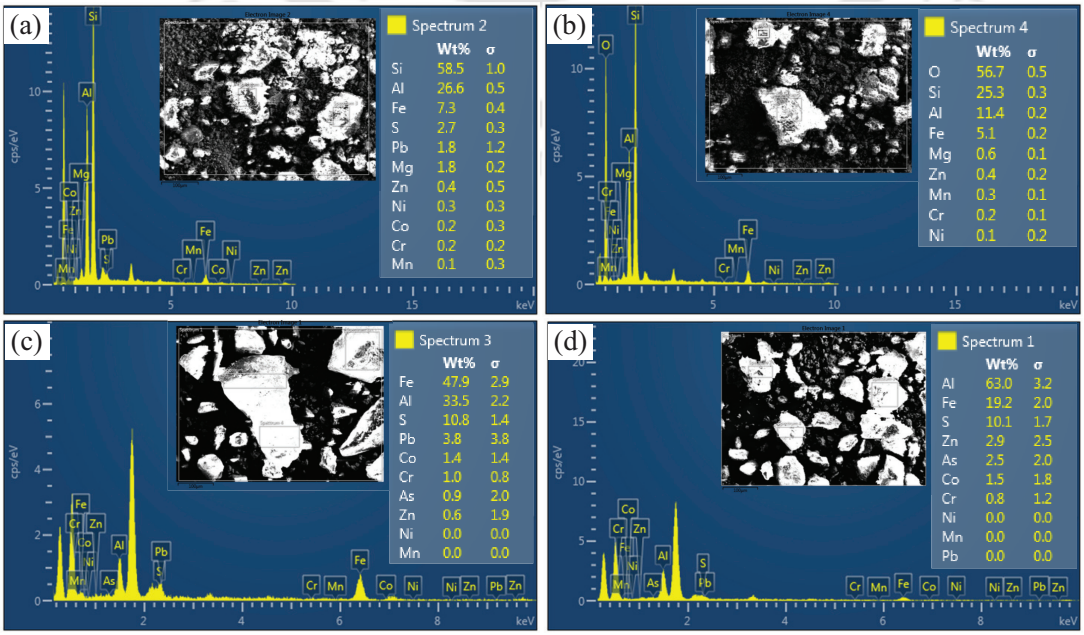

Fig. 2.8 EDX spectrum of soil from (a) Tirap, (b) Ledo, (c) Tikak and (d) Tipong colliery.

Table 2.9 Metal content (in mg kg^{-1}) in the surrounding soil of NEC.

Soil sample	Metals										
	Mg	Cd	Cu	Co	Pb	Zn	Fe	Al	Mn	Ni	Cr
Tirap	1230 ± 213	244 ± 5.38	185 ± 24.50	450 ± 29.78	1.86 ± 0.28	108 ± 2.44	21575 ± 470	7170 ± 846	190 ± 1.98	100 ± 0.42	82.76 ± 6.36
Ledo	531 ± 58.81	248 ± 2.43	65.15 ± 9.19	436 ± 9.65	7.10 ± 0.87	141 ± 2.52	26776 ± 99.88	6924 ± 342	449 ± 25.34	101 ± 5.34	77.08 ± 2.57
Tikak	416 ± 33.92	254 ± 12.20	265 ± 45.28	461 ± 29.12	3.08 ± 0.31	90.16 ± 48.21	23106 ± 520	4132 ± 103	81.23 ± 0.76	48.10 ± 10.48	33 ± 0.30
Tipong	1132 ± 224	248 ± 0.30	1.96 ± 0.25	503 ± 39.08	8.24 ± 1.33	115 ± 2.44	27043 ± 71.29	14172 ± 203	642 ± 34.67	78.77 ± 23.50	136 ± 1.65
World background[a] (average values)	–	1.10	14	6.90	25	62	–	–	418	–	42
WHO SQG[b]	–	0.20	32	13	16	127	–	–	750	49	90
USEPA SQG[c]	–	6	25	–	–	123	–	–	–	20	25
CEQG[d]	–	0.60	35.70	–	35	123	–	–	–	–	37.30
CSG (grade I)[e]	–	0.20	35	–	35	100	–	–	–	40	90.0
IS[f]	–	–	3–6	–	–	135–270	300–600	–	–	–	250–500
TEL[g]	–	0.68	18.70	–	30.20	124	–	–	–	15.90	52.30

[The data is presented in the 'xx ± yy' format, where 'xx' is the average of three independent values and 'yy' is the standard deviation]

SQG: sediment quality guideline; CEQG: Canadian environmental quality guidelines; CSG: Chinese soil guidelines; IS: Indian standard of potential toxic element for agricultural soils; TEL: threshold effects level.

[a](Kabata-Pendias and Pendias, 1999, 2001)

[b]WHO (2004)

[c]USEPA (1999)

[d]CCME (1999)

[e]Liu et al. (2019)

[f]Awashthi (2000)

[g]Long et al. (1995)

SQGs of USEPA (1999) and CCME (1999). Thus, soil samples collected from nearby collieries showed a high concentration of heavy metals, indicating soil contamination directly linked with anthropogenic activities and AMD (Ahn et al., 2020; Equeenuddin et al., 2013).

2.5 Summary

The coal mine discharge from Tirap and Tikak was extremely acidic and highly contaminated with heavy metals and sulfate ions. On the other hand, Ledo and Tipong collieries produced less acidic drainage (pH > 5.0) with relatively low dissolved metals. The change in the season had a predominant effect on the oxidative leaching of sulfide minerals and AMD formation. A high dissolution rate of sulfate salts and release of hazardous elements was observed during the monsoon season, followed by an increase in the concentration of all solutes due to surface evaporation in the post-monsoon season. The findings revealed a strong control of local climatic conditions on AMD chemistry. In addition, the surrounding soil of the collieries was enriched with heavy metals, which could potentially control metal mobility.

Large variations were recorded in pH, sulfate and metal concentration among various coal mines in different seasons. Tirap and Tikak collieries generated AMD having the lowest pH (2.7–2.9) and highest sulfate concentration (3170–7231 mg L^{-1}) during monsoon and post-monsoon seasons. However, all other collieries released moderate sulfate (502–1776 mg L^{-1}). High acidity alleviation is most challenging and chiefly responsible for metal mobilization in the sediments. Therefore, acidic pH (2.0–2.5) and sulfate in the range of 1000–1500 mg L^{-1} were chosen for further studies. It was observed that metal release is a consequence of the dissolution of sulfidic minerals at low pH; therefore, metals (such as Fe, Al, Mn, Zn, Co, Ni and Cr) exceeding the discharge limits substantially were taken into consideration and the highest metal concentration corresponding to the selected sulfate range was opted.

References

Ahn, Y., Yun, H. S., Pandi, K., Park, S., Ji, M., and Choi, J. (2020). Heavy metal speciation with prediction model for heavy metal mobility and risk assessment in mine-affected soils. *Environmental Science and Pollution Research*, 27(3):3213–3223.

Akcil, A. and Koldas, S. (2006). Acid mine drainage (AMD): Causes, treatment and case studies. *Journal of Cleaner Production*, 14(12-13):1139–1145.

APHA (2012). *Standard Methods for the Examination of Water and Wastewater*. American Public Health Association, Washington, DC.

Awashthi, S. K. (2000). *Prevention of Food Adulteration Act no. 37 of 1954*. Central and State Rules as Amended for 1999, Ashoka Law House, New Delhi.

Aykol, A., Budakoglu, M., Kumral, M., Gultekin, A. H., Turhan, M., Esenli, V., Yavuz, F., and Orgun, Y. (2003). Heavy metal pollution and acid drainage from the abandoned Balya Pb-Zn sulfide Mine, NW Anatolia, Turkey. *Environmental Geology*, 45(2):198–208.

Barooah, P. K. and Baruah, M. K. (1996). Sulphur in Assam coal. *Fuel Processing Technology*, 46(2):83–97.

Bhagabati, R. and Borkotoki, A. (2014). Status of Patkai lake near tikak open cast mine, Assam: A hydro-biological approach. *Biolife*, 2(2):615–626.

CCME (1999). Canadian water quality guidelines for the protection of aquatic life: CCME Water Quality Index. Report, Canadian Council of Ministers of the Environment, Winnipeg, Canada.

Chabukdhara, M. and Singh, O. P. (2016). Coal mining in northeast India: An overview of environmental issues and treatment approaches. *International Journal of Coal Science & Technology*, 3(2):87–96.

Chattaraj, S., Sanga, B., Akanksha, H. G., and Mohanty, D. (2016). Insights into the abnormal characteristics of tertiary coals in Makum coalfield, Assam for their efficient end utilization. In *International Seminar on Mineral Processing Technology*, Pune, India.

Choudhury, A., Lahkar, J., Saikia, B. K., Singh, A. K. A., Chikkaputtaiah, C., and Boruah, H. P. D. (2021). Strategies to address coal mine-created environmental issues and their feasibility study on northeastern coalfields of Assam, India: A review. *Environment, Development and Sustainability*, 23:9667–9709.

CPCB (1993). *General Standards for Discharge of Environmental Pollutants Part-A: Effluents, Schedule - VI (Rule 3A)*. Central Pollution Control Board, New Delhi, India.

Dutta, M., Islam, N., Rabha, S., Narzary, B., Bordoloi, M., Saikia, D., Silva, L. F., and Saikia, B. K. (2020). Acid mine drainage in an Indian high-sulfur coal mining area: Cytotoxicity assay and remediation study. *Journal of Hazardous Materials*, 389:121851.

Dutta, M., Saikia, J., Taffarel, S. R., Waanders, F. B., de Medeiros, D., Cutruneo, C. M. N. L., Silva, L. F. O., and Saikia, B. K. (2017). Environmental assessment and nano-mineralogical characterization of coal, overburden and sediment from Indian coal mining acid drainage. *Geoscience Frontiers*, 8(6):1285–1297.

EPA (2002). *Standards for Effluent Discharge Regulations. General Notice No. 44. of 2003*. Environmental Protection Agency. (accessed on 17.04.19).

Equeenuddin, S. M., Tripathy, S., Sahoo, P. K., and Panigrahi, M. K. (2010). Hydrogeochemical characteristics of acid mine drainage and water pollution at Makum Coalfield, India. *Journal of Geochemical Exploration*, 105(3):75–82.

Equeenuddin, S. M., Tripathy, S., Sahoo, P. K., and Panigrahi, M. K. (2013). Metal behavior in sediment associated with acid mine drainage stream: Role of pH. *Journal of Geochemical Exploration*, 124:230–237.

Guttikunda, S. K., Thongboonchoo, N., Arndt, R. L., Calori, G., Carmichael, G. R., and Streets, D. G. (2001). Sulfur deposition in Asia: Seasonal behavior and contributions from various energy sectors. *Water, Air, and Soil Pollution*, 131:383–406.

Hammack, R. W. and Watzlaf, G. R. (1990). The effect of oxygen on pyrite oxidation. In *Proceedings America Society of Mining and Reclamation*, pages 257–264. West Virginia University.

Jhajharia, D., Yadav, B. K., Maske, S., Chattopadhyay, S., and Kar, A. K. (2012). Identification of trends in rainfall, rainy days and 24 h maximum rainfall over subtropical Assam in Northeast India. *Comptes Rendus Geoscience*, 344(1):1–13.

Kabata-Pendias, A. and Pendias, H. (1999). Biogeochemistry of trace elements. *PWN, Warsaw*. (in Polish).

Kabata-Pendias, A. and Pendias, H. (2001). *Trace Elements in Soils and Plants*. CRC Press, Boca Raton, FL, USA.

Liu, X., Bai, Z., Shi, H., Zhou, W., and Liu, X. (2019). Heavy metal pollution of soils from coal mines in China. *Natural Hazards*, 99:1163–1177.

Long, E. R., Macdonald, D. D., Smith, S. L., and Calder, F. D. (1995). Incidence of adverse biological effects within ranges of chemical concentrations in marine and estuarine

sediments. *Environmental Management*, 19(1):81–97.

Misra, B. K. (1992). Optical properties of some Tertiary coals from northeastern India: Their depositional environment and hydrocarbon potential. *International Journal of Coal Geology*, 20(1-2):115–144.

Mukherjee, S. and Srivastava, S. K. (2006). Minerals transformations in northeastern region coals of India on heat treatment. *Energy & Fuels*, 20(3):1089–1096.

Murray, J., Nordstrom, D. K., Dold, B., and Kirschbaum, A. (2021). Seasonal fluctuations and geochemical modeling of acid mine drainage in the semi-arid Puna region: The Pan de Azúcar Pb–Ag–Zn mine, Argentina. *Journal of South American Earth Sciences*, 109:103197.

Olıas, M., Nieto, J. M., Sarmiento, A. M., Cerón, J. C., and Cánovas, C. R. (2004). Seasonal water quality variations in a river affected by acid mine drainage: The Odiel River (South West Spain). *Science of the Total Environment*, 333(1-3):267–281.

Piper, A. M. (1944). A graphic procedure in the geochemical interpretation of water-analyses. *Transactions American Geophysical Union*, 25(6):914–923.

Plumlee, G. S., Smith, K. S., Montour, M. R., Ficklin, W. H., and Mosier, E. L. (1999). Geologic controls on the composition of natural waters and mine waters draining diverse mineral-deposit types. In *The Environmental Geochemistry of Mineral Deposits*, pages 373–432. Society of Economic Geologists.

Rajarathnam, S., Chandra, D., and Handique, G. K. (1996). An overview of chemical properties of marine-influenced Oligocene coal from the northeastern part of the Assam-Arakan basin, India. *International Journal of Coal Geology*, 29(4):337–361.

Sahoo, P. K., Tripathy, S., Panigrahi, M. K., and Equeenuddin, S. M. (2014). Geochemical characterization of coal and waste rocks from a high sulfur bearing coalfield, India: Implication for acid and metal generation. *Journal of Geochemical Exploration*, 145:135–147.

Sahoo, P. K., Tripathy, S., Panigrahi, M. K., and Equeenuddin, S. M. (2017). Anthropogenic contamination and risk assessment of heavy metals in stream sediments influenced by acid mine drainage from a northeast coalfield, India. *Bulletin of Engineering Geology and the Environment*, 76:537–552.

Saikia, B. K., Saikia, A., Choudhury, R., Xie, P., Liu, J., Das, T., and Dekaboruah, H. P. (2016). Elemental geochemistry and mineralogy of coals and associated coal mine overburden from Makum coalfield (Northeast India). *Environmental Earth Sciences*, 75(8):660.

Singh, G. (1987). Mine water quality deterioration due to acid mine drainage. *International Journal of Mine Water*, 6(1):49–61.

Todd, D. K. and Mays, L. W. (2004). *Groundwater Hydrology*. John Wiley & Sons, Hoboken, NJ.

Tutu, H., McCarthy, T. S., and Cukrowska, E. (2008). The chemical characteristics of acid mine drainage with particular reference to sources, distribution and remediation: The Witwatersrand Basin, South Africa as a case study. *Applied Geochemistry*, 23(12):3666–3684.

USEPA (1996). *Method 3050B: Acid Digestion of Sediments, Sludges, and Soils*. Environmental Protection Agency, Washington, DC.

USEPA (1999). *Screening Level Ecological Risk Assessment Protocol for Hazardous Waste Combustion Facilities*. Environmental Protection Agency, Washington, DC.

WHO (2004). *Guidelines for Drinking Water Quality*. World Health Organization, Geneva.

3

Exploration and Utilization of Organic Media for Treating Acid Mine Drainage

This chapter provides an insight about the utilization and comparative evaluation of organic wetland media for the bioremediation of AMD and also assesses the metal accumulation and mobilization within various wetland components.

3.1 Introduction

The biological treatment approach of AMD in CWs is widely applied in lab-scale and field-scale studies (Chen et al., 2021; Younger and Henderson, 2014). From the previous findings of Chapter 2, it was observed that AMD from various collieries of the NEC was deficient in organic carbon and exhibited very low COD (3.10–116 mg L^{-1}). Therefore, for the efficacy of the biological treatment, a continuous supply of organic carbon is essential to ensure the effective removal of metal and sulfate ions by a bacterially mediated sulfate reduction process, as represented by equations (1.7–1.8). The potential application of organic-rich media for heavy metal retention from AMD is highlighted in many studies (Choudhary and Sheoran, 2012; Gibert et al., 2005; Manios et al., 2003a; Ruehl and Hiibel, 2020). Dann et al. (2009) utilized agricultural waste for the bioremediation of acidic iron and sulfate-rich wastewater from titanium mineral processing. Gandy et al. (2016) investigated the potential of compost-based wetland for zinc removal from low strength and near-neutral pH mine drainage in the UK. Chen et al. (2021) observed better sequestration of metals and biogenic metal abatement in cellulosic waste-amended CWs than the control systems established to treat synthetic AMD. However, the possible mitigation and treatment strategies for high strength and low pH mine drainage, as generated in the NEC, Assam using passive organic-based CWs, are not available.

Although wetlands provide long-term metal retention, these can also become sources of metal release under certain conditions (Szkokan-Emilson et al., 2014). For example, reductions in pH can result in the release of metals from peat through competition of binding sites between metal cations and protons (Brown et al., 2000). Additionally, the metal removal

process is seasonally regulated, Xu and Mills (2018) found sulfide oxidation as the dominant reaction in sulfur cycling during the cool months, which increased metal bioavailability. Therefore, the stability of the accumulated metal deposits in wetland media is unpredictable and susceptible to leach over time with the fluctuations in water chemistry. Biermann et al. (2014) reported the remobilization of previously retained metals from the municipal waste organics employed as the wetland media to treat extremely acidic saline groundwater in Australia. Hence, understanding metal removal mechanisms and appropriate investigation for the immobilization of metals to avoid the risk of metal release needs to be carried out before implementing organic-based media in field applications.

The present study aims to evaluate the performance of lab-scale HSSF-CWs using low-cost organic media to treat of synthetic mine wastewater laden with a high content of dissolved metals and sulfate. Due to logistical constraints, experiments were conducted with synthetic mine wastewater simulating similar chemical compositions of AMD generated in the collieries of NEC, Assam, India. As low pH is one of the major concerns of AMD formation, therefore lowest pH and moderate sulfate release with corresponding highest metal concentration exceeding permissible limits were selected. A metal speciation study and Toxicity Characteristic Leaching Procedure (TCLP) test were conducted to identify the metal retention phase and assess the environmental impact of metal mobilization. The contribution of plants in heavy metals uptake was investigated. Further, metagenomics analysis was performed to identify taxa and the relative abundance of microbial communities.

3.2 Materials and methods

3.2.1 Chemicals and reagents

Chemicals and reagents used in the present study were of AR grade as described in section 2.3.2 of Chapter 2. For the preparation of synthetic AMD, analytical grade ferrous sulfate heptahydrate, manganese sulfate monohydrate, aluminium sulfate hydrate, zinc sulfate heptahydrate, cobaltous sulfate heptahydrate, nickel sulfate heptahydrate and chromium sulfate hydrate were procured from SRL/Merck/HiMedia, India. Perchloric acid, ammonium acetate, methyl orange and phenolphthalein indicator were obtained from Merck, India. Hydroxylamine hydrochloride was procured from Himedia, India.

3.2.2 Composition of synthetic AMD

Synthetic AMD was prepared in the laboratory and modelled to represent AMD from the NEC, Assam, India (Table 3.1). As discussed in Chapter 2, highly acidic (pH 2.0–2.5) discharge and moderate sulfate concentration (1000–1500 mg L^{-1}), which consistently released from the various collieries of NEC were selected. Metals exceeding the PDL were chosen and accordingly, the highest metal concentration corresponding to the selected sulfate range was opted. The required amount of metal sulfate salts was added to the tap water. Feed pH was maintained at 2.0, adjusted by adding 5N sulfuric acid. Characteristics of tap water are enlisted in Appendix–III.

Table 3.1 Composition of simulated AMD feed.

Component	Concentration (mg L^{-1}), except pH	Source
pH	2.0 ± 0.4	5N H_2SO_4
Sulfate	1000–1500	–
Fe	100	$FeSO_4.7H_2O$
Mn	6.00	$MnSO_4.H_2O$
Al	25	$Al_2(SO_4)_3.16H_2O$
Zn	5.00	$ZnSO_4.7H_2O$
Co	1.00	$CoSO_4.7H_2O$
Ni	1.00	$NiSO_4.7H_2O$
Cr	1.00	$Cr_2(SO_4)_3.15H_2O$

3.2.3 Design configuration of lab-scale CWs

Lab-scale HSSF-CWs (A, B and C) were designed, consisting of a rectangular acrylic tank (0.95 m long, 0.32 m wide, 0.55 m depth) with four perforated baffles placed in an up and downside fashion along the length of the reactor, thus forming five zones (I, II, III, IV and V) as shown in Fig. 3.1 (a). The operational details of HSSF-CW (B) are discussed in Chapter 5. Sampling ports ($A_1/B_1/C_1$–$A_{11}/B_{11}/C_{11}$) were placed along the length at the mid-depth to collect samples periodically or remained clamped otherwise. CWs were kept outdoor under clear shed on the rooftop of the Environmental Engineering Laboratory, IIT Guwahati.

Common cattail (*Typha latifolia*) collected from natural wetlands of the IITG (average height of 40–50 cm) were planted at a planting density of 25 plants m^{-2} in zones II, III and IV. *Typha* was chosen for the study due to its low pH tolerance (pH < 3.0) and its ability to grow under iron-rich sediments, as documented by (Fyson, 2000). Inlet and outlet zones (I and V) were filled with coarser sized gravel (12.5 mm < ϕ< 20 mm, 50 cm thickness), whereas coarse gravel (10 mm < ϕ< 12.5 mm, 5 cm thickness) was placed at the bottom of zone II, III and IV. Primary reactive media comprised of bamboo chips (20%, v/v) and cow manure (60%, v/v) in HSSF-CW (A); and areca palm husk (20%, v/v) and goat manure (60%, v/v) in the case of HSSF-CW (C) [Fig. 3.1 (b)] was employed. A top soil layer (10%, v/v) was provided over the reactive zones. The use of mixed organic media is intended to provide a good carbon source for the growth of microbes and plants and is also expected to give good hydraulic conductivity, which would prevent clogging or short-circuiting of the system (Herrera-Melián et al., 2014; Wu et al., 2015). The photographic image of the HSSF-CWs (A and C) is shown in Fig. 3.2.

3.2.4 Operational conditions

HSSF-CWs were operated under a continuous flow regime throughout the study. For the estimation of effective volume, the wetland bed was completely saturated with tap water. The effective volume for HSSF-CW (A) and (C) were 66 and 70 L, yielding a porosity of 0.50 and 0.53, respectively. The continuous loading was accomplished using single-channel peristaltic pumps (Miclins, India), adjusted at an influent flow rate of 9.43 and 10 L d^{-1} for HSSF-CW

(A) and (C), respectively, resulting in 7 d HRT. The surface area of each zone was calculated from the length and width of the respective zones. Thus, the applied HLR of the CWs was about 0.03 $m^3\ m^{-2}\ d^{-1}$ (Equation 3.1). After the completion of each feeding cycle, the storage tank was replenished with fresh AMD. For the establishment and acclimatization of microbes, as well as to sustain the growth of plants, a diluted concentration of AMD (10–70% of full strength) was introduced into the CWs from phase I to IV and thereafter full strength AMD was discharged (phase V) (Table 3.2).

$$\text{Hydraulic loading rate (HLR, } m^3m^{-2}d^{-1}) = \frac{\text{Flow rate } (m^3d^{-1})}{\text{Surface area } (m^2)} \quad (3.1)$$

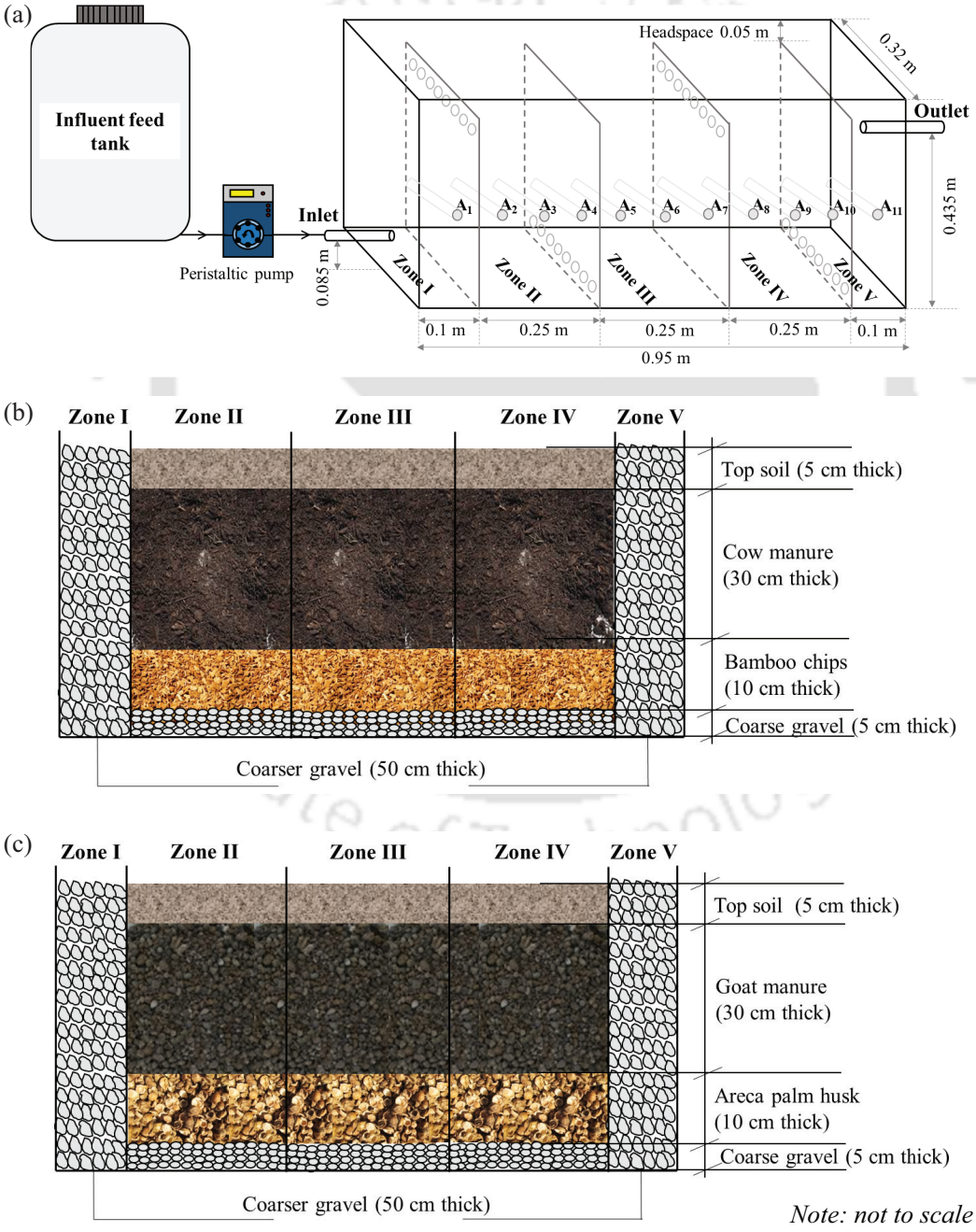

Fig. 3.1 (a) Schematic diagram of lab-scale HSSF-CWs and media layout of (b) HSSF-CW (A) and (c) HSSF-CW (C).

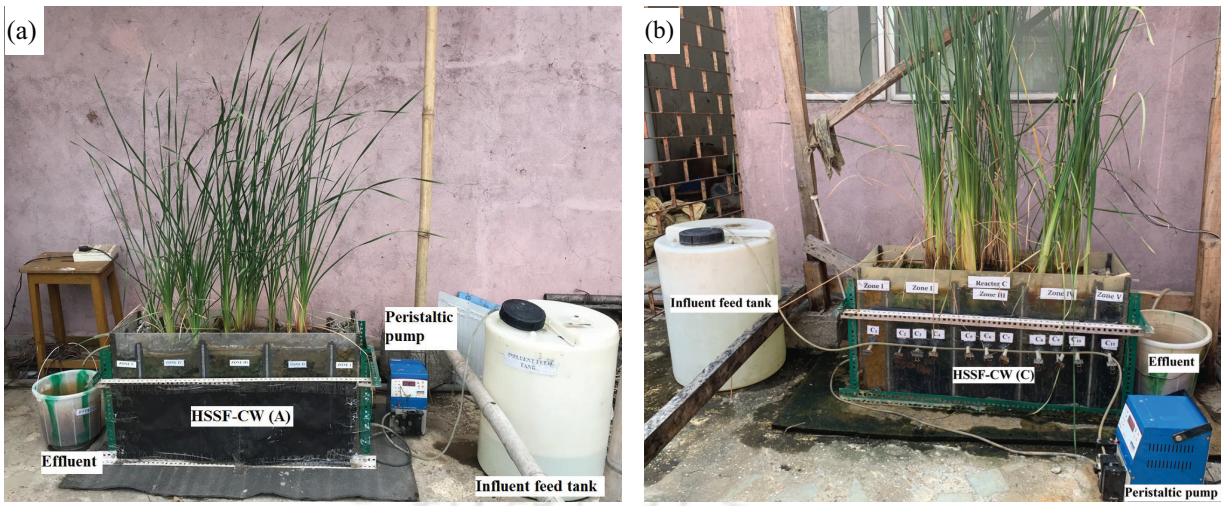

Fig. 3.2 Photographic image of (a) HSSF-CW (A) and (b) HSSF-CW (C).

Table 3.2 Details of operational strategy and feed concentrations during various phases.

Operational phases		Duration (d)	AMD strength (%)	Pollutant concentration (mg L^{-1}, except acidity expressed as mg L^{-1} as $CaCO_3$)	pH
Acclimatization phases	**Phase I**	14	10	Acidity (–), Fe (10), Al (2.50), Mn (0.60), Zn (0.50), Co (0.10), Ni (0.10), Cr (0.10) and SO_4^{2-} (105–162)	4.8–5.9
	Phase II	14	25	Acidity (60–95), Fe (25), Al (6.33), Mn (1.50), Zn (1.25), Co (0.25), Ni (0.25), Cr (0.25) and SO_4^{2-} (236–307)	3.7–3.8
	Phase III	14	45	Acidity (260–280), Fe (45), Al (11.25), Mn (2.70), Zn (2.25), Co (0.45), Ni (0.45), Cr (0.45) and SO_4^{2-} (450–490)	2.6–2.7
	Phase IV	21	70	Acidity (520–596), Fe (70), Al (18), Mn (4.20), Zn (3.50), Co (0.70), Ni (0.70), Cr (0.70) and SO_4^{2-} (869–923)	2.3–2.4
Treatment phase	**Phase V**	120–219	100	Acidity (672–795), Fe (100), Al (25), Mn (6), Zn (5), Co (1), Ni (1), Cr (1) and SO_4^{2-} (1025–1515)	1.8–2.3

3.2.5 Media characterization and batch experiments

Organic materials derived from animal and agricultural waste, which are locally available in abundant quantity at a low cost, were selected to examine the suitability of such materials for the treatment of AMD. Organic wastes (cow manure, goat manure) were collected from local dairy farms in Amingaon, Guwahati, while cellulosic wastes (bamboo chips, areca palm husk) were obtained from the local farm units outside the IIT Guwahati campus. Before elemental analysis, all samples were dried and ground to a fine powder (< 2 mm). pH and EC of the samples were measured by intermittent mixing of solids with deionized water in a horizontal shaker (Reico, India) in 1:10 (w/v) ratio for 1 h (USEPA, 2004). For soluble COD, samples were analyzed after mechanical shaking of solids with deionized water in 1:10 ratio (w/v) in a rotary shaker (GE Motors, India) for 2 h as described by Zagury et al. (2006). The moisture content of a sample was calculated by subtracting the weight of the sample dried at 105°C overnight from the initial sample weight. Volatile solids fraction was estimated by calculating the weight loss of oven-dried sample on ignition at 550°C in a muffle furnace (Karam, 1993).

The total metal concentration in the virgin organic media was estimated according to USEPA (1996). The chemical characterization of different organic media is presented in Table 3.3.

The batch precipitation test was carried out in different sets of conical flasks (50 mL AMD) without any media at a varying initial pH (2.0–9.0) using 1M Na_2CO_3 under constant stirring of 250 rpm based on the earlier study (Seo et al., 2017). After each neutralization step, samples were immediately filtered through 0.45 μm filter paper and analyzed for metal concentration. The test was replicated thrice. The removal efficiency of metal ions after precipitation was calculated by equation (3.2).

$$\text{Metal removal efficiency (\%)} = \frac{C_0 - C_1}{C_0} \times 100 \tag{3.2}$$

where 'C_0' and 'C_1' represent the metal concentration (mg L^{-1}) before and after precipitation.

Another batch study was carried out with various organic materials employed as CW media. Batch experiments were performed in 250 mL Erlenmeyer flasks containing AMD (50 mL) and desired dose of the organic material (0 to 200 g L^{-1}), agitated at 120 rpm in a horizontal mechanical shaker for 24 h. Samples were filtered at the end of the agitation period and analyzed for the change in pH.

Table 3.3 Characterization of different organic media.

Parameters	Bamboo chips	Cow manure	Areca husk	Goat manure
Physicochemical parameters				
pH	7.3 ± 0.1	6.6 ± 0.0	7.7 ± 0.1	7.5 ± 0.1
EC (mS m^{-1})	295 ± 11	43.13 ± 9.39	327 ± 4.58	82.63 ± 1.85
Dry density (g cm^{-3})	0.20 ± 0.02	0.22 ± 0.01	0.10 ± 0.03	0.24 ± 0.01
Moisture content (%)	8.53 ± 0.10	58.97 ± 1.44	12.77 ± 0.27	13.64 ± 1.94
Total volatile solids (%)	95.88 ± 0.16	50.06 ± 6.45	93.01 ± 0.33	71.76 ± 1.97
Soluble COD (mg g^{-1})	6.03 ± 0.95	9.32 ± 0.95	19.81 ± 2.70	27.54 ± 2.28
Specific gravity	1.34 ± 0.04	1.77 ± 0.04	1.23 ± 0.10	1.55 ± 0.04
Elemental analysis (%)				
C	42.51	18.78	44.03	32.08
H	5.42	2.56	5.54	4.38
N	2.30	1.33	2.92	4.69
S	<0.01	<0.01	<0.01	<0.01
C/N ratio	18.48	14.12	15.08	6.84
Metal analysis (mg kg^{-1})				
Fe	124 ± 12.75	865 ± 64	188 ± 31.66	790 ± 84.07
Al	48.33 ± 5.51	157 ± 24.43	112 ± 11.15	111 ± 11.62
Mn	88.89 ± 1.35	441 ± 48.47	37.74 ± 2.95	393 ± 30.50
Zn	8.14 ± 1.46	358 ± 36.32	12.79 ± 2.17	387 ± 34.92
Co	1.21 ± 0.18	25.92 ± 2.27	0.69 ± 0.09	27.54 ± 4.54
Ni	0.94 ± 0.08	14.01 ± 3.15	0.31 ± 0.04	11.16 ± 0.46
Cr	0.17 ± 0.05	13.03 ± 4.12	0.06 ± 0.02	9.87 ± 1.61

Parameters are presented in the 'xx ± yy' format, where 'xx' is the average of three independent values and 'yy' is the standard deviation.

3.2.6 Biomass activity assays

Assessment of microbial biomass activity of the active microorganisms in HSSF-CW (A) and (C) was performed after the acclimatization phase and at the end of the study to account for the overall change in treatment efficiency over time. Biomass activity assays (S1 and S2) were conducted to determine the heterotrophic substrate utilization and specific sulfidogenic activity. Initially, a known amount of wet solid (as biomass) was taken from the CW and total volatile solids (TVS) was measured as per APHA (2012). The assays were conducted in serum bottles having provisions for feed/purging and pressure release tubes with 1 L liquid volume (Fig. 3.3). All assays were performed under continuous stirring mode. A known amount of wetland media was added to each serum bottle to get TVS in the range of 1–1.50 g L^{-1}.

For the S1 assay, only a simple carbon substrate (dextrose) was added such that the initial COD concentration was about 1.50 g L^{-1}. For the S2 assay, carbon and sulfate source were added as dextrose (COD = 1.20 g L^{-1}) and Na_2SO_4 (SO_4^{2-} = 1.70 g L^{-1}) to maintain COD/SO_4^{2-} ratio of 0.68–0.70. A blank assay (B) was also conducted without any substrate addition to determine the COD exerted by the media itself. Nutrients (nitrogen, phosphorous and trace elements) were not supplemented to restrict the biomass growth during the test period. Bottles were tightly sealed, purged with nitrogen for about 15 min and immediate samples at t = 0 were withdrawn using a syringe (5 mL), filtered and stored at 4°C until analysis for COD and sulfate. Samples were drawn initially at shorter intervals (0.25 h) and later at longer intervals (up to 6 h) for 48 h after stirring was stopped. Note that the pressure tube was clamped when withdrawing samples. After the first feeding cycle, the supernatant was carefully decanted and refilled with a similar feed, which constituted the second feeding. Likewise, the procedure was repeated for the third feeding cycle and finally, the amount of TVS was determined at this stage. The biomass activity was estimated by the final TVS and slope of the linear portion of the cumulative COD removed (or sulfate reduced) in the third feed cycle and calculated by modifying the methanogenic activity of Jawed and Tare (1999) (Equation 3.3).

$$\text{Biomass activity}\left(\frac{\text{mg COD or } SO_4^{2-} \text{ removed}}{\text{mg TVS d}}\right) = \text{Slope}\left(\frac{\text{mg COD or } SO_4^{2-} \text{ removed}}{\text{h}}\right) \times \frac{24\ \text{h}}{\text{d}} \times \frac{1}{\text{mg TVS}} \quad (3.3)$$

3.2.7 Microbial metagenomics

The taxonomic profiling of microbial communities involved in the bioremediation of AMD in HSSF-CWs was performed using 16S MicroBiome Profiling. A representative homogenized media samples from HSSF-CW (A) and wastewater samples from the triplicate sampling of middle zones from HSSF-CW (C) were sent to Eurofins Genomics (Bangalore, India) for 16S (V3–V4) ribosomal ribonucleic acid (rRNA) sequencing using Illumina MiSeq platform. The sequencing data have been deposited on National Center for Biotechnology Information (NCBI) in the bioprojects PRJNA734092 and PRJNA777238 as Sequence Read Archives (SRA) (SRR14886503, SRR14886504, SRR16925072 and SRR17024153) with sample accession

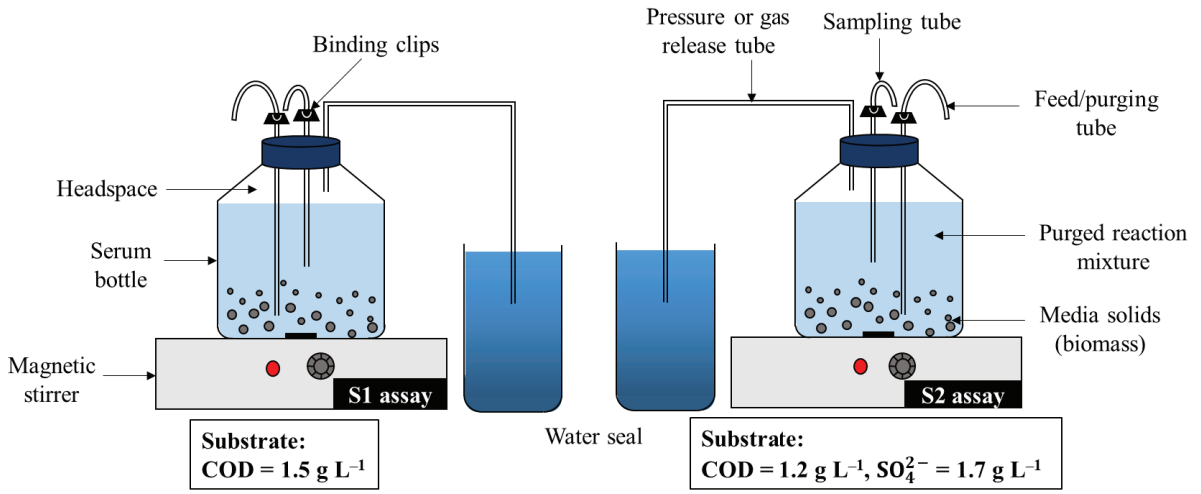

Fig. 3.3 Schematic of the biomass activity test set-up.

numbers SAMN19471447, SAMN19471448, SAMN22837305 and SAMN23393983. The detailed procedure adopted for DNA extraction, amplification, library preparation, sequencing and sequence data analysis by Eurofins Genomics, India, are summarized below.

- *Genomic DNA extraction, amplification, library preparation and sequencing by Eurofins Genomics, India*: Metagenomic DNA was isolated using a commercially available kit (Nucleospin Soil, Macherey-Nagel) and the quality of the isolated metagenomic DNA sample was quantified using NanoDrop spectrophotometer (NanoDrop One, ThermoScientific). The first amplicon polymerase chain reaction (PCR) was set up using the isolated metagenomic DNA along with a bacterial 16S V3–V4 region-specific primer set. Forward and reverse primers used for the amplification of 16S rRNA targeting bacteria were GCCTACGGGNGGCWGCAG and ACTACHVGGGTATCTAATCC, respectively. The PCR product (3 μL) was resolved on 1.2% agarose gel at 120 V for approximately 60 min (or till the sample reached $3/4^{th}$ of the gel). The first amplicon generation was followed by next-generation sequencing (NGS) library preparation using Nextera XT Index Kit (Illumina Inc.). The library was sequenced on the MiSeq platform using 2 × 300 bp chemistry. The amplicon with the Illumina adaptor was amplified using i5 and i7 primers that added multiplexing index sequences and common adapters required for cluster generation (P5 and P7). The amplicon library was purified by AMPure XP beads and quantified using Qubit Fluorometer (Qubit 3.0 Fluorometer, Life Technology). The amplified library was analyzed on the 4200 TapeStation system (Agilent Technologies, USA) using D1000 Screen tape as per manufacturer instructions. After obtaining the mean peak sizes from the tapestation profile, the library was loaded onto MiSeq at an appropriate concentration (10–20 pM) for cluster generation and sequencing. The kit reagents (MiSeq Reagent Kit v3, Illumina) were used in the binding of samples to complementary adapter oligoes on paired-end flow cell. The adapters were designed to allow selective cleavage of the forward strands after re-synthesis of the reverse strand during sequencing. The copied reverse strand was then used to sequence from the opposite end of the fragment.

- *Sequence data analysis*: Quantitative Insights Into Microbial Ecology (QIIME) pipeline (v1.8) was used to process raw reads. High-quality clean pair end (PE) reads were obtained using Trimmomatic (v0.38) and then stitching of PE data into single end reads. Operational taxonomic units (OTUs) were obtained by comparing sequence similarity to the Greengenes database (version 13_8). All the sequences from the samples were clustered into Operational Taxonomic Units (OTUs) based on their sequence similarity using UCLUST algorithm at 97% sequence similarity.

3.2.8 Analytical methods

3.2.8.1 Analysis of water samples

In general, standard techniques, as mentioned in the Standard Methods (APHA, 2012) have been followed for the analysis of influent and effluent samples. Collection of influent and effluent water samples was performed regularly on every alternate day in two sets of sterile polystyrene specimen tubes. Samples were immediately filtered and analyzed for pH, EC, temperature, acidity and alkalinity. pH was measured by a digital pH meter (μpH System 361, Systronics, India) with 0.01 sensitivity and temperature correction facility. The pH meter was calibrated using standard buffer solutions (pH 4.0 and 7.0) periodically. Conductivity was measured by a conductivity meter (VSI-04 Deluxe, VSI Electronics, India) and was calibrated using 0.1N KCl solution at room temperature before any analysis and temperature was measured by a thermometer. Acidity and alkalinity were determined by the titrimetric procedure as detailed in APHA (2012). Measurement of ammonia, nitrite, nitrate, COD, TDS and sulfate followed the same procedure as described in section 2.3.3 of Chapter 2.

Another set of samples was acidified (pH < 2.0) using two drops of 60% nitric acid, filtered with a 0.45 μm filter and aspirated to direct air-acetylene flame ionization for the determination of Fe, Mn, Zn, Cr, Co and Ni, whereas direct nitrous oxide-acetylene flame mode was used for the determination of Al using FAAS. The standard calibration curves for various metals are provided in Appendix–II. The metal removal efficiency (%) was obtained using equation (3.4).

$$\text{Metal removal efficiency (\%)} = \frac{\text{Change in metal concentration}(C_{in} - C_{eff})}{\text{Initial concentration } (C_{in})} \times 100 \quad (3.4)$$

where 'C_{in}' and 'C_{eff}' represent mean metal concentration (mg L^{-1}) in the influent and effluent, respectively.

3.2.8.2 Analysis of plant samples

The growth of the plants in different zones was monitored periodically by measuring the height of plants, plant density and chlorophyll content of the leaves. Total chlorophyll content (chlorophyll a, b and c) was determined by the trichromatic method (APHA, 2012) and represented as mg per g fresh weight (FW) of the leaves.

After the completion of the experiment, the emergent plants reached maturity and were harvested for chemical analyses. Heavy metal estimation in plant parts was performed

as per Allen et al. (1974). Plants were segregated into shoots (aboveground) and roots (belowground) parts. The surface impurities of plant parts were removed by repeated washing with tap water and finally with distilled water. The dry plant biomass consisting of both shoots and roots parts was calculated by oven drying for 24 h at 80°C (Mishra et al., 2008). The dried samples were then homogenized to fine-textured powder; 1 g of powdered plant sample was digested using a tri-acid digestion mixture (HNO_3, $HClO_4$ and H_2SO_4; 5:1:1) at 80°C until clear solution. The digested samples after filtration were stored for metal analysis. The concentration of heavy metals in fresh plants obtained from the natural habitat before planting into the CW was analyzed and referred to as 'unpolluted' throughout this chapter.

The bio-concentration factor (BCF) denotes the phytoaccumulation ability of plants, which is defined as the ratio of total metal content in plant tissues (C_p, mg kg^{-1}) to total metal content in the top layer of soil (C_s, mg kg^{-1}), assuming the homogeneous distribution of metals throughout the soil layer in each zone. It is given by equation (3.5) (Dan et al., 2017).

$$BCF = \frac{C_p}{C_s} \tag{3.5}$$

The translocation factor (TF) depicts the ability of plants to translocate the heavy metals from the belowground (roots) to aboveground (shoots and leaves) parts of a plant. It is defined as the ratio of metal content in the aboveground (C_a, mg kg^{-1}) to the belowground plant tissues (C_b, mg kg^{-1}). It is given by equation (3.6) (Sasmaz et al., 2008).

$$TF = \frac{C_a}{C_b} \tag{3.6}$$

3.2.8.3 Speciation of metals in wetland media

At the end of the experimental period, the media samples were collected from different depths of each zone of the HSSF-CW (A). The five-step sequential extraction procedure was used to assess the partitioning of various metals among the various forms that exist in geochemical phases. Samples were partitioned into each fraction using suitable extracting reagents at every step as described by Tessier et al. (1979). After each step, the supernatant was decanted from the residual soil and stored until metal analysis, whereas the residue was rinsed with 8 mL deionized water after centrifugation at 10,000 rpm for 5 min and this second supernatant was discarded to ensure removal of reagents used in the previous steps.

(a) Exchangeable fraction (F_1)

1 g of dried samples were extracted at room temperature by agitating the sample and extracting solution continuously for 1 h in a horizontal shaker. The extracting reagent used was 8 mL magnesium chloride solution (1M $MgCl_2$) at pH 7.0. Metals extracted in the exchangeable fraction include weakly adsorbed metals and can be easily released by the ion-exchange.

(b) Bound to carbonates (F_2)

The residue of fraction F_1 was extracted using 8 mL of sodium acetate (1M NaOAc) by agitating

the mixture at room temperature for 5 h. The pH of the extracting reagent was adjusted to pH 5.0 using acetic acid. A significant amount of trace metals can be co-precipitated with carbonates at the appropriate pH.

(c) Bound to iron and manganese oxides (F_3)

The residue from fraction F_2 was further extracted using 20 mL of hydroxylamine hydrochloride (0.4M $NH_2OH.HCl$) in 25% (v/v) acetic acid in a water bath (ICT, India) at 96°C for 6 h with occasional agitation. Under reducing conditions, Fe (III) and Mn (IV) could release adsorbed trace metals.

(d) Bound to organics and sulfides (F_4)

The residue from faction F_3 was then extracted using 3 mL of 0.02M HNO_3 and 5 mL of 30% (v/v) H_2O_2. The mixture was heated to 85°C in a water bath for 2 h with occasional agitation and allowed to cool down. Another 3 mL of 30% H_2O_2 was then added. The mixture was heated again at 85°C for 3 h with occasional agitation and allowed to cool down. Then 5 mL of 3.2M ammonium acetate in 20% (v/v) nitric acid was added, followed by dilution to a final volume of 20 mL. Under oxidizing conditions, organic matter can be degraded, leading to a release of soluble trace metals.

(e) Residual fraction (F_5)

The residue from fraction F_4 was digested with 10 mL of H_2SO_4:$HClO_4$ mixture in the ratio 5:1 (v/v) for 2 h at 300°C in the block digestion system (Pelican, India). This fraction largely consists of mineral compounds, where metals are firmly bonded within the crystal structure of the minerals comprising the soil. These metals are not expected to be released in solution over a reasonable period under the conditions typically encountered in nature.

The potential leaching of metals from wetland media was studied by TCLP as per SW 846 test Method 1311 (USEPA, 1992). TCLP test was conducted to investigate the mobility of metals into the environment concerning the safe disposal of media onto the land. Wetland media from each zone was collected and samples were dried, crushed and homogenized to pass through a 9.5 mm standard sieve. Before the leaching procedure, pH of the samples was measured in accordance to USEPA (1992) for deciding the appropriate extraction fluid and accordingly extraction solution consisting of glacial acetic acid and 1N sodium hydroxide at pH 4.93 ± 0.05 was selected as the extraction solution because pH of all samples was < 5.0. Powdered samples were extracted in screw cap vessels (Teflon bottles), keeping solids to extraction fluid ratio of 1:20 (w/v basis). The mixture was agitated continuously for 18 ± 2 h at 30 ± 2 rpm in a rotary shaker under ambient temperature. Following extraction, liquid part (supernatant) after centrifugation at 6000 rpm was separated using 0.45 μm filter paper and later analyzed for metal concentration in FAAS.

3.2.8.4 Mineralogical characterization of wetland solids

The solid wet media (or precipitate) collected from CWs were immediately transferred into the sterile falcon tubes with minimal headspace, sealed and preserved at 4°C. Further,

for obtaining mineralogy, samples were powdered by lyophilization procedure and X-ray powder diffraction (XRD) (Rigaku SmartLab X-ray Diffractometer) was performed over a scanning range of 2θ ranging from 5° to 80° (at a step size of 0.02°) with Cu Kα anode (wavelength, λ= 0.154 nm, 40 mA, 40 kV). The resulting peaks in the XRD spectra were analyzed in the PANalytical X'Pert HighScore Plus (v2.2b) by retrieving the Joint Committee on Powder Diffraction Standards (JCPDS) reference number in the Powder Diffraction File (PDF) database. The surface morphology was observed by FESEM images (Gemini 300, Zeiss). The elemental composition was obtained as described in Chapter 2 (section 2.3.3).

3.3 Results and discussions

3.3.1 Batch precipitation and adsorption using organic media

The results of metal removal from the batch precipitation experiments at different pH are given in Table 3.4. The metal removal efficiency increased with the pH of the solution, achieving 100% removal at pH 9.0, except manganese (84.83%). In general, the precipitation of the metals at pH 6.0–9.0 was in the order: Fe (100%) > Al (92.88–100%) > Cr (83.38–100%) > Zn (82.10–100%) > Ni (44.92–100%) > Co (34.44–100%) > Mn (22.40–84.83%), which follows the order of metal precipitation according to the pK_{sp} values [Fe (III): 37.40, Zn (II):16.92, Cr (II): 15.70, Ni (II): 14.70, Co (II): 12.85, Mn (II): 10.74, Al: 4.74], except aluminium. The precipitation behavior of metals like Fe, Al and Mn were similar to Seo et al. (2017). pH is the most critical physical parameter that governs the metal removal process from an aqueous solution. The precipitation of metal ions, as well as the binding of metal ions with the surface of media, depends on the pH of the solution. Fig. 3.4 depicts the increase in pH of AMD with the increase in media dose. At the highest media dose of 200 g L^{-1}, pH increased to 7.4, 7.9, 7.1 and 7.2 with cow manure, goat manure, bamboo chips and areca palm husk, respectively. Animal wastes were most effective in raising the pH and exhibited strong buffering capacity, which could further assist in metal removal as seen in Table 3.4.

Table 3.4 Results of batch precipitation experiment at different pH.

Initial pH[a]	Metal removal[b] (%)						
	Fe	Mn	Al	Zn	Co	Ni	Cr
2.0	0.98 ± 0.30	0.00	0.00	0.00	0.00	1.10	0.00
2.5	13.88 ± 0.51	1.64 ± 0.05	0.00	3.24 ± 0.10	0.00	1.30	0.85
3.0	29.14 ± 0.39	3.26 ± 0.02	0.04 ± 0.01	23.38 ± 0.05	0.50 ± 0.01	1.60	6.03 ± 0.01
3.5	30.91 ± 0.03	9.11 ± 0.16	3.48 ± 0.76	29.44 ± 0.03	0.60	2.00	9.35 ± 0.02
4.0	31.79 ± 0.03	14.72 ± 0.13	16.20 ± 0.45	33.53 ± 0.05	1.10	2.50 ± 0.01	13.48 ± 0.02
4.5	32.54 ± 1.05	16.67 ± 0.04	27.41 ± 0.89	37.48 ± 0.03	2.00	3.10 ± 0.01	14.44 ± 0.02
5.0	39.29 ± 1.13	20.11 ± 0.11	66.59 ± 0.19	39.02 ± 0.06	3.40 ± 0.01	9.30 ± 0.03	22.92 ± 0.01
5.5	79.26 ± 0.89	22.31 ± 0.11	90.60 ± 0.24	49.33 ± 0.13	21.72 ± 0.02	23.14 ± 0.01	33.30 ± 0.01
6.0	100	22.40 ± 0.11	92.88 ± 0.13	82.10 ± 0.02	34.44 ± 0.01	44.92 ± 0.01	83.38 ± 0.01
7.0	100	43.05 ± 0.09	100	99.14	76.61 ± 0.02	65.34 ± 0.05	98.06
8.0	100	51.79 ± 0.06	100	99.40	94.39 ± 0.01	91.58 ± 0.02	100
9.0	100	84.83 ± 0.03	100	99.64	100	100	100

[a]Initial metal concentration (mg L^{-1}): Fe (100), Mn (6), Al (25), Zn (5), Co (1), Ni (1) and Cr (1).

[b]The data is presented in the 'xx' or 'xx ± yy' format, where 'xx' is the average of three independent values and 'yy' is the standard deviation.

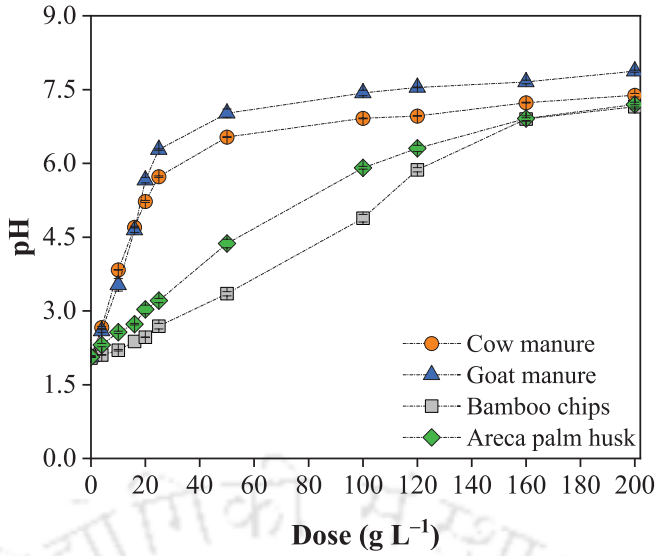

Fig. 3.4 Change in pH with different doses of organic media.

This is attributed to buffering from bicarbonates and organic acids (such as humic acids) in manure and the dissolution of the surface-bound hydroxyl ion from organic materials (Song et al., 2012). In addition, the presence of functional groups (phenolic, hydroxyl and methoxyl, etc.) in agro-organic media aid in metal binding by chelation (Komy et al., 2013). Therefore, the sorption mechanism would govern the short-term metal retention during initial operation, whereas acidity alleviation and precipitation at pH > 6.0 would be the major long-term metal retention route. However, fluxes in the ionic composition of wastewater and the redox state of the wetland control the re-dissolution of the adsorbed metals.

3.3.2 Performance of organic media amended HSSF-CW (A)

3.3.2.1 Physicochemical characteristics of effluent

Fig. 3.5 shows the effluent characteristics profile of HSSF-CW (A) for various physicochemical parameters. Mean effluent pH was 7.1 (phase I–IV) and 6.3 (phase V). Release of ions during the mineralization process of organic matter contributed to higher EC and TDS values at the beginning of operation (Moreno et al., 1999). EC and TDS exhibited a positive correlation (Appendix–IV). In phase V, effluent pH, EC and TDS ranged from 4.5 to 7.2, 86 to 191 mS m^{-1} (averaged 129 mS m^{-1}) and 856 to 2088 mg L^{-1} (averaged 1260 mg L^{-1}), respectively.

No external carbon was added in the influent as carbon-rich solid organic media (cow manure and bamboo chips) were expected to provide the carbon required for the biological process. Effluent COD was very high in the range of 1500 mg L^{-1} during phase I and II; however, from phase III, it declined to much lower values meeting the PDL (< 250 mg L^{-1}) due to the depletion of more soluble and readily available organics. Influent ammonia concentration was < 1 mg L^{-1}, whereas a relatively higher concentration (10–45 mg L^{-1}) was observed in the effluent in phase I–III due to the release of ammonia from the decomposition of organics, which eventually declined to 1.12 mg L^{-1} in phase V. Effluent ammonia and COD varied from 0.32 to 6.86 mg L^{-1} and 23.85 to 243 mg L^{-1}, respectively in the treatment phase V. All through the experimental period, nitrite and nitrate concentrations measured in the

effluent were about 0.01–2.98 and 0.04–6.48 mg L^{-1}, respectively.

Dissimilatory sulfate reduction is an important biological process that explains the effective removal of sulfate ions and alkalinity generation in the HSSF-CW (A). Initially,

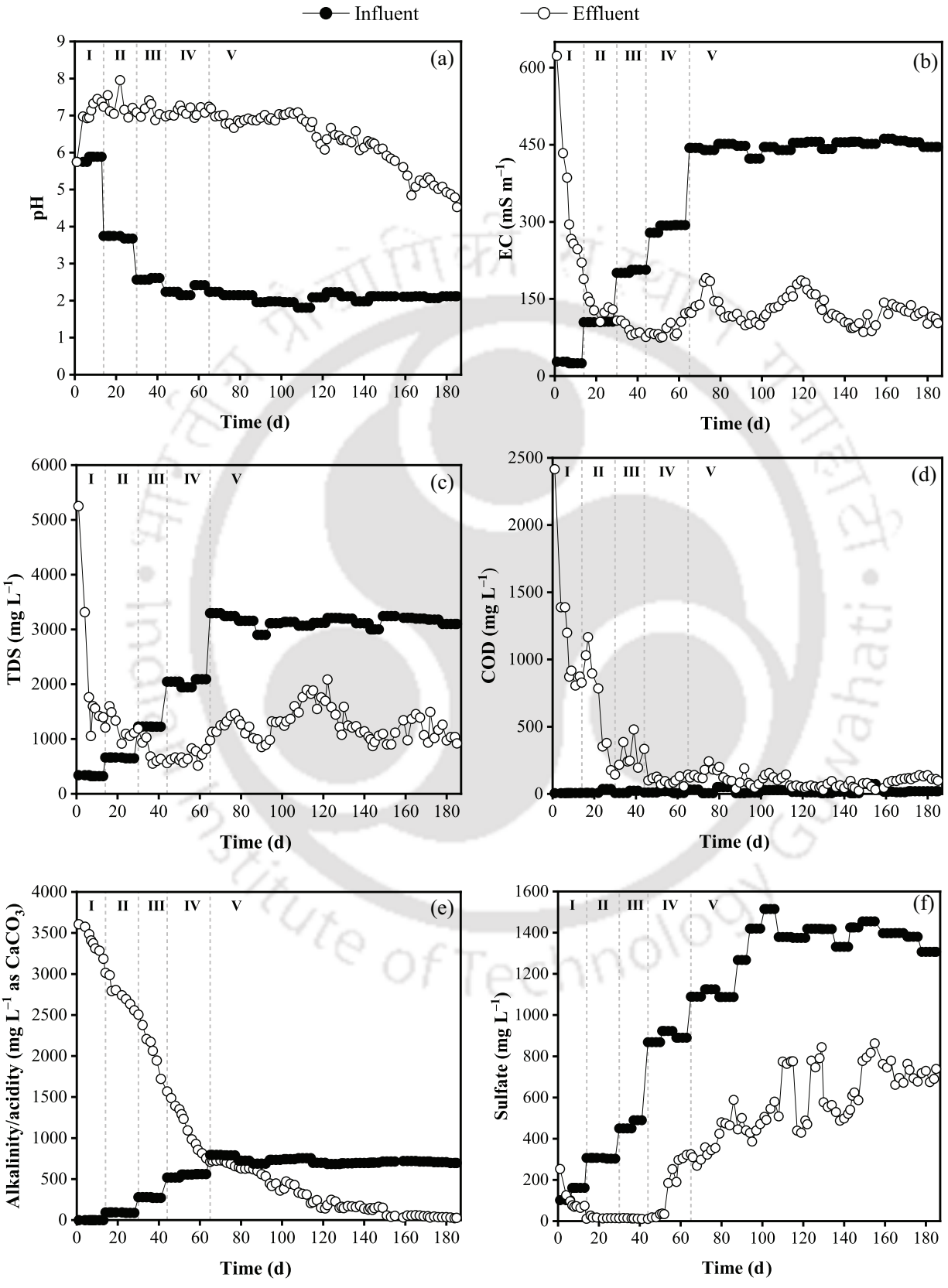

Fig. 3.5 Influent and effluent profile of HSSF-CW (A) for (a) pH, (b) EC, (c) TDS, (d) COD, (e) acidity (influent)/alkalinity (effluent) and (f) sulfate.

during the acclimatization period, an average sulfate removal efficacy of 22.74, 94.85, 97.35 and 81.80% was obtained in phase I, II, III and IV, respectively. Some fluctuations in the influent sulfate concentration (1100–1500 mg L^{-1}) were measured in the phase V. However, higher sulfate removal (40.41–75.29%) was achieved as compared to other studies (Collins et al., 2005; Sheoran, 2017) at a mean influent sulfate concentration of 1300 mg L^{-1}. The effluent sulfate concentration persisted below the permissible discharge (750 mg L^{-1}) (EPA, 2002), except few occurrences with an average effluent sulfate concentration of about 581 mg L^{-1}. For about 150 days, effluent pH > 6.0 was recorded and then a gradual decrease in pH was observed. Similarly, high alkalinity generation (∼ 600 mg L^{-1} as $CaCO_3$) was observed initially at the start-up, which eventually decreased twenty-fold (∼ 30 mg L^{-1} as $CaCO_3$) at the end of phase V. This could be due to the depletion of buffering capacity of the media and limited sulfate reduction with minimal organics (COD of 80.79 mg L^{-1} inside CW) available for sustaining biological processes. An attempt was made to compare the measured alkalinity values and theoretical bicarbonate alkalinity production based on the amount of sulfate reduced. Stoichiometrically, 1 mg L^{-1} of sulfate reduced produces 1.04 mg L^{-1} as $CaCO_3$ bicarbonate alkalinity according to equation (1.7). The measured effluent alkalinity production averaged 290 mg L^{-1} as $CaCO_3$ in the CW, much lower than the theoretical alkalinity value of 787 mg L^{-1} as $CaCO_3$. The difference between the measured and calculated alkalinity values suggests significant alkalinity consumption for the elimination of strong influent acidity (averaged 722 mg L^{-1} as $CaCO_3$). The measured alkalinity in the effluent is essentially the residual alkalinity after AMD neutralization. In addition to the microbial-mediated sulfate reduction, various other biological processes such as photosynthesis (Equation 3.7), ammonification (Equation 3.8), denitrification, methanogenesis (Equation 3.9), and iron and manganese reduction (Equation 3.10) occur in wetland ecosystems which contribute to the acid-neutralization (Bechard, 1994; Hallberg and Johnson, 2005; Johnson and Hallberg, 2002) and may account for the residual or net alkalinity.

$$6HCO_3^- \text{ (weak base)} + 6H_2O \longrightarrow C_6H_{12}O_6 + 6O_2 + 6OH^- \text{ (strong base)} \quad (3.7)$$

$$NH_3 + H^+ \longrightarrow NH_4^+ \quad (3.8)$$

$$CH_3COO^- + H^+ \longrightarrow CH_4 + CO_2 \quad (3.9)$$

$$CH_2O + 4Fe(OH)_3 \longrightarrow H_2CO_3 + 4Fe^{2+} + 8OH^- + 2H_2O \quad (3.10)$$

3.3.2.2 Results of biomass activity test from HSSF-CW (A)

The heterotrophic activity was determined from the maximum slope of the S1 assay, which represents the maximum substrate utilization. The specific sulfidogenic activity was determined from the S2 assay. The amount of sulfate reduced corresponding to COD metabolized by SRB was calculated as each mole of sulfate reduced corresponds to 64 g COD. After acclimatization of HSSF-CW (A), the heterotrophic activity and specific sulfidogenic activity were 3.19 mg COD removed mg TVS^{-1} d^{-1} and 0.83 mg sulfate reduced mg TVS^{-1}

d^{-1}, respectively (Fig. 3.6). However, a significant reduction was observed at the end of the study as heterotrophic activity and specific sulfidogenic activity reduced to 1.43 mg COD removed mg TVS^{-1} d^{-1} and 0.60 mg sulfate reduced mg TVS^{-1} d^{-1}, respectively. This could be possibly due to the lowering of effluent pH affecting microbial growth (or functioning) or microbial death after prolonged exposure to AMD. The final TVS measured was slightly higher than the initial TVS, implying that biomass growth was not completely restricted with considerably higher cumulative COD or sulfate removal in the last cycle (cycle 3).

3.3.2.3 Identification of taxa and abundance of microbial communities

The 16S rRNA sequencing was performed during the treatment phase V, yielding about 60,000 sequences per sample. Kingdom Archaea consisted of about 21.52%, whereas the remaining (78.48%) consisted of the bacterial kingdom, indicating that most bacterial taxa present in the media sample were targeted and identified. At the phylum level, archaea identified were Euryarchaeota (18.60%) and Crenarchaeota (2.92%). The metagenomics of the bacterial flora revealed the major dominant phyla included Firmicutes (36.08%), Proteobacteria (16.07%), Actinobacteria (8.81%), Planctomycetes (7.79%), Chloroflexi (3.52%), Acidobacteria (1.85%) and Fibrobacteres (1.47%). Other additional phyla identified

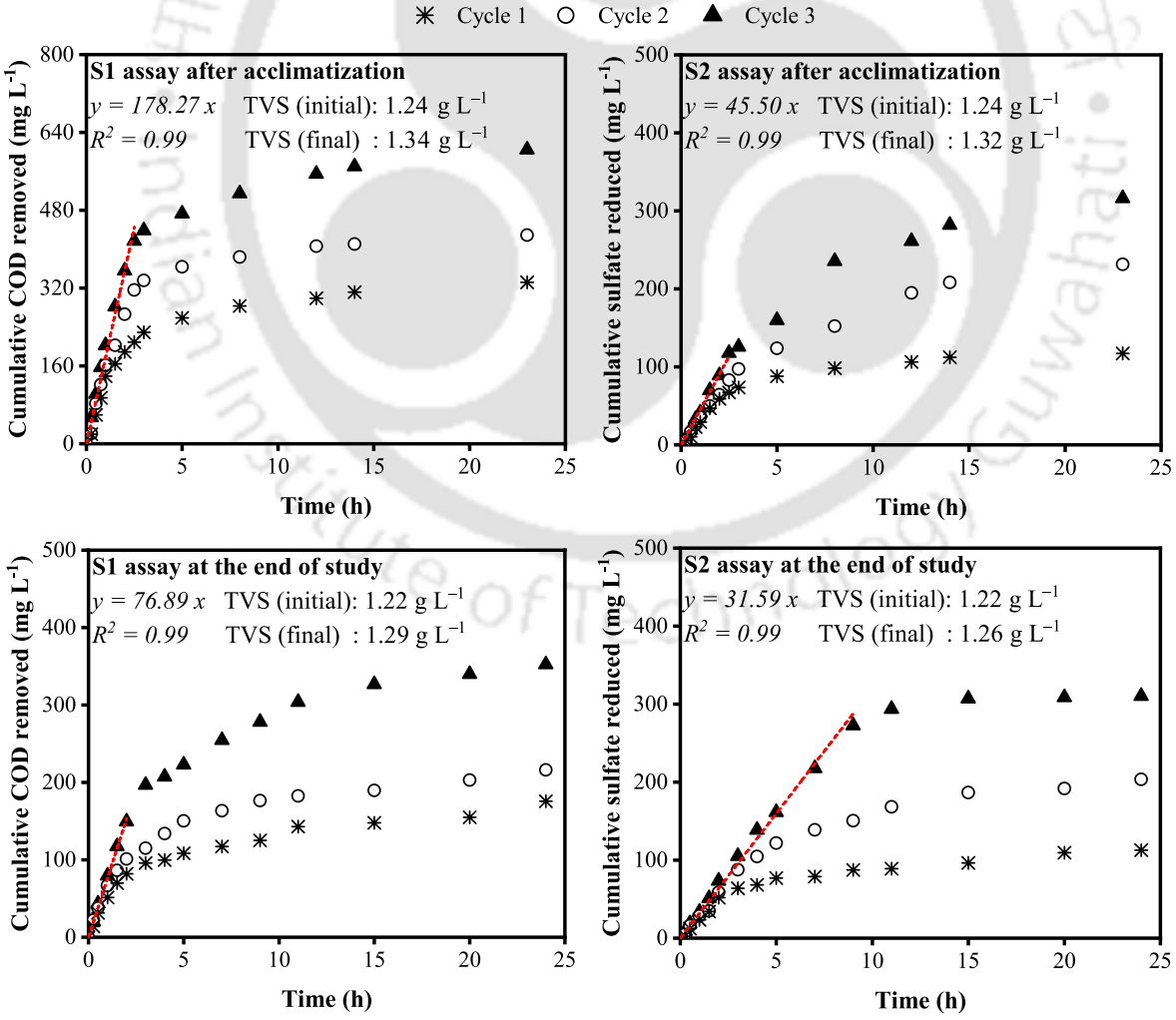

Fig. 3.6 Cumulative COD removal (mg L^{-1}) and sulfate reduction (mg L^{-1}) with time for HSSF-CW (A).

(< 1%) were Bacteroidetes (0.51%), Chlamydiae (0.36%), Verrucomicrobia (0.22%), Spirochaetes (0.19%), Nitrospirae (0.19%) and Chlorobi (0.13%). Many authors have also revealed similar bacterial groups in AMD impacted streams and sediments (Fan et al., 2016; Ly et al., 2019). The most abundant classes detected were Clostridia (20.14%), Bacilli (15.94%), Methanomicrobia (14.82%), Alphaproteobacteria (9.27%), Planctomycetia (7.04%), Actinobacteria (6.40%) and Deltaproteobacteria (4.95%), while some less detected classes (< 5%) were Methanobacteria (3.35%), MCG (2.90%), Anaerolineae (2.16%), TG3 (1.47%) and Acidimicrobiia (1.44%). The relative abundance of acid-tolerant Gammaproteobacteria and Betaproteobacteria were similar. At the order level, most abundant orders were Clostridiales (18.51%), Bacillales (13.53%), Methanosarcinales (12.42%), Rhizobiales (7.11%) and Actinomycetales (6.39%). The most abundant family identified were Methanosarcinaceae (12.19%), Clostridiaceae (11.25%) and Planococcaceae (9.26%) followed by Hyphomicrobiaceae (4.17%) and Micromonosporaceae (4%), while many remained unclassified (16.82%). The relative abundance of different microbial communities at the phylum and genus level is shown in Fig. 3.7.

The abundance of Firmicutes and Proteobacteria has been reported in extreme environmentally stressed conditions, such as hypersaline sediments and heavy metal contaminated soils (Emmerich et al., 2012). Therefore, the dominance of Firmicutes, Proteobacteria, Actinobacteria, Planctomycetes and Chloroflexi indicated their ability to adapt and grow in an acidic metal-rich environment. Some less dominant genera of sulfur metabolizing and sulfur-reducing bacteria (≤ 1%) identified were *Desulfobacca*, *Desulfomonile*, *Desulfarculus*, *Desulfovibrio*, *Sulfuricurvum*, *Desulfosporosinus*, *Desulfococcus*, *Desulfomicrobium*, *Desulfotomaculum* and *Desulfitobacter*. Thus, their presence confirms the SRB activity in the HSSF-CW (A).

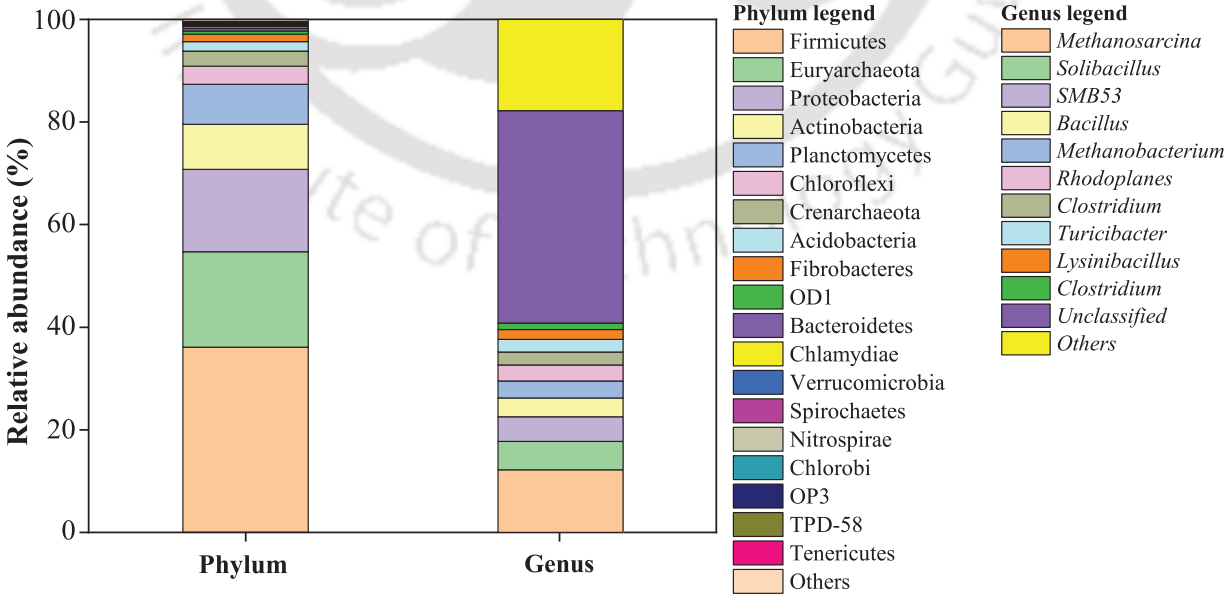

Fig. 3.7 Relative abundances (%) of dominant lineages at phylum and genus levels in media samples from HSSF-CW (A) (top 19 categories at phyla and genera taxonomical levels).

3.3.2.4 Metal removal profile

The highest metal removal efficiency was recorded for Cr (99.75%), followed by Ni (95.46%), Zn (94.42%), Co (91.61%), Fe (90.90%) and Al (60.52%) in the treatment phase V. Manganese removal was inconsistent in phase V and eventually, concentration increased in the effluent to 15 mg L^{-1}. Despite good removal efficiency, iron, aluminium and cobalt concentration in the effluent did not meet the permissible discharge limit (Fig. 3.8). It should be noted that CPCB (1993) guideline was followed for iron and manganese, whereas a more stringent EPA (2002) guideline was followed for other metals (Al, Zn, Co, Ni and Cr).

Hydrolysis or oxidation of aluminium at a neutral pH 7.0 to form insoluble oxides, oxyhydroxides and hydroxides are the major removal pathways for aluminium. Many metals very often undergo co-precipitation with iron and manganese hydroxides (or oxyhydroxides) and thus, get subsequently removed. Additionally, metals (such as nickel) precipitate and form very stable insoluble metal sulfides under anaerobic conditions (Tchobanoglous et al., 2003). Iron plaque formation near the plant roots and oxides/hydroxides precipitate on gravel surface was visible (Fig. 3.9), where co-precipitation and sequestration of zinc and nickel are often reported (Pi et al., 2011). Thus, the high removal efficiency of zinc is explained by the complex interaction of bio-chemical routes involving precipitation as oxides and sulfides (Stein et al., 2007), co-precipitation reactions with iron oxides and plant uptake (about 1–3% of Zn removal) (Gillespie Jr. et al., 2000). In general, higher removal efficacy of nickel (31–99%) and chromium (65–100%) is reported in small and full-scale CWs (Dan et al., 2017; Lesage, 2006; Ranieri, 2012) and thus, very comparable with the present study. Besides adsorption to the organic matter, sulfide precipitation and rhizofiltration contribute largely to nickel and chromium retention (Dan et al., 2017; Kröpfelová et al., 2009). However, major reduced sulfur compounds, which predominantly exist at pH $\leq$ 7.0 are mostly H_2S and to some degree HS^-, therefore, most of the metals would precipitate as metal oxides or hydroxides and sulfides (Equation 1.8).

Although cobalt was effectively removed, very limited information is available on the effectiveness of cobalt removal in CWs; therefore, it is difficult to understand the governing mechanism of its removal and compare with the existing literature. Ye et al. (2001) reported high cobalt removal (39–96%) in full-scale CWs from coal combustion leachate containing a lower concentration of cobalt (0.02 mg L^{-1}) and identified major accumulation in the sediments as the largest sink with a minor fraction (0.19–2.75%) as plant uptake. In contrast, very low cobalt removal (0.76–24%) was detected in horizontal flow CW treating municipal sewage with a much lower cobalt concentration (1.31–2.46 μg L^{-1}) (Kröpfelová et al., 2009).

The kinetics of manganese precipitation as (oxy-)hydroxides is slower as compared to ferrous iron at pH < 9.0 (Neculita and Rosa, 2019) and it is challenging to remove biologically by means of SRB in anaerobic wetlands (Hallberg and Johnson, 2005). In addition, the formation of insoluble manganese sulfide is very difficult because most of the other metals preferentially complex with sulfides before Mn does (Stumm and Morgan, 1981); therefore,

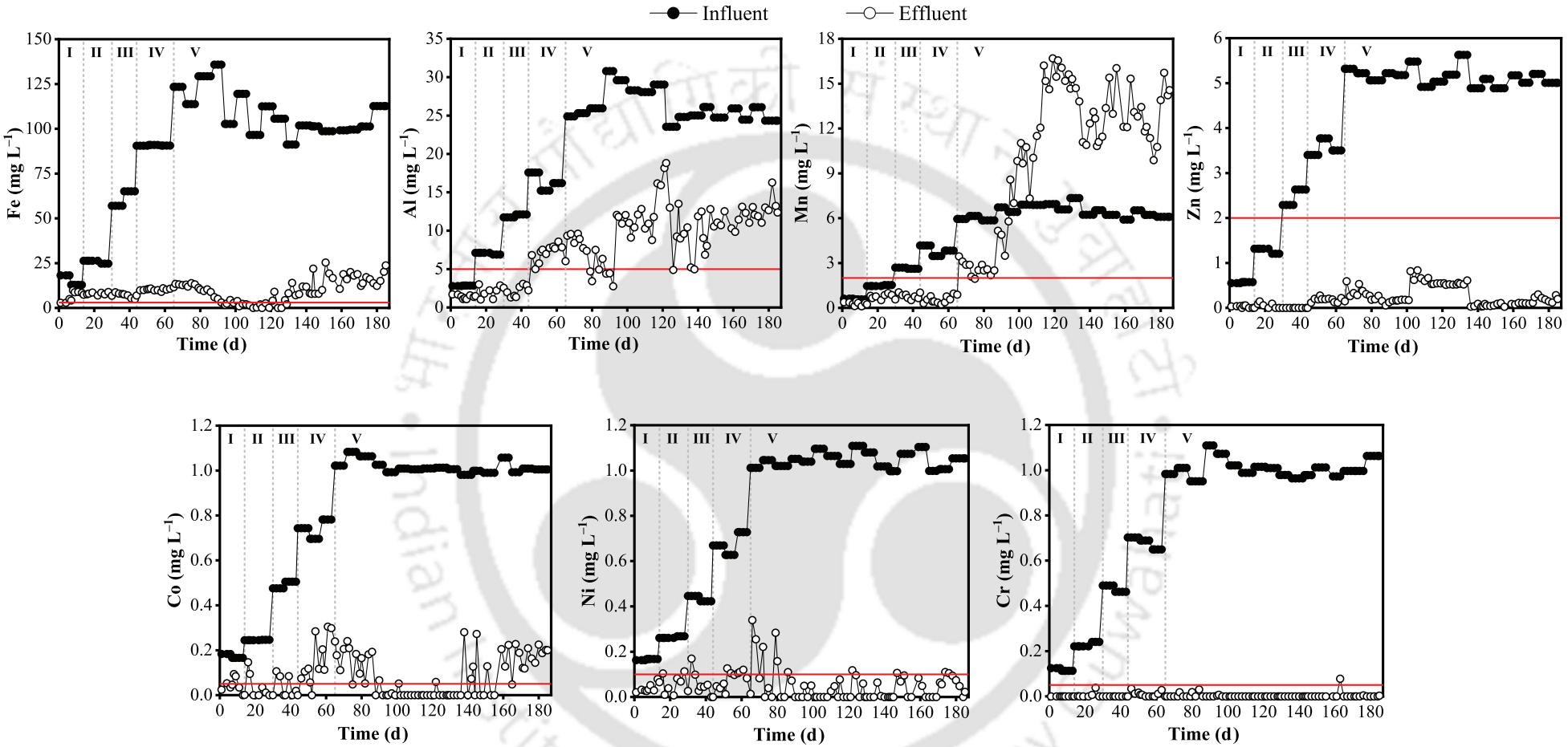

Fig. 3.8 Metal profile of influent and effluent in HSSF-CW (A). The red line denotes the permissible discharge limit (PDL) as recommended by CPCB (1993) and EPA (2002).

Fig. 3.9 Photographic image of (a) ferric hydroxide coating on gravel and (b) iron plaque formations on the roots after treatment in HSSF-CW (A).

it could be easily released. Because of the anoxic status inside the bed, Mn^{2+} remained in a reduced dissolved state and exhibited complete leaching (no net removal) without undergoing any treatment. Manganese concentration in the effluent increased by about 2.5 times the influent concentration after passing through the wetland bed. These results elucidated manganese accumulation during the start-up of the CW and subsequent re-release of adsorbed manganese once pH started to decline and the bed became mostly anaerobic (Hallberg and Johnson, 2005; Kröpfelová et al., 2009). Very limited to negative removal is reported in many studies dealing with manganese removal from various wastewaters in CWs, especially in the case of anaerobic wetlands when dissolved iron is present at higher concentration in the wastewater (Kröpfelová et al., 2009; Lesage, 2006; Vymazal, 2005; Xu et al., 2009). Poor removal of Mn in the CW suggested the necessary post-treatment of AMD (for Mn > 0.05 mg L^{-1}) by complete oxidation of Mn to form $Mn(OH)_2$ or preferably MnO_2, which is extremely insoluble.

3.3.2.5 Metal speciation

Metal speciation study revealed the fractionation of different metals in the wetland media. Metals could exist in several complexed forms associated with organic matter, oxides and hydroxides of iron and manganese and as a mineral component. Various chemical reagents of specific strength and reactivity in each step depict the release of metals from different fractions of the examined soil. Zone-wise distribution of metals along the depth of each zone is depicted in Fig. 3.10. It was found that iron mostly occurred in residual fractions and some in organics and sulfide bound fractions, indicating that iron is firmly trapped in minerals and would not release into the environment even under extreme conditions. Chromium was

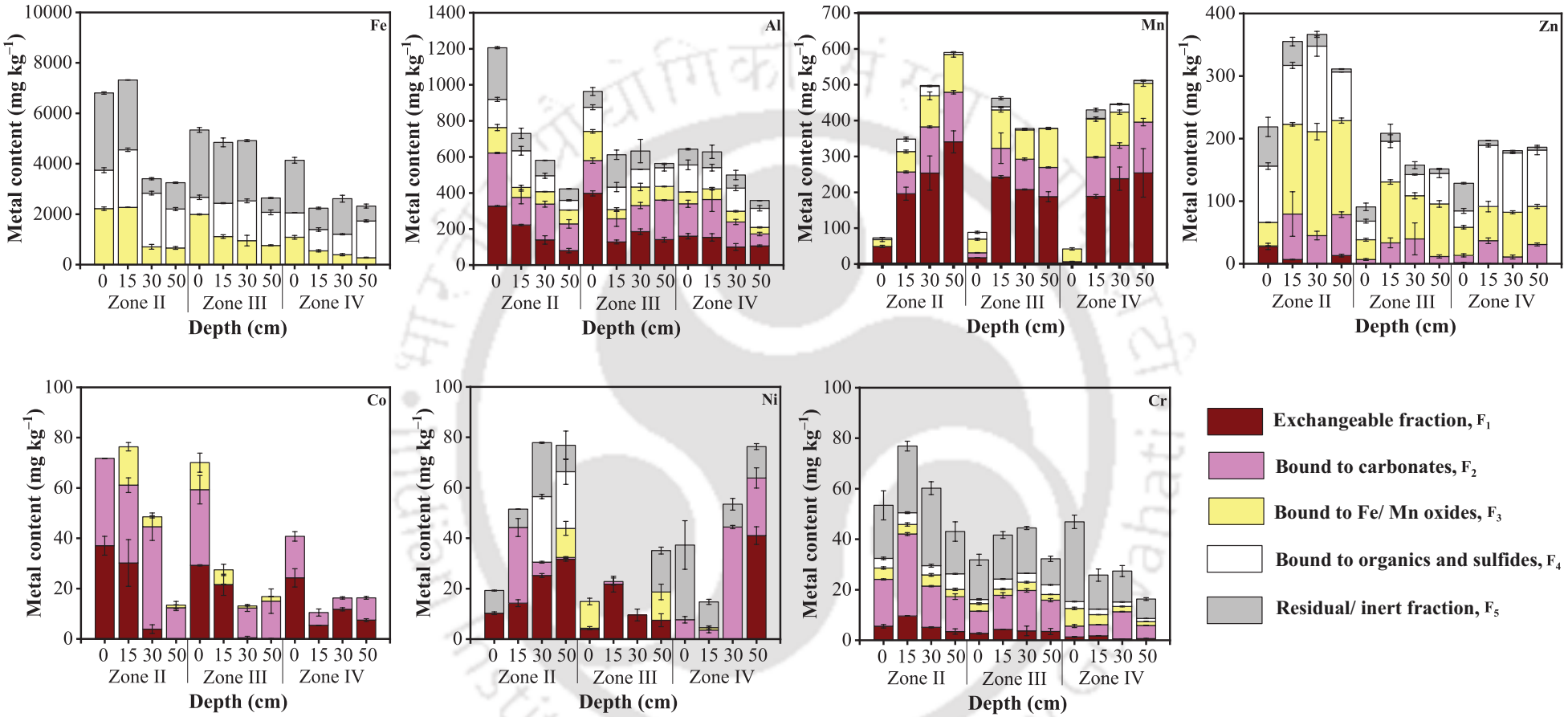

Fig. 3.10 Plots of Fe, Al, Mn, Zn, Co, Ni and Cr content (mg kg^{-1}) obtained in various fractions of sequential extraction procedure of media from zone II, III and IV at different depths (0, 15, 30 and 50 cm) of the HSSF-CW (A).

majorly carbonate bound and occurred mostly in inert fractions, indicating that chromium was distinctly immobilized and unavailable to the surrounding biota. These results also provide an idea about the form of metal retention and indirectly suggest metal removal mechanisms. It was observed that an average aluminium concentration of about 192, 213 and 130 mg kg^{-1} in exchangeable fraction (F_1) whereas about 199, 169 and 149 mg kg^{-1} in carbonate bound fraction (F_2) appeared in zone II, III and IV, respectively. Thus, it describes the precipitation of aluminium mostly as (oxy-)hydroxides. Zinc majorly appeared as organically, sulfide and Fe- and Mn- oxide bound, while some also appeared in residual fraction. Mean zinc concentration of about 124, 70.47 and 58 mg kg^{-1} in the F_3 fraction, whereas about 99.62, 44.34 and 77.24 mg kg^{-1} in the F_4 fraction was found in zone II, III and IV, respectively. Thus, these results indicated that zinc was mostly immobilized and would not leach or back-release under ambient environmental conditions. However, cobalt and manganese presented mostly as the inorganically bound fraction, which revealed that these metals were weakly adsorbed and, thus, more bioavailable, which would eventually turn into a secondary source of metal pollution. Therefore, cobalt and manganese removal occurred as oxides or carbonates, which mostly represented in the F_1 and F_2 fractions. In addition, some fractions of nickel also appeared in loosely bound inorganic and carbonate fractions, which could potentially release under an adverse environmental state. As a substantial amount of Co, Mn, Al and Ni were present in the loosely bound fractions, necessary post-treatment measures should be considered to meet environmental compliant disposal, further discussed in Chapter 4.

3.3.2.6 Mineralogy of media deposits

The precipitate morphology was observed in FESEM and the elemental analysis was performed in EDX [Fig. 3.11 (a) and (b)]. The X-ray diffraction pattern of the solid samples from the reactor was analyzed [Fig. 3.11 (c)]. Sharp characteristics peaks of quartz were present in the sample. XRD pattern indicated the distinctive peaks of goethite (FeOOH; JCPDS 00-001-0401), zinc hydroxide ($Zn(OH)_2$; JCPDS 01-076-0778) and cobalt oxide (CoO; JCPDS 01-075-0533). Due to the poor crystalline nature of the precipitates, weak peak intensities were recorded. Besides, iron sulfide precipitation (FeS; JCPDS 00-023-1120) and manganese sulfite ($MnSO_3$; JCPDS 00-031-0837) was indicated.

3.3.2.7 TCLP leaching results

The TCLP results are presented in Table 3.5. The leached chromium concentration from the media sample of all the zones of CW was lower than the USEPA hazardous waste criteria of 5 mg L^{-1} (USEPA, 1994). Thus, it can be inferred that media can be safely disposed on land without posing an environmental menace. The leachability ratio (L_m/T_m), which is given by the ratio of leached metal concentration (mg kg^{-1}) during the TCLP study to the total metal concentration (mg kg^{-1}), gives a direct idea of metal extraction and immobilization ability. A high leachability ratio reflects the weak immobilization of metal within the media matrix. A high leachability ratio (> 0.50) was obtained for iron and manganese, indicating iron and manganese are more prone to 'extractability' than other metals.

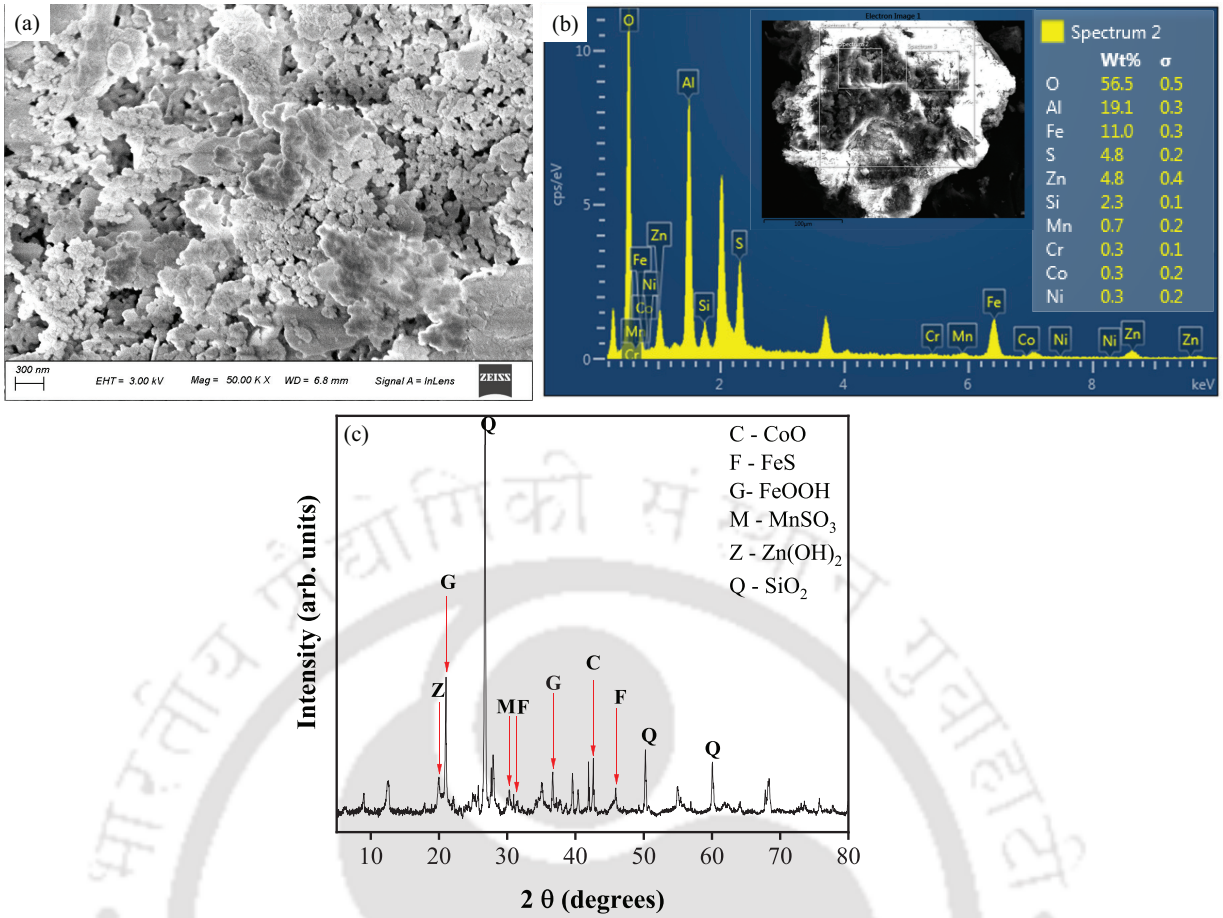

Fig. 3.11 (a) FESEM image, (b) EDX analysis and (c) powder XRD pattern of the precipitate from HSSF-CW (A).

Table 3.5 Leachability of metals by TCLP test.

Metal	Metal concentration* (mg L^{-1})			TCLP	L_m/T_m		
	Zone II	Zone III	Zone IV	criteria[a]	Zone II	Zone III	Zone IV
Fe	113 ± 5.66	124 ± 6.23	86.83 ± 1.52	–	0.66	0.50	0.66
Mn	13.82 ± 1.40	10.38 ± 0.64	10.77 ± 0.28	–	0.55	0.56	0.48
Al	12.67 ± 1.08	13.13 ± 0.36	9.96 ± 0.12	–	0.44	0.42	0.40
Zn	4.93 ± 0.17	4.22 ± 0.28	3.62 ± 0.35	–	0.27	0.54	0.40
Co	0.42 ± 0.04	0.15 ± 0.02	0.16 ± 0.02	–	0.17	0.23	0.20
Ni	0.60 ± 0.02	0.10 ± 0.02	0.54 ± 0.02	–	0.16	0.22	0.20
Cr	0.37 ± 0.02	0.31 ± 0.01	0.33 ± 0.01	5	0.12	0.14	0.24

*Represented as average value ± standard deviation of three independent replicates.

[a]USEPA (1994) hazardous waste criteria in mg L^{-1}.

T_m was obtained from the sum of averaged exchangeable, carbonate bound, Fe/Mn oxide bound, organics/sulfide bound and residual fractions for 30 cm depth media samples of each zone.

3.3.2.8 Plant growth and metal uptake

At the end of the experimental period, the plant density increased from initial 25 to 75, 138 and 113 plants m^{-2} in zone II, III and IV, respectively. Table 3.6 exhibits the plant growth, biomass production and chlorophyll content from each zone. The highest total plant biomass production of 3.42 kg m^{-2} was recorded in zone III, which explains better adaptability and growth of plants due to improvement in water quality along the length of the wetland bed.

As many metals precipitated and retained near the inlet zone II, plants were exposed to high toxicity and therefore, the lowest plant density and plant biomass production was observed in zone II. The total chlorophyll in plants was 3.13–4.02 mg g^{-1} FW, thus significantly varying from the total chlorophyll content of unpolluted plants (5.44 mg g^{-1} FW). This reduction in total chlorophyll could be due to inhibition caused by the build-up of heavy metals (toxic effect) in plants (Manios et al., 2003b; Mufarrege et al., 2014).

The metal uptake in shoots and roots of plants harvested from the HSSF-CW (A) is depicted in Fig. 3.12. CW cultivated plants exhibited higher heavy metal accumulation than the unpolluted plant. Cobalt and chromium content was neither detected in roots nor shoots of the unpolluted plant. The heavy metals concentration was considerably higher in roots than shoots, except for Mn and Co. These results were consistent with the findings of previous studies on heavy metal uptake by macrophytes (Dan et al., 2017; Mungur et al., 1995). The Fe and Al content in the roots of the common cattail was as high as about 7952–10702 mg kg^{-1} and 308–492 mg kg^{-1}, respectively. However, iron content in shoots was < 2000 mg kg^{-1}. In contrast, shoots exhibited higher Mn and Co concentration than the roots, indicating higher translocation ability of common cattail for these metals. Mn and Co content in leaves/stems of common cattail were 59.75–117 mg kg^{-1} and 26.15–63.94 mg kg^{-1}, respectively. Sasmaz et al. (2008) also reported a higher accumulation of manganese in leaf (990 mg kg^{-1}) than in root (860 mg kg^{-1}), indicating that cattails can be considered as bio-indicator organs for manganese. Cr and Ni content was least in plants, accounting for only about 7.69–15.45 mg kg^{-1} and 0.59–7.64 mg kg^{-1} in roots and shoots, respectively. Low accumulation of Co, Ni and Cr can be suggested as the protective mechanism of the plants against such toxic metals.

The highest BCF values were obtained for Fe, followed by Mn, Co, Ni and Cr (Table 3.7). Although cattail accumulated more iron than other metals, most of it remained in the roots, showing excellent iron extraction capability of the plant from the surrounding environment, which is in line with the previous study reported by Anning et al. (2013). Manganese exhibited the highest TF (> 2.5), whereas lower TF (< 1.0) was obtained for other metals, which indicated that the cattail did not effectively transfer heavy metals from root to body and that is why cattail was able to grow well even under extremely low pH metal-rich environment.

Table 3.6 Plant parameters in zone II, III and IV of HSSF-CW (A) at the end of study.

Parameters	Zone II	Zone III	Zone IV	Unpolluted
Plant density (plant nos. per m^2)	75	138	113	–
Average plant height, cm	110 ± 35	137 ± 37	124 ± 33	–
Dry plant biomass (aboveground), kg m^{-2}	0.56	2.61	1.17	–
Dry plant biomass (belowground), kg m^{-2}	0.41	0.81	0.66	–
Total plant biomass, kg m^{-2}	0.98	3.42	1.83	–
Chlorophyll a, mg g^{-1} FW	2.24	2.04	1.73	3.13
Chlorophyll b, mg g^{-1} FW	1.64	1.50	1.31	2.15
Chlorophyll c, mg g^{-1} FW	0.08	0.11	0.10	0.14

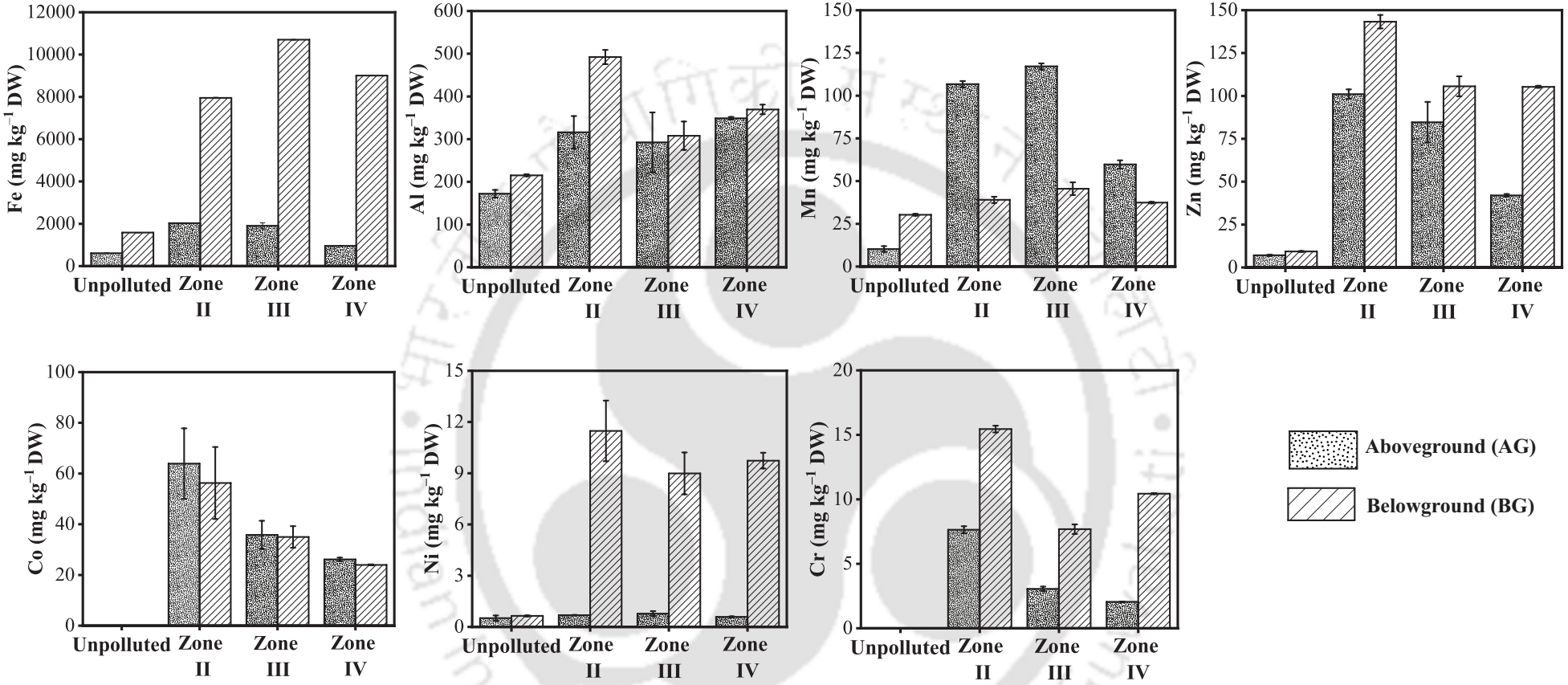

Fig. 3.12 Heavy metal concentration (mg kg^{-1} dry weight) in aboveground (AG) and belowground (BG) parts of the plant (*Typha latifolia*).

3.3.2.9 Metal accumulation – A mass balance approach

Wetland media is eventually a major sink for the retention of almost every metal. Media samples were collected from zone II, III and IV at different depths (0, 15, 30 and 50 cm) to quantify each metal at varying depths. An estimate of metal accumulation (or retention) within the wetland media was performed based on the mass balance analysis (Table 3.8). Some of the assumptions made for this approach were: (a) Precipitation and evapotranspiration terms have been neglected such that $Q = Q_{in} = Q_{out} = 9.43$ L d^{-1}; (b) Influent (C_{in}, mg L^{-1}) and effluent (C_{eff}, mg L^{-1}) metal concentration have been assumed constant and equal to average values as observed during each feeding cycle; (c) The influent and effluent mass were calculated by multiplying the number of days (n, days) operated and daily flow rate with an average concentration of influent and effluent, respectively; (d) The mass removed from the system is given by the difference between the influent and effluent mass; (e) The metal retained (R_m, g) within the wetland media represents a total of an average metal load of each zone, where the metal load was obtained by multiplying the average metal concentration (mg kg^{-1}) of each zone with the respective mass of the particular media (either soil or cow manure, kg) added in zones; (f) Metal uptake by the plants (U_p, g) represents the total metal concentration in the plant biomass of each zone. The unaccounted mass represents the untraced amount of metal, calculated from the difference between influent mass and the sum of mass in the effluent, retained in media and plant uptake. Fig. 3.13 shows the percent contribution of various biochemical processes (or routes) in metal removal. It was evident that media was the major sink of the metal accumulation (> 50%), whereas metal uptake in

Table 3.7 BCF and TF values of cattail at the end of the study.

Metal	BCF*			TF*		
	Zone II	Zone III	Zone IV	Zone II	Zone III	Zone IV
Fe	1.47	2.36	2.41	0.26	0.18	0.11
Al	0.67	0.66	1.12	0.64	0.94	1.06
Mn	2.00	1.85	2.31	2.74	2.58	1.60
Zn	1.12	2.09	1.15	0.71	0.80	0.40
Co	1.68	1.01	1.23	1.14	1.04	1.09
Ni	0.63	0.66	0.28	0.06	0.09	0.06
Cr	0.43	0.34	0.27	0.50	0.40	0.20

*Dimensionless.

Table 3.8 Metal mass balance after 6-month experimental period of HSSF-CW (A).

Metal	Influent mass, nQC_{in} (g)	Effluent mass, nQC_{eff} (g)	Mass removed, $nQ(C_{in}-C_{eff})$ (g)	Mass retained in media, R_m (g)	Uptake by plants, U_p (g)	Unaccounted mass, $nQC_{in}-(nQC_{eff} + R_m + U_p)$ (g)
Fe	153.27	16.18	137.09	129.88	4.60	2.62
Al	35.62	13.79	21.84	20.58	0.14	1.11
Zn	7.29	0.38	6.91	6.07	0.09	0.76
Co	1.46	0.15	1.31	1.16	0.04	0.12
Ni	1.49	0.09	1.40	1.14	0.01	0.25
Cr	1.32	0.01	1.31	1.25	0.01	0.05

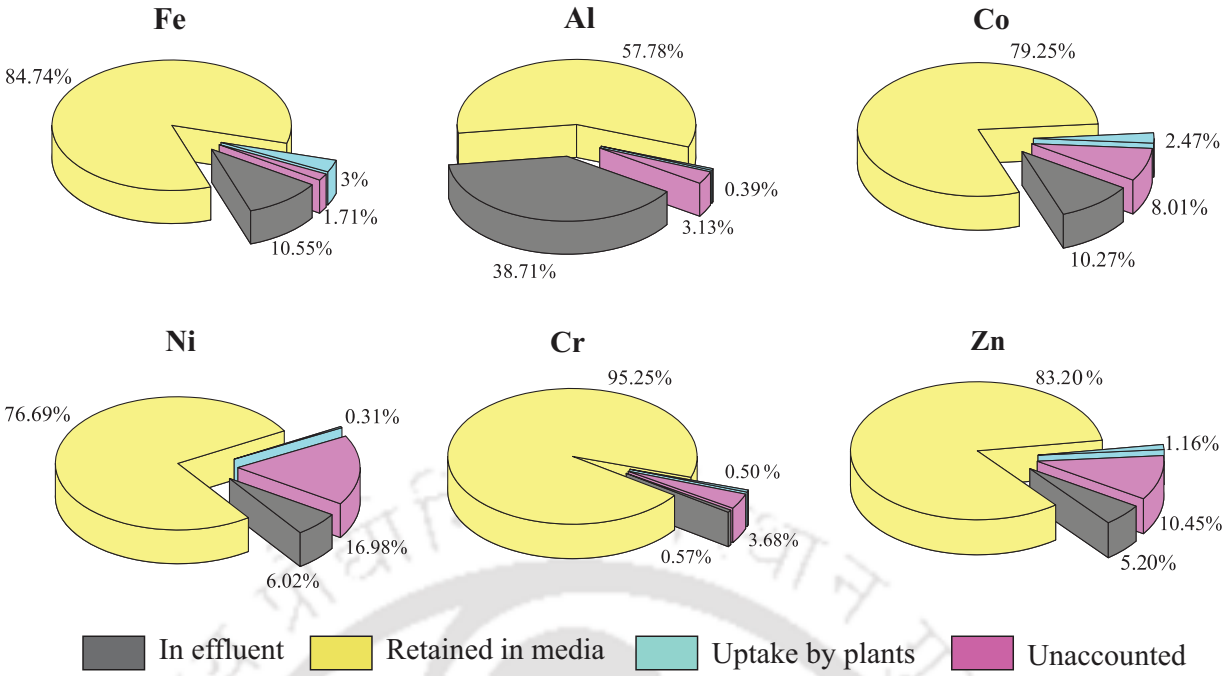

Fig. 3.13 Metal distribution (expressed in %) among different components of HSSF-CW (A).

plants was merely 3% of the initial influent metal concentration. Heavy metal accumulation in different wetland plant species has been reported to be about 2–10% (Dan et al., 2017; Gill et al., 2017; Lesage et al., 2007), implying that plant biomass does not contribute greatly in metal removal.

3.3.3 Performance of organic media amended HSSF-CW (C)

3.3.3.1 AMD treatment and water quality improvement

HSSF-CW (C) employed a different mixture of organic media consisting of goat manure and areca palm husk, which operated in continuous mode, as described in Table 3.2. The effluent water quality measured in terms of pH, alkalinity, EC, TDS, COD and sulfate is shown in Fig. 3.14. High effluent pH 7.3–8.0 (averaged 7.6) and 7.1–7.7 (averaged 7.4) were recorded in the acclimatization and treatment phase, respectively. Instantaneous release of easily degradable organics and ions from the organic media caused higher measurement of EC (192–580 mS m^{-1}) and TDS (1204–10940 mg L^{-1}) in the effluent during the start-up of the CW. Thereafter, in the steady treatment phase, EC varied in the range 114–241 mS m^{-1}, whereas TDS stabilized to 1240 ± 182 mg L^{-1}, presenting a positive correlation (Appendix–IV). In general, goat manure and areca husk presented an effective carbon-rich source and provided long-term carbon availability (COD = 71.97 ± 33.45 mg L^{-1}), coupled with the higher acidity alleviation and alkalinity production (380–1300 mg L^{-1} as $CaCO_3$). In contrast, HSSF-CW (A) demonstrated a significantly lower effluent pH (4.5–7.2) and alkalinity generation (24–730 mg L^{-1} as $CaCO_3$) in the treatment phase. Choudhary and Sheoran (2012) observed similar results in passive bioreactors with different manures, where goat manure (pH = 7.5; sulfate removal = 54%) exhibited superior performance followed by cow manure (pH = 7.1; sulfate removal = 48%). This explains that the efficiency of AMD treatment by SRB is primarily determined by the availability of carbon, nitrogen and

protein content. Rapid discharge of high amounts of sulfate (493–1227 mg L^{-1}) in phase I, followed by steadied concentration (43–278 mg L^{-1}) in the subsequent acclimatization phases. However, effluent sulfate concentration increased significantly after 200 days, accounting for sulfate removal of 23.72–84.39% in the treatment phase, which could be due to the limited supply of carbon (COD = 30.87–170 mg L^{-1}) with the depletion of available organics after continuous treatment for a longer period.

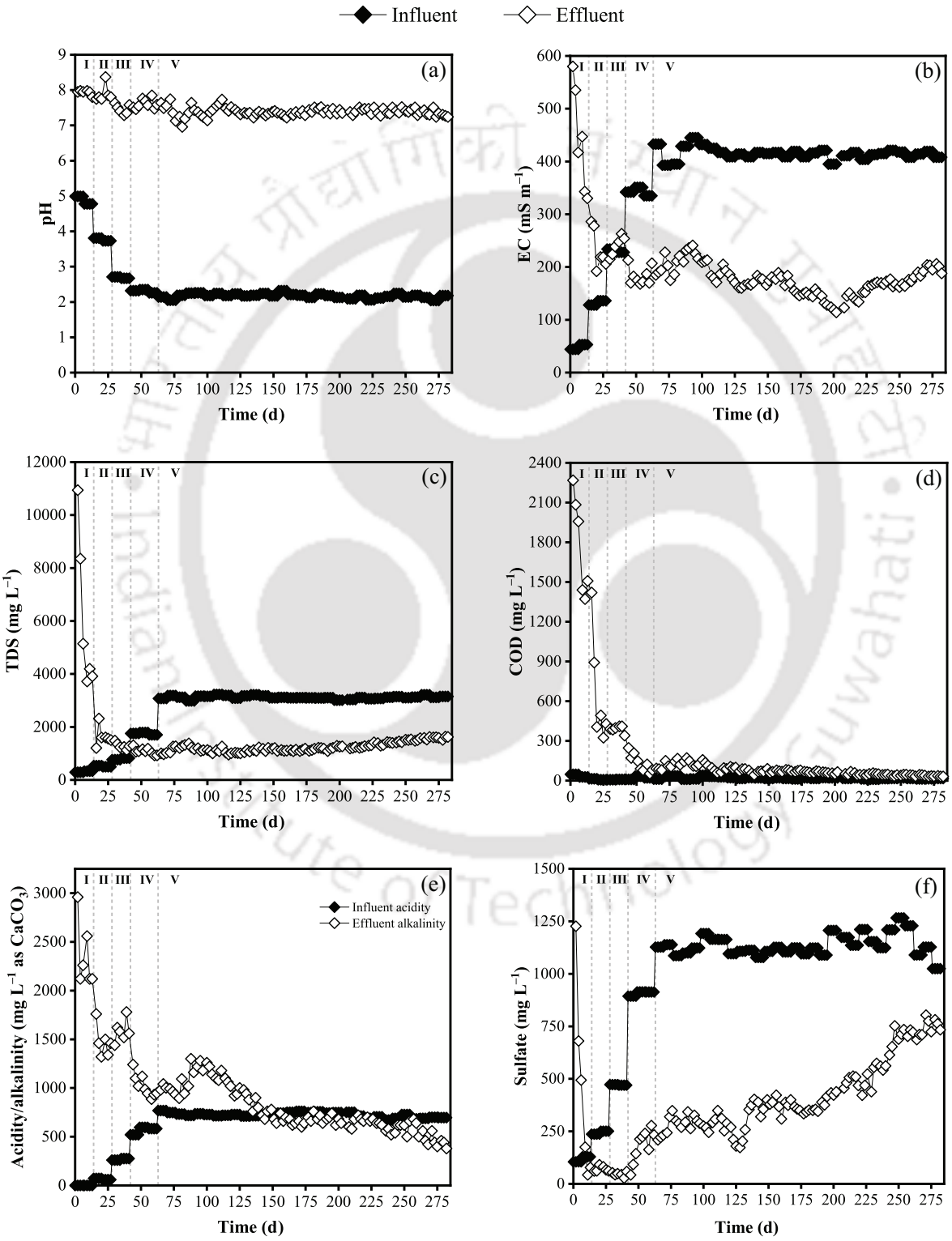

Fig. 3.14 (a) pH, (b) EC, (c) TDS, (d) COD, (e) acidity/alkalinity and (f) sulfate profile of HSSF-CW (C).

HSSF-CW (C) exhibited excellent metal removal efficiency for all metals, except manganese. The formation of a thick layer coating of ferric hydroxides was observed on the top soil surface in zone III and IV (Fig. 3.15). The metal profile of the HSSF-CW (C) is depicted in Fig. 3.16. Average metal removal efficiency achieved in the following order: Fe (99.92%) > Cr (99.06%) > Ni (98.25%) > Co (98.19%) > Zn (97.78%) > Al (86.63%) and least for Mn in the treatment phase V. The obtained results were coherent with the batch precipitation results. High removal of iron and chromium is attributed to precipitation as oxides or hydroxides and adsorption by the organic media at pH > 7.0. As the measured effluent pH > 7.0 in all phases, therefore most of the metals are expected to be retained as metal precipitates. The concentration of metals like Fe, Al, Zn, Ni and Cr in the effluent remained below the permissible limits and thus, it can be safely discharged in the water bodies. Cobalt exhibited fair removal in the treatment phase; however, higher concentrations (> 0.05 mg L^{-1}) exceeding the PDL were also occasionally recorded. Manganese removal was inconsistent, which eventually leached out of the wetland as observed in HSSF-CW (A) and thus, did not meet the permissible discharge criteria. Short-term removal of manganese during the initial operation phases is explained by several metal retention mechanisms such as physical adsorption, complexation, chelation and ion exchange on the surfaces and micro-precipitation (Pagnanelli et al., 2003). These findings revealed the superior performance of goat manure and areca palm husk as the wetland media for AMD remediation by demonstrating high metal removal and pH increment. Table 3.9 gives a brief comparison of AMD treatment using CWs in terms of sulfate and metal removal as reported in the literature. Compared to similar studies, the current work presented better metal removal efficacy for Fe, Zn, Co, Ni and Cr and achieved comparable sulfate removal.

3.3.3.2 Mineralogy of the metal precipitates

The mineralogical characteristics of the precipitate from HSSF-CW (C) are illustrated in Fig. 3.17. SEM and EDX analysis revealed the formation and accumulation of metal precipitates in the wetland media, suggesting media as the major sink. Further, from the powder XRD analysis, various mineral phases were identified. Sharp peaks of quartz (SiO_2; JCPDS 01-085-0794) and indistinctive peaks of low intensities were also identified, which indicated the amorphous nature of the precipitate. Characteristic peaks of metal precipitate include cobalt

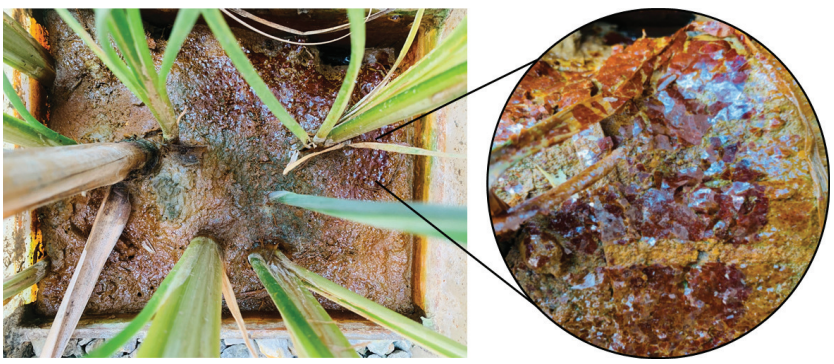

Fig. 3.15 Photographic image of iron (oxy-)hydroxides coating on the top soil surface from zone IV of HSSF-CW (C).

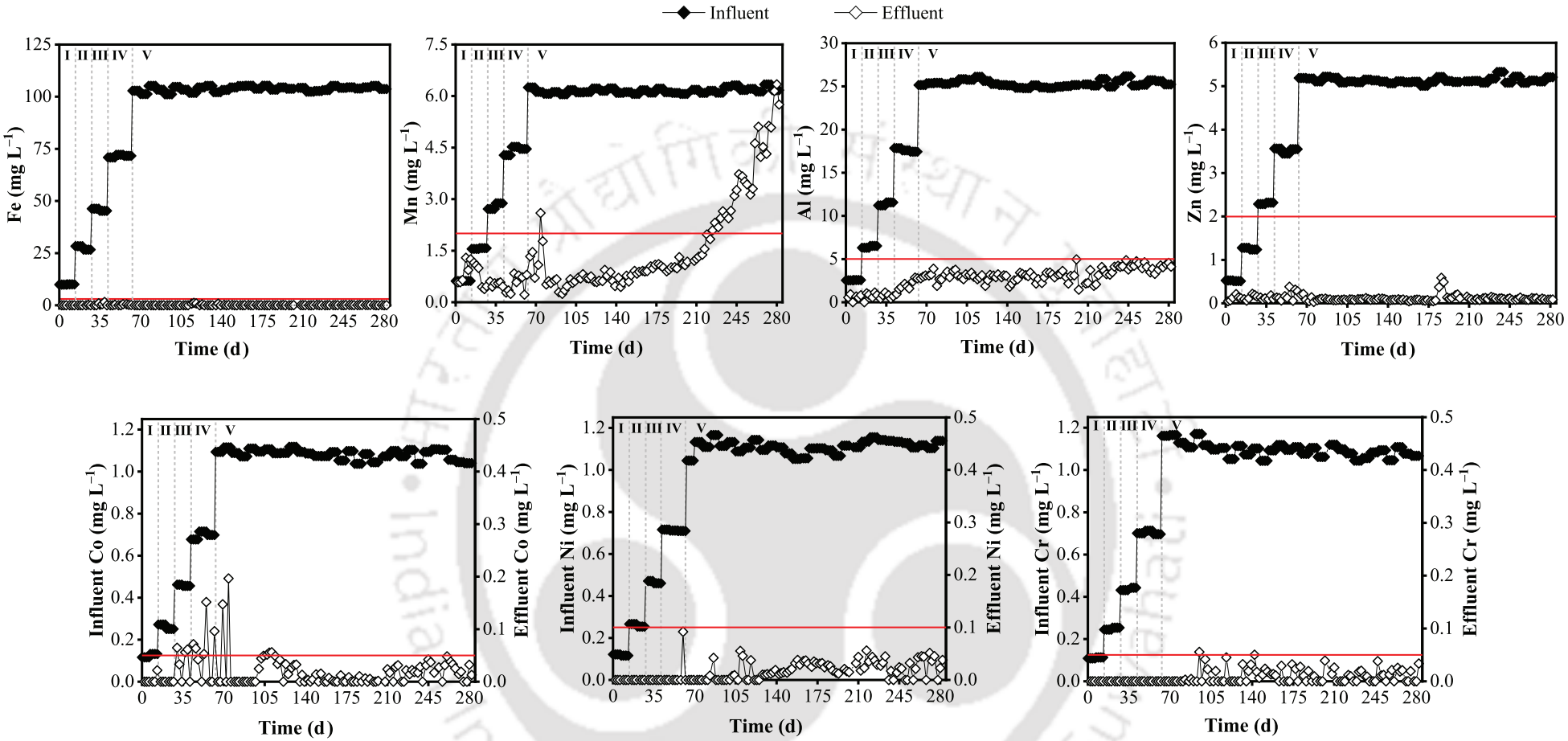

Fig. 3.16 Metal profile of influent and effluent in HSSF-CW (C). The red line denotes the permissible discharge limit (PDL) as recommended by CPCB (1993) and EPA (2002).

Table 3.9 Comparative performance evaluation of CWs employed for the treatment of AMD.

Type of CW	Media	Nature of wastewater	Pollutant concentration* (mg L^{-1})	Removal efficiency* (%)	Reference
VF (lab-scale)	Gravel and walnut shell	Synthetic AMD	Fe (50), Zn (5), Cu (5), Cd (5), Cr (5), SO_4^{2-} (568) and pH (4.0)	Fe (73), Zn (85), Cu (99), Cd (99) and Cr (90), SO_4^{2-} (38) and pH (6.5)	Chen et al. (2021)
SF (lab-scale)	Spent mushroom	Synthetic AMD	Al (150), Zn (90), Cu (5), Fe (130), Pb (1.50), Mn (6), SO_4^{2-} (1965) and pH (3.1)	Al (99), Zn (99), Cu (99), Fe (97), Pb (97), Mn (no removal), SO_4^{2-} (negative removal) and pH (3.0–6.0)	Jordan et al. (2021)
FWS (lab-scale)	Zambian soil	Synthetic AMD	Co (3), Cu (5), Pb (1), Mn (2) and pH (8)	Cu and Pb (83–86) at pH (< 7.9), Co and Mn exhibited negative removal	Nabuyanda et al. (2019)
FWS (bench-scale)	Goat manure, wood shavings and soil	Synthetic AMD	Fe (18), Cu (15), Zn (30), Pb (1.80), Co (0.34), Ni (0.40), Mn (2.20) and SO_4^{2-} (445) and pH (2.9)	Fe (95), Cu (92), Zn (77), Pb (89), Co (68), Ni (30), Mn (26), SO_4^{2-} (28) and pH (7.2)	Sheoran (2017)
VF (pilot-scale)	Compost, wood chips and sludge	Rampgill mine discharge, England	Zn (2.32), SO_4^{2-} (134) and pH (7.7)	Zn (68), SO_4^{2-} (13) and pH (7.3)	Gandy et al. (2016)
HSF (bench-scale)	Sandy soil, cattle manure, peat and limestone	Synthetic AMD	Fe (38), Mn (2.60), Ni (0.40), Zn (9) and pH (4.2)	Fe (90), Mn (–20), Ni (58), Zn (96) and pH (7.6)	Dufresne et al. (2015)
HSF (pilot-scale)	Municipal waste organics and 10% recycled limestone	Acid drainage from Dongolocking Creek, Australia	Fe (0–340), Al (0–370), SO_4^{2-} (1690–15300) and pH (1.9–7.0)	Fe (23–99), Al (36–100), SO_4^{2-} (–48–96) and pH (4.6–7.3)	Biermann et al. (2014)
VF (lab-scale)	Cocopeat	Synthetic AMD	As (3.08), B (32), Fe (107), SO_4^{2-} (907) and pH (2.0)	As (9.60), B (6.30), Fe (46), SO_4^{2-} (–5.10) and pH (1.8)	Lizama-Allende et al. (2012)
VF (large-scale)	Limestone and composted waste	Coal pile runoff, South Carolina, USA	Fe (142), Al (84), Mn (3.90), Zn (1.60), SO_4^{2-} (1500) and pH (2.4)	Fe (89), Al (100), Mn (13), Zn (97), SO_4^{2-} (20) and pH (6.4)	Collins et al. (2005)
SF wetland ponds (pilot-scale)	Spent mushroom compost	Alkaline mine wastewater from Tara Mines, Ireland	Pb (0.15), Zn (2) and SO_4^{2-} (900)	Pb (32), Zn (74) and SO_4^{2-} (32)	O'Sullivan et al. (2004)
HSSF (lab-scale)	Gravel, cow manure, bamboo chips and soil	Synthetic AMD (NEC, India)	Fe (109), Mn (6.43), Al (26), Zn (5.14), Co (1.02), Ni (1.05), Cr (1.01), SO_4^{2-} (1336) and pH (2.1)	Fe (91), Mn (no net removal), Al (61), Zn (94), Co (92), Ni (96), Cr (100), SO_4^{2-} (56.81) and pH (6.3)	Present study
HSSF (lab-scale)	Gravel, goat manure, areca husk and soil	Synthetic AMD (NEC, India)	Fe (104), Mn (6.15), Al (25), Zn (5.13), Co (1.08), Ni (1.11), Cr (1.10), SO_4^{2-} (1136) and pH (2.2)	Fe (100), Mn (no net removal), Al (87), Zn (98), Co (98), Ni (98), Cr (99), SO_4^{2-} (61.58) and pH (7.4)	Present study

*Except pH (unitless).

oxide (CoO; JCPDS 01-075-0533), aluminium oxide (Al_2O_3; JCPDS 01-076-0144), nickel sulfide (NiS; JCPDS 01-077-1624), chromium oxide hydroxide (CrOOH; JCPDS 01-074-2386), iron oxide (Fe_2O_3; JCPDS 00-016-0653) and zinc hydroxide ($Zn(OH)_2$; JCPDS 01-076-1778).

3.3.3.3 Taxonomical composition of microbial communities

The 16S rRNA gene sequencing was performed to determine the taxonomical composition and phylogenetic distribution of bacteria and archaea communities inhabiting the environment with prolonged AMD exposure and to identify the dynamic shifts during the bioremediation. Fig. 3.18 depicts the relative abundance and microbial diversity distribution in HSSF-CW (C) after the acclimatization and treatment phase. The category 'others' includes the rest of the classifications.

In the acclimatization phase, dominant lineages of Proteobacteria (44.96%), Bacteroidetes (26.02%), Euryarchaeota (7.63%), Chlorobi (5.08%), Firmicutes (3.46%), OP3 (2.72%), Actinobacteria (1.90%), WS6 (1.87%), Planctomycetes (1.34%), OD1 (1.22%), Chloroflexi (0.84%) and Acidobacteria (0.52%) were detected at phylum level along with other phyla (< 0.5%) such as OP11, Verrucomicrobia, Crenarchaeota, Spirochaetes and Parvarchaeota. However, in the treatment phase, bacterial assemblages reformed greatly with taxonomical groups from the kingdom Archaea completely disappeared and abundance of

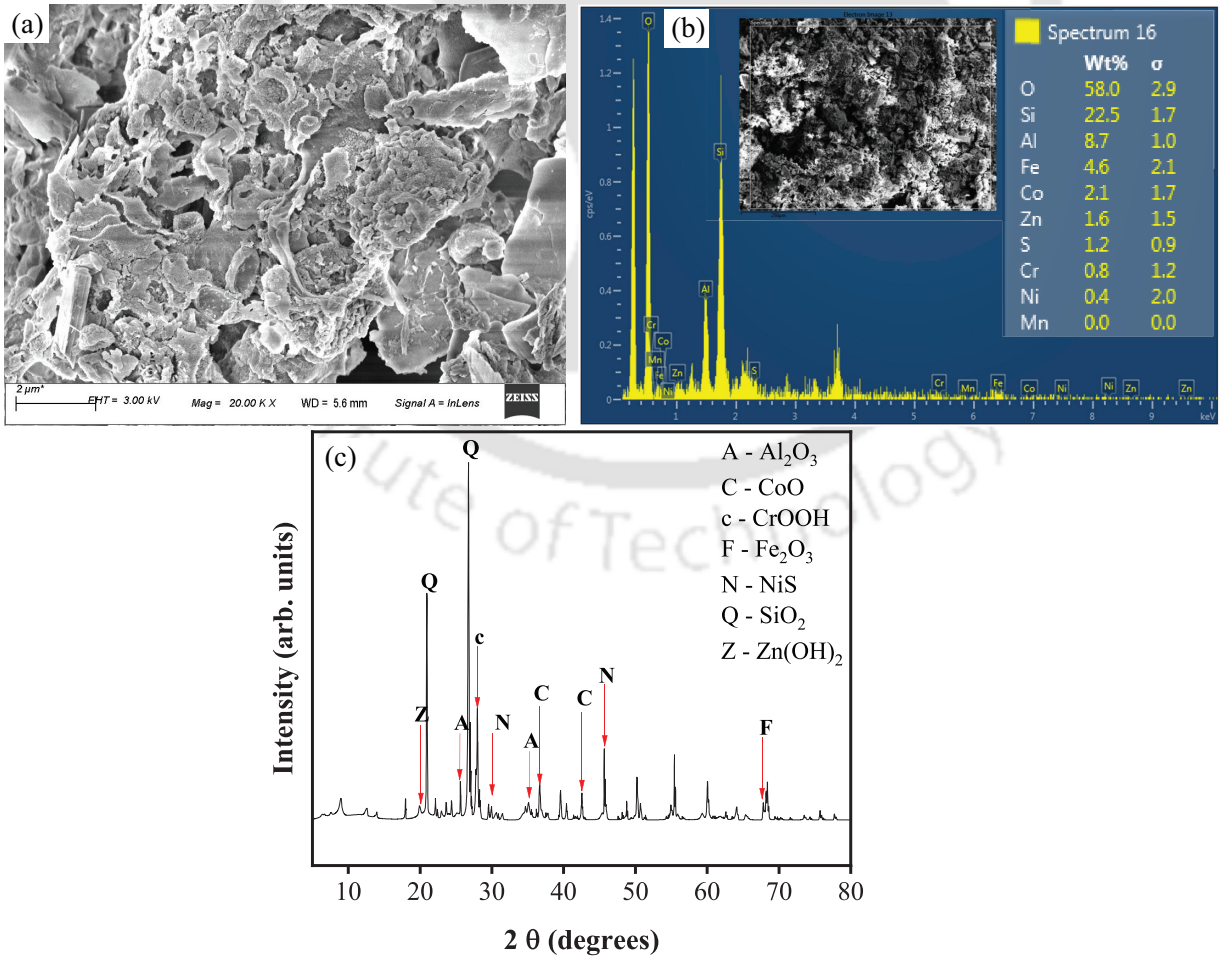

Fig. 3.17 (a) SEM micrograph, (b) EDX spectra and (c) XRD spectra of the precipitate from HSSF-CW (C).

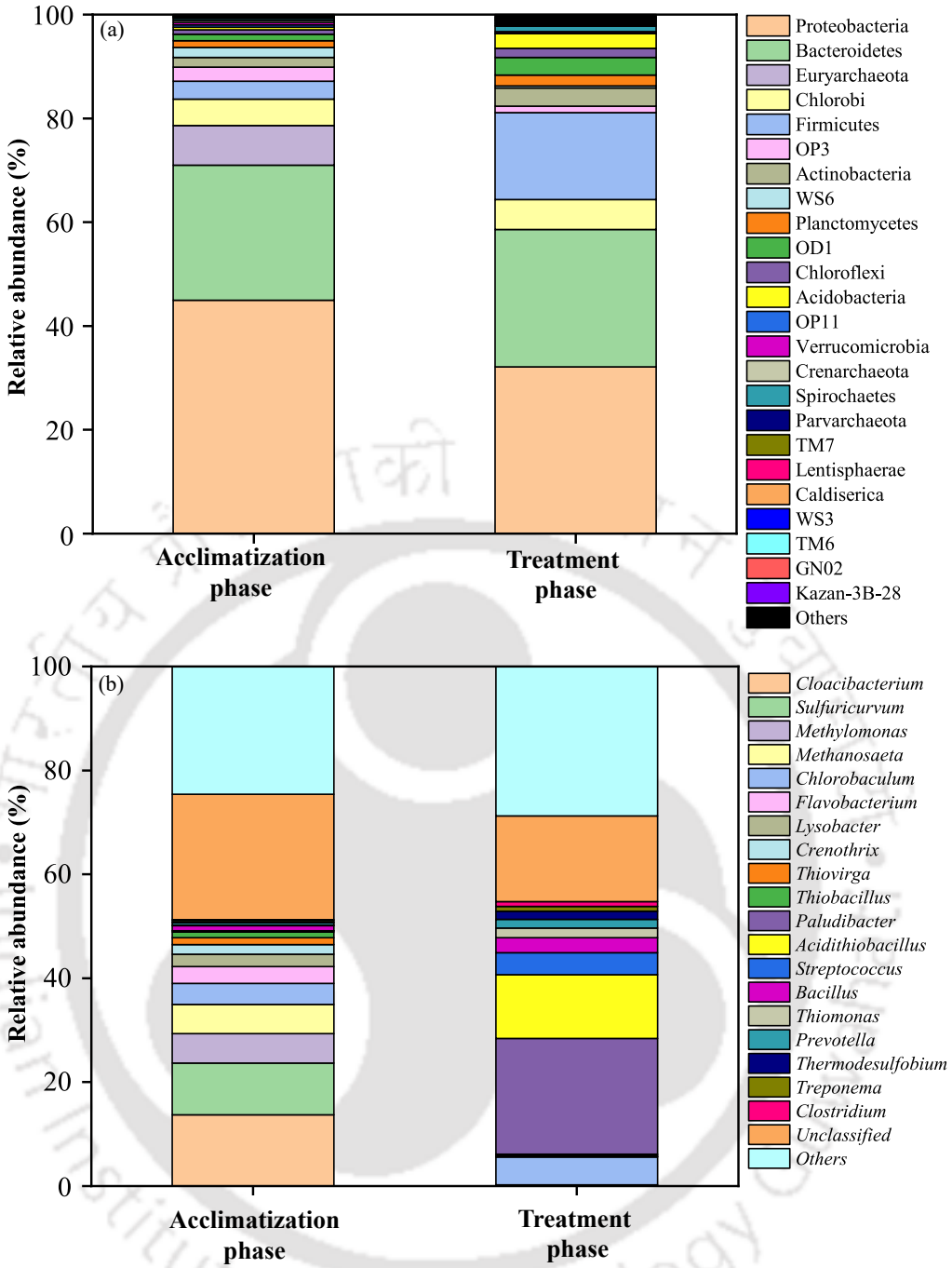

Fig. 3.18 Microbial community structure of HSSF-CW (C) during operation at the (a) phylum and (b) genus level (top 19 categories at phyla and genera taxonomical levels).

Firmicutes (16.77%), Actinobacteria (3.49%), Planctomycetes (2.14%), OD1 (3.39%), Chloroflexi (1.75%) and Acidobacteria (2.82%) increased, while those of Proteobacteria (32.13%) decreased. Proteobacteria consisting of all five classes, mostly dominated by Gammaproteobacteria (14.87–16.21%), followed by Alphaproteobacteria (5.31–7.26%), Epsilonproteobacteria (4.70–10.22%), Betaproteobacteria (3.69–7.05%) and Deltaproteobacteria (3.55–4.20%), declined to some extent due to the elimination of aerobic strains with the establishment of anaerobic conditions. The emergence of ammonia-oxidizing archaea (such as *Nitrososphaera* and *Nitrosopumilus*), as well as the abundance of methanogenic archaea such as *Methanosaeta*, *Methanospirillum*, *Methanosarcina*, *Methanoregula*, *Methanobrevibacter*, *Methanocorpusculum*

and *Methanosphaera*, were detected at the start-up after the acclimatization period, whereas these groups were suppressed after long-term operation possibly due to the existence of competition from sulfate and iron-reducers (Baek et al., 2019; Liu et al., 2019). Bacteroidetes revealed dominancy throughout the operational period, which are regarded as the major degraders of complex carbohydrates to produce simpler compounds (such as sugars, organic acids and alcohols) for easier utilization by SRB (Vasquez et al., 2018), whereas Actinobacteria and Firmicutes metabolize organic matter, and Acidobacteria is diverse heterotrophs capable of degrading sugars to cellulose/hemicellulose in acidic environments (pH 3.0–6.0) (Auld et al., 2013; Villegas-Plazas et al., 2019; Ward et al., 2009). The co-existence and abundance of the phyla Bacteroidetes and Firmicutes affirms the stable operation of the AMD treatment, as described by Aoyagi et al. (2017). An increase in the dominance of these phyla, particularly Firmicutes and Actinobacteria, revealed their ability to adapt to the acidic environment by utilizing their autotrophic capabilities, ferric iron respiration and chemolithotrophic metabolism (Ogbughalu et al., 2020). Planctomycetes are a diverse group of aerobic/facultative chemoorganotrophs, which are involved in carbon fixation and carbohydrate metabolism (cellular respiration) (Dedysh and Kulichevskaya, 2013) as well as some species of this phylum are identified as anaerobic autotrophs that are known for facilitating anaerobic ammonium oxidation (anammox process) (Sinninghe Damsté et al., 2005). In addition, the presence of Chlorobi was found to be consistent, which are essentially obligate anaerobic photoautotrophs and capable of fixing carbon by oxidizing reduced sulfur compounds using the reverse tricarboxylic acid (rTCA) cycle (Ogbughalu et al., 2020). The taxonomic genus identified includes *Chlorobaculum* from the family Chlorobiaceae (green sulfur bacteria). Members of the phylum Chloroflexi are diversified, comprising filamentous aerobic heterotrophs and phototrophs (green non-sulfur bacteria). Some of the identified class of Chloroflexi includes Anaerolineae, Dehalococcoidetes, Thermomicrobia and Ktedonobacteria. These findings demonstrated that a wide range of anaerobic/facultative autotrophs and heterotrophs were present within the HSSF-CW (C).

The iron-metabolizing and sulfur-metabolizing bacteria were present abundantly in HSSF-CW (C). The microbiome of wetland presented an abundance of sulfur-oxidizing bacteria (SOB), such as *Cloacibacterium* (13.72%), *Sulfuricurvum* (9.94%), *Chlorobaculum* (3.91%), *Flavobacterium succinicans* (3.21%), *Thiobacillus* (1.11%), *Thiovirga* (1.34%) and *Thiomonas* (0.07%) in the acclimatization phase. However, the total abundance of SOB decreased substantially in the treatment phase to 0.01–0.29%, except for *Thiomonas* (1.88%). Besides the oxidation of reduced sulfur compounds, moderately acidophiles, *Thiomonas* and *Halothiobacillus* spp. are also described as iron-oxidizing bacteria (Hallberg, 2010) and Johnson and Hallberg (2005) mentioned the possibility that these bacteria can couple the oxidation of reduced sulfur (including sulfide) to the reduction of ferric iron in anaerobic environments and might therefore be important in the biological reductive dissolution of ferric iron. Besides, the abundance of *Acidithiobacillus* spp., consisting of sulfur oxidizers (e.g., *Acidithiobacillus thiooxidans*) and ferrous iron oxidizers (e.g., *Acidithiobacillus ferrooxidans*)

(Hallberg, 2010) increased significantly in the treatment phase. Some of the iron-oxidizing bacteria (FeOB) were detected during the initial operational phase of HSSF-CW (C), with the highest relative abundance of *Lysobacter* (2.35%) and *Crenothrix* (1.83%), followed by *Dechloromonas*, while in the steady operation phase, these groups were not detected. *Crenothrix* is known to oxidize not only iron but also manganese, only after the complete oxidation of ferrous iron (Cheng et al., 2019). Manganese-oxidizing genera reported in Mn deposits, e.g., *Flavobacterium*, *Sphingomonas* and *Acinetobacter* (Cai et al., 2015), were also present within the wetland throughout the study phases. In addition, some iron-reducing bacteria (FeRB) such as *Geothrix*, *Acidiphilium* and *Geobacter* were also present at low abundance. Many bacterial species from the order Rhodobacterales, Rhodospirillales, Rhizobiales and Rhodocyclales of the phylum Proteobacteria were detected and reported to perform versatile metabolic activities and survive under various extreme environmental conditions, especially in neutral to acidic mine drainage (Kisková et al., 2018).

The richness of SRB increased in phase V, majorly consisting of *Thermodesulfobium* sp., *Syntrophobacter* spp., *Desulfomonile* sp., *Desulfovibrio aminophilus*, *Desulfosporosinus meridiei*, *Desulfotomaculum* sp., *Desulfovirga adipica*, *Desulfobacca* sp., *Desulfovibrio mexicanus* and *Desulfurispora* sp. whereas *Desulfomicrobium* sp., *Desulfobulbus* spp. and *Desulfovibrio sulfodismutans* were detected only at the start-up phase. In the presence of high sulfate concentration, bacterial species capable of sulfate metabolism affiliated with Firmicutes and Proteobacteria dominated over methanogenic groups, particularly, *Thermodesulfobium* sp., a moderately thermophilic autotroph that can utilize H_2/CO_2 by sulfate respiration in acidic conditions (Campos-Quevedo et al., 2021; Sánchez-Andrea et al., 2011).

3.3.4 Results of biomass activity test from HSSF-CW (C)

Similar observations were made in HSSF-CW (C), the cumulative COD and sulfate removal is depicted in Fig. 3.19. High biomass activity values in terms of cumulative COD removal and sulfate reduction were observed as 1.56 mg COD removed mg TVS^{-1} d^{-1} and 0.88 mg sulfate reduced mg TVS^{-1} d^{-1}, respectively, after the acclimatization phase. After operating for about 196 days in the treatment phase, a gradual decrease in the heterotrophic activity and specific sulfidogenic activity to 1.05 mg COD removed mg TVS^{-1} d^{-1} and 0.79 mg sulfate reduced mg TVS^{-1} d^{-1} were recorded, indicating inactive biomass which contributed to significantly lower sulfate reduction efficiency at the end of the study.

3.3.5 Comparative performance assessment of HSSF-CW (A) and (C)

The comparative treatment results of HSSF-CW (A) and (C) are given in Table 3.10. Goat manure amended HSSF-CW (C) exhibited superior treatment performance than cow manure amended HSSF-CW (A). Significantly higher effluent pH, EC and alkalinity values were recorded for HSSF-CW (C) than HSSF-CW (A). However, both HSSF-CWs exhibited similar TDS values (~1200 mg L^{-1}), which exceeded the permissible discharge limit of 500 mg L^{-1} as recommended by EPA (2002). This implied that despite the effective removal of sulfate, metals and other dissolved ions, the oxidation and decomposition processes of organic media

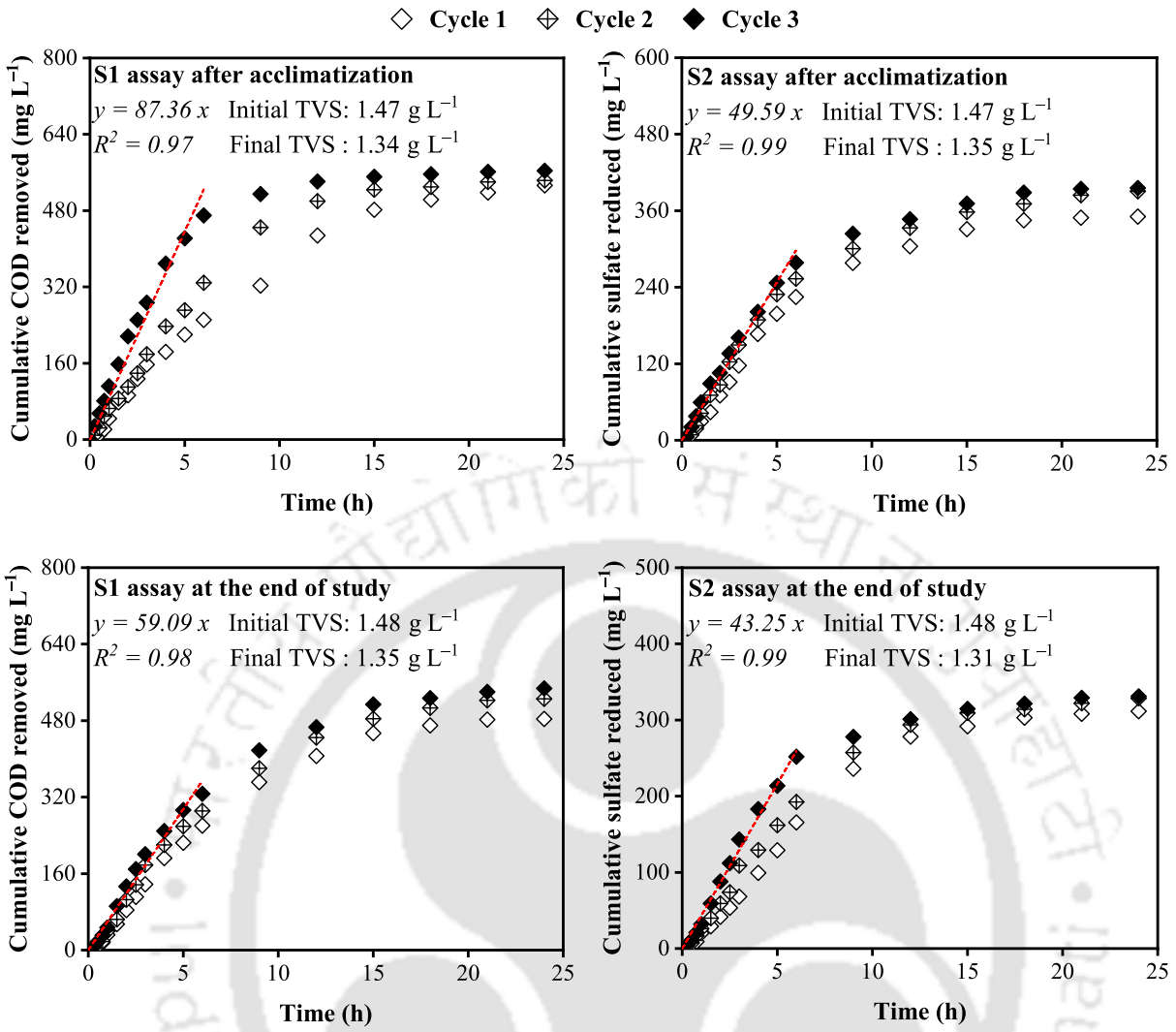

Fig. 3.19 Cumulative COD removal (mg L^{-1}) and sulfate reduction (mg L^{-1}) with time for HSSF-CW (C).

produced carboxyl and phenolic groups and further, the release of Ca^{2+}, Na^{+}, K^{+} and Mg^{2+} (Lax et al., 1986) contributed to the higher TDS and ionic strength of the effluent. Comparable sulfate removal (57–62%) was achieved in both HSSF-CWs, which was also confirmed by the results of high specific sulfidogenic activity in HSSF-CW (A) (0.60–0.83 mg sulfate reduced mg TVS^{-1} d^{-1}) and HSSF-CW (C) (0.79–0.88 mg sulfate reduced mg TVS^{-1} d^{-1}).

Organic media contain a high proportion of humified organic matter and are capable of heavy metal retention by adsorption and/or forming stable metal-organic complexes (Shuman, 1999). However, goat manure reportedly has high ion exchange capability than any other manures due to its relatively high pH raising ability (pH > 6.5) (Gichangi et al., 2012), which allows the weakly acidic sites of the goat manure to dissociate becoming negatively charged and thus provide greater metal ion binding capacity. Thus, HSSF-CW (C) achieved higher removal efficacy for metals like Fe, Al, Zn, Ni and Cr and metal concentration in the effluent remained below the permissible limits, except Co and Mn. While in HSSF-CW (A), regardless of good removal efficiency, metals including Fe, Al, Co, Ni and Mn concentration in the effluent exceeded permissible discharge limit.

Table 3.10 Performance comparison of HSSF-CW (A) and (C) in the treatment phase.

Parameters		Influent	Treated effluent		Removal[a] (%)	
			HSSF-CW (A)	HSSF-CW (C)	HSSF-CW (A)	HSSF-CW (C)
pH		2.1 ± 0.1	6.3 ± 0.7	7.4 ± 0.1	–	–
EC (mS m^{-1})		427 ± 19	129 ± 26	175 ± 27	56.59–80.97	41.98–71.14
TDS (mg L^{-1})		3131 ± 71	1260 ± 281	1243 ± 180	34.99–72.21	48.16–70.07
COD (mg L^{-1})		20.64 ± 12	97.54 ± 46	71.97 ± 34	–	–
Acidity (mg L^{-1} as $CaCO_3$)		723 ± 28	–	–	–	–
Alkalinity (mg L^{-1} as $CaCO_3$)		–	290 ± 240	771 ± 228	–	–
Sulfate (mg L^{-1})		1206 ± 29	581 ± 160	430 ± 169	40.41–75.29	23.72–84.39
Metals	Fe (mg L^{-1})	106 ± 7.50	9.68 ± 6.63	0.18 ± 0.08	74.25–100	98.93–100
	Al (mg L^{-1})	26 ± 1.30	10.28 ± 3.38	3.25 ± 0.74	20.05–91.04	77.69–94.25
	Mn (mg L^{-1})	6.25 ± 0.28	10.36 ± 4.81	1.71 ± 1.48	–159.80–85.17	–2.77–96.10
	Zn (mg L^{-1})	5.14 ± 0.13	0.29 ± 0.22	0.11 ± 0.07	84.75–99.47	88.72–99.13
	Co (mg L^{-1})	1.06 ± 0.04	0.09 ± 0.07	0.02 ± 0.01	71.43–100	72.48–100
	Ni (mg L^{-1})	1.09 ± 0.04	0.05 ± 0.03	0.02 ± 0.01	66.41–100	95.02–100
	Cr (mg L^{-1})	1.06 ± 0.06	0.00	0.01	91.99–100	95.25–100

[a]Removal data presented as the min–max value. Values exceeding the discharge limits as recommended by CPCB (1993) and EPA (2002) are marked in red.

3.4 Summary

HSSF-CW (C) demonstrated significantly superior treatment performance in terms of alkalinity generation (771 mg L^{-1} as $CaCO_3$) and metal removal below the recommended discharge standards as compared to HSSF-CW (A). This emphasizes the importance of organic media selection and intrinsic properties for the suitability of wetland media in CWs. Altogether, organic media amended HSSF-CWs exhibited effective removal of metals: Fe (91–100%), Al (61–87%), Zn (94–98%), Co (92–98%), Ni (96–98%) and Cr (99–100%), except Mn. Microbial-assisted sulfate reduction (57–62%) was observed by SRB groups (*Thermodesulfobium*, *Syntrophobacter*, *Desulfomonile*, *Desulfovibrio* and *Desulfosporosinus*). However, the longevity of the organic-rich amended CWs is debatable and would require consistent replacement of exhausted bed, and thereby disposal of metal-rich media. Metal speciation results revealed possible metal toxicity due to more bioavailable manganese and cobalt ions from the wetland media under unfavorable environmental conditions. Therefore, necessary post-treatment and recovery measures need to be further considered. The metal mass balance analysis indicated media as the major sink of metal retention (58–95%). In comparison, the metal uptake by *T. latifolia* was minimal (0.31–3%) and did not significantly contribute to metal removal. A higher accumulation of heavy metals was observed in the belowground plant tissues, but manganese. Thus, *T. latifolia* exhibited high BCF and TF (> 1.0), suggesting that the plant could be a hyperaccumulator of manganese.

References

Allen, S. E., Grimshaw, H. M., Parkinson, J. A., and Quarmby, C. (1974). *Chemical Analysis of Ecological Materials*. Blackwell Scientific Publications, Oxford, UK.

Anning, A. K., Korsah, P. E., and Addo-Fordjour, P. (2013). Phytoremediation of wastewater with *Limnocharis flava*, *Thalia geniculata* and *Typha latifolia* in constructed wetlands. *International Journal of Phytoremediation*, 15(5):452–464.

Aoyagi, T., Hamai, T., Hori, T., Sato, Y., Kobayashi, M., Sato, Y., Inaba, T., Ogata, A., Habe, H., and Sakata, T. (2017). Hydraulic retention time and pH affect the performance and microbial communities of passive bioreactors for treatment of acid mine drainage. *AMB Express*, 7:1–11.

APHA (2012). *Standard Methods for the Examination of Water and Wastewater*. American Public Health Association, Washington, DC.

Auld, R. R., Myre, M., Mykytczuk, N. C. S., Leduc, L. G., and Merritt, T. J. S. (2013). Characterization of the microbial acid mine drainage microbial community using culturing and direct sequencing techniques. *Journal of Microbiological Methods*, 93(2):108–115.

Baek, G., Kim, J., and Lee, C. (2019). A review of the effects of iron compounds on methanogenesis in anaerobic environments. *Renewable and Sustainable Energy Reviews*, 113:109282.

Bechard, G. M. (1994). *Microbiological process for the treatment of acid mine drainage using cellulosic substrates*. PhD Thesis, Department of Biology, Carleton University, Ottawa, Ontario.

Biermann, V., Lillicrap, A. M., Magana, C., Price, B., Bell, R. W., and Oldham, C. E. (2014). Applicability of passive compost bioreactors for treatment of extremely acidic and saline waters in semi-arid climates. *Water Research*, 55:83–94.

Brown, P. A., Gill, S. A., and Allen, S. J. (2000). Metal removal from wastewater using peat. *Water Research*, 34:3907–3916.

Cai, Y., Li, D., Liang, Y., Luo, Y., Zeng, H., and Zhang, J. (2015). Effective start-up biofiltration method for Fe, Mn, and ammonia removal and bacterial community analysis. *Bioresource Technology*, 176:149–155.

Campos-Quevedo, N., Moreno-Perlin, T., Razo-Flores, E., Stams, A. J. M., Celis, L. B., and Sánchez-Andrea, I. (2021). Acetotrophic sulfate-reducing consortia develop active biofilms on zeolite and glass beads in batch cultures at initial pH 3. *Applied Microbiology and Biotechnology*, 105:52135227.

Chen, J., Li, X., Jia, W., Shen, S., Deng, S., Ji, B., and Chang, J. (2021). Promotion of bioremediation performance in constructed wetland microcosms for acid mine drainage treatment by using organic substrates and supplementing domestic wastewater and plant litter broth. *Journal of Hazardous Materials*, 404:124125.

Cheng, Q., Huang, Y., Nengzi, L., Liu, J., and Zhang, J. (2019). Performance and microbial community profiles in pilot-scale biofilter for ammonia, iron and manganese removal at different dissolved oxygen concentrations. *World Journal of Microbiology and Biotechnology*, 35:1–11.

Choudhary, R. P. and Sheoran, A. S. (2012). Performance of single substrate in sulphate reducing bioreactor for the treatment of acid mine drainage. *Minerals Engineering*, 39:29–35.

Collins, B. S., Sharitz, R. R., and Coughlin, D. P. (2005). Elemental composition of native wetland plants in constructed mesocosm treatment wetlands. *Bioresource Technology*, 96(8):937–948.

CPCB (1993). *General Standards for Discharge of Environmental Pollutants Part-A: Effluents, Schedule - VI (Rule 3A)*. Central Pollution Control Board, New Delhi, India.

Dan, A., Oka, M., Fujii, Y., Soda, S., Ishigaki, T., Machimura, T., and Ike, M. (2017). Removal of heavy metals from synthetic landfill leachate in lab-scale vertical flow constructed wetlands. *Science of the Total Environment*, 584:742–750.

Dann, A. L., Cooper, R. S., and Bowman, J. P. (2009). Investigation and optimization of

a passively operated compost-based system for remediation of acidic, highly iron-and sulfate-rich industrial waste water. *Water Research*, 43(8):2302–2316.

Dedysh, S. N. and Kulichevskaya, I. S. (2013). Acidophilic planctomycetes: Expanding the horizons of new planctomycete diversity. In *Planctomycetes: Cell Structure, Origins and Biology*, pages 125–139. Humana Press, Totowa, NJ.

Dufresne, K., Neculita, C., Brisson, J., and Genty, T. (2015). Metal retention mechanisms in pilot-scale constructed wetlands receiving acid mine drainage. In *Proceedings of the 10th ICARD (International Conference on Acid Rock Drainage)-IMWA (International Mine Water Association)*, pages 21–24, Santiago, Chile.

Emmerich, M., Bhansali, A., Lösekann-Behrens, T., Schröder, C., Kappler, A., and Behrens, S. (2012). Abundance, distribution, and activity of Fe (II)-oxidizing and Fe (III)-reducing microorganisms in hypersaline sediments of Lake Kasin, southern Russia. *Applied and Environmental Microbiology*, 78(12):4386–4399.

EPA (2002). *Standards for Effluent Discharge Regulations. General Notice No. 44. of 2003*. Environmental Protection Agency. (accessed on 17.04.19).

Fan, M., Lin, Y., Huo, H., Liu, Y., Zhao, L., Wang, E., Chen, W., and Wei, G. (2016). Microbial communities in riparian soils of a settling pond for mine drainage treatment. *Water Research*, 96:198–207.

Fyson, A. (2000). Angiosperms in acidic waters at pH 3 and below. *Hydrobiologia*, 433:129–135.

Gandy, C. J., Davis, J. E., Orme, P. H., Potter, H. A., and Jarvis, A. P. (2016). Metal removal mechanisms in a short hydraulic residence time subsurface flow compost wetland for mine drainage treatment. *Ecological Engineering*, 97:179–185.

Gibert, O., de Pablo, J., Cortina, J. L., and Ayora, C. (2005). Municipal compost-based mixture for acid mine drainage bioremediation: Metal retention mechanisms. *Applied Geochemistry*, 20(9):1648–1657.

Gichangi, E. M., Mnkeni, P. N. S., and Muchaonyerwa, P. (2012). Evaluation of the heavy metal immobilization potential of pine bark-based composts. *Journal of Plant Nutrition*, 35(12):1853–1865.

Gill, L. W., Ring, P., Casey, B., Higgins, N. M. P., and Johnston, P. M. (2017). Long term heavy metal removal by a constructed wetland treating rainfall runoff from a motorway. *Science of the Total Environment*, 601:32–44.

Gillespie Jr., W. B., Hawkins, W. B., Rodgers Jr., J. H., Cano, M. L., and Dorn, P. B. (2000). Transfers and transformations of zinc in constructed wetlands: Mitigation of a refinery effluent. *Ecological Engineering*, 14(3):279–292.

Hallberg, K. B. (2010). New perspectives in acid mine drainage microbiology. *Hydrometallurgy*, 104(3-4):448–453.

Hallberg, K. B. and Johnson, D. B. (2005). Biological manganese removal from acid mine drainage in constructed wetlands and prototype bioreactors. *Science of the Total Environment*, 338(1-2):115–124.

Herrera-Melián, J. A., González-Bordón, A., Martín-González, M. A., García-Jiménez, P., Carrasco, M., and Araña, J. (2014). Palm tree mulch as substrate for primary treatment wetlands processing high strength urban wastewater. *Journal of Environmental Management*, 139:22–31.

Jawed, M. and Tare, V. (1999). Microbial composition assessment of anaerobic biomass through methanogenic activity tests. *Water SA*, 25(3):345–350.

Johnson, D. B. and Hallberg, K. B. (2002). Pitfalls of passive mine water treatment. *Reviews*

in Environmental Science and Biotechnology, 1:335–343.

Johnson, D. B. and Hallberg, K. B. (2005). Biogeochemistry of the compost bioreactor components of a composite acid mine drainage passive remediation system. *Science of the Total Environment*, 338(1-2):81–93.

Jordan, S. N., Redington, W., and Holland, L. B. (2021). Remediation of metal contaminated simulated acid mine drainage using a lab-scale spent mushroom substrate wetland. *Water, Air, & Soil Pollution*, 232:220.

Karam, A. (1993). Chemical properties of organic soils. In *Soil Sampling and Methods of Analysis*, pages 459–471. Lewis Publishers, Boca Raton, FL.

Kisková, J., Perháčová, Z., Vlčko, L., Sedláková, J., Kvasnová, S., and Pristaš, P. (2018). The bacterial population of neutral mine drainage water of Elizabeth's Shaft (Slovinky, Slovakia). *Current Microbiology*, 75:988–996.

Komy, Z. R., Abdelraheem, W. H., and Ismail, N. M. (2013). Biosorption of Cu^{2+} by *Eichhornia crassipes*: Physicochemical characterization, biosorption modeling and mechanism. *Journal of King Saud University - Science*, 25(1):47–56.

Kröpfelová, L., Vymazal, J., Švehla, J., and Štíchová, J. (2009). Removal of trace elements in three horizontal sub-surface flow constructed wetlands in the Czech Republic. *Environmental Pollution*, 157(4):1186–1194.

Lax, A., Roig, A., and Costa, F. (1986). A method for determining the cation-exchange capacity of organic materials. *Plant and Soil*, 94(3):349–355.

Lesage, E. (2006). *Behaviour of heavy metals in constructed treatment wetlands*. PhD Thesis, Faculty of Bioscience Engineering, Ghent University, Ghent, Belgium.

Lesage, E., Rousseau, D. P. L., Meers, E., Tack, F. M. G., and De Pauw, N. (2007). Accumulation of metals in a horizontal subsurface flow constructed wetland treating domestic wastewater in Flanders, Belgium. *Science of the Total Environment*, 380(1-3):102–115.

Liu, Y., Gu, M., Yin, Q., and Wu, G. (2019). Inhibition mitigation and ecological mechanism of mesophilic methanogenesis triggered by supplement of ferroferric oxide in sulfate-containing systems. *Bioresource Technology*, 288:121546.

Lizama-Allende, K., Fletcher, T. D., and Sun, G. (2012). The effect of substrate media on the removal of arsenic, boron and iron from an acidic wastewater in planted column reactors. *Chemical Engineering Journal*, 179:119–130.

Ly, T., Wright, J. R., Weit, N., McLimans, C. J., Ulrich, N., Tokarev, V., Valkanas, M. M., Trun, N., Rummel, S., Grant, C. J., and Lamendella, R. (2019). Microbial communities associated with passive acidic abandoned coal mine remediation. *Frontiers in Microbiology*, 10(1955):1–13.

Manios, T., Stentiford, E. I., and Millner, P. (2003a). Removal of heavy metals from a metaliferous water solution by *Typha latifolia* plants and sewage sludge compost. *Chemosphere*, 53(5):487–494.

Manios, T., Stentiford, E. I., and Millner, P. A. (2003b). The effect of heavy metals accumulation on the chlorophyll concentration of *Typha latifolia* plants, growing in a substrate containing sewage sludge compost and watered with metaliferus water. *Ecological Engineering*, 20(1):65–74.

Mishra, V. K., Upadhyaya, A. R., Pandey, S. K., and Tripathi, B. D. (2008). Heavy metal pollution induced due to coal mining effluent on surrounding aquatic ecosystem and its management through naturally occurring aquatic macrophytes. *Bioresource Technology*, 99(5):930–936.

Moreno, J. L., Hernández, T., and Garcia, C. (1999). Effects of a cadmium-contaminated

sewage sludge compost on dynamics of organic matter and microbial activity in an arid soil. *Biology and Fertility of Soils*, 28(3):230–237.

Mufarrege, M. M., Hadad, H. R., Di Luca, G. A., and Maine, M. A. (2014). Metal dynamics and tolerance of *Typha domingensis* exposed to high concentrations of Cr, Ni and Zn. *Ecotoxicology and Environmental Safety*, 105:90–96.

Mungur, A. S., Shutes, R. B. E., Revitt, D. M., and House, M. A. (1995). An assessment of metal removal from highway runoff by a natural wetland. *Water Science & Technology*, 32(3):169–175.

Nabuyanda, M. M., van Bruggen, J., Kelderman, P., and Irvine, K. (2019). Investigating Co, Cu, and Pb retention and remobilization after drying and rewetting treatments in greenhouse laboratory-scale constructed treatments with and without *Typha angustifolia*, and connected phytoremediation potential. *Journal of Environmental Management*, 236:510–518.

Neculita, C. M. and Rosa, E. (2019). A review of the implications and challenges of manganese removal from mine drainage. *Chemosphere*, 214:491–510.

Ogbughalu, O. T., Vasileiadis, S., Schumann, R. C., Gerson, A. R., Li, J., Smart, R. S. C., and Short, M. D. (2020). Role of microbial diversity for sustainable pyrite oxidation control in acid and metalliferous drainage prevention. *Journal of Hazardous Materials*, 393:122338.

O'Sullivan, A. D., Moran, B. M., and Otte, M. L. (2004). Accumulation and fate of contaminants (Zn, Pb, Fe and S) in substrates of wetlands constructed for treating mine wastewater. *Water, Air, and Soil Pollution*, 157(1-4):345–364.

Pagnanelli, F., Mainelli, S., Vegliò, F., and Toro, L. (2003). Heavy metal removal by olive pomace: Biosorbent characterisation and equilibrium modelling. *Chemical Engineering Science*, 58(20):4709–4717.

Pi, N., Tam, N. F. Y., and Wong, M. H. (2011). Formation of iron plaque on mangrove roots receiving wastewater and its role in immobilization of wastewater-borne pollutants. *Marine Pollution Bulletin*, 63(5-12):402–411.

Ranieri, E. (2012). Chromium and nickel control in full- and small-scale subsuperficial flow constructed wetlands. *Soil & Sediment Contamination*, 21(7):802–814.

Ruehl, M. D. and Hiibel, S. R. (2020). Evaluation of organic carbon and microbial inoculum for bioremediation of acid mine drainage. *Minerals Engineering*, 157:106554.

Sánchez-Andrea, I., Rodríguez, N., Amils, R., and Sanz, J. L. (2011). Microbial diversity in anaerobic sediments at Rio Tinto, a naturally acidic environment with a high heavy metal content. *Applied and Environmental Microbiology*, 77(17):6085–6093.

Sasmaz, A., Obek, E., and Hasar, H. (2008). The accumulation of heavy metals in *Typha latifolia* L. grown in a stream carrying secondary effluent. *Ecological Engineering*, 33(3-4):278–284.

Seo, E. Y., Cheong, Y. W., Yim, G. J., Min, K. W., and Geroni, J. N. (2017). Recovery of Fe, Al and Mn in acid coal mine drainage by sequential selective precipitation with control of pH. *Catena*, 148(1):11–16.

Sheoran, A. S. (2017). Management of acidic mine waste water by constructed wetland treatment systems: A bench scale study. *European Journal of Sustainable Development*, 6(2):245.

Shuman, L. M. (1999). Organic waste amendments effect on zinc fractions of two soils. *Journal of Environmental Quality*, 28:1442–1447.

Sinninghe Damsté, J. S., Rijpstra, W. I. C., Geenevasen, J. A., Strous, M., and Jetten, M. S. M. (2005). Structural identification of ladderane and other membrane lipids of planctomycetes capable of anaerobic ammonium oxidation (anammox). *The FEBS Journal*,

272(16):4270–4283.

Song, H., Yim, G.-J., Ji, S.-W., Neculita, C. M., and Hwang, T. (2012). Pilot-scale passive bioreactors for the treatment of acid mine drainage: Efficiency of mushroom compost vs. mixed substrates for metal removal. *Journal of Environmental Management*, 111:150–158.

Stein, O. R., Borden-Stewart, D. J., Hook, P. B., and Jones, W. L. (2007). Seasonal influence on sulfate reduction and zinc sequestration in subsurface treatment wetlands. *Water Research*, 41(15):3440–3448.

Stumm, W. and Morgan, J. J. (1981). *Aquatic chemistry: An introduction emphasizing chemical equilibria in natural waters*. Wiley, New York.

Szkokan-Emilson, E. J., Watmough, S. A., and Gunn, J. M. (2014). Wetlands as long-term sources of metals to receiving waters in mining-impacted landscapes. *Environmental Pollution*, 192:91–103.

Tchobanoglous, G., Burton, F. L., Stensel, H. D., Metcalf, and Eddy (2003). *Wastewater Engineering: Treatment and Reuse*. McGraw-Hill Education, India.

Tessier, A., Campbell, P. G. C., and Bisson, M. (1979). Sequential extraction procedure for the speciation of particulate trace metals. *Analytical Chemistry*, 51(7):844–851.

USEPA (1992). *Method 1311: Toxicity Characteristic Leaching Procedure*. Environmental Protection Agency, Washington, DC.

USEPA (1994). *EPA-902-B-94-001: Technical Assistance Document for Complying with the TC Rule and Implementing the Toxicity Characteristic Leaching Procedure (TCLP)*. Environmental Protection Agency, Washington, DC.

USEPA (1996). *Method 3050B: Acid Digestion of Sediments, Sludges, and Soils*. Environmental Protection Agency, Washington, DC.

USEPA (2004). *Method 9045D: Soil and Waste pH*. Environmental Protection Agency, Washington, DC.

Vasquez, Y., Escobar, M. C., Saenz, J. S., Quiceno-Vallejo, M. F., Neculita, C. M., Arbeli, Z., and Roldan, F. (2018). Effect of hydraulic retention time on microbial community in biochemical passive reactors during treatment of acid mine drainage. *Bioresource Technology*, 247:624–632.

Villegas-Plazas, M., Sanabria, J., and Junca, H. (2019). A composite taxonomical and functional framework of microbiomes under acid mine drainage bioremediation systems. *Journal of Environmental Management*, 251:109581.

Vymazal, J. (2005). Removal of heavy metals in a horizontal sub-surface flow constructed wetland. *Journal of Environmental Science and Health*, 40(6-7):1369–1379.

Ward, N. L., Challacombe, J. F., Janssen, P. H., Henrissat, B., Coutinho, P. M., Wu, M., Xie, G., Haft, D. H., Sait, M., Badger, J., Ravi, D. B., Bradley, B., Brettin, T. S., Brinkac, L. M., Bruce, D., Creasy, T., Daugherty, S. C., Davidsen, T. M., DeBoy, R. T., Detter, J. C., Dodson, R. J., Durkin, A. S., Ganapathy, A., Gwinn-Giglio, M., Han, C. S., Khouri, H., Kiss, H., Kothari, S. P., Madupu, R., Nelson, K. E., Nelson, W. C., Paulsen, I., Penn, K., Ren, Q., Rosovitz, M. J., Selengut, J. D., Shrivastava, S., Sullivan, S. A., Tapia, R., Thompson, L. S., Watkins, K. L., Yang, Q., Yu, C., Zafar, N., Zhou, L., and Kuske, C. R. (2009). Three genomes from the phylum Acidobacteria provide insight into the lifestyles of these microorganisms in soils. *Applied and Environmental Microbiology*, 75(7):2046–2056.

Wu, H., Zhang, J., Ngo, H. H., Guo, W., Hu, Z., Liang, S., Fan, J., and Liu, H. (2015). A review on the sustainability of constructed wetlands for wastewater treatment: Design and operation. *Bioresource Technology*, 175:594–601.

Xu, J. C., Chen, G., Huang, X. F., Li, G. M., Liu, J., Yang, N., and Gao, S. N. (2009). Iron and

manganese removal by using manganese ore constructed wetlands in the reclamation of steel wastewater. *Journal of Hazardous Materials*, 169(1-3):309–317.

Xu, X. and Mills, G. L. (2018). Do constructed wetlands remove metals or increase metal bioavailability? *Journal of Environmental Management*, 218:245–255.

Ye, Z. H., Whiting, S. N., Lin, Z. Q., Lytle, C. M., Qian, J. H., and Terry, N. (2001). Removal and distribution of iron, manganese, cobalt, and nickel within a Pennsylvania constructed wetland treating coal combustion by-product leachate. *Journal of Environmental Quality*, 30(4):1464–1473.

Younger, P. L. and Henderson, R. (2014). Synergistic wetland treatment of sewage and mine water: Pollutant removal performance of the first full-scale system. *Water Research*, 55:74–82.

Zagury, G. J., Kulnieks, V. I., and Neculita, C. M. (2006). Characterization and reactivity assessment of organic substrates for sulphate-reducing bacteria in acid mine drainage treatment. *Chemosphere*, 64(6):944–954.

4

Effect of Influencing Factors on Acid Mine Drainage Treatment and Prospects of Resource Recovery

The role of vegetation and the impact of operational as well as environmental factors on the bioremediation of AMD are discussed in this chapter along with the metal recovery prospects.

4.1 Introduction

In general, the efficacy of CWs largely depends on the type of CW (surface/sub-surface flow, horizontal/vertical and anaerobic/aerobic), surface area, depth, type of plants, organic media, HLR, HRT, flow regime, AMD composition (net acidic or net alkaline) and environmental factors such as temperature, evapotranspiration and rainfall (Acharya and Kharel, 2020; Johnson and Hallberg, 2005). Wetland plants such as common reed (*Phragmites* spp.) and cattail (*Typha* spp.) are most widely studied for heavy metal removal (Türker et al., 2013; Galletti et al., 2010). However, literature presents a very controversial aspect of wetland plants involved in the remediation of AMD (Scholz, 2006). Some previous studies have illustrated minor to insignificant contribution of plants in heavy metal uptake (Lizama-Allende et al., 2021; Manios et al., 2003; Mays and Edwards, 2001). On the contrary, several studies have shown a significantly beneficial role of plant species with respect to metal uptake and phytoremediation ability (Gaballah et al., 2021; Gikas et al., 2013; Rahman et al., 2011).

So far, numerous studies have focused primarily on the metal uptake ability of wetland plants. However, AMD also has other pollutants like high acidity and sulfate ions in addition to heavy metals. Therefore, an assessment of the role of plants in other biochemical processes involved in the remediation of AMD is necessary. Further, the metal removal process in any CWs is a function of plant species, growth conditions, ability to grow in the media or organics supplemented, tolerance to metal stress and adaptability to the varying concentration of different metals present in AMD. Similarly, previous research has shown wide variability in

the sulfate removal efficiencies by incorporating plants in CWs (Kadlec and Wallace, 2008).

CW functions rely on natural processes, which are strongly influenced by weather conditions. Kadlec and Wallace (2008) highlighted the importance of meteorological effects on the CW function and it is hypothesized that there is a significant difference between the treatment efficiency of CWs during different seasons (dry and wet period) under natural conditions. Although the effects of climatic conditions are realized as a crucial aspect dictating the efficiency of CWs, only a few studies have considered the role of climatic variations and seasonality on the treatment performance of AMD in CWs (Gupta et al., 2020; Stein et al., 2007). The northeastern region of India is one of the highest rainfall-receiving regions on Earth (Jhajharia et al., 2012; Singh et al., 2021). Therefore, in the present study, rainfall is considered, which is a primary atmospheric parameter of the climate system. So far, no study has described the effect of rainfall on the bioremediation of AMD using CWs in subtropical climatic conditions. Therefore, understanding the dynamic nature of AMD treatment in CW associated with seasonal variation is a prerequisite for predicting and improvising the treatment efficiency in field applications.

Chapter 3 elucidated the major retention of metals in the wetland bed (or media) of CWs and revealed the leaching of a few metals to some extent. Likewise, many authors have raised concerns regarding the metal leaching from CWs due to the increased metal bioavailability (Khan et al., 2019; Xu and Mills, 2018). Thus, after many years of use, CWs may become contaminant sinks or secondary source of metal pollution when water chemistry and environmental conditions change drastically. Therefore, the recovery of metals from the wetland media is essential for environmentally friendly disposal. Ethylenediaminetetraacetic acid (EDTA) has been largely employed in soil washings for the extraction of Cd, Pb and Ni (Di Palma et al., 2003; Goel and Gautam, 2010). Besides, mineral acids have been extensively practiced in metal leaching (Chen et al., 2014), but its associated hazardous and non-eco-friendly nature limits its use and paves the way for organic acids (Musariri et al., 2019).

The current study evaluates the role of vegetation (*Typha latifolia*) and the effect of HLRs on the performance efficiency of small-scale CWs. It also considers the effect of rainfall on AMD treatment and metal retention in CWs under subtropical climatic conditions. Further, this study demonstrates the possibility of metal extraction and recovery from wetland deposits using a chelating agent and organic acids to meet environmental compliance.

4.2 Materials and methods

4.2.1 Chemicals and reagents

Chemicals and reagents used in the present study were of AR grade as described in Chapter 2 (section 2.3.2) and Chapter 3 (section 3.2.1). EDTA ($C_{10}H_{14}N_2O_8Na_2.2H_2O$) was procured from SRL, India. Potassium bromide and n-hexane were obtained from Merck, India, while L-ascorbic acid ($C_6H_8O_6$), calcium hydroxide and sodium sulfide flakes were purchased from Himedia, India. Stock solutions were prepared using milli-Q water.

4.2.2 Description of the weather conditions

The research area was located on the rooftop of M-block, IIT Guwahati (26.1878°N, 91.6916°E). The weather station facility equipped with instruments (Davis Vantage Pro, USA) was located at the nearest opposite block (Annexure building, IIT Guwahati). The weather conditions have been continuously monitored and recorded since January 2021. The meteorological data included, among others, temperature, humidity, dew point, wind speed, wind direction, solar radiation, heat index, evapotranspiration and rainfall depth. Fig. 4.1 shows the average atmospheric temperature (in °C) and accumulated rainfall (in mm) per day. These values can be considered typical of a subtropical climate.

4.2.3 Design and operation of wetland microcosms

Four small-scale HSSF-CW microcosms were fabricated using commercially available high-density polyethylene (HDPE) crates (Supreme, India) having dimensions 0.565 m × 0.365 m × 0.30 m (length × width × height). Three sampling ports were provided at mid-depth and about 0.15 m center-to-center distance [(C_1, C_2, C_3) or (P_1, P_2, P_3) or (S_1, S_2, S_3) or (U_1, U_2, U_3)] along the length of the CWs (Fig. 4.2). Wetland media comprised of bottom-most pea-sized gravel (10 mm < ϕ< 12.5 mm, 3 cm thick), overlaid by layers of bamboo chips, cow manure, and soil having a thickness of 6, 18 and 3 cm, respectively, provided in the same proportion (v/v) as HSSF-CW (A). The detailed media characterization is provided in Chapter 3 (Table 3.3).

Two CW microcosm units, designated as CCW (unplanted) and PCW (planted), were designed to assess the role of plants (*Typha latifolia*) and the impact of HLRs on the treatment efficacy of CWs. Plants growing in natural wetlands inside the IITG campus were transplanted in PCW at a planting density of 25 plants m^{-2}, whereas CCW was kept unplanted. The effective volume for CCW and PCW were 27 and 26 L; therefore, the overall porosities of the bed were about 0.44 and 0.42, respectively. CCW and PCW were operated under varying HLRs of

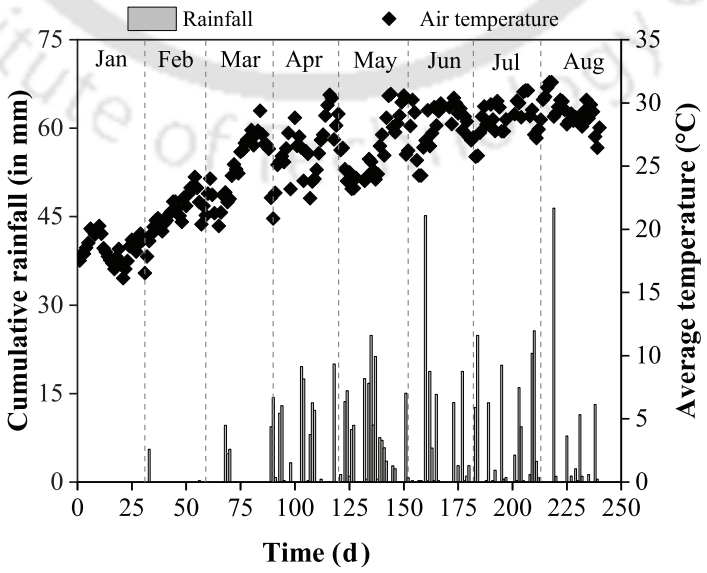

Fig. 4.1 Average temperature and cumulative rainfall depth during Jan–Aug 2021. (*Source: Air Pollution Laboratory, IIT Guwahati*)

0.019, 0.026 and 0.033 m^3 m^{-2} d^{-1}, controlled by regulating flow discharge at 2.68, 3.75 and 4.51 mL min^{-1}, respectively. The photographic image of CCW and PCW is shown in Fig. 4.3.

The other two units, having similar design and media configuration as CCW/PCW, were assigned as SCW (sheltered) and UCW (unsheltered), designed to study the effect of rainfall on the bioremediation of AMD in subtropical climatic conditions. SCW and UCW were planted with *Typha latifolia* at 15 plants m^{-2}. The effective volume determined for SCW and UCW were 20 and 19.60 L, which yielded a porosity of about 0.32. AMD was discharged at 1.95 mL min^{-1} to attain an HLR of 0.014 m^3 m^{-2} d^{-1}. As described in section 3.2.2, synthetic AMD was prepared and discharged from an influent feed tank (capacity 60 L each) using two-channel peristaltic pumps. The diluted concentration of AMD (10–70% of full strength) was fed into CWs for the first 35 days (acclimatization phase I–IV) and thereafter, full-strength AMD was discharged (treatment phase V). CW microcosms were placed outdoor under a temporary structure (sheltered from rain), whereas UCW was kept unsheltered on the rooftop of Environmental Engineering Laboratory, IIT Guwahati.

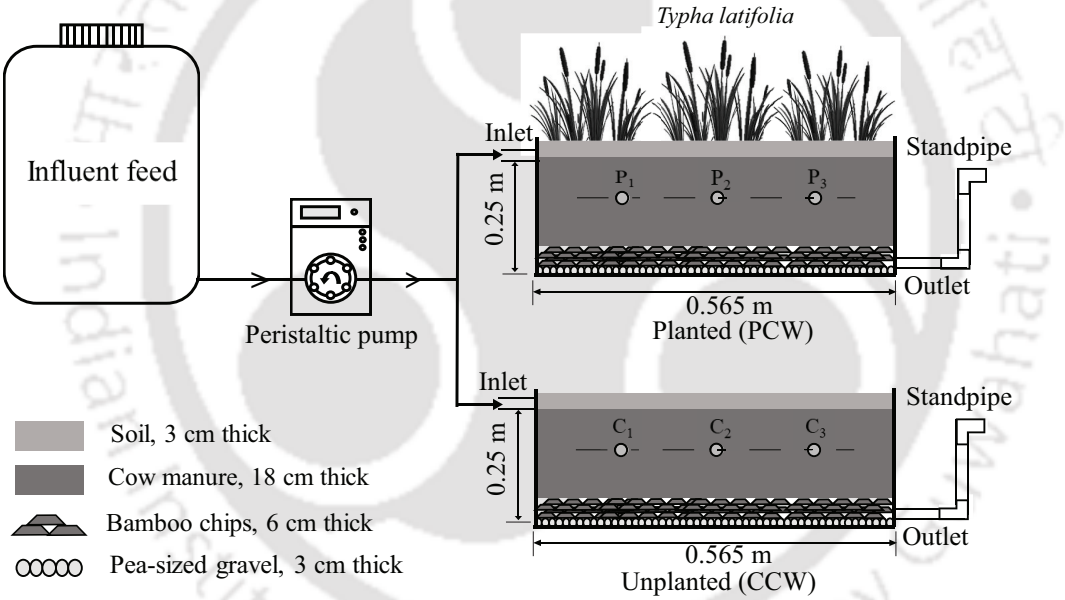

Fig. 4.2 Schematic diagram of the experimental CW microcosms (CCW and PCW).

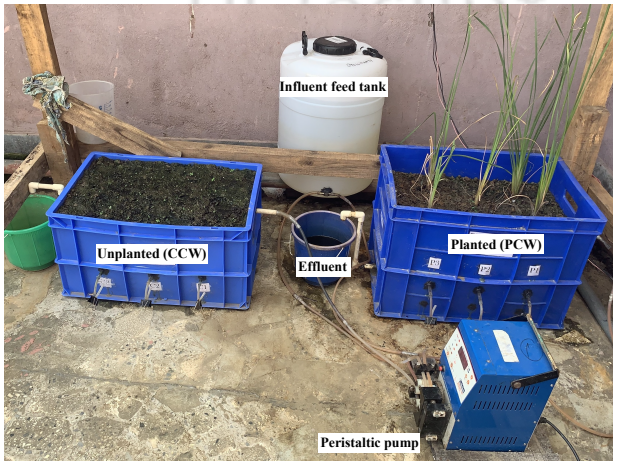

Fig. 4.3 Photographic image of CCW and PCW microcosms.

4.2.4 Analytical methods

All the analytical techniques used in this study are mentioned in Chapter 2 (section 2.3.3) and Chapter 3 (section 3.2.8). Biomass activity determination is provided in Chapter 3 (section 3.2.6). DO of water samples from occasional port sampling was measured in triplicates using modified Winkler's method for small volume samples (Shriwastav et al., 2010). Total dissolved sulfide was measured as per the Iodometric method of APHA (2012).

For the characterization of the basic classes of the chemical groups in wetland media, Fourier Transform Infrared Spectroscopy (FTIR) was used (PerkinElmer, Spectrum Two, Waltham, MA). Samples were prepared using the KBr pellet method at room temperature by mixing samples (about 1 mg) uniformly with KBr in a 1:100 ratio. The spectra were recorded over the range of 400–4000 cm^{-1} wavenumber at 1.0 cm^{-1} resolution by transmittance mode.

4.2.4.1 Metal extraction and recovery process

The estimation of total metal concentration in media was determined by destroying CWs after the completion of the study. The wetland media from random triplicate sampling was oven-dried at 105°C and homogenized to pass < 2 mm sieve. The samples were subjected to acid-digestion procedure as described in section 2.3.3 of Chapter 2 (Equation 4.1).

$$\text{Total metal concentration in media } (M_0,\ \text{mg kg}^{-1}) = \frac{C_{ext} \times V_{ext}}{D_w} \tag{4.1}$$

where 'C_{ext}' represents the total metal concentration in extractant solution (mg L^{-1}); 'V_{ext}' is the final volume of extractant solution (0.1 L) and 'D_w' is the dry weight of the media (kg).

For metal extraction (or leaching), 2 g of powdered media samples were taken and transferred to the 250 mL conical flasks containing specific lixiviants of varying concentrations (each 100 mL). A control test was also set up using millipore water as the extracting solution to determine the amount of water-elutable heavy metals. All tests were performed in triplicates to ascertain reproducibility and the data represented are the mean values. All leaching experiments were conducted at a fixed liquid-to-solid ratio (L/S, mL/g) of 50 at constant shaking in the end-to-end rotatory shaker at room temperature (28–30°C) for 24 h (Fig. 4.4). After the completion of batch leaching experiments, the media slurries were first centrifuged at 5000 rpm for 10 min and the supernatant was separated and then later acidified (pH < 2.0). The acidified supernatant was filtered through a 0.45 μm filter and later analyzed for metal concentration in FAAS. In the case of EDTA chelation, this acidification step allows the splintering of the EDTA-metal complex and free EDTA gets precipitated out of the solution overnight, which can be again recycled by subsequent washing with distilled water (Goel and Gautam, 2010). The metal extraction efficiency was calculated using the equation (4.2).

$$\text{Metal extraction efficiency } (\%) = \frac{M_1}{M} \times 100 \tag{4.2}$$

where 'M_1' and 'M' represent total metal (in mg) present in the leached solution and media, respectively.

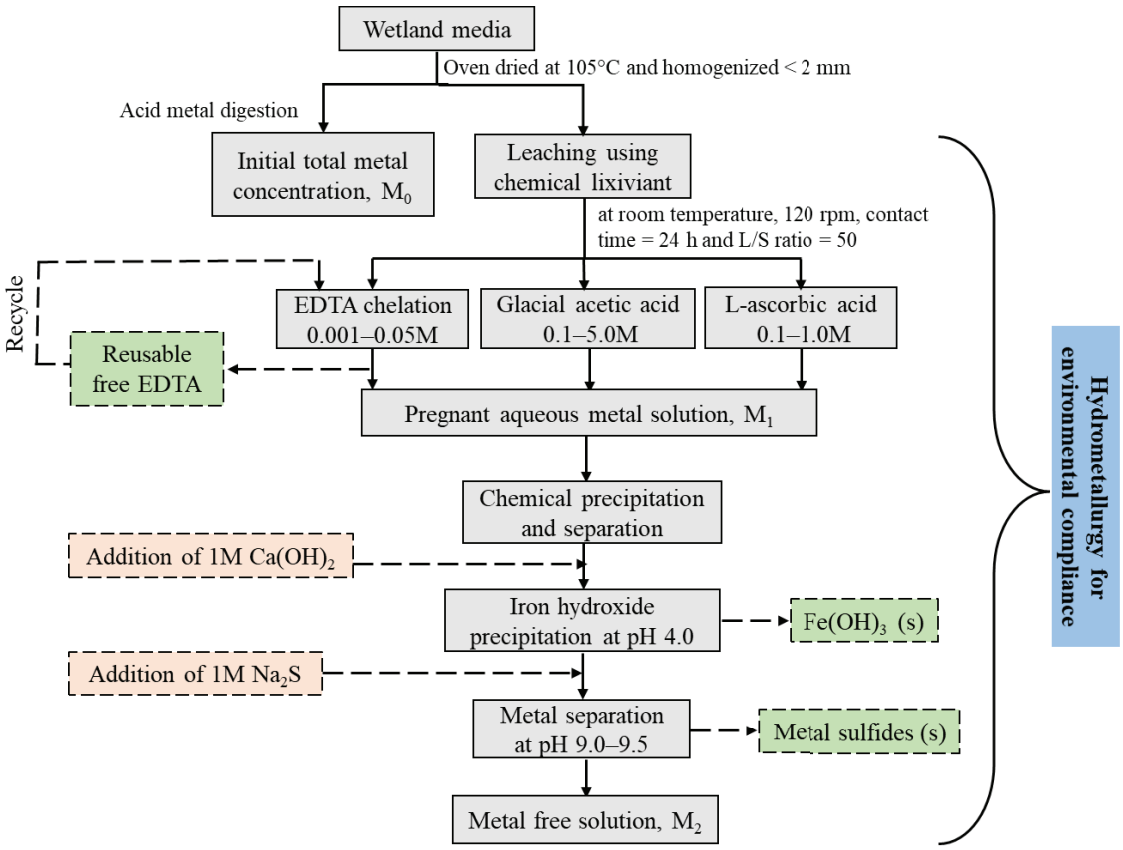

Fig. 4.4 Flowchart of metal extraction and recovery process from wetland media.

Following the extraction procedure, metal pregnant filtrates of each lixiviant (0.05M EDTA, 5M CH_3COOH, 1M $C_6H_8O_6$) were subjected to chemical precipitation steps using 1M $Ca(OH)_2$ and 1M Na_2S. At first, 1M $Ca(OH)_2$ solution was added dropwise to raise the pH of the solution to 4.0 and stirred continuously at 300 rpm, causing Fe to be precipitated out first as hydroxides. The filtrate obtained from the previous step was next subjected to precipitation using 1M Na_2S and the remaining metals were precipitated as metal sulfides up to pH 9.0–9.5. The solid precipitates obtained after final precipitation were oven-dried at 90°C overnight and analyzed. The metal concentration remaining in the final filtrate was determined and metal recovery (%) was estimated using the equation (4.3).

$$\text{Metal recovery (\%)} = \frac{M_1 - M_2}{M} \times 100 \tag{4.3}$$

where 'M_2' represents the total metal (in mg) remaining in the solution after final precipitation.

4.2.5 Statistical analyses

The statistical relations between effluent water characteristics of planted and unplanted CWs for various physicochemical parameters such as pH, TDS, EC, COD, sulfate and metal removal efficiency were determined by a one-way Analysis of Variance (ANOVA) test using the Microsoft Office Excel program (Professional Plus 2016). Correlations between various physicochemical parameters of water samples and metal removal efficiencies were analyzed by Pearson's correlation coefficient. Statistical confidence was set at $p < 0.05$ before performing ANOVA.

The difference between the effluent characteristics of SCW and UCW were compared statistically for various parameters and metal constituents using the Data Analysis tool embedded in Microsoft Office Excel. Statistical comparison of the measured experimental data were performed, including Student's T-test and Fisher F-test. Before conducting the Student T-test, the Fisher F-test was performed to determine the variance similarity between the measured values of SCW and UCW (null hypothesis: there exists no difference in variance, $p > 0.05$). If the F-test value > 0.05, a T-test assuming equal variances was conducted whereas if the F-test value < 0.05, a T-test assuming unequal variances was used. T-test value > 0.05 demonstrated no significant statistical difference (equivalent) whereas T-test value < 0.05 indicated significant statistical difference (non-equivalent) between the SCW and UCW for the measured parameter.

4.3 Results and discussions

4.3.1 Comparative performance evaluation of CCW and PCW

4.3.1.1 Treatment performance

The change in pH, EC, TDS, COD, alkalinity and sulfate at different HLRs of CCW and PCW is depicted in Fig. 4.5. The mean effluent pH of CCW and PCW was 6.3 and 6.4, respectively, throughout the study. Many studies have reported the positive influence of wetland plants on raising the pH of metal-rich wastewater, possibly due to the release of organic acids and exudates from the roots of plants (Dean et al., 2013; Javed et al., 2013). The pH values of PCW were found to be slightly higher than CCW; however, statistical analysis showed no significant differences between the effluent pH of PCW and CCW ($p > 0.05$). Similarly, no significant difference was observed between effluent EC values of CCW and PCW ($p > 0.05$) with mean EC measured as 227 and 246 mS m^{-1} in CCW and PCW, respectively. TDS demonstrated a very similar trend with EC, which is considered a surrogate measurement of TDS. Therefore, Pearson correlation analysis showed a significant relationship between EC and TDS of CCW and PCW ($R^2 = 0.94–0.96$, $p < 0.05$) (Appendix–IV). Essentially, parameters such as pH, EC and TDS were similar and the difference was insignificant between CCW and PCW.

The sulfate concentration in the effluent of CCW (158.14 ± 23.48 mg L^{-1}) and PCW (177.81 ± 23.39 mg L^{-1}) was comparatively higher than the influent (121 ± 2.43 mg L^{-1}) for the first 3 days in phase I, which could be the result of oxidation of carbon bound S and release of sulfate from organic media. The formation of powdered white flakes at the bottom of plant shoots in PCW was evident and it could be from the volatilization of sulfates or transitions to sulfur oxides or sulfide minerals as explained by Kiiskila et al. (2017). It was further observed that sulfate concentration in the effluent of PCW was always higher than CCW. This probably indicated the formation of micro-aerobic zones due to the release of oxygen near roots and this could have suppressed the microbial-assisted sulfate reduction in PCW, as reported by many authors (Stein et al., 2007; Wiessner et al., 2010). Matsui and Tsuchiya (2006) estimated about 0.18–0.33 nmol O_2 g^{-1} root dry weight s^{-1} as the ROL from

the roots of *Typha latifolia*. Therefore, the presence of plants revealed significant impairment of microbial activity involved in sulfate reduction. Statistical analysis also demonstrated a significant difference between the sulfate concentration in the effluent of planted and unplanted CWs ($p < 0.05$). In phase V, the good sulfate removal efficiency was obtained in CCW (36.80–93.27%, averaged 61.57%) and PCW (23.95–90.09%, averaged 50.28%). In phase V, alkalinity generation of about 20–1000 and 32–1640 mg L^{-1} was observed in CCW and PCW, respectively, with no significant difference. A significant correlation was observed between alkalinity generation and sulfate reduction in both CWs. This explains

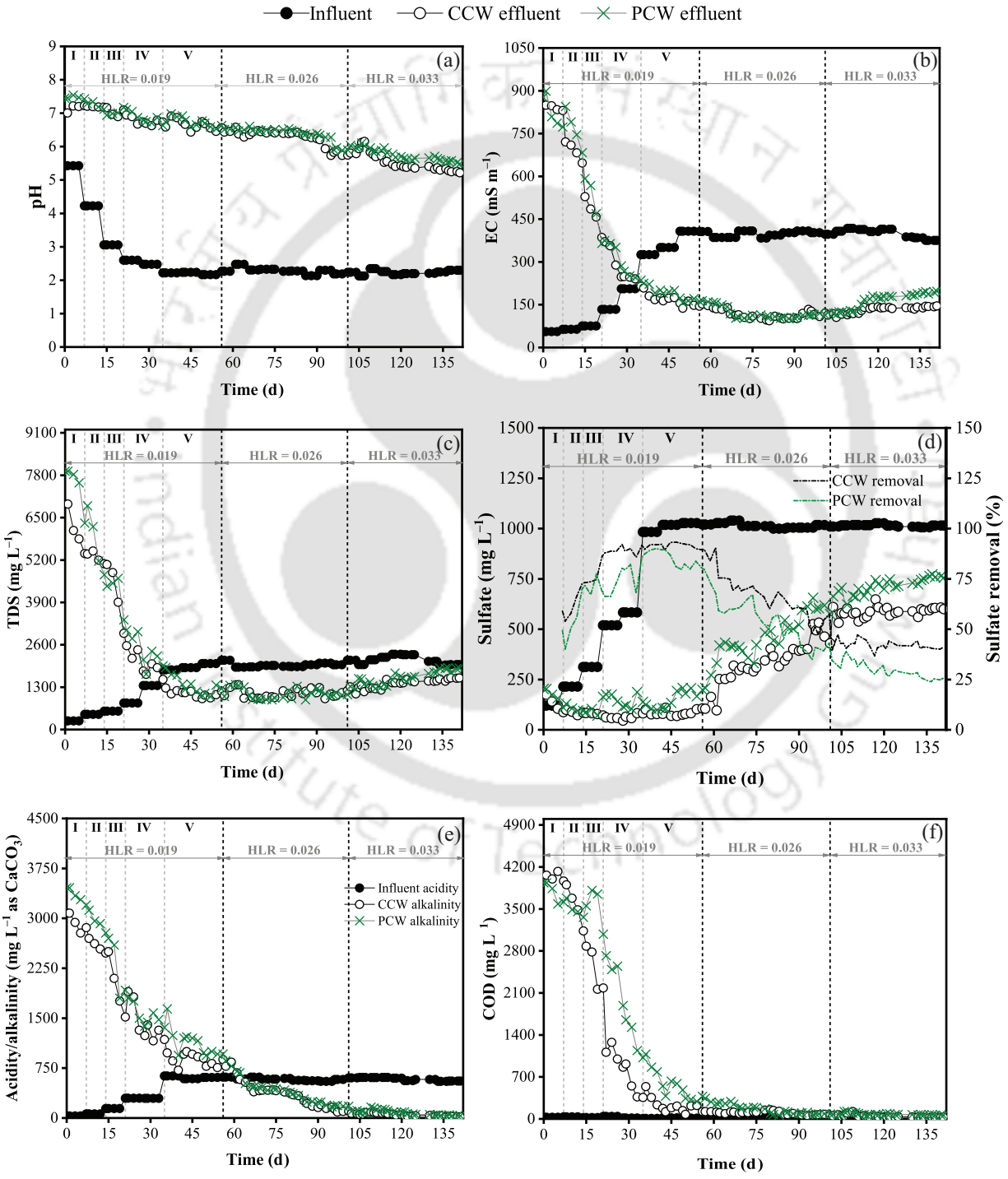

Fig. 4.5 (a) pH, (b) EC, (c) TDS, (d) sulfate, (e) acidity/alkalinity and (f) COD profile of CCW and PCW. The unit of HLR is in m^3 m^{-2} d^{-1}.

that despite significantly lower sulfate reduction in PCW, other biochemical processes (such as photosynthesis represented by Equation 3.7) occurred in the presence of plants , which sufficiently generated comparable alkalinity as CCW.

The COD concentration in the influent was 21.47 ± 8.80 mg L^{-1} throughout the study. Effluent COD values were very high and ranged to about 4064–2185 mg L^{-1} (averaged 3419 mg L^{-1}) and 3936–3079 mg L^{-1} (averaged 3622 mg L^{-1}) in CCW and PCW, respectively, during phase I–III. Thus, there was a rapid washout of the organic carbon during the initial operation of CWs, which gradually stabilized in phase V to 98.68 and 198.62 mg L^{-1} in CCW and PCW, respectively. It was observed that soluble COD measured in the effluent samples of PCW were consistently higher than CCW [Fig. 4.5 (f)]; however, a statistical p-value > 0.05 suggested an insignificant difference between effluent COD of CCW and PCW. The possible reasons for the increase in COD of PCW could be either from the release of some organic carbon from the decomposition of the plant's detritus and root exudates due to metal stress (Javed et al., 2018; White et al., 2011) or more COD consumption in CCW due to higher sulfate reduction.

The port sampling profile of CCW and PCW was measured at a depth of 15 cm during various operational phases (Fig. 4.6). Influent DO remained stable at 6.30–6.73 mg L^{-1} throughout the study. Relatively higher DO was present near the inlet sampling port (C_1 or P_1) during the initial operation of CWs, which gradually declined and stabilized to 2.21–3.07 mg L^{-1}. Further, DO levels decreased along the length of the wetland bed (as measured from C_2/P_2 and C_3/P_3 sampling ports). This suggests that DO was consumed inside the CWs due to the development of autotrophic/heterotrophic biological activity and chemical oxidation of ferrous iron to ferric iron while simultaneously raising pH (Equation 1.2). Microbial profiling from Chapter 3 has also revealed the presence of SOB as well as aerobic/facultative microbes. DO concentration inside CCW (1.11–1.43 mg L^{-1}) and PCW (1.63–1.94 mg L^{-1}) revealed the existence of hypoxic conditions as DO levels remained below the hypoxic threshold concentration of 2.30 mg L^{-1} (Vaquer-Sunyer and Duarte, 2008). Gupta et al. (2020) revealed the existence of sulfate reduction activity by a large proportion of SRB (*Desulfobacterales*, *Desulfuromonadales* and *Syntrophobacterales*) at 0.81–1.78 mg L^{-1} DO in shallow floating CW treating AMD impacted water. Therefore, circumneutral pH and lower DO conditions inside CWs allowed the growth of SRB as SRB can survive in 0–2 mg L^{-1} DO (Qin et al., 2022; Willow and Cohen, 2003) and allowed sulfate reduction to occur. At lower pH, the unionized end-product (H_2S) of dissimilatory sulfate reduction is predominant and tends to react with many metal species (Equation 1.8) and exolve from the solution. Therefore, the total dissolved sulfide concentration measured in CCW and PCW represented a very small fraction (0.37–2.87 mg L^{-1}). It was likely that higher DO during the acclimatization period (0–35 days) rapidly oxidized the sulfide to elemental sulfur or similar intermediates (Gutierrez et al., 2008), and as DO concentration decreased within CWs, some amount of sulfide accumulated. However, as sulfate reduction efficiency deteriorated over time, sulfide formation also diminished. Thus, besides sulfate reduction by SRB, other biochemical reactions such as oxidation of organics, iron and sulfide occurred concurrently in the CWs.

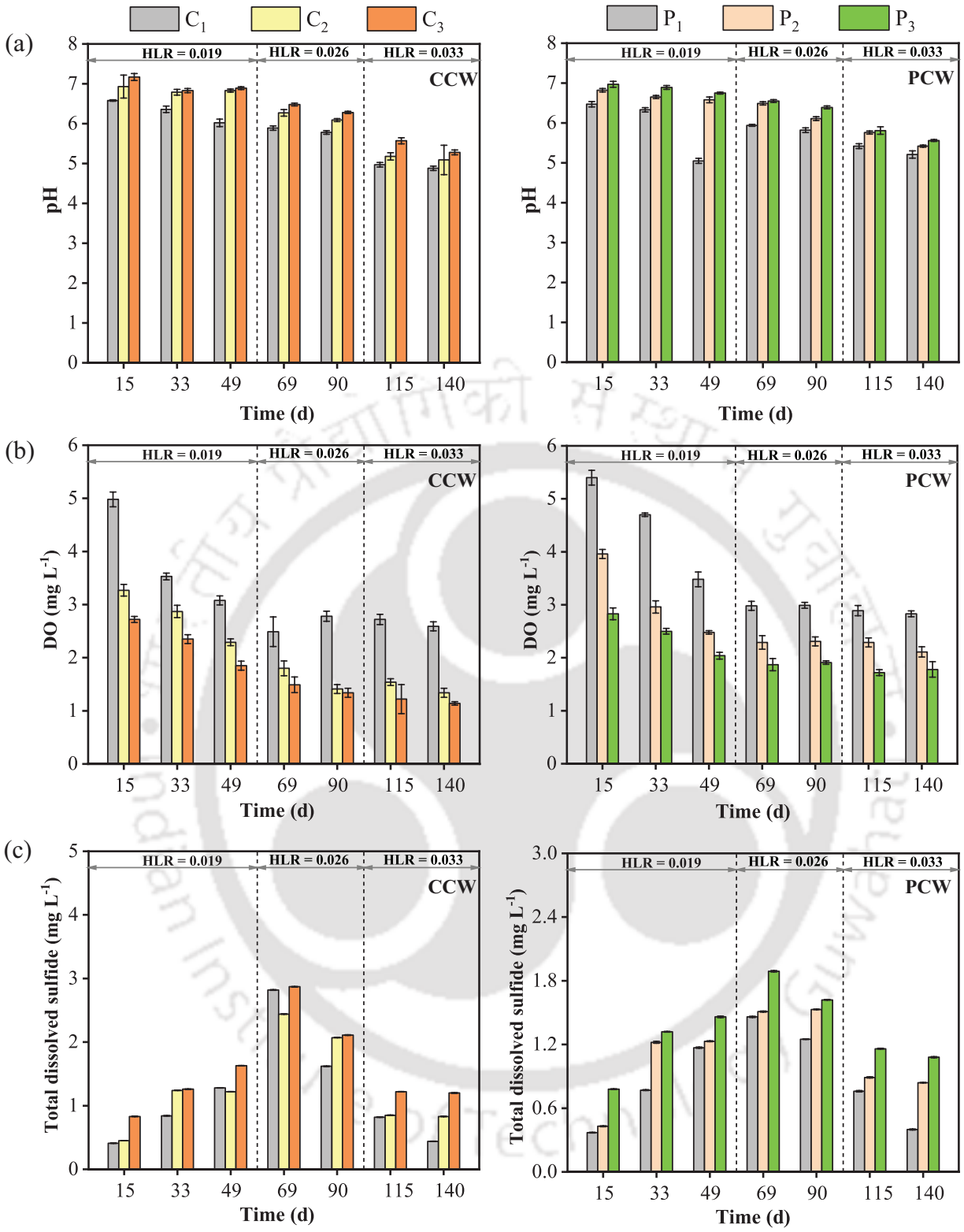

Fig. 4.6 Port sampling profile of (a) pH, (b) DO and (c) total dissolved sulfide in CCW and PCW. The unit of HLR is in $m^3\ m^{-2}\ d^{-1}$.

4.3.1.2 Effect of HLRs

CCW and PCW were operated at various HLRs of 0.019, 0.026 and 0.033 $m^3\ m^{-2}\ d^{-1}$, corresponding to HRT of 7, 5 and 4 days, respectively. On increasing HLR, water quality parameters such as pH, EC, TDS, alkalinity production and sulfate removal deteriorated significantly (Fig. 4.5). pH rapidly declined whereas EC and TDS values considerably increased

in both CWs at HLR of 0.033 m^3 m^{-2} d^{-1}. Similarly, the high sulfate removal efficiency of CCW (92%) and PCW (85%) at HLR of 0.019 m^3 m^{-2} d^{-1} decreased drastically to 42 and 30% when operated at HLR of 0.033 m^3 m^{-2} d^{-1}, respectively. It was evident that faster depletion of available organics and shorter residence time at higher loading rates promoted incomplete sulfate reduction. For AMD treatment in anaerobic solid media bioreactors and SSF-CWs, Drury (2000) recommended required HRT from 8 days (at 17°C) to 41 days (at 1°C) for 50% bacterial sulfate reduction. Chen et al. (2021) attributed shorter HRT (1 day) and subsequent rapid intrusion of oxygen with influent feeding for lower sulfate reduction (3.70–38%) in organic-amended SSF-CWs treating AMD. Meanwhile, Genty et al. (2018) reported increased alkalinity generation at longer HRT (7 days) with no significant improvement in the sulfate removal (8–11%) on increasing the HRT from 5 to 7 days in passive bioreactor applied for ferriferous AMD treatment. HRT is dependent on the reactor configuration and packing media. In general, shorter HRT cannot sustain biosulfidogenesis and results in decrease in treatment performance, possibly due to the washout of slow growing SRB and active cells from the suspended broth of the system (Dev et al., 2017; Hernández et al., 2022; Sato et al., 2022). Additionally, higher HRT might cause a reduction in the porosity and permeability of the reactive mixture (or media), leading to hydraulic related problems as well as lower availability of organic matter or nutrients (Neculita et al., 2008; Sato et al., 2022).

The effluent metal concentration profile of CCW and PCW is depicted in Fig. 4.7. Statistical analysis showed a significant difference ($p < 0.05$) between overall metal removal efficiencies of CCW and PCW, except for Al, Mn and Cr. Plants have higher aerobic activity, which assisted in higher metal removal in PCW. Further, plants can directly participate in metal uptake. However, increasing the HLRs, Fe, Mn, Al and Co concentration exceeded the effluent PDL. A significant difference was observed in metal removal efficiencies between different HLRs in CCW and PCW ($p < 0.05$) (Fig. 4.8). Removal efficiencies of metals like Fe, Mn and Al decreased remarkably in CCW and PCW. Results emphasized that longer HRT is necessary and seems that the 7-day HRT was adequate for acceptable removal of various metals. Genty et al. (2018) obtained decrease in Fe removal on decreasing the HRT from 7 to 5 days and explained that shorter HRT did not provide the appropriate conditions for precipitation of iron hydroxides and SRB was probably not efficient enough in producing soluble sulfides. Interestingly, on increasing HLR, Zn removal exhibited a slight reduction while other metals such as Co, Ni and Cr showed negligible change on increasing HLRs in both CWs. Besides, the depletion of organic matter from wetland media seems to have also influenced the deleterious impacts of higher HLRs in CWs. Several studies have also highlighted the positive aspect of lower HLRs in CWs for achieving maximum efficiency of metals (Taheri Ghannad et al., 2015; You et al., 2014). These results elucidated that operational parameters such as HLR (or HRT) have a more important role on the efficacy of passive treatment of AMD than the presence of vegetation in CWs. Table 4.1 shows the comparative summary of AMD treatment performance of CCW and PCW.

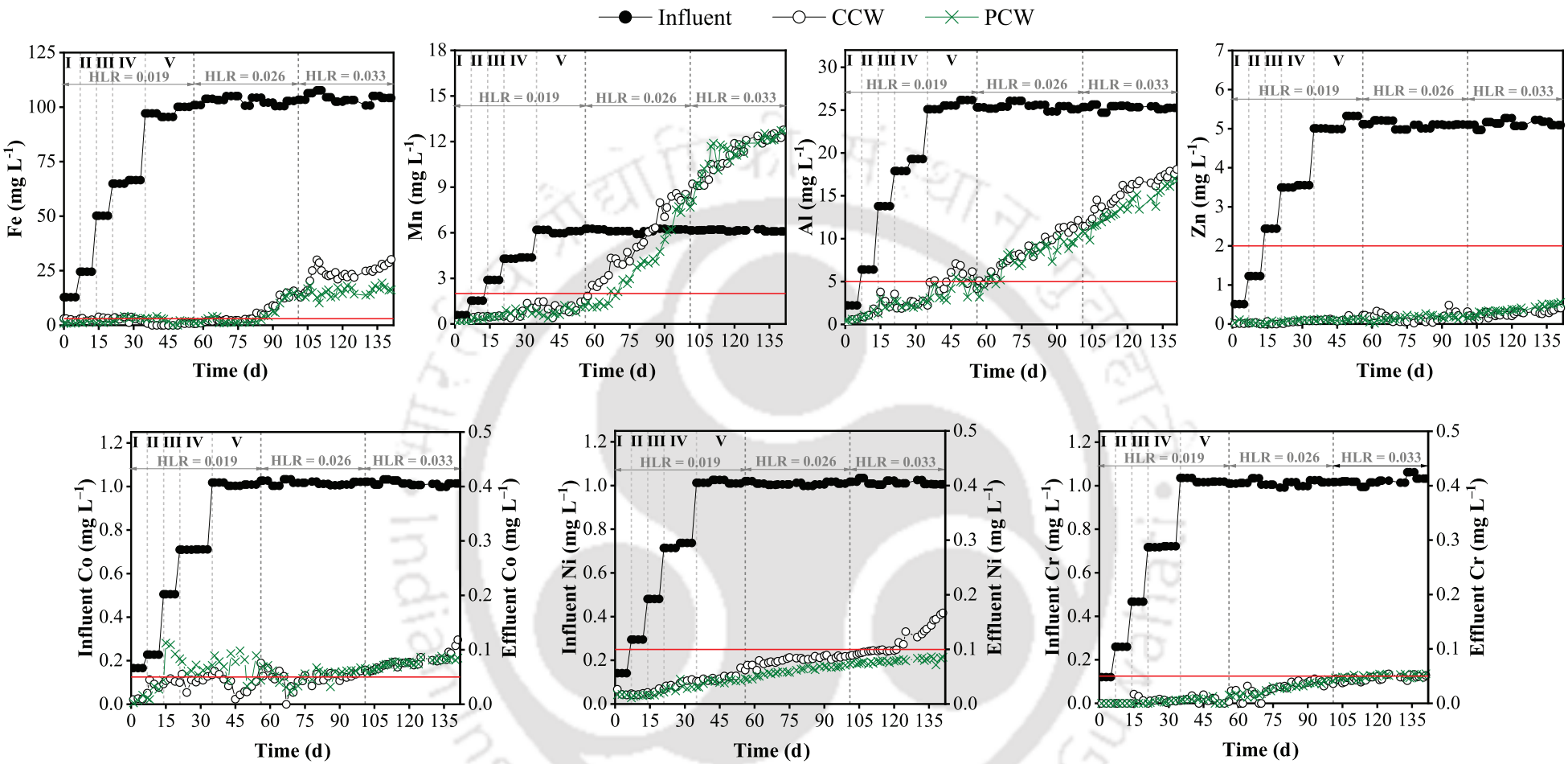

Fig. 4.7 Metal profile of influent and effluent in CCW and PCW. The unit of HLR is in $m^3\ m^{-2}\ d^{-1}$. The red line denotes the permissible discharge limit (PDL) as recommended by CPCB (1993) and EPA (2002).

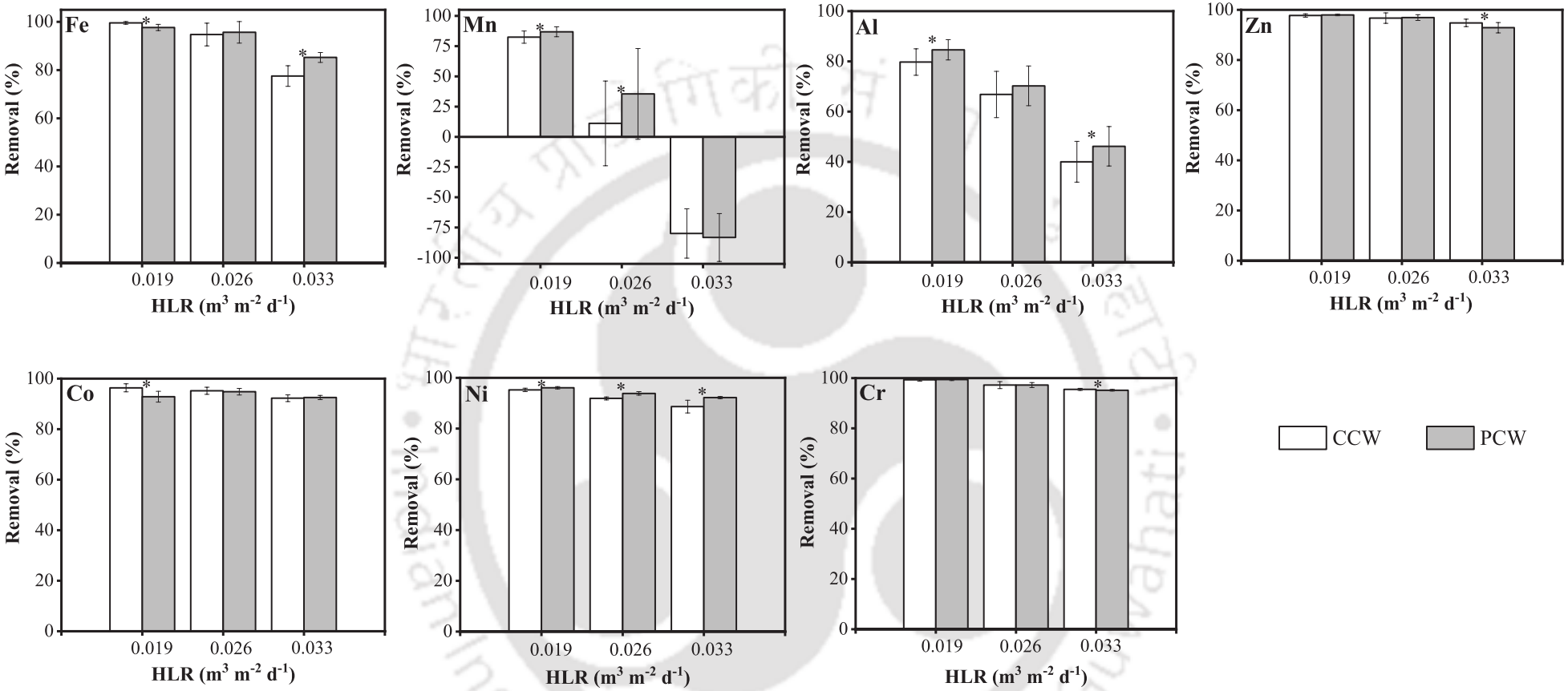

Fig. 4.8 Comparison between metal removal efficiencies (%) of CCW and PCW at varying HLRs. (*) indicates a significant difference ($p < 0.05$) between CCW and PCW at a specific HLR.

Table 4.1 Performance comparison of CCW and PCW in the treatment phase at different HLRs.

Parameters	Influent	Treated effluent						Removal[d] (%)					
		CCW			PCW			CCW			PCW		
		HLR1[a]	HLR2[b]	HLR3[c]	HLR1	HLR2	HLR3	HLR1	HLR2	HLR3	HLR1	HLR2	HLR3
pH	2.3 ± 0.1	6.7 ± 0.2	6.3 ± 0.2	5.6 ± 0.3	6.7 ± 0.1	6.4 ± 0.2	5.8 ± 0.2	–	–	–	–	–	–
EC (mS m^{-1})	393 ± 24	172 ± 22	118 ± 17	132 ± 12	194 ± 25	121 ± 22	160 ± 30	34–66	62–76	61–74	28–62	59–75	48–72
TDS (mg L^{-1})	2034 ± 129	1133 ± 159	1115 ± 130	1405 ± 138	1409 ± 325	1102 ± 155	1562 ± 230	16–53	28–53	20–49	7.85–50	28–54	4.69–50
COD (mg L^{-1})	21 ± 8.80	238 ± 127	102 ± 28	45 ± 23	612 ± 271	171 ± 92	78 ± 17	–	–	–	–	–	–
Acidity (mg L^{-1} as $CaCO_3$)	590 ± 24	–	–	–	–	–	–	–	–	–	–	–	–
Alkalinity (mg L^{-1} as $CaCO_3$)	–	903 ± 127	384 ± 222	51 ± 23	1153 ± 208	420 ± 217	81 ± 38	–	–	–	–	–	–
Sulfate (mg L^{-1})	1015 ± 12	84 ± 13	327 ± 117	582 ± 38	147 ± 42	452 ± 122	708 ± 48	89–93	48–91	37–58	80–90	35–81	24–43
Fe (mg L^{-1})	103 ± 3	0.41 ± 0.54	5.37 ± 4.78	23.45 ± 4.52	2.20 ± 1.19	4.45 ± 4.58	15.40 ± 2.14	99–100	85–99	71–88	96–100	85–99	81–91
Al (mg L^{-1})	25 ± 0.35	5.10 ± 1.40	8.43 ± 2.31	15.18 ± 2.05	3.83 ± 1.05	7.47 ± 2.02	13.63 ± 1.96	72–91	52–84	28–55	78–90	59–87	33–61
Mn (mg L^{-1})	6.15 ± 0.08	1.08 ± 0.32	5.25 ± 2.26	11 ± 1.31	0.80 ± 0.25	3.74 ± 2.28	11 ± 1.35	76–93	–38–75	No removal	80–94	–34–83	No removal
Zn (mg L^{-1})	5.12 ± 0.10	0.12 ± 0.04	0.17 ± 0.11	0.27 ± 0.07	0.11 ± 0.02	0.16 ± 0.06	0.37 ± 0.11	96–99	90–100	92–98	97–99	95–100	89–97
Co (mg L^{-1})	1.01 ± 0.01	0.04 ± 0.02	0.05 ± 0.01	0.08 ± 0.01	0.07 ± 0.02	0.05 ± 0.01	0.08 ± 0.01	94–99	93–100	88–94	90–97	93–98	91–94
Ni (mg L^{-1})	1.01 ± 0.01	0.05 ± 0.01	0.08 ± 0.01	0.11 ± 0.02	0.04 ± 0.01	0.06 ± 0.01	0.08 ± 0.01	93–96	91–94	83–91	96–97	93–96	91–93
Cr (mg L^{-1})	1.02 ± 0.01	0.01 ± 0.01	0.03 ± 0.01	0.05 ± 0.02	0.02 ± 0.01	0.03 ± 0.01	0.05 ± 0.01	98–100	96–100	95–96	99–100	96–99	95–96

[a]HLR1 = 0.019 m^3 m^{-2} d^{-1}; [b]HLR2 = 0.026 m^3 m^{-2} d^{-1}; [c]HLR3 = 0.033 m^3 m^{-2} d^{-1}; [d]Removal data presented as the min–max value. Values exceeding the discharge limits as recommended by CPCB (1993) and EPA (2002) are marked in red.

4.3.1.3 *Biomass activity results*

The maximum COD utilization and specific sulfidogenic activity were determined for CCW and PCW at 0.026 and 0.033 m^3 m^{-2} d^{-1} HLR. Biomass activity of both CWs reduced over time due to the exhaustion of media organics and increased HLRs (Fig. 4.9 and Fig. 4.10). At 0.026 m^3 m^{-2} d^{-1} HLR, CCW exhibited higher heterotrophic activity (2.55 mg COD removed mg TVS^{-1} d^{-1}) and specific sulfidogenic activity (0.79 mg sulfate reduced mg TVS^{-1} d^{-1}) than PCW. At a higher HLR of 0.033 m^3 m^{-2} d^{-1}, biomass activity of both CWs noticeably decreased in terms of heterotrophic activity and specific sulfidogenic activity (Fig. 4.11). These results showed that higher biomass activity was achieved in CCW than in PCW, indicating the presence of more active biomass in CCW than PCW due to the higher COD consumption and existence of limited oxygen inside CCW.

4.3.1.4 *Wetland mineralogy*

The wetland media from CCW and PCW was analyzed in XRD (Fig. 4.12). In both samples, sharp peaks representative of quartz (SiO_2) were identified. In addition, some distinctive peaks of aluminium oxide (JCPDS 00-001-1303/01-076-0144), cobalt oxide (JCPDS 01-075-0393/

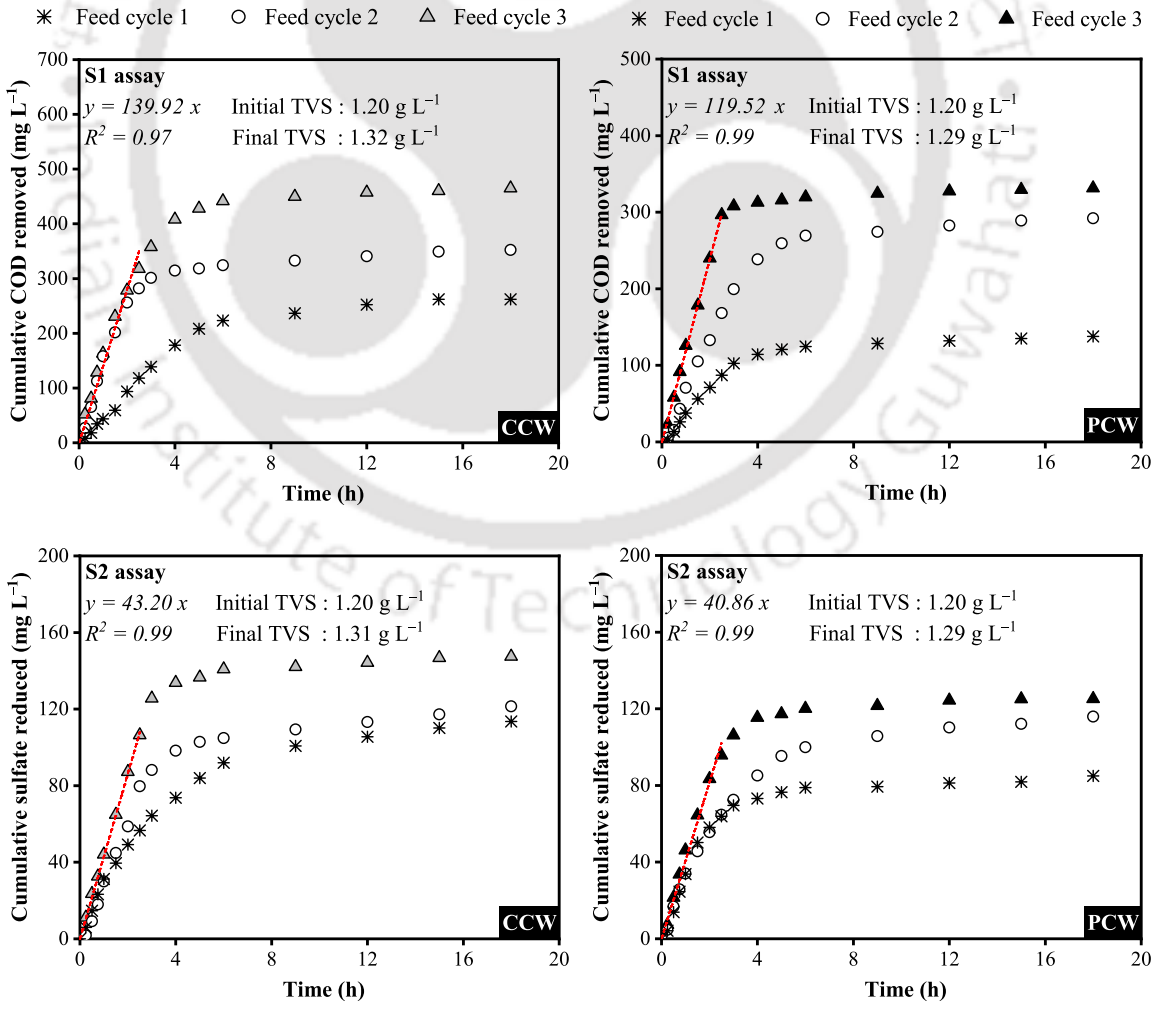

Fig. 4.9 Cumulative COD removal (mg L^{-1}) and sulfate reduction (mg L^{-1}) at HLR of 0.026 m^3 m^{-2} d^{-1}.

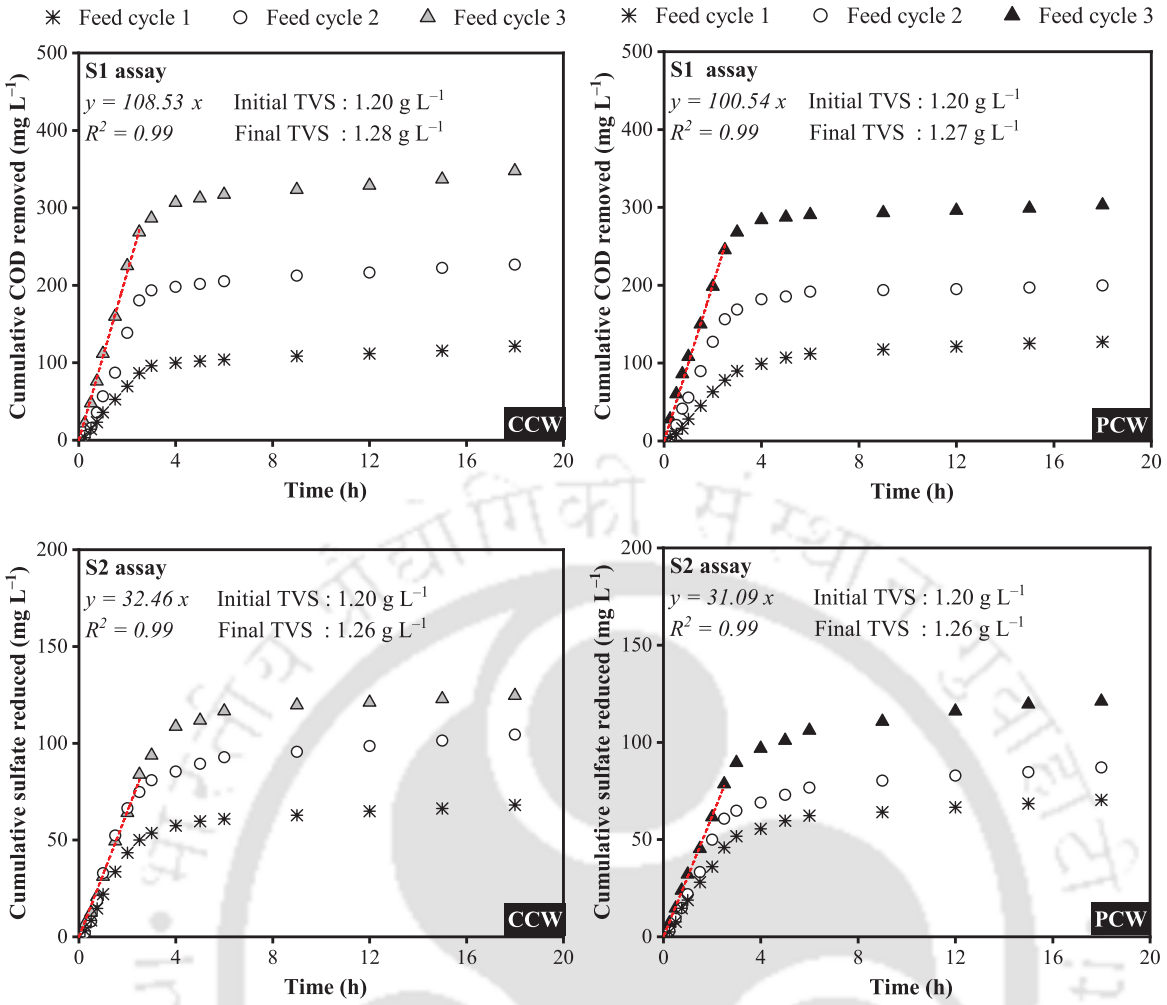

Fig. 4.10 Cumulative COD removal (mg L^{-1}) and sulfate reduction (mg L^{-1}) at HLR of 0.033 m^3 m^{-2} d^{-1}.

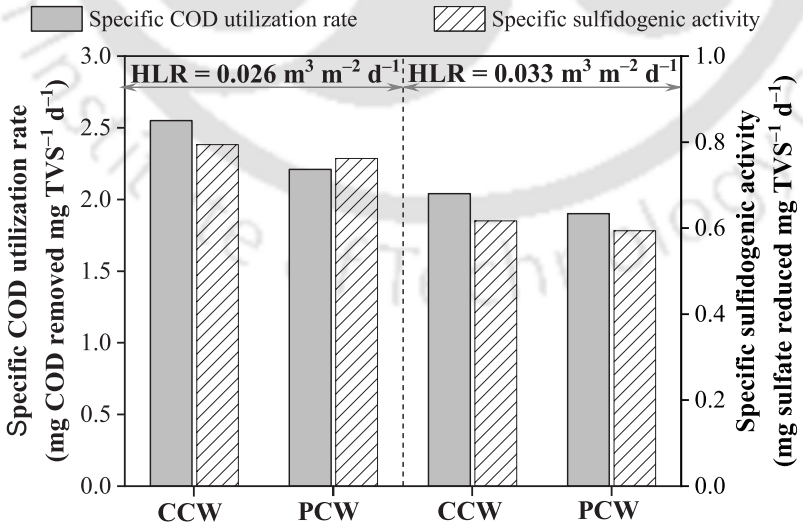

Fig. 4.11 Biomass activity of CCW and PCW at HLR of 0.026 and 0.033 m^3 m^{-2} d^{-1}.

01-074-2392) and zinc oxide or zincite (JCPDS 00-001-1136/01-075-1526) were also identified in CCW and PCW. Wetland media being mostly amorphous; thus, some characteristics of weak peaks intensities of metal precipitates were also recorded. The presence of iron sulfide (JCPDS 00-076-0965), manganese oxide or maganosite (JCPDS 01-072-1533),

nickel sulfide (JCPDS 00-014-0358) and chromium oxide (JCPDS 00-008-0254) was indicated in CCW while, precipitation of manganese oxide or groutellite (JCPDS 00-012-0720) and nickel sulfide or millerite (JCPDS 00-001-1286) were recorded in case of PCW.

4.3.1.5 Metal extraction and recovery

Metal mobilization increased considerably with the increment in the concentration of the extracting solution (Fig. 4.13). The unusual property of EDTA is its ability to chelate or complex metal ions in 1:1 metal-to-EDTA complexes. The fully deprotonated form (all acidic hydrogens removed) of EDTA binds to the metal ion (Singh, 2009). Therefore, it was observed that most of the metals leached effectively into the solution at 0.005M EDTA (equivalent EDTA: metal [Fe + Al + Zn + Co + Ni + Cr] molar ratio is 4.24). EDTA achieved higher extraction efficiency for Fe (97.64%), Zn (98.77%) and Cr (87.07%), whereas acetic acid exhibited higher extraction efficiency for Al (61.27%) and Co (77.26%), and ascorbic acid showed the highest leachability for Ni (89.23%). EDTA is a strong chelating agent, whereas acetic and ascorbic acids are weak natural chelating agents. Based on the first acidity value, ascorbic acid ($pK_a = 4.10$) is a much stronger acid than acetic acid ($pK_a = 4.76$), in addition to the presence of a double bond in ascorbic acid that allows for stabilization by delocalization. The metal solubilization by complexing agents takes place due to the competition between solid adsorption and complexation. The extraction efficiency of an organic ligand is metal-specific and governed by its complexing affinity for metal and affinity between solid and metal (Goel and Gautam, 2010).

The recovery of metals was performed in two steps, first $Ca(OH)_2$ raised the pH to 4.0 and mostly Fe was precipitated out (22.37–41.39%), followed by Zn (3.16–25.39%) and Al (1.70–4.87%). In the final precipitation step, pH was raised to 9.5 and good metal recovery values were obtained in the order: Fe (49.13–97.63%) > Zn (57.41–94.94%) > Ni (67.03–86.46%) > Cr (68.25–83.80%) > Co (50.30–73.56%) > Al (29.68–47.93%). Although metal extraction using different lixiviants revealed appreciable recovery of metals, the precipitated sludge might contain a mixture of metals and would result in low purity

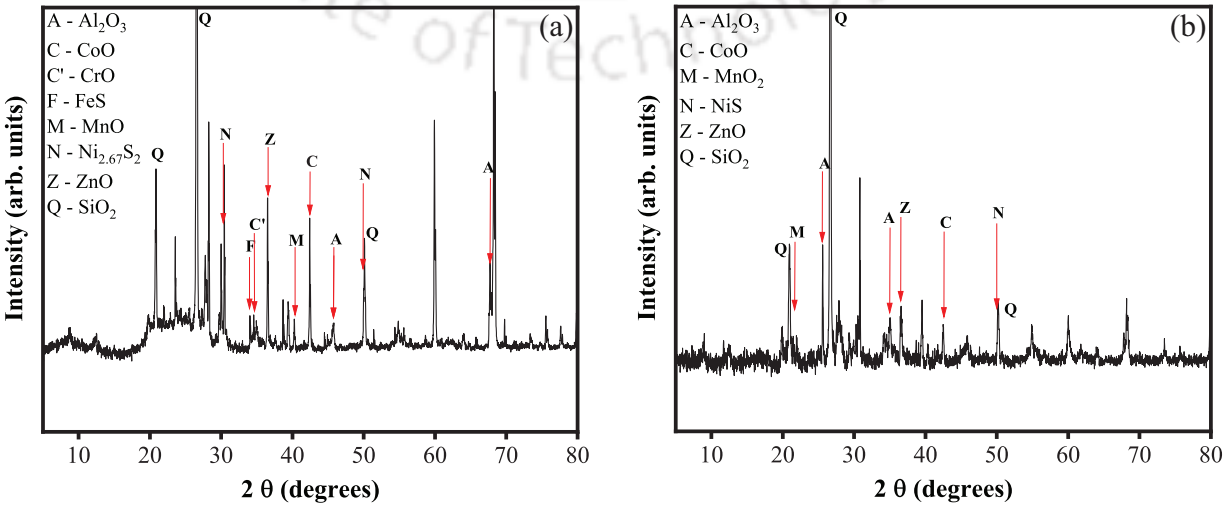

Fig. 4.12 X-ray powder diffraction pattern of (a) CCW and (b) PCW media.

precipitates. Therefore, fractional precipitation and selective separation are recommended to ensure economic feasibility. A complete metal mass balance of the metal recovery process is presented in Table 4.2. It can be seen that a high recovery yield of Fe (52.80 g) and Al (4.69 g) was obtained from wetland media. From the EDX spectrum (Fig. 4.14), it can be observed that amount of metals (percent by weight) present in media decreased variably when extracted using 0.05M EDTA, 5M acetic acid and 1M ascorbic acid, whereas the recovered precipitate revealed high metal-rich composition in the order of the amount of metal extracted.

The media samples were further investigated using FTIR to identify the change in chemical bonds and composition before and after the chemical extraction (Fig. 4.15). All samples showed the presence of amorphous silica, which was recognized by bands at 800 and 1100 cm^{-1} (Vithanage et al., 2014). The dissolution of metal-Si oxides was indicated by the changes in the peak position and intensities at 535, 693 and 790 cm^{-1}, which are related to SiO_2 vibrations (Wei et al., 2018). The band at 469–470 cm^{-1} observed in all samples was attributed to O–Si–O bending vibrations. The bands in the 1610–1654 cm^{-1} region highlighted the presence of carboxylate groups for asymmetric stretching vibration, and a new peak appeared at 1762 cm^{-1}, indicating the absorbed C=O group in the case of extraction with ascorbic acid. These results showed the complexation of the C=O group with

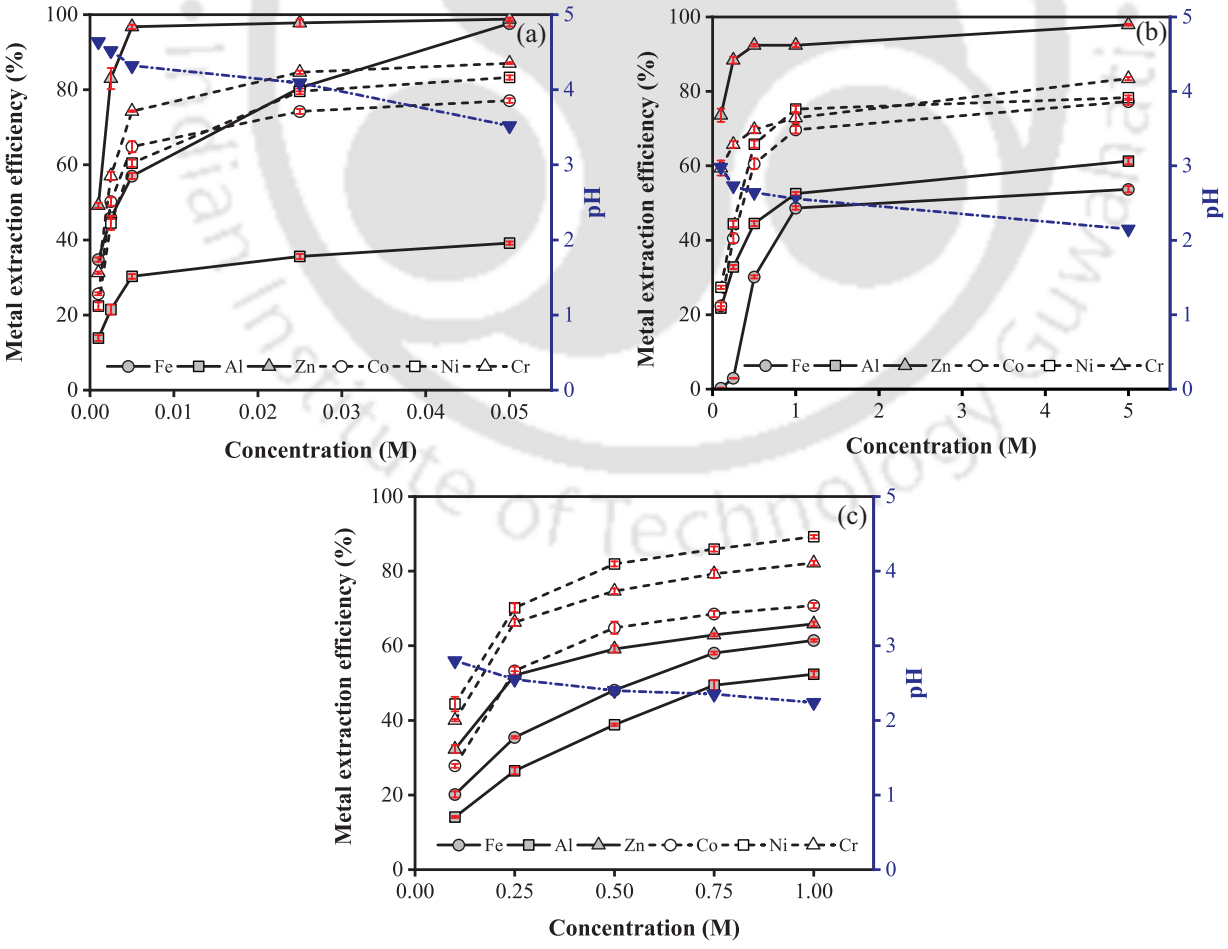

Fig. 4.13 Metal extraction efficiencies (%) using (a) 0.001–0.05M EDTA, (b) 0.1–5M acetic acid and (c) 0.1–1M L-ascorbic acid.

Table 4.2 Mass balance of the metal extraction and recovery process from wetland media of CCW.

Metal	Influent mass (g)	Effluent mass (g)	Total metal concentration in media[a] (mg kg^{-1})	Mass retained in media[b] (g)	Unaccounted mass[c] (g)	Metal extracted (g) using			Metal recovered (g) by precipitation		
						0.05M EDTA	5M CH_3COOH	1M $C_6H_8O_6$	0.05M EDTA	5M CH_3COOH	1M $C_6H_8O_6$
Fe	63.57	6.14 ± 1.49	2272 ± 91	54.05 ± 2.21	3.38	52.80	29.05	33.23	52.79	26.57	32.11
Al	15.88	5.90 ± 0.49	411 ± 21	9.78 ± 0.50	0.21	3.83	5.99	5.13	2.90	4.69	4.38
Zn	3.18	0.13 ± 0.02	125 ± 0.19	2.97 ± 0.01	0.08	2.94	2.91	1.96	2.82	2.80	1.71
Co	0.63	0.04 ± 0.01	23.45 ± 0.21	0.56 ± 0.01	0.03	0.43	0.43	0.40	0.28	0.41	0.34
Ni	0.63	0.05 ± 0.01	23.70 ± 0.47	0.56 ± 0.01	0.02	0.47	0.44	0.50	0.41	0.38	0.49
Cr	0.63	0.02 ± 0.01	24.88 ± 0.07	0.59 ± 0.02	0.02	0.52	0.49	0.49	0.50	0.44	0.40

[a]Total metal concentration was calculated from the acid-digestion procedure as described by USEPA (1996); [b]Mass retained in media was obtained by multiplying the total metal concentration in media (mg kg^{-1}) with the mass of the organic media added (kg); [c]Unaccounted mass was derived as [influent mass – (effluent mass + mass retained in media)].

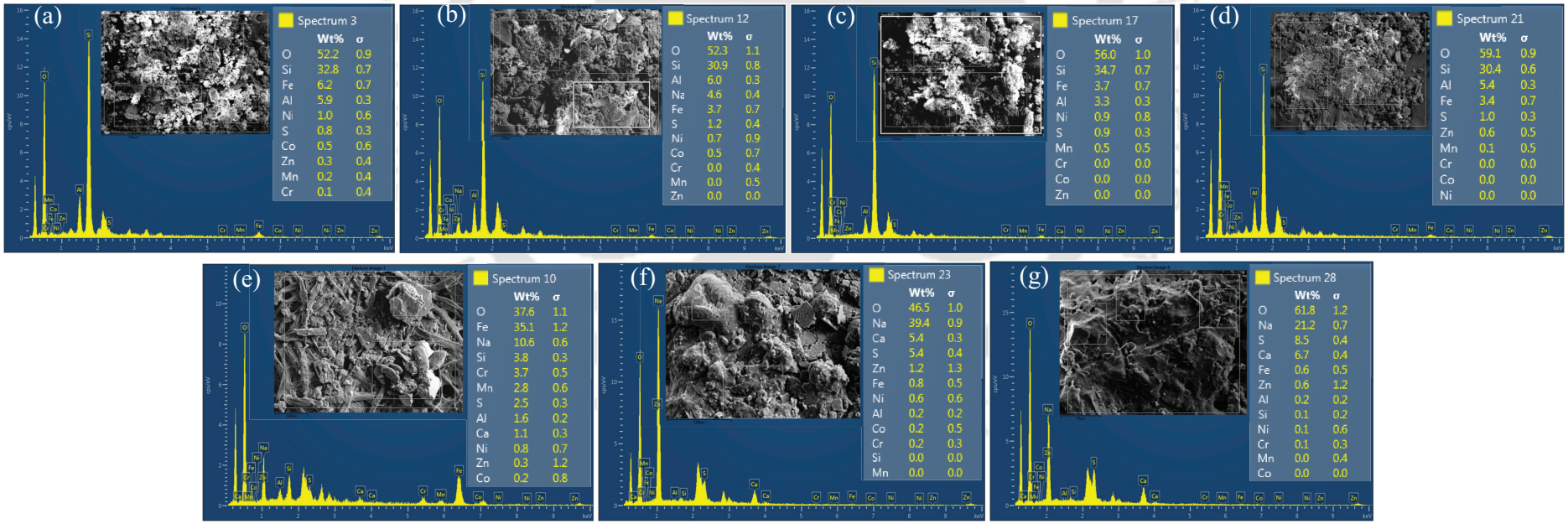

Fig. 4.14 EDX spectrum of (a) parent media before extraction and after extraction using (b) 0.05M EDTA, (c) 5M acetic acid, (d) 1M L-ascorbic acid; and recovered metal precipitate sludge following extraction using (e) 0.05M EDTA, (f) 5M acetic acid and (g) 1M L-ascorbic acid.

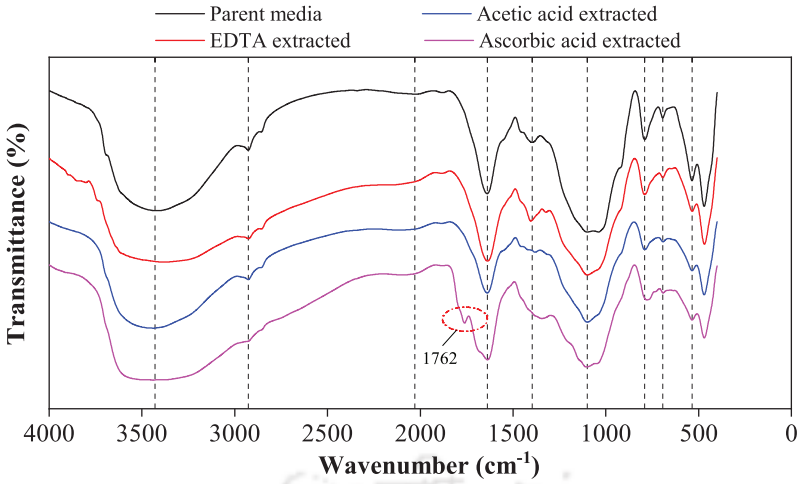

Fig. 4.15 FTIR spectrum of media before and after extraction using 0.05M EDTA, 5M acetic acid and 1M L-ascorbic acid.

metals (Alikhani and Manceron, 2015). Significant changes were observed in 3500–3100 cm^{-1}, 2940–2850 cm^{-1} and 1400–1300 cm^{-1} corresponding to –OH, C–H_n stretch and COOH, respectively (Feng et al., 2018). The peaks between 3440 and 3397 cm^{-1} shifted (or decreased) and broadened, indicating the desorption of heavy metal ions with intermolecular bonded –OH groups. The bands at 2927–2925 cm^{-1} are assigned to asymmetric and symmetric –CH_2 groups, which remarkably reduced in all extracted samples.

4.3.2 Performance evaluation of sheltered (SCW) and unsheltered (UCW) CWs

4.3.2.1 Pollutant removal and effluent water quality

The time series chart of the effluent characteristics of SCW and UCW is presented in Fig. 4.16. Mean effluent pH recorded during the acclimatization period of SCW and UCW were 7.4 and 7.5, while during phase V, pH steadily declined to 6.1 and 5.7, respectively. Statistical analysis showed significant differences ($p < 0.05$) between the pH values of SCW and UCW. Likewise, high EC values were observed at the start-up of SCW (249 ± 97 mS m^{-1}) and UCW (328 ± 91 mS m^{-1}), which gradually stabilized to 166 ± 30 and 188 ± 36 mS m^{-1} in SCW and UCW, respectively. Additionally, short-lived low rainfall intensities were observed in the dry season, which caused a relatively higher release of ions and organics in UCW. However, throughout the study period, the EC values of UCW were found to be higher than SCW, illustrating significant differences between SCW and UCW ($p < 0.05$). These results suggest that rainfall events likely increased the EC values by shortening the hydraulic residence time of the UCW (Poach et al., 2004). Similarly, high TDS values (1076–6452 mg L^{-1}) were measured in SCW and UCW during phase (I–IV) alleviated to 1197 ± 230 and 1333 ± 332 mg L^{-1} in SCW and UCW, respectively. TDS values of UCW increased exceptionally in the wet period and revealed significant differences between SCW and UCW ($p < 0.05$).

Rapid release and washout of organics (2070–823 mg L^{-1}) occurred at the initial phase and sooner depleted to about 87 ± 47 and 71 ± 48 mg L^{-1} in SCW and UCW, respectively. The heterotrophic oxidation of organics catalyzed by sulfate reducers contributed to high sulfate removal in SCW (82.10%) and UCW (80.05%) in phase (I–IV). During the dry season,

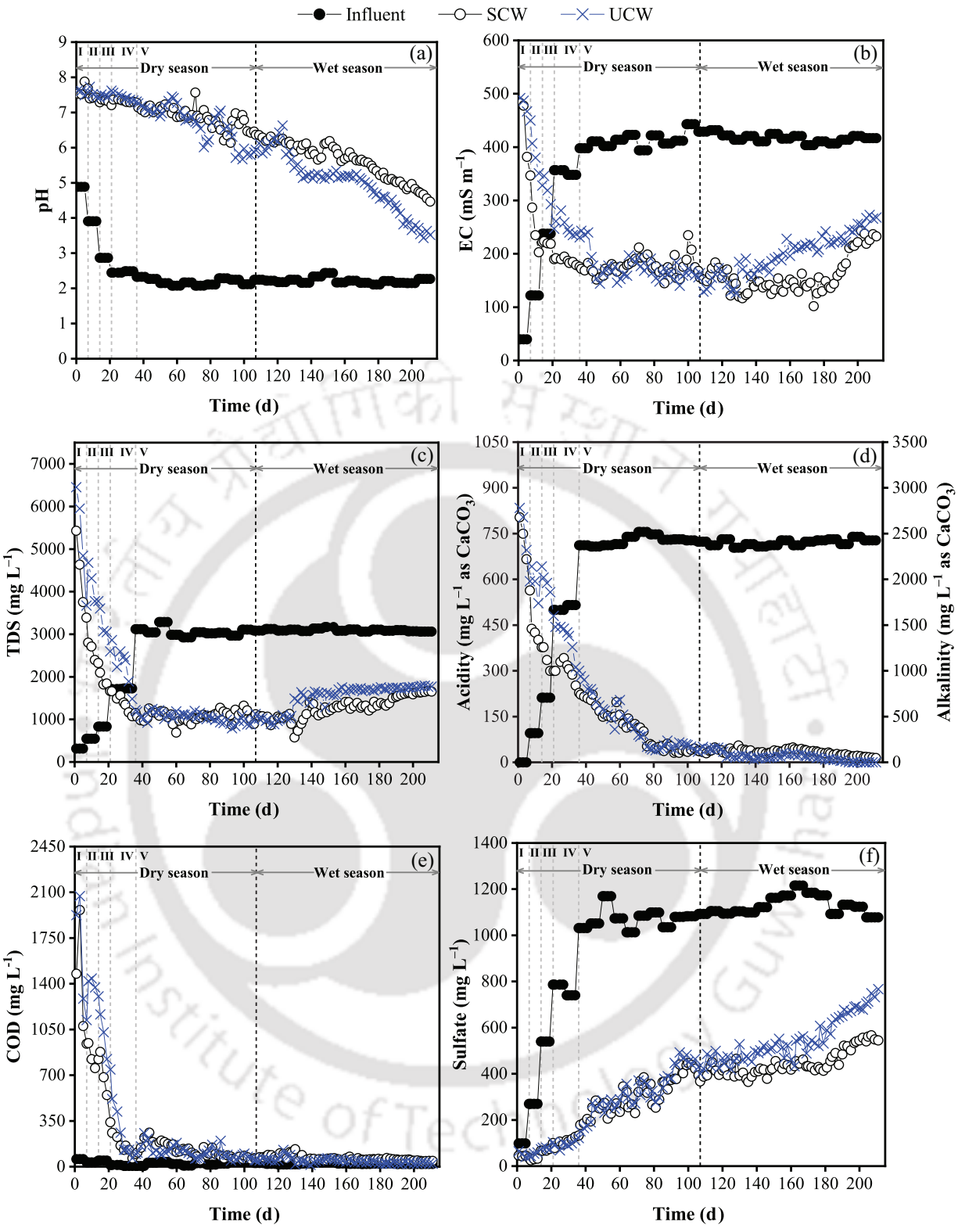

Fig. 4.16 Influent and effluent profile of SCW and UCW for (a) pH, (b) EC, (c) TDS, (d) acidity (influent) and alkalinity (effluent), (e) COD and (f) sulfate.

SCW and UCW accounted 70.89 and 69.46% sulfate removal, respectively, with no significant differences between effluent sulfate concentration of SCW and UCW ($p > 0.05$). On the contrary, during the wet season, findings showed significant differences between the sulfate removal efficiency of SCW (60.29%) and UCW (51.34%) with the highest effluent sulfate concentration in UCW (767 mg L^{-1}), indicating a minimal possible effect of dilution on

wastewater from rainfall in UCW (Liolios et al., 2014). However, no statistically significant difference was indicated between the alkalinity values of SCW and UCW ($p > 0.05$). Rainfall inflicted disturbance in the wetland bed, leading to less anoxic conditions because of rainwater infiltration and a possible decline in sulfate reduction. In addition, the decrease in the abundance of SRB from rapid washout during heavy rainfall and the incapability of microbes to adapt to sudden environmental changes might have suppressed sulfate reduction in UCW.

4.3.2.2 Heavy metal removal

The time series metal profile in the water samples from SCW and UCW is depicted in Fig. 4.17. Average metal removal efficiency during treatment phase V was recorded as Cr (96.24 and 90.36%), Zn (93.88 and 92.48%), Ni (90.67 and 82.52%), Fe (89.69 and 84.85%), Al (79.36 and 70.33%), Co (92.35 and 81.92%) and Mn (22.74 and 20.46%) in SCW and UCW, respectively. Statistical analysis revealed significant differences ($p < 0.05$) between metal removal efficiencies of SCW and UCW, except for manganese. After months of operation in phase V, iron concentration in the effluent of SCW as well as UCW exceeded the permissible limit (CPCB, 1993), possibly due to the re-dissolution of complexes of iron oxides (or hydroxides) or microbial assisted dissimilatory ferric iron reduction (Coupland and Johnson, 2008). Results indicated a significant deterioration of iron removal in the UCW (76.35%) than SCW (85.18%), particularly in the wet season. Wiessner et al. (2006) reported the negative influence of heavy rain events causing intermittent or total breakdowns in the Fe removal processes, resulting in a drastic decrease from 97 to 17% Fe removal in planted SSF CWs.

A similar observation was recorded for other metals such as Al, Co, Ni and Cr. Abiotic removal of aluminium via hydrolysis and precipitation is reported to occur at pH > 6.0 (Wei et al., 2005), which considerably reduced in SCW (74.87%) and UCW (59.18%) when pH dropped to 3.5–6.4 during the wet period in phase V and did not meet the recommended discharge criteria (EPA, 2002). Zinc exhibited excellent removal in SCW (82.85–99.71%) and UCW (73.95–99.38%), meeting the discharge limit throughout the treatment period, which is in agreement with the earlier studies (Wiessner et al., 2006; Yang et al., 2006). The removal efficiency achieved for trace metals such as Co, Ni and Cr during the dry period were 97.48, 97.80 and 98.74% in SCW, and 96.52, 98.48 and 99.55% in UCW, respectively. However, despite good removal efficiency, Co, Ni and Cr exceeded the permissible discharge concentration in the effluent due to the overall performance deterioration of CWs. Further, the rainfall events in the wet season severely impacted the performance of UCW, which showed a significant reduction in Co (72.16%), Ni (71.90%) and Cr (84.24%) removal in comparison with SCW (88.93% Co, 85.88% Ni and 94.59% Cr).

Manganese being the most difficult metal, exhibited inferior removal and mostly leached out. The manganese concentration in the effluent of both CWs varied largely over the operating period; however, large fluctuations were recorded for UCW. Due to the high activation energy of Mn^{2+} oxidation and higher solubility, the chemical precipitation of Mn is

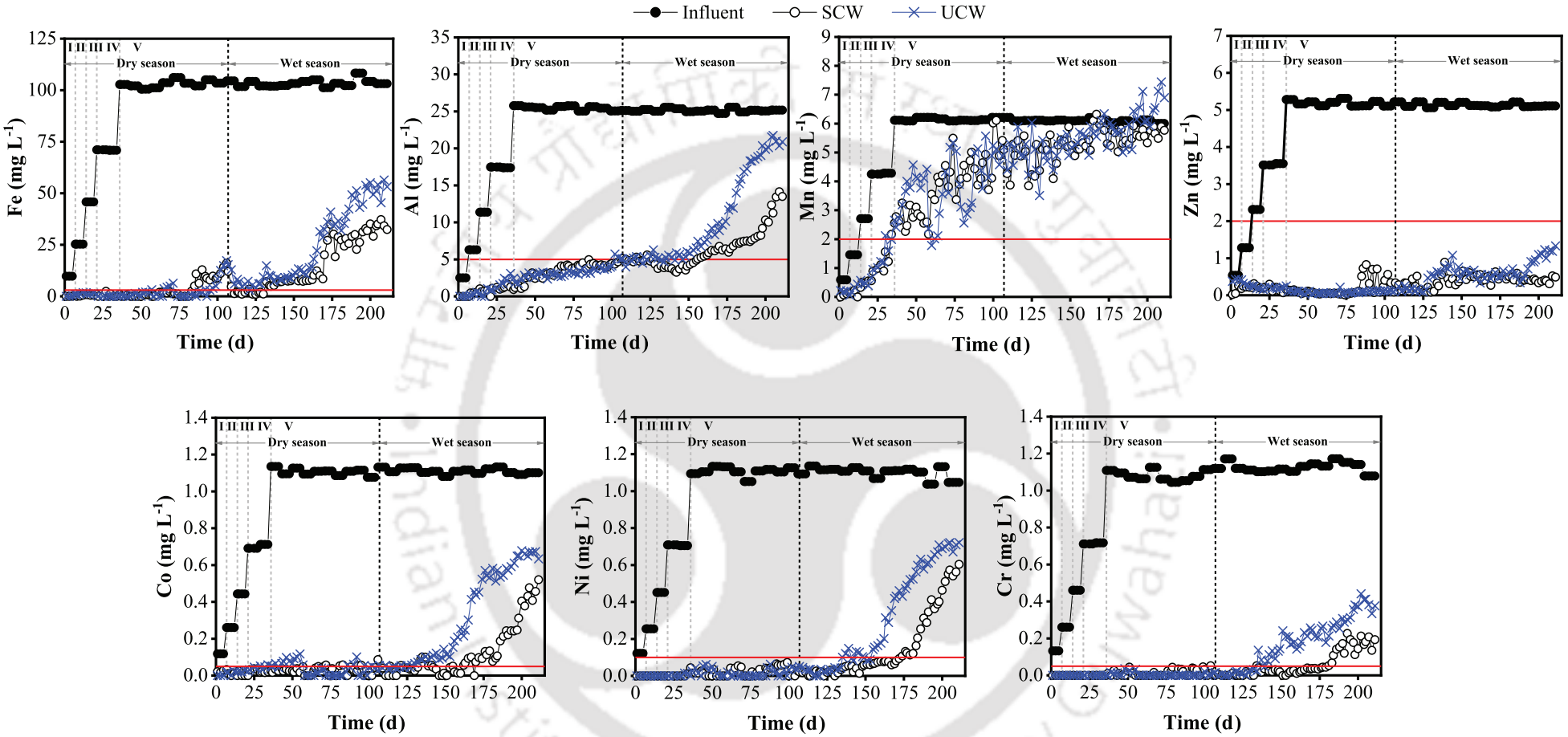

Fig. 4.17 Metal profile of influent and effluent in SCW and UCW. The red line denotes the permissible discharge limit (PDL) as recommended by CPCB (1993) and EPA (2002).

not possible at the existing pH of 5.5–6.0. Therefore, manganese removal could be partly attributed to media adsorption, sulfide precipitation and bacterial mediated immobilization mechanisms as the minor sinks. Complete or partial oxidation of 1 mg L^{-1} of Mn^{2+} to Mn^{4+} (or Mn^{3+}) requires approximately 0.15–0.30 mg L^{-1} of DO (Johnson and Younger, 2005), which was sufficiently available in CWs (0.55–1.22 mg L^{-1} in SCW and 0.48–1.51 mg L^{-1} in UCW) for biological manganese oxidation, even reported to occur at pH 5.0–6.0 (Pacini et al., 2005; Xu et al., 2009). However, manganese and other adsorbed metals were eventually released as the experiment continued. Table 4.3 shows the comparative summary of AMD treatment in SCW and UCW.

4.3.2.3 Mineralogical characteristics of wetland media and plant growth

The elemental composition from the EDX spectrum image of the wetland media from SCW and UCW (Fig. 4.18) revealed a higher deposition of iron and aluminium followed by zinc. Results conveyed accumulation of metals in SCW and UCW (such as Zn, Cr, Co and Ni), while manganese was least retained in UCW media due to more rapid washout under rainfall events. From the morphological analysis in Fig. 4.18 (b, e), the formation of metal precipitates having rod-like structures (encircled with red) and the presence of microbial biofilm (encircled with yellow) is depicted. The identification of various mineral phases present in the wetland media was analyzed from XRD spectra and presented in Fig. 4.18 (c, f). Being non-crystalline samples (amorphous solid), media from SCW and UCW exhibited sharp distinctive peaks of SiO_2 along with other small peak intensities such as zinc aluminium sulfide ($ZnAl_2S_4$) (JCPDS 00-040-1075), cobalt oxide (CoO) (JCPDS 01-075-0418/ 01-075-0533) and nickel sulfide (NiS) (JCPDS 01-075-0613). In addition, metal precipitates such as wurtzite or zinc sulfide (ZnS) (JCPDS 01-079-2204), iron sulfide (FeS) (JCPDS 00-023-1123), aluminium oxide (Al_2O_3) (JCPDS 01-077-2135) and chromium oxide (CrO_2) (JCPDS 01-084-1819) were recorded in

Table 4.3 Performance comparison of SCW and UCW in the treatment phase.

Parameters		Influent (AMD)	Treated effluent		Removal[a] (%)	
			SCW	UCW	SCW	UCW
pH		2.2 ± 0.1	6.1 ± 0.8	5.7 ± 1.1	–	–
EC (mS m^{-1})		416 ± 11	167 ± 30	189 ± 36	42.28–74.75	34.53–69.93
TDS (mg L^{-1})		3082 ± 68	1197 ± 230	1333 ± 332	45.42–81.34	41.44–73.32
COD (mg L^{-1})		24.41 ± 7.70	87.21 ± 47	70.65 ± 48	–	–
Acidity (mg L^{-1} as $CaCO_3$)		724 ± 13	–	–	–	–
Alkalinity (mg L^{-1} as $CaCO_3$)		–	215 ± 191	199 ± 238	–	–
Sulfate (mg L^{-1})		1107 ± 50	390 ± 96	455 ± 147	47.44–82.67	28.91–85.41
Metals	**Fe (mg L^{-1})**	103 ± 1.68	10.70 ± 11	15.72 ± 18	63.87–100	45.36–100
	Al (mg L^{-1})	25 ± 0.29	5.21 ± 2.51	7.47 ± 5.81	43.83–95.85	13.62–93.25
	Mn (mg L^{-1})	6.12 ± 0.06	4.73 ± 1.04	4.87 ± 1.20	–1.89–65.00	–23.88–71.36
	Zn (mg L^{-1})	5.16 ± 0.07	0.31 ± 0.21	0.39 ± 0.34	82.85–99.71	73.95–99.38
	Co (mg L^{-1})	1.11 ± 0.02	0.08 ± 0.12	0.20 ± 0.23	52.70–100	37.93–100
	Ni (mg L^{-1})	1.10 ± 0.03	0.10 ± 0.15	0.19 ± 0.25	42.34–100	31.16–100
	Cr (mg L^{-1})	1.11 ± 0.03	0.04 ± 0.06	0.11 ± 0.13	80.28–100	61.36–100

[a]Removal data presented as the min–max value. Values exceeding the discharge limits as recommended by CPCB (1993) and EPA (2002) are marked in red.

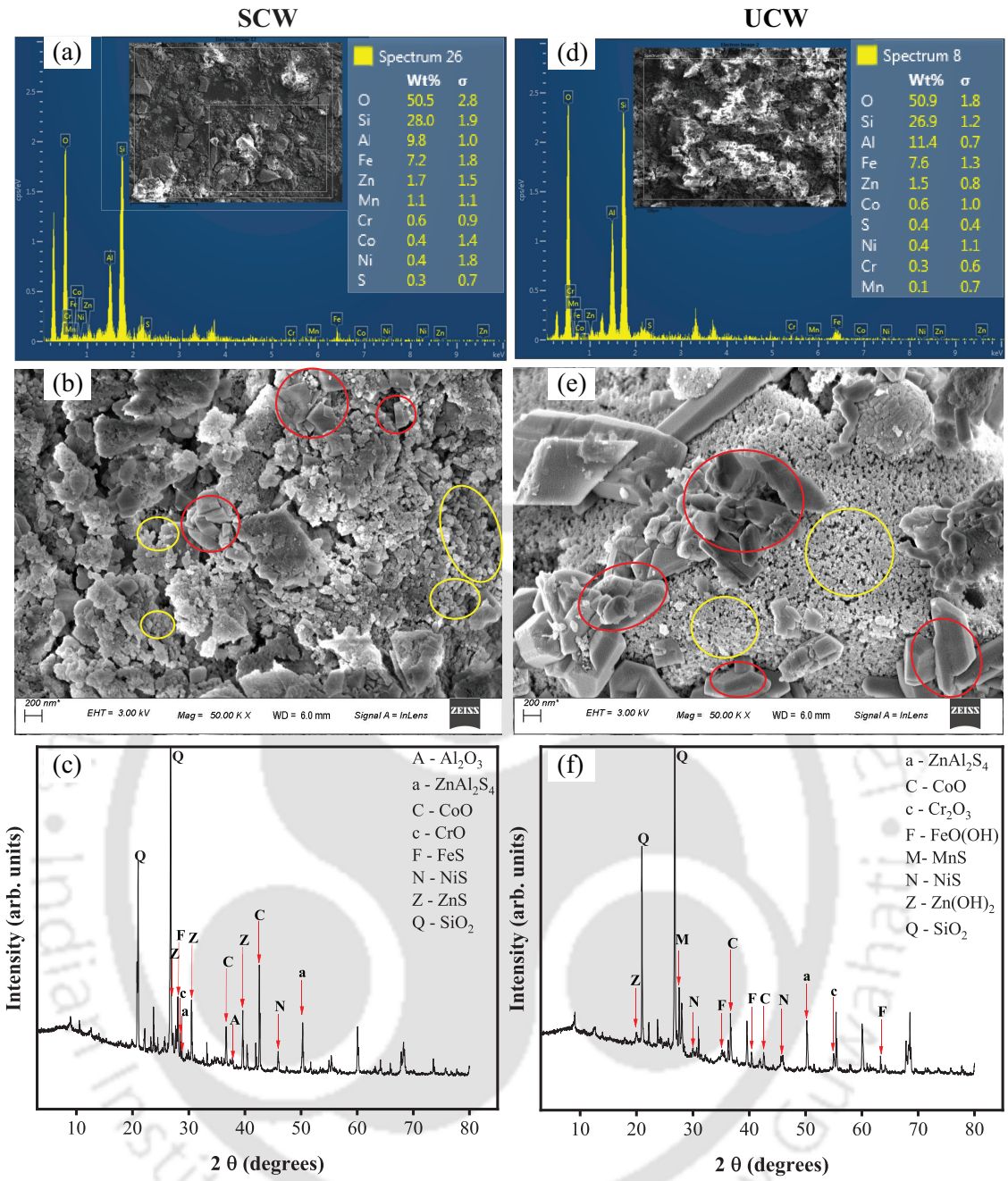

Fig. 4.18 Illustration of mineralogical composition (a and d), FESEM images (b and e) and XRD spectra (c and f) of the media from SCW (left) and UCW (right).

SCW. On the other hand, precipitation of manganese sulfide (MnS) (JCPDS 00-040-1288), zinc hydroxide ($Zn(OH)_2$) (JCPDS 01-076-1778), iron oxide hydroxide (FeO(OH)) (JCPDS 00-013-0518) and chromium oxide (Cr_2O_3) (JCPDS 00-001-1294) were indicated in UCW.

The comparative parameters of plant growth in SCW and UCW are presented in Table 4.4. Both CWs showed a similar number of plants; however, there was a considerable difference in the height of the plants, resulting in higher plant biomass production (expressed as dry weight basis) in UCW. Thus, high rainfall positively influenced the overall growth of plants in UCW. Furthermore, total chlorophyll measured in UCW (chlorophyll a: 1.53, b: 0.22 and c: 0.11 mg g^{-1}) was relatively higher than SCW (chlorophyll a: 1.19, b: 0.28 and c: 0.06 mg g^{-1}), which could be due to the higher metal retention and absorption by plants in SCW.

4.3.2.4 *Results of biomass activity test*

Maximum COD utilization or heterotrophic activity and specific sulfidogenic activity were estimated during the dry and wet seasons in SCW and UCW (Fig. 4.19 and Fig. 4.20). Comparable COD utilization rate of 1.06 and 0.91 mg COD mg TVS^{-1} d^{-1} were observed in SCW and UCW during the dry period, which decreased to 0.84 and 0.62 mg COD mg TVS^{-1} d^{-1} in SCW and UCW during the wet period, respectively. Similarly, sulfidogenic activity in terms of sulfate reduction decreased from 0.66 to 0.57 mg sulfate mg TVS^{-1} d^{-1} in SCW, while in UCW, significantly decreased sulfidogenic activity of 0.36 mg sulfate mg TVS^{-1} d^{-1} was observed in wet period than dry period (0.57 mg sulfate mg TVS^{-1} d^{-1}) (Fig. 4.21).

Table 4.4 Plant growth parameters in SCW and UCW.

Parameters	SCW	UCW
Plant density (plants per m^2)	102	102
Average plant height (cm)	124.76	156.48
Dry plant biomass of aboveground parts (kg m^{-2})	2.11	2.64
Dry plant biomass of belowground parts (kg m^{-2})	0.62	0.73
Total dry biomass (kg m^{-2})	2.73	3.36
Total chlorophyll (mg g^{-1})	1.53 ± 0.11	1.86 ± 0.09

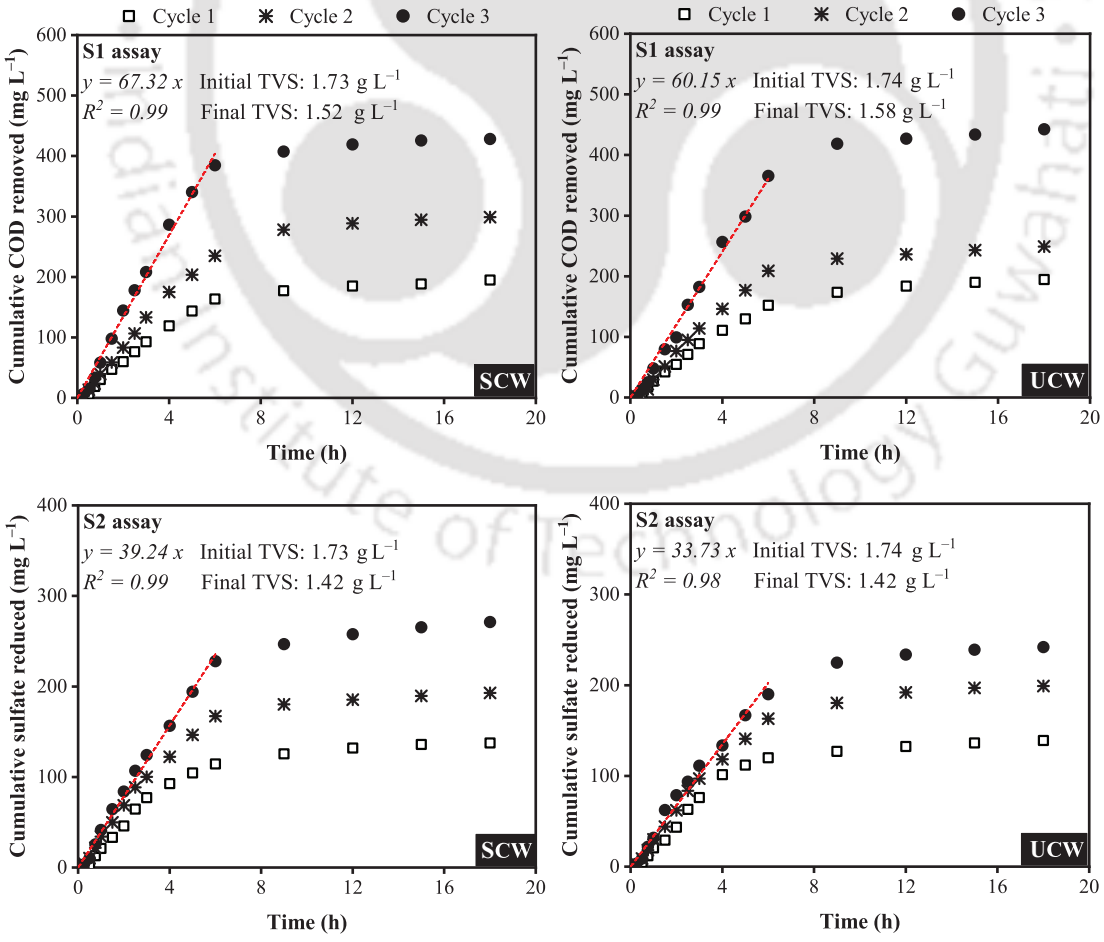

Fig. 4.19 Cumulative COD removal (mg L^{-1}) and sulfate reduction (mg L^{-1}) during the dry season.

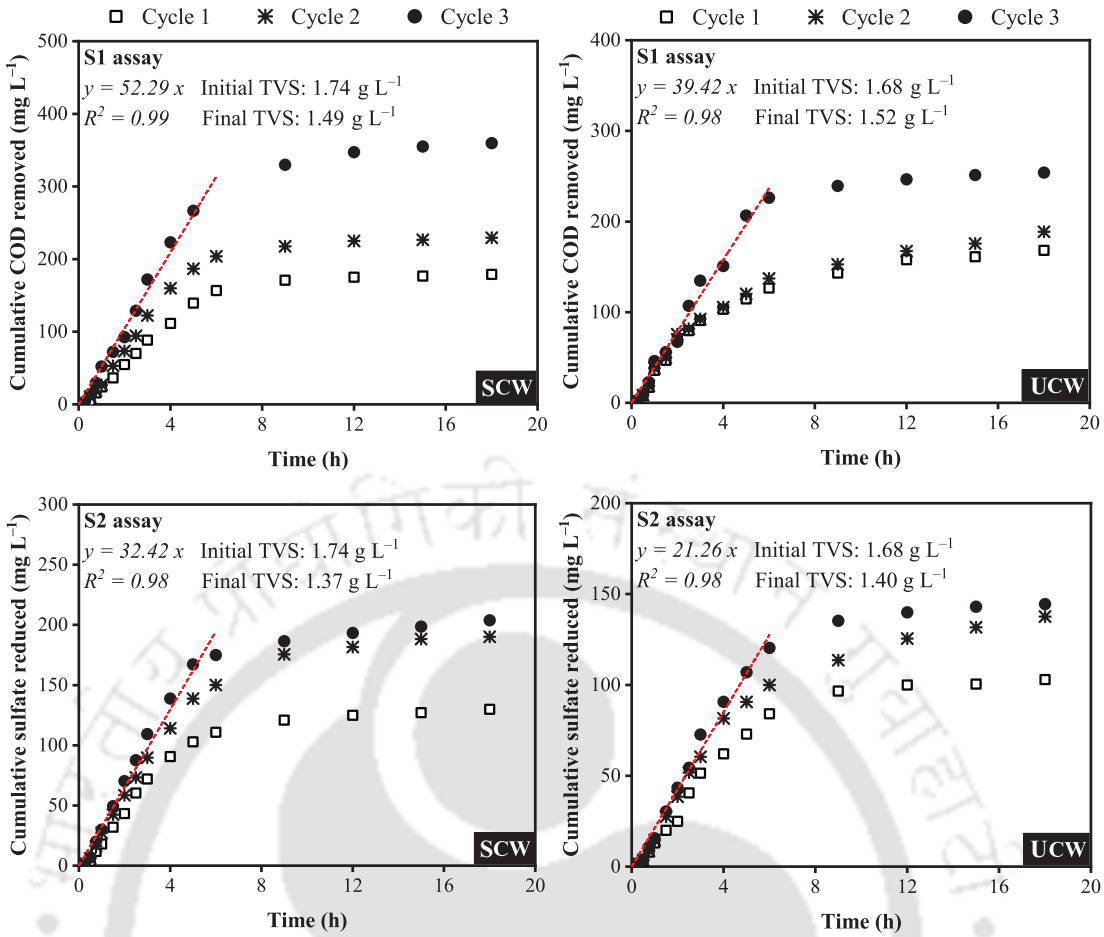

Fig. 4.20 Cumulative COD removal (mg L^{-1}) and sulfate reduction (mg L^{-1}) during the wet season.

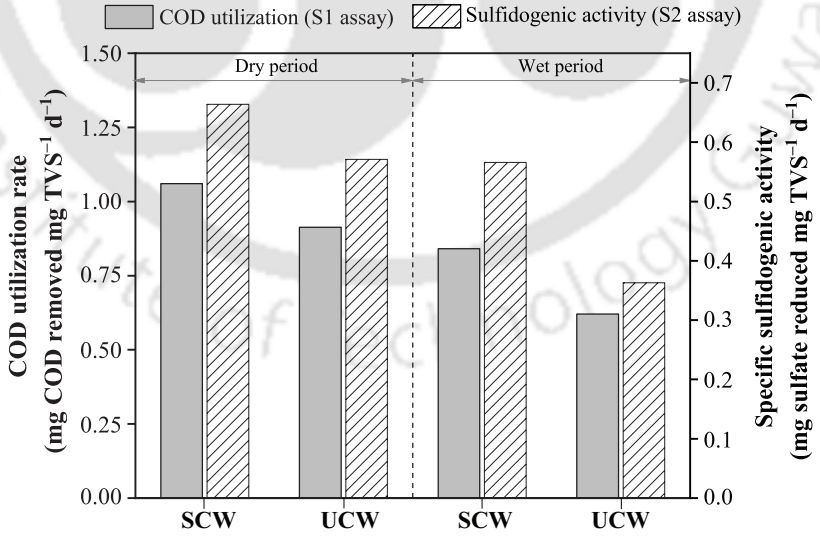

Fig. 4.21 Biomass activity of SCW and UCW during the dry and wet season.

The results inferred that with the onset of the wet period, the microbial activity in terms of COD utilization and sulfate reduction decreased significantly in UCW. The overall decline of biomass activity was also observed in SCW, which could be related to the organics depletion with time. Additionally, heavy rainfall caused excess flooding and a higher outflow rate in the UCW, which hampered the biological activities and pH dropped significantly (<

5.0). Many of the SRB are sensitive to even mild acidity and most of them are inhibited at pH 5.5 (Johnson et al., 2006). Cohen (2006) pointed pH as the predominant controlling factor for optimal sulfate reduction, which explains the lower biomass activity and deteriorating performance in UCW.

4.4 Summary

The incorporation of plants (*Typha latifolia*) does not contribute significantly to the remediation of AMD in terms of various physicochemical parameters. The presence of plants caused significant impairment and suppressed the microbial-assisted sulfate reduction in PCW. Both CCW and PCW exhibited excellent removal of metals like Fe (78–100%), Al (40–85%), Zn (93–98%), Co (92–96%), Ni (89–96%) and Cr (95–99%), except Mn. Further, the metal removal efficiency of Fe and Al was drastically reduced on increasing HLRs. Although metal removal efficiency is significant at 7-day HRT, at exceptionally higher loading during seasonal fluctuations (particularly monsoon season), a higher HRT with provision of additional supply of organics is recommended. EDTA exhibited higher metal extraction efficiency for Fe, Zn and Cr; nevertheless, organic acids also achieved comparable extraction efficiencies. The choice of EDTA as a suitable chemical lixiviant is limited in large-scale applications due to its high cost and low biodegradability (persistent organic pollutant); therefore, acetic acid is recommended, as it is quite cheap and readily biodegradable. The recovered metal precipitate could be further refined and recycled, adding economic value and environmentally friendly disposal of wetland media retaining metals. SCW demonstrated superior metal removal for Fe, Al, Zn, Co, Ni and Cr, which significantly differed from UCW, except manganese. UCW achieved only 51% sulfate removal, which significantly varied from SCW (60%) during the wet season. Thus, UCW exhibited significantly lower treatment efficiency for all constituents with the onset of the rainfall period, indicating possible shortening of the HRT due to heavy rainfall with minimal or no significant dilution effect. Taking high surface flow and infiltration rates into consideration, a large wetland area than the nominal design may be implemented in rainfall-prone areas of subtropical region. Furthermore, regardless of plants or seasonal effects, the depletion of carbon from organic wetland media limited the treatment efficacy of CWs over time.

References

Acharya, B. S. and Kharel, G. (2020). Acid mine drainage from coal mining in the United States–An overview. *Journal of Hydrology*, 588:125061.

Alikhani, M. E. and Manceron, L. (2015). The copper carbonyl complexes revisited: Why are the infrared spectra and structures of copper mono and dicarbonyl so different? *Journal of Molecular Spectroscopy*, 310:32–38.

APHA (2012). *Standard Methods for the Examination of Water and Wastewater*. American Public Health Association, Washington, DC.

Chen, J., Li, X., Jia, W., Shen, S., Deng, S., Ji, B., and Chang, J. (2021). Promotion of bioremediation performance in constructed wetland microcosms for acid mine drainage treatment by using organic substrates and supplementing domestic wastewater and plant

litter broth. *Journal of Hazardous Materials*, 404:124125.

Chen, T., Lei, C., Yan, B., and Xiao, X. (2014). Metal recovery from the copper sulfide tailing with leaching and fractional precipitation technology. *Hydrometallurgy*, 147-148:178–182.

Cohen, R. R. H. (2006). Use of microbes for cost reduction of metal removal from metals and mining industry waste streams. *Journal of Cleaner Production*, 14(12-13):1146–1157.

Coupland, K. and Johnson, D. B. (2008). Evidence that the potential for dissimilatory ferric iron reduction is widespread among acidophilic heterotrophic bacteria. *FEMS Microbiology Letters*, 279(1):30–35.

CPCB (1993). *General Standards for Discharge of Environmental Pollutants Part-A: Effluents, Schedule - VI (Rule 3A)*. Central Pollution Control Board, New Delhi, India.

Dean, A. P., Lynch, S., Rowland, P., Toft, B. D., Pittman, J. K., and White, K. N. (2013). Natural wetlands are efficient at providing long-term metal remediation of freshwater systems polluted by acid mine drainage. *Environmental Science & Technology*, 47(21):12029–12036.

Dev, S., Roy, S., and Bhattacharya, J. (2017). Optimization of the operation of packed bed bioreactor to improve the sulfate and metal removal from acid mine drainage. *Journal of Environmental Management*, 200:135–144.

Di Palma, L., Ferrantelli, P., Merli, C., and Biancifiori, F. (2003). Recovery of EDTA and metal precipitation from soil flushing solutions. *Journal of Hazardous Materials*, 103(1-2):153–168.

Drury, W. J. (2000). Modeling of sulfate reduction in anaerobic solid substrate bioreactors for mine drainage treatment. *Mine Water and the Environment*, 19:19–29.

EPA (2002). *Standards for Effluent Discharge Regulations. General Notice No. 44. of 2003*. Environmental Protection Agency. (accessed on 17.04.19).

Feng, C., Zhang, S., Li, L., Wang, G., Xu, X., Li, T., and Zhong, Q. (2018). Feasibility of four wastes to remove heavy metals from contaminated soils. *Journal of Environmental Management*, 212:258–265.

Gaballah, M. S., Ismail, K., Aboagye, D., Ismail, M. M., Sobhi, M., and Stefanakis, A. I. (2021). Effect of design and operational parameters on nutrients and heavy metal removal in pilot floating treatment wetlands with *Eichhornia Crassipes* treating polluted lake water. *Environmental Science and Pollution Research*, 28:25664–25678.

Galletti, A., Verlicchi, P., and Ranieri, E. (2010). Removal and accumulation of Cu, Ni and Zn in horizontal subsurface flow constructed wetlands: Contribution of vegetation and filling medium. *Science of the Total Environment*, 408(21):5097–5105.

Genty, T., Bussière, B., Benzaazoua, M., Neculita, C. M., and Zagury, G. J. (2018). Changes in efficiency and hydraulic parameters during the passive treatment of ferriferous acid mine drainage in biochemical reactors. *Mine Water and the Environment*, 37(4):686–695.

Gikas, P., Ranieri, E., and Tchobanoglous, G. (2013). Removal of iron, chromium and lead from waste water by horizontal subsurface flow constructed wetlands. *Journal of Chemical Technology and Biotechnology*, 88(10):1906–1912.

Goel, S. and Gautam, A. (2010). Effect of chelating agents on mobilization of metal from waste catalyst. *Hydrometallurgy*, 101(3-4):120–125.

Gupta, V., Courtemanche, J., Gunn, J., and Mykytczuk, N. (2020). Shallow floating treatment wetland capable of sulfate reduction in acid mine drainage impacted waters in a northern climate. *Journal of Environmental Management*, 263:110351.

Gutierrez, O., Mohanakrishnan, J., Sharma, K. R., Meyer, R. L., Keller, J., and Yuan, Z. (2008). Evaluation of oxygen injection as a means of controlling sulfide production in a sewer system. *Water Research*, 42(17):4549–4561.

Hernández, P., Recio, G., Canales, C., Schwarz, A., Villa-Gomez, D., Southam, G., and Nancucheo, I. (2022). Evaluation of operating conditions on sulfate reduction from acidic wastewater in a fixed-bed bioreactor. *Minerals Engineering*, 177:107370.

Javed, M. T., Akram, M. S., Habib, N., Tanwir, K., Ali, Q., Niazi, N. K., Gul, H., and Iqbal, N. (2018). Deciphering the growth, organic acid exudations, and ionic homeostasis of *Amaranthus viridis* L. and *Portulaca oleracea* L. under lead chloride stress. *Environmental Science and Pollution Research*, 25:2958–2971.

Javed, M. T., Stoltz, E., Lindberg, S., and Greger, M. (2013). Changes in pH and organic acids in mucilage of *Eriophorum angustifolium* roots after exposure to elevated concentrations of toxic elements. *Environmental Science and Pollution Research*, 20:1876–1880.

Jhajharia, D., Yadav, B. K., Maske, S., Chattopadhyay, S., and Kar, A. K. (2012). Identification of trends in rainfall, rainy days and 24 h maximum rainfall over subtropical Assam in Northeast India. *Comptes Rendus Geoscience*, 344(1):1–13.

Johnson, D. B. and Hallberg, K. B. (2005). Acid mine drainage remediation options: A review. *Science of the Total Environment*, 338(1-2):3–14.

Johnson, D. B., Sen, A. M., Kimura, S., Rowe, O. F., and Hallberg, K. B. (2006). Novel biosulfidogenic system for selective recovery of metals from acidic leach liquors and waste streams. *Mineral Processing and Extractive Metallurgy*, 115(1):19–24.

Johnson, K. L. and Younger, P. L. (2005). Rapid manganese removal from mine waters using an aerated packedbed bioreactor. *Journal of Environmental Quality*, 34(3):987–993.

Kadlec, R. H. and Wallace, S. D. (2008). *Treatment Wetlands*. CRC press, Boca Raton, FL.

Khan, U. A., Kujala, K., Nieminen, S. P., Räisänen, M. L., and Ronkanen, A.-K. (2019). Arsenic, antimony, and nickel leaching from northern peatlands treating mining influenced water in cold climate. *Science of the Total Environment*, 657:1161–1172.

Kiiskila, J. D., Sarkar, D., Feuerstein, K. A., and Datta, R. (2017). A preliminary study to design a floating treatment wetland for remediating acid mine drainage-impacted water using vetiver grass (*Chrysopogon zizanioides*). *Environmental Science and Pollution Research*, 24(36):27985–27993.

Liolios, K. A., Moutsopoulos, K. N., and Tsihrintzis, V. A. (2014). Comparative modeling of HSF constructed wetland performance with and without evapotranspiration and rainfall. *Environmental Processes*, 1(2):171–186.

Lizama-Allende, K., Ayala, J., Jaque, I., and Echeverría, P. (2021). The removal of arsenic and metals from highly acidic water in horizontal subsurface flow constructed wetlands with alternative supporting media. *Journal of Hazardous Materials*, 408:124832.

Manios, T., Stentiford, E. I., and Millner, P. (2003). Removal of heavy metals from a metaliferous water solution by *Typha latifolia* plants and sewage sludge compost. *Chemosphere*, 53(5):487–494.

Matsui, T. and Tsuchiya, T. (2006). A method to estimate practical radial oxygen loss of wetland plant roots. *Plant and Soil*, 279(1):119–128.

Mays, P. A. and Edwards, G. S. (2001). Comparison of heavy metal accumulation in a natural wetland and constructed wetlands receiving acid mine drainage. *Ecological Engineering*, 16(4):487–500.

Musariri, B., Akdogan, G., Dorfling, C., and Bradshaw, S. (2019). Evaluating organic acids as alternative leaching reagents for metal recovery from lithium ion batteries. *Minerals Engineering*, 137:108–117.

Neculita, C.-M., Zagury, G. J., and Bussière, B. (2008). Effectiveness of sulfate-reducing passive bioreactors for treating highly contaminated acid mine drainage: I. Effect of hydraulic

retention time. *Applied Geochemistry*, 23(12):3442–3451.

Pacini, V. A., Ingallinella, A. M., and Sanguinetti, G. (2005). Removal of iron and manganese using biological roughing up flow filtration technology. *Water Research*, 39(18):4463–4475.

Poach, M. E., Hunt, P. G., Reddy, G. B., Stone, K. C., Johnson, M. H., and Grubbs, A. (2004). Swine wastewater treatment by marsh-pond-marsh constructed wetlands under varying nitrogen loads. *Ecological Engineering*, 23(3):165–175.

Qin, M., He, G., Liao, K., Zou, Q., Zhao, S., Jiang, X., and Zhang, S. (2022). CO_2-O_2-SRB-Cl^- multifactor synergistic corrosion in shale gas pipelines at a low liquid flow rate. *Journal of Materials Engineering and Performance*, pages 1–16.

Rahman, K. Z., Wiessner, A., Kuschk, P., van Afferden, M., Mattusch, J., and Müller, R. A. (2011). Fate and distribution of arsenic in laboratory-scale subsurface horizontal-flow constructed wetlands treating an artificial wastewater. *Ecological Engineering*, 37(8):1214–1224.

Sato, Y., Hamai, T., Hori, T., Aoyagi, T., Inaba, T., Hayashi, K., Kobayashi, M., Sakata, T., and Habe, H. (2022). Optimal start-up conditions for the efficient treatment of acid mine drainage using sulfate-reducing bioreactors based on physicochemical and microbiome analyses. *Journal of Hazardous Materials*, 423:127089.

Scholz, M. (2006). *Wetland Systems to Control Urban Runoff*. Elsevier, Amsterdam, The Netherlands.

Shriwastav, A., Sudarsan, G., Bose, P., and Tare, V. (2010). Modification of Winkler's method for determination of dissolved oxygen concentration in small sample volumes. *Analytical Methods*, 2(10):1618–1622.

Singh, A., Thakur, S., and Adhikary, N. C. (2021). Analysis of spatial and temporal rainfall characteristics of the North East region of India. *Arabian Journal of Geosciences*, 14(885):1–16.

Singh, B. (2009). Treatment of spent catalyst from the nitrogenous fertilizer industry–A review of the available methods of regeneration, recovery and disposal. *Journal of Hazardous Materials*, 167(1-3):24–37.

Stein, O. R., Borden-Stewart, D. J., Hook, P. B., and Jones, W. L. (2007). Seasonal influence on sulfate reduction and zinc sequestration in subsurface treatment wetlands. *Water Research*, 41(15):3440–3448.

Taheri Ghannad, S., Boroomandnasab, S., Moazed, H., and Jaafarzadeh, N. (2015). The effects of substrate type, HRT and reed on the lead removal in horizontal subsurface-flow constructed wetland. *Desalination and Water Treatment*, 56(12):3357–3367.

Türker, O. C., Böcük, H., and Yakar, A. (2013). The phytoremediation ability of a polyculture constructed wetland to treat boron from mine effluent. *Journal of Hazardous Materials*, 252:132–141.

USEPA (1996). *Method 3050B: Acid Digestion of Sediments, Sludges, and Soils*. Environmental Protection Agency, Washington, DC.

Vaquer-Sunyer, R. and Duarte, C. M. (2008). Thresholds of hypoxia for marine biodiversity. *Proceedings of the National Academy of Sciences*, 105(40):15452–15457.

Vithanage, M., Rajapaksha, A. U., Wijesekara, H., Weerarathne, N., and Ok, Y. S. (2014). Effects of soil type and fertilizer on As speciation in rice paddy contaminated with As-containing pesticide. *Environmental Earth Sciences*, 71:837–847.

Wei, M., Chen, J., and Wang, Q. (2018). Remediation of sandy soil contaminated by heavy metals with Na_2EDTA washing enhanced with organic reducing agents: element distribution and spectroscopic analysis. *European Journal of Soil Science*, 69(4):719–731.

Wei, X., Viadero Jr, R. C., and Buzby, K. M. (2005). Recovery of iron and aluminum

from acid mine drainage by selective precipitation. *Environmental Engineering Science*, 22(6):745–755.

White, R. A., Freeman, C., and Kang, H. (2011). Plant-derived phenolic compounds impair the remediation of acid mine drainage using treatment wetlands. *Ecological Engineering*, 37(2):172–175.

Wiessner, A., Kuschk, P., Buddhawong, S., Stottmeister, U., Mattusch, J., and Kastner, M. (2006). Effectiveness of various small-scale constructed wetland designs for the removal of iron and zinc from acid mine drainage under field conditions. *Engineering in Life Sciences*, 6(6):584–592.

Wiessner, A., Rahman, K. Z., Kuschk, P., Kastner, M., and Jechorek, M. (2010). Dynamics of sulphur compounds in horizontal sub-surface flow laboratory-scale constructed wetlands treating artificial sewage. *Water Research*, 44(20):6175–6185.

Willow, M. A. and Cohen, R. R. H. (2003). pH, dissolved oxygen, and adsorption effects on metal removal in anaerobic bioreactors. *Journal of Environmental Quality*, 32:1212–1221.

Xu, J. C., Chen, G., Huang, X. F., Li, G. M., Liu, J., Yang, N., and Gao, S. N. (2009). Iron and manganese removal by using manganese ore constructed wetlands in the reclamation of steel wastewater. *Journal of Hazardous Materials*, 169(1-3):309–317.

Xu, X. and Mills, G. L. (2018). Do constructed wetlands remove metals or increase metal bioavailability? *Journal of Environmental Management*, 218:245–255.

Yang, B., Lan, C. Y., Yang, C. S., Liao, W. B., Chang, H., and Shu, W. S. (2006). Long-term efficiency and stability of wetlands for treating wastewater of a lead/zinc mine and the concurrent ecosystem development. *Environmental Pollution*, 143(3):499–512.

You, S.-H., Zhang, X.-H., Liu, J., Zhu, Y.-N., and Gu, C. (2014). Feasibility of constructed wetland planted with *Leersia hexandra* Swartz for removing Cr, Cu and Ni from electroplating wastewater. *Environmental Technology*, 35(2):187–194.

5

Influence of Electron Donor on the Long-term Biochemical Treatment of Acid Mine Drainage

This chapter aims to understand the influence of simple carbon source on the long-term treatment performance of CW in response to different COD/SO_4^{2-} ratios and to develop the biochemical mechanisms.

5.1 Introduction

AMD is devoid of organics; hence the carbon source for biological treatment is accomplished either as a simple organic carbon or as a complex organic material. The utilization of organic material as wetland media (such as mushroom compost, manure and agricultural waste) for the bioremediation of AMD in CWs is extensively employed (Chen et al., 2021; Dann et al., 2009). However, findings from previous chapters underlined that organic media provided a limited supply of carbon over time due to rapid depletion of the readily degradable organics and thus, requires consistent replacement of media bed for sustaining microbial activity (Neculita et al., 2011). On the other hand, the use of simple, low-cost and easily available carbon (such as alcohols, sugars and organic acids) allows better control of the quantity of carbon release and management of COD/SO_4^{2-} ratio for the optimum operation in bioreactors (Bekmezci et al., 2011; Sahinkaya et al., 2018; Santos et al., 2021). Unlike bioreactors, the biogeochemistry and microbiology of the CWs are highly complex and influenced by several other environmental factors (such as the season and presence of plants). With the current state of knowledge, there is potential to understand the functioning of different fundamental processes that co-occur in CWs. Lactate has been acknowledged as an efficient electron donor for the high biomass yield of SRB and high alkalinity production in lab-scale operations (Kaksonen and Puhakka, 2007; Santos et al., 2021). However, the performance appraisal of CWs supplied with a simple carbon for AMD treatment is not explored yet.

Sulfidogenesis and methanogenesis pathway is favored at low and high COD/SO_4^{2-} ratio, respectively, which has a strong influence on the microbial community and regulates electron flows (Dar et al., 2008). Therefore, COD/SO_4^{2-} ratio is a governing factor that affects the biochemical mechanisms of sulfate reduction and organic matter utilization. The sulfate reduction process by SRB using lactate as an electron donor is represented in equation (5.1) (Oyekola et al., 2009).

$$2CH_3CHOHCOO^- + 3SO_4^{2-} \longrightarrow 6HCO_3^- + 3HS^- + H^+ \quad (5.1)$$

In this context, the primary focus of the study was to evaluate the performance of gravel-based CW operating under varying COD/SO_4^{2-} ratios using a simple carbon (lactate) for the bioremediation of AMD. The role of different wetland components in the treatment matrix was assessed to determine the metal removal mechanisms. Further, the genetic composition of diverse microbial communities and relative abundance were identified using metagenomics analysis.

5.2 Materials and methods

5.2.1 Chemicals and reagents

Chemicals and reagents used in the present study were of AR grade as described in Chapter 2 (section 2.3.2) and Chapter 3 (section 3.2.1).

5.2.2 Experimental set-up and wetland operation

HSSF-CW (B) was fabricated having the same design configuration as mentioned in Chapter 3 (section 3.2.3). Zones I and V were packed with coarser gravel bed (12.5 mm < ϕ < 20 mm), whereas the middle zones were filled with different layers of the gravel bed, consisting of coarser gravel (5 cm thick) at the bottom followed by a layer of coarse gravel (10 mm < ϕ < 12.5 mm, 10 cm depth), fine gravel (6.3 mm < ϕ < 10 mm, 30 cm depth) and top-most soil (5 cm depth). The layout of media arrangement in HSSF-CW (B) is illustrated in Fig. 5.1 (a). Fresh and healthy saplings of *Typha latifolia* (25 stems per m^2) were planted in the middle zones (II, III and IV). A photographic image of HSSF-CW (B) is presented in Fig. 5.1 (b).

Synthetic AMD was prepared according to section 3.2.2 of Chapter 3 with the addition of sodium lactate as a carbon source to vary COD/SO_4^{2-} ratio. In addition, micro and macronutrients (56 mg L^{-1} KH_2PO_4, 110 mg L^{-1} NH_4Cl and 11 mg L^{-1} ascorbic acid) were also supplemented, as described by Bekmezci et al. (2011). The effective volume and porosity were about 64 L and 0.48, respectively. The influent discharge was regulated at 9.14 L d^{-1} by a peristaltic pump to achieve an applied HLR of 0.03 m^3 m^{-2} d^{-1} and a corresponding HRT of 7 d. During the acclimatization phase (phase I–IV), a diluted concentration of AMD was discharged (10, 25, 45 and 70%), whereas in the treatment phase (phase V–VI), full-strength (100%) AMD was fed. HSSF-CW (B) was operated at COD/SO_4^{2-} ratio of 0.65–0.69 and 0.32–0.35 during phase (I–V) and phase VI, respectively (Table 5.1).

(a)

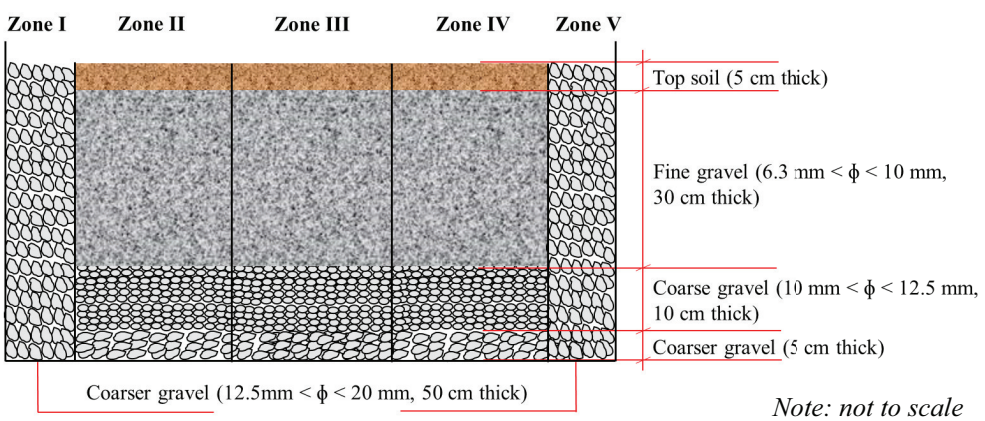

(b)

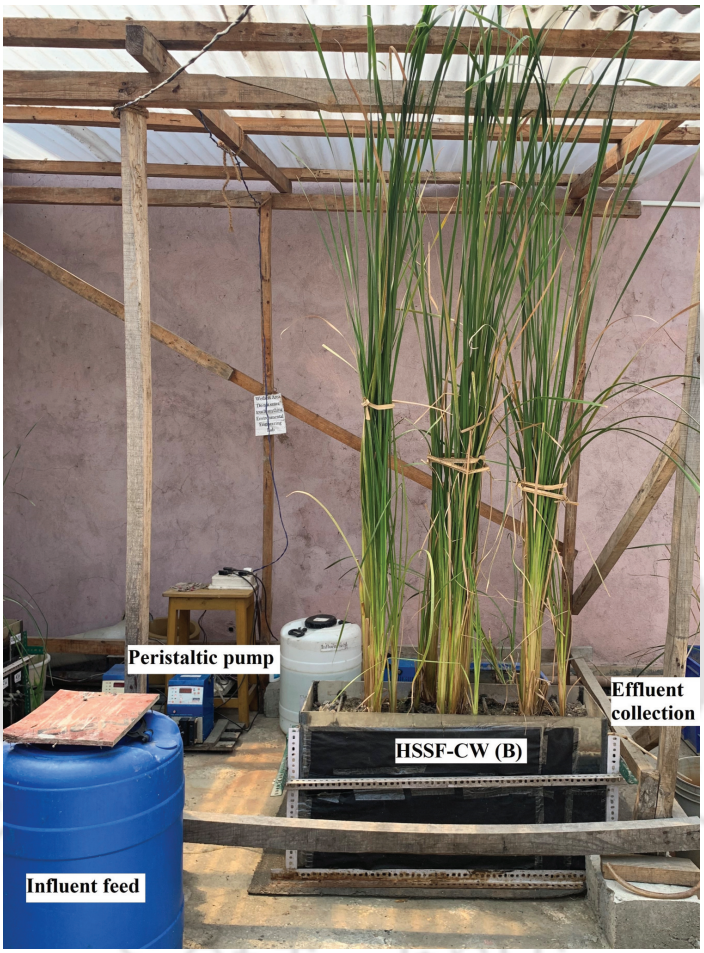

Fig. 5.1 (a) Media layout and (b) photographic image of HSSF-CW (B).

Table 5.1 Details of operational conditions of HSSF-CW (B).

	Operational phases	Duration (d)	AMD strength (%)	COD (mg L^{-1})	Sulfate (mg L^{-1})	COD/SO_4^{2-}
Acclimatization phases	**Phase I**	14	10	87.57 ± 5.60	128.71 ± 3.69	0.65–0.69
	Phase II	14	25	227.36 ± 4.96	326.76 ± 1.45	
	Phase III	14	45	447.85 ± 4.05	648.86 ± 0.74	
	Phase IV	21	70	593.14 ± 3.34	877.00 ± 10.78	
Treatment phases	**Phase V**	71	100	727.67 ± 31.17	1085.26 ± 43.86	
	Phase VI	84	100	355.85 ± 13.85	1064.30 ± 31.98	0.32–0.35

5.2.3 Batch adsorption experiment

For the adsorption study, the desired dose of the autoclaved gravel media (adsorbent dose, 100 g L^{-1}) was added to the series of AMD solutions (50 mL) maintained at different pH (2.0, 3.0, 4.0, 5.0, 6.0 and 7.0). The pH of the solution was adjusted using 1M Na_2CO_3 or 1N H_2SO_4. The mixtures were agitated in an end-over-end rotary shaker for 24 h at room temperature (28 ± 2°C). After agitation, the mixture was separated and filtered through 0.45 µm filter paper and analyzed for the remaining metal concentration in the solution after adsorption. All batch experiments were conducted in triplicates and data are represented as the average value. The adsorption capacity was obtained using equation (5.2).

$$\text{Adsorption capacity (q, mg kg}^{-1}) = \frac{V \times (C_1 - C_2)}{m} \tag{5.2}$$

where 'C_1' is the metal concentration after precipitation (mg L^{-1}) (from section 3.2.5), 'C_2' is the final metal concentration remaining in the solution after adsorption (mg L^{-1}), 'V' is the volume of the solution (L) and 'm' is the dry mass of the media (kg).

5.2.4 Biomass activity test

Biomass activity assays were performed with slight modification from the method mentioned in Chapter 3 (section 3.2.6). For the initial volatile suspended solids (VSS) estimation, a measured quantity of gravel mass (as attached biomass) was taken from the HSSF-CW (B), agitated with distilled water (50 mL), filtered and VSS was computed (APHA, 2012). VSS of the homogenous water sample (as suspended biomass) taken from the ports of the CW was also determined. For the biomass activity test, the biomass of 1–1.50 g L^{-1} was used in the same ratio as available in the CW. Three assays (S1, S2 and S3) were performed, such that in the S1 assay, solely carbon (as dextrose) was added (COD = 1.50 g L^{-1}), whereas, for S2 and S3 assays, carbon (as dextrose) and sulfate (as Na_2SO_4) were added in the ratio of 0.67 (COD = 1.20 g L^{-1}, SO_4^{2-} = 1.70 g L^{-1}) and 0.32 (COD = 0.54 g L^{-1}, SO_4^{2-} = 1.70 g L^{-1}), respectively. Thereafter, the estimation of biomass activity in terms of heterotrophic activity and specific sulfidogenic activity was done by following the same procedure as described in Chapter 3 up to three feed cycles and finally computed by considering the linear portion (slope) of the third cycle (Equation 3.3).

5.2.5 Analytical methods

All the analytical techniques used in this study are mentioned in Chapter 2 (section 2.3.3), Chapter 3 (section 3.2.8) and Chapter 4 (section 4.2.4). For microbial metagenomics, a homogenous wastewater sample from triplicate sampling was sent to Eurofins Genomics (Bangalore, India). The detailed procedure for DNA extraction, amplification, library preparation, sequencing, and sequence data analysis is mentioned in Chapter 3. The sequencing data have been deposited on NCBI in the bioproject PRJNA743990 as SRA (SRR15524177) with sample accession number SAMN20064651.

The specific metal mass removal rate was calculated as the difference between the

inflow and outflow loading rates given by equation (5.3).

$$\text{Specific metal mass removal rate (in mg m}^{-2}\text{ d}^{-1}) = \frac{(C_{in} - C_{out}) \times Q}{A} \quad (5.3)$$

where 'C_{in}' is the inflow metal concentration (mg L^{-1}), 'C_{out}' is the outflow metal concentration (mg L^{-1}), 'Q' is the flow rate ($Q_{in} = Q_{out} = Q$) (L d^{-1}) and 'A' is the surface area (m^2).

5.3 Results and discussions

5.3.1 Batch adsorption results

The results of metal removal in the presence of gravel at different pH are provided in Table 5.2. Metal removal achieved in the absence of gravel was principally due to precipitation (Table 3.4) and in the presence of gravel was due to both precipitation and adsorption. From the difference between the two results, the surplus metal removal at a specific pH is attributed to the adsorption mechanism. The results showed that adsorption capacity increased with pH increment due to lower H^+ ionic activity or decreased competition from H^+ ions against metal ions at higher pH (Sizirici et al., 2018). Gravel exhibited the highest adsorption capacity (in mg kg^{-1}) for iron (20.32–243.13) and aluminium (3.20–11.23), followed by manganese (1.52–5.51), zinc (1.46–3.76), nickel (0.13–1.24), cobalt (0.18–1.12) and chromium (0.062–0.44). Sizirici et al. (2018) reported comparatively lower metal removal efficiency for iron (78.60%), zinc (90.20%) and nickel (25.80%) at pH 7.0 using gravel.

5.3.2 Effluent water quality

The time series profile for various physiochemical parameters measured during different operational phases is shown in Fig. 5.2. Higher mean effluent pH of 7.1–7.4 was recorded during the acclimatization phase, whereas the mean pH varied from 5.4 to 5.9 in the treatment phase. Initial alkalinity production during phase I–IV (108–368 mg L^{-1} as $CaCO_3$) dropped gradually to 190.83 ± 105.07 in phase V, which further decreased to 62.75 ± 17.05 mg L^{-1} in

Table 5.2 Metal removal efficiency and adsorption capacity as a function of pH using gravel.

Initial pH	Final pH	Metal removal[a] (%)						
		Fe	Al	Mn	Zn	Co	Ni	Cr
2.0	2.1	3.01 (20.32)[b]	1.18 (3.20)	0.00 (0.00)	2.93 (1.46)	0.00 (0.00)	2.50 (0.14)	0.00 (0.00)
3.0	3.2	35.48 (63.43)	2.54 (6.17)	5.79 (1.52)	26.41 (1.51)	2.33 (0.18)	2.93 (0.13)	6.65 (0.06)
4.0	4.2	44.10 (122.65)	19.53 (8.33)	18.20 (2.10)	38.12 (2.31)	2.93 (0.35)	5.23 (0.27)	15.81 (0.23)
5.0	5.3	63.57 (243.13)	70.84 (10.70)	24.20 (2.48)	45.72 (3.35)	12.57 (0.92)	14.70 (0.54)	26.32 (0.34)
6.0	6.2	100 (–)	97.37 (11.23)	30.07 (4.59)	89.66 (3.76)	45.27 (1.09)	51.87 (0.70)	87.79 (0.44)
7.0	7.2	100 (–)	100 (–)	52.30 (5.51)	100 (0.45)	87.83 (1.12)	77.73 (1.24)	100 (0.20)

[a]Metal removal values indicate total metal removal by precipitation and adsorption route.

[b]Adsorption capacity, expressed as mg kg^{-1} is presented inside the parentheses.

phase VI due to less availability of electron donor. Assuming complete lactate oxidation, the theoretical alkalinity estimation based on the sulfate reduction accounted about 844 and 502 mg L^{-1} as $CaCO_3$ in phase V and VI, respectively. The measured alkalinity of the effluent was comparable to the net residual alkalinity after high acidity (averaged 722 mg L^{-1} as $CaCO_3$)

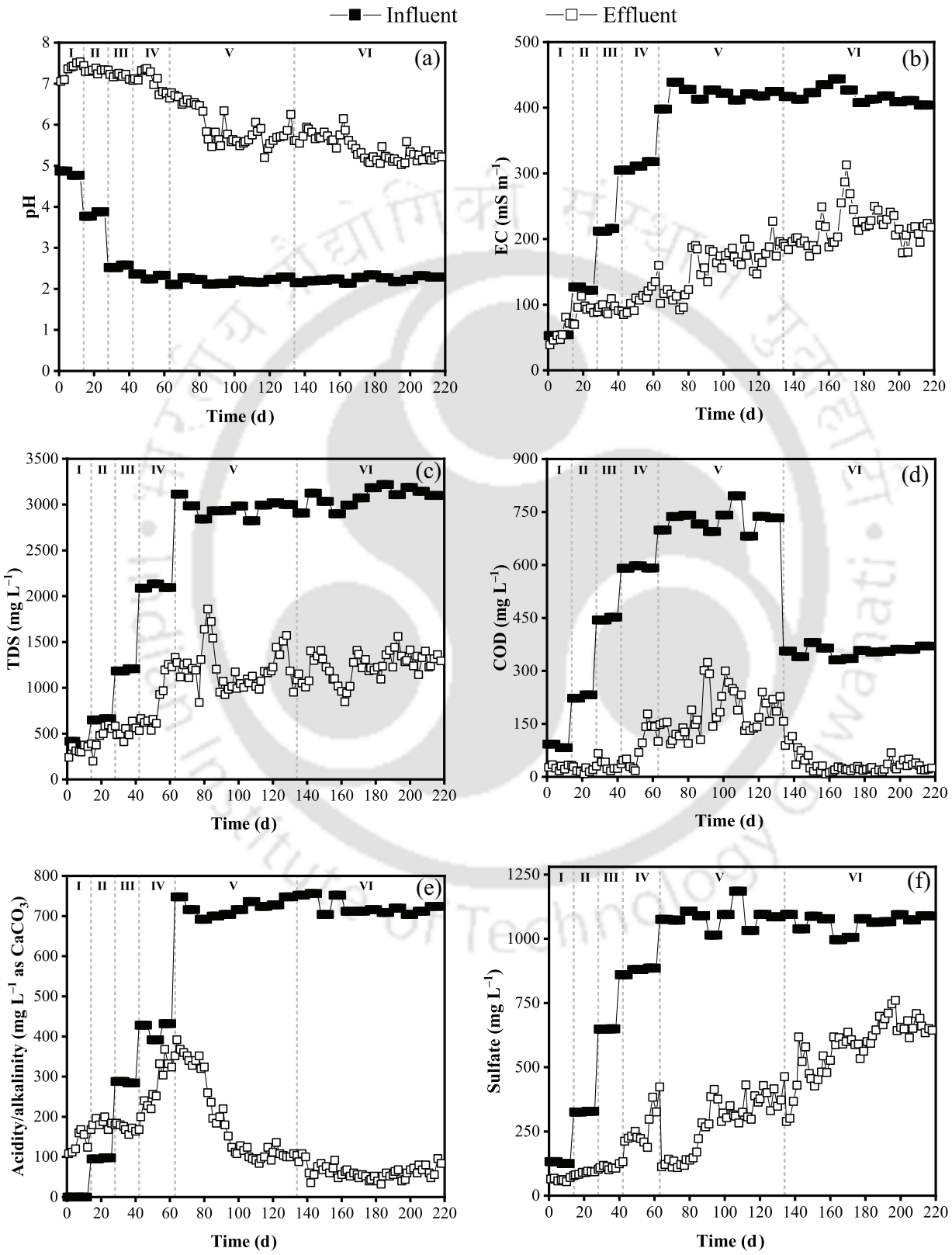

Fig. 5.2 Inflow and outflow profile of HSSF-CW (B) for (a) pH, (b) EC, (c) TDS, (d) COD, (e) acidity (inflow) and alkalinity (outflow) and (f) sulfate.

neutralization of the influent in phase V. However, a significant disparity was observed between theoretical alkalinity and residual alkalinity of the effluent measured in phase VI. Therefore, other biochemical reactions such as oxidation or reduction of iron (Equation 1.2, 3.10, 5.4–5.5) consumed protons and contributed significantly to alkalinity in addition to sulfate reduction, which could not be accounted due to cyclic reactions co-occurring in the CW. The alkalinity production coupled with the generation of bicarbonate ions by oxidation of electron donor predominantly controlled the effluent pH. A declining pH trend was directly linked with the deteriorating sulfate removal efficiency in phase V and VI. Mean effluent EC was 90.17 mS m^{-1} during the acclimatization period and gradually increased from 158.90 to 216.90 mS m^{-1} in phase V to VI. This increase in EC values is associated with the low pH (more H^+ ions) and the presence of metal and sulfate ions due to lower removal efficiency in phase VI. Similarly, effluent TDS varied between 200–1332 mg L^{-1} during phase I–IV, which increased to 1198.45 ± 229.78 and 1238.13 ± 149.44 mg L^{-1} in phase V and VI, respectively. Contrary to the EC results, mean effluent TDS increased marginally from phase V to VI due to a significant decrease in effluent COD, measured as 180.64 and 34.21 mg L^{-1} in phase V and VI, respectively.

The COD removal efficiency of 85.02% was accounted during phase I–IV, which reduced to 75.20% in phase V, whereas no significant change in sulfate removal efficiency was observed during phase I–IV (70.19%) and V (74.10%). The establishment of SRB was confirmed by the presence of black deposits in the gravel bed and on the walls of the CW, as well as the incidence of a strong sulfurous odor accompanied by the production of total dissolved sulfide (15.60–25.70 mg L^{-1}) as discussed by Lyew and Sheppard (2001). Relatively higher dissolved sulfide concentrations were observed in HSSF-CW (B) compared to organic-amended CWs, suggesting the promotion of microbial degradation and SRB metabolism with oxygen depletion in the presence of sufficient organics. However, in phase VI, about 90.28% COD removal was measured, while sulfate removal (44%) reduced significantly and a high concentration of sulfate (585.17 ± 106.07 mg L^{-1}) in the effluent samples and lower dissolved sulfide (13.59 ± 8.74 mg L^{-1}) was detected (Fig. 5.3).

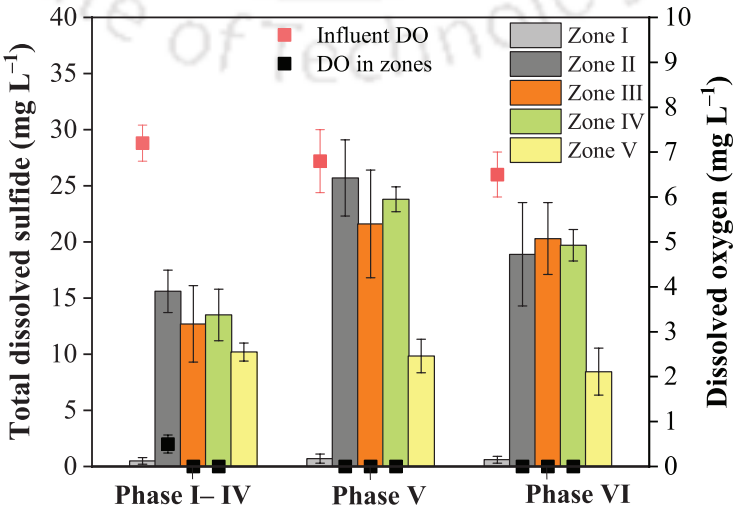

Fig. 5.3 Profile of dissolved oxygen and total dissolved sulfide in HSSF-CW (B).

5.3.3 Metal removal

The time series metal profile from HSSF-CW (B) is illustrated in Fig. 5.4. The specific metal mass removal rate and removal efficiency during various operational phases is depicted in Fig. 5.5. Metal removal efficiencies for different metals ranged between 91.23–99.53% during the acclimatization period and effluent metal concentration remained far below the permissible discharge limits (CPCB, 1993; EPA, 2002). However, during the treatment period, the concentration of metals like Fe, Mn and Co started to increase and exceeded the effluent discharge standards. Interestingly, other metals such as Al, Zn, Ni and Cr exhibited excellent removal efficiency of 63.16–94.09%, 95.49–100%, 94.04–100% and 93.64–100%, respectively, during the treatment period. The oxidation and formation of reddish ferric precipitates on the soil layer and gravel of zone I was noticeable and accounted mainly for iron removal. However, an anoxic condition of the wetland bed resulted in the bacterial reduction of Fe^{3+} and consequent release of the reduced form of Fe^{2+}, which was manifested by the reduced iron removal efficiency from 98.98 (phase I–IV) to 81.74 and 65.80% in phase V and VI, respectively. Reduction of Fe^{3+} may involve both microbial dissimilatory reduction (Equation 3.10) and chemical reduction by the involvement of sulfide as described in equations (5.4) and (5.5) (Johnson and Hallberg, 2002; Wu et al., 2019). The presence of iron-reducing anaerobes is identified and further discussed in the subsequent section 5.3.7.

$$2FeOOH + 4H^+ + H_2S \longleftrightarrow 2Fe^{2+} + S^0 + 4H_2O \quad (5.4)$$

$$6FeOOH + 10H^+ + S^0 \longleftrightarrow 6Fe^{2+} + SO_4^{2-} + 8H_2O \quad (5.5)$$

Aluminium exhibited good average removal efficiency of about 93.89, 85.76 and 74.07% in phase (I–IV), V and VI, respectively. Biologically-induced removal of soluble aluminium mediated by SRBs may occur in two steps: (i) by the formation of hydroxysulfate precipitates with the increase in pH after proton consumption and (ii) by acting as a sink for the protons released during hydrolysis and precipitation (Falagán et al., 2017). The oxides, hydroxides and oxyhydroxides species of Al are least soluble at pH 7.0. However, the hydrous oxides of Al are unstable in reducing conditions, which might cause the release of Al and co-precipitated metals with the substantial change in pH and redox conditions (Lesage, 2006). Zinc and nickel showed effective retention (~97%) throughout the study. The highest removal efficiency was achieved for chromium, exhibiting more than 99% in all the operational phases. Throughout the study, excessive fluctuations were recorded in the cobalt concentration. Removal of cobalt was less as it exceeded the permissible discharge limit by a considerable amount in phase V and VI. Cobalt likely did not precipitate as sulfides and instead primarily precipitated as CoO (confirmed by XRD analysis). Similarly, Hedrich and Johnson (2014) detected no cobalt removal in the sulfide precipitation vessel (using hydrogen sulfide) of the sulfidogenic bioreactor applied for mine wastewater. Table 5.3 provides a comprehensive summary of AMD treatment performance in HSSF-CW (B).

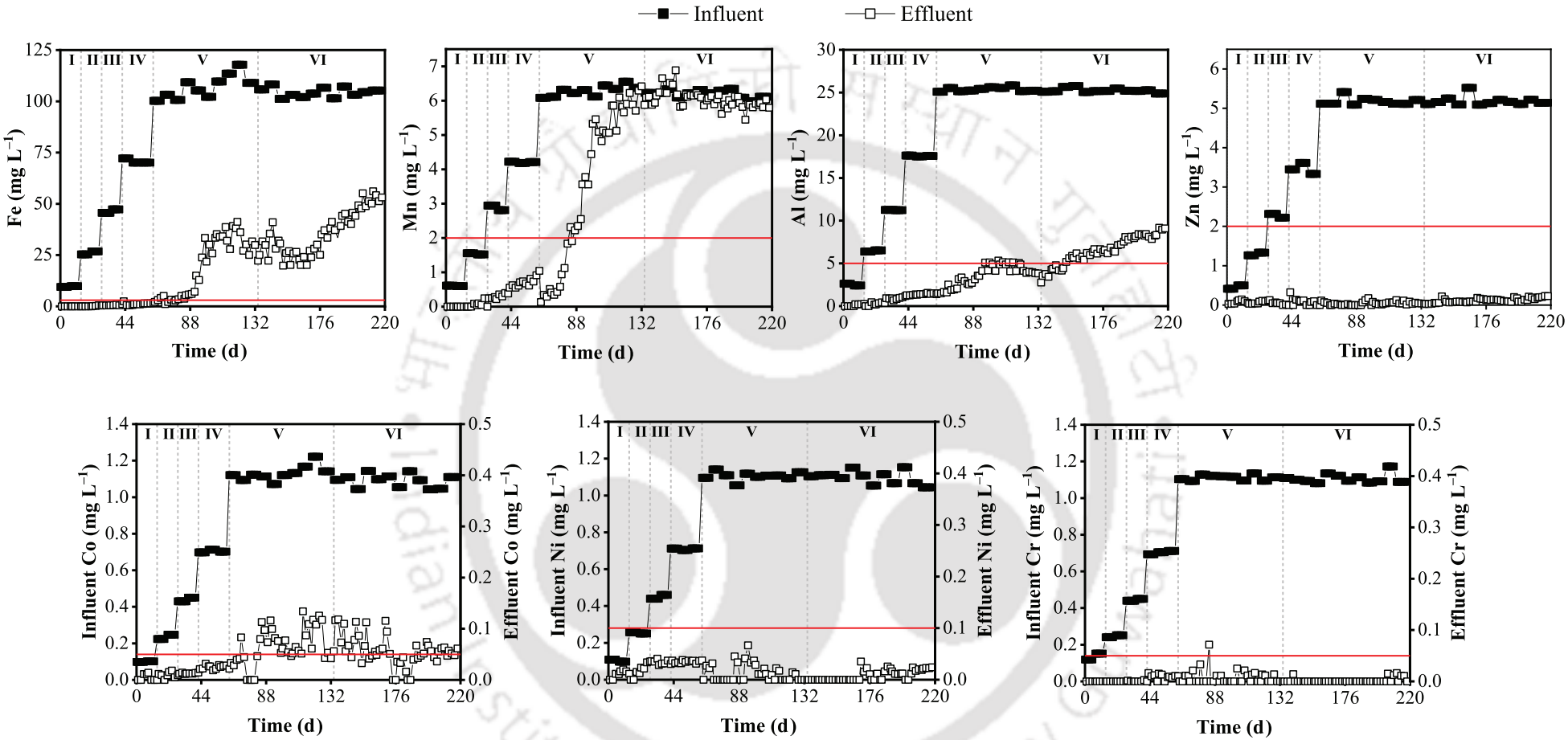

Fig. 5.4 Metal profile of influent and effluent in HSSF-CW (B). The red line denotes the permissible discharge limit (PDL) as recommended by CPCB (1993) and EPA (2002).

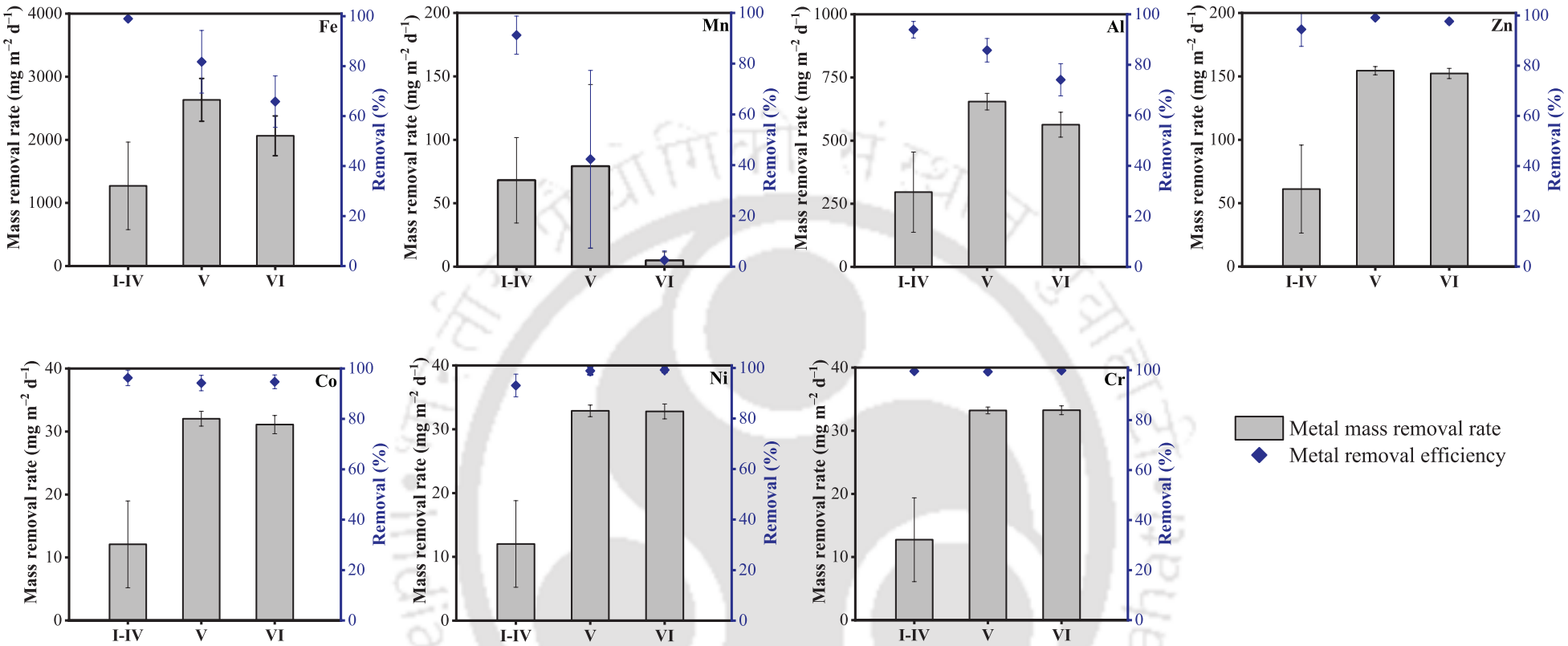

Fig. 5.5 Specific metal mass removal rate and metal removal efficiency in different operational phases of HSSF-CW (B).

Table 5.3 AMD treatment performance of HSSF-CW (B).

Parameters		Influent (AMD)	Treated effluent		Removal[a] (%)	
			Phase V	Phase VI	Phase V	Phase VI
pH		2.2 ± 0.1	5.9 ± 0.4	5.4 ± 0.3	–	–
EC (mS m^{-1})		419.15 ± 11.13	158.88 ± 33.07	216.90 ± 28.18	46.59–79.04	26.70–58.87
TDS (mg L^{-1})		3029.08 ± 109.18	1198.45 ± 229.78	1238.13 ± 149.44	34.60–71.89	49.81–70.76
COD (mg L^{-1})						
Phase V		727.67 ± 31.17	180.64 ± 61.36	34.21 ± 24.09	54.66–87.22	67.71–97.31
Phase V		355.85 ± 13.85				
Acidity (mg L^{-1} as $CaCO_3$)		722.07 ± 18.45	–	–	–	–
Alkalinity (mg L^{-1} as $CaCO_3$)		–	186.80 ± 103.15	62.75 ± 17.05	–	–
Sulfate (mg L^{-1})		1073.72 ± 38.99	280.42 ± 111.14	585.17 ± 106.07	57.33–89.79	29.97–73.62
Metals	Fe (mg L^{-1})	105.61 ± 4.26	19.54 ± 14.12	35.75 ± 10.91	64.74–98.94	46.69–80.44
	Al (mg L^{-1})	25.31 ± 0.24	3.62 ± 1.19	6.55 ± 1.59	79.20–94.09	63.16–86.29
	Mn (mg L^{-1})	6.24 ± 0.13	3.66 ± 2.24	6.04 ± 0.25	1.28–97.81	–8.70–10.76
	Zn (mg L^{-1})	5.18 ± 0.10	0.05 ± 0.04	0.12 ± 0.06	96.63–100	95.49–99.44
	Co (mg L^{-1})	1.11 ± 0.04	0.07 ± 0.04	0.06 ± 0.03	89.13–100	88.51–100
	Ni (mg L^{-1})	1.10 ± 0.03	0.02 ± 0.01	0.01 ± 0.01	96.82–100	94.04–100
	Cr (mg L^{-1})	1.11 ± 0.02	0.01 ± 0.01	0.00	98.62–100	93.64–100

[a]Removal data presented as the min–max value. Values exceeding the discharge limits as recommended by CPCB (1993) and EPA (2002) are marked in red.

5.3.4 Effect of COD/SO_4^{2-} ratio

In phase V, influent COD/SO_4^{2-} ratio of 0.65–0.69 was maintained and the observed average COD and sulfate removal were 547.03 and 804.84 mg L^{-1}, respectively. Theoretically, a COD/SO_4^{2-} of 0.67 suffice the sulfate requirement for complete oxidation of organic matter as represented by equation (5.1). The obtained COD removal was comparable with the theoretical COD (539 mg L^{-1}). This signifies that COD removal was contributed solely by the sulfidogenesis (99%) if complete oxidation was the main pathway. However, an appreciable amount of residual COD was present in the effluent (180.64 ± 61.36 mg L^{-1}), suggesting incomplete oxidation or utilization of COD supplied. Santos et al. (2021) reported the highest COD and sulfate removal rates for all electron donors (cheese whey, ethanol and lactate) at COD/SO_4^{2-} ratio of 1.0, where 79% COD removal (with lactate) was due to sulfidogenesis, explaining that sufficient electrons were provided to reduce sulfate to sulfide. Incomplete oxidation of lactate to acetate by SRB occurs as represented by equations (5.6) and (5.7) (Nevatalo et al., 2010).

$$2CH_3CHOHCOO^- + SO_4^{2-} \longrightarrow 2CH_3COO^- + 2HCO_3^- + H_2S \quad (5.6)$$

$$CH_3COO^- + SO_4^{2-} \longrightarrow 2HCO_3^- + HS^- \quad (5.7)$$

The supply of electron donor increases operational cost, thus the influent COD/SO_4^{2-} ratio was adjusted to 0.32–0.35 in phase VI to minimize the residual COD concentration in the effluent. Additionally, Song et al. (1998) suggested an optimum COD/SO_4^{2-} ratio of 0.33 for the effective utilization of carbon source in sulfate reduction. The average COD and

sulfate removal measured were 316.29 and 461.83 mg L^{-1}, respectively. Thus, only negligible COD was detected in the effluent, accounting 90.28% COD removal, which implied that as COD became a limiting factor, the sulfate removal efficiency dropped sharply. In another study, similar findings by Zhao et al. (2008) reported a sudden decline in the sulfate removal efficiency to about 20% when the COD/SO_4^{2-} ratio changed from 2.0 to 0.5. Contrary, Dar et al. (2008) identified only sulfate, sulfide, and acetate in the effluent, which explained the quantitative oxidation of lactate to acetate coupled with sulfate reduction as a dominant reaction at lower COD/SO_4^{2-} of 0.34 using lactate. Although sulfate reduction substantially decreased at lower COD/SO_4^{2-}, it did not surpass the PDL of 750 mg L^{-1}. In addition, other water quality parameters were comparable and consistent as in phase V, except for Al. Metals like Fe, Co and Mn exceeded the PDL in both phase V and VI (Table 5.3). Therefore, from an economic perspective, COD/SO_4^{2-} ratio of 0.33 may be recommended, provided necessary post-treatment measures are considered to remove remaining constituents below the PDL. Additional aerobic treatment may be provided to enhance Fe, Mn and Al removal.

5.3.5 Effect of AMD on the ecophysiology of plants

The plant density in zone II, III and IV increased from 25 to 50, 100 and 75 plants m^{-2}, respectively and a positive increase in the plant biomass was observed in the subsequent phases (Fig. 5.6). Total chlorophyll is a unifying parameter as it indicates the effect of heavy metals on a plant's growth. Few metals can affect enzymes involved in chlorophyll biosynthesis and interrupt electron transport in light reactions and affect various enzymes in dark reactions (Rai et al., 2016). The total chlorophyll measured in plants before transplantation was 4.70 ± 0.23 mg g^{-1} FW, which reduced significantly to 2.53–3.23 mg g^{-1} FW in phase (I–IV). This reduction in total chlorophyll concentration could be due to the inhibition of enzymes by the accumulation of heavy metals in plants (Manios et al., 2003; Mufarrege et al., 2014). Total

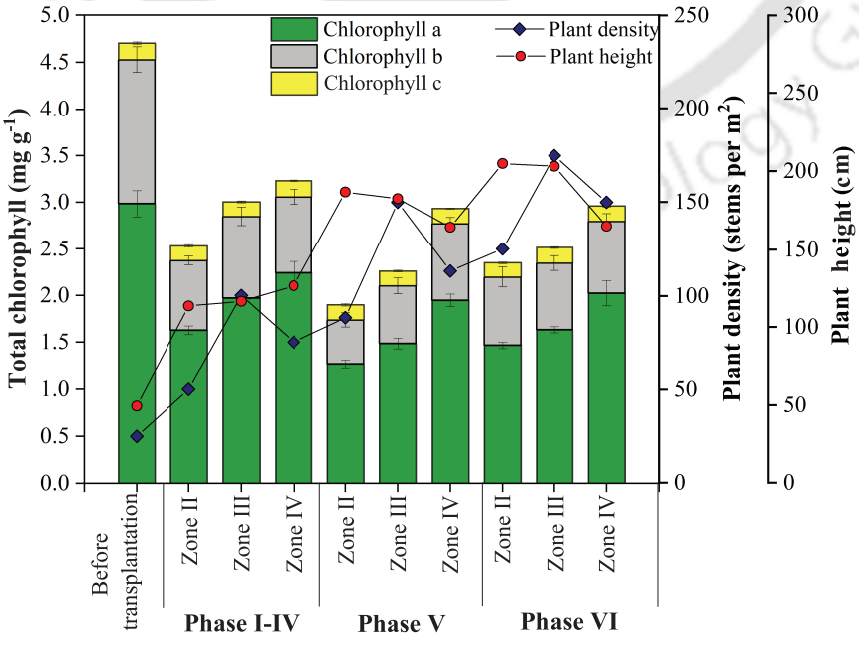

Fig. 5.6 Plant growth parameters in different zones of HSSF-CW (B) during different operational phases.

chlorophyll further decreased in phase V to 1.90–2.94 mg g^{-1} FW. In phase V, plants reached maturity and were in the senescence stage, which could have been attributed to the low estimation due to chlorophyll degradation (Hörtensteiner, 2006). In contrast, plants exhibited relatively higher total chlorophyll content (2.35–2.96 mg g^{-1} FW) in phase VI.

The structural changes in the root and leaf of the plant before transplantation and after treatment in the CW are shown in the SEM micrographs (Fig. 5.7 a, c). The metal-treated plant showed slight changes in the root and leaf structure with the accumulation of heavy metals. The root tissues of the treated plant displayed significant structural changes, the vascular cylinder damaged and cortex cells distorted with minimal intercellular spaces. The leaves of the plant (after treatment) exhibited less foliar structural change, including a loss in intercellular spaces and thickened cell walls compared to the untreated plant. Probst et al. (2009) reported the thickening of root cell walls of *Vicia faba* growing in mine tailings as a response to stress defense against the uptake of toxic metals. Similar alterations in the physiological and morphological characteristics of *Brassica juncea* exposed to Zn and Cd were observed by Sridhar et al. (2005). The SEM-EDX analysis of root and leaf samples of *Typha latifolia* demonstrated a higher accumulation of metals in roots than shoots (Fig. 5.7 b, d), indicating both absorption and translocation mechanisms of plants.

5.3.6 Mineralogy of wetland bed

The morphology characterization and elemental composition of the precipitate collected from HSSF-CW (B) are depicted in Fig. 5.8. From the SEM-EDX analysis, precipitate exhibited a highly metal-rich composition, mostly consisting of iron, aluminium and sulfur with the least amount of manganese, thus following the order of observed metal removal and evidenced the formation of metal sulfides. The XRD pattern reflected poor crystallinity of the solid precipitate, representing distinct peaks of quartz (SiO_2; JCPDS 01-086-1628) and other peaks of low intensities were recognized. The precipitation of metals as oxy-(hydroxides) and sulfides was indicated, such as the presence of iron oxide hydroxide (FeO(OH); JCPDS 00-005-0499), aluminium oxide (Al_2O_3; JCPDS 00-010-0425), manganese sulfide (MnS; JCPDS 00-040-1288), zinc sulfide (ZnS; JCPDS 00-010-0434), cobalt oxide (CoO; JCPDS 01-074-2391) and nickel sulfide (Ni_3S_2; JCPDS 00-027-0341) were identified.

5.3.7 Microbial biomass activity and community structure

The heterotrophic substrate utilization and specific sulfidogenic activity were obtained from the biomass activity assays (S1, S2 and S3). In the S1 assay, the observed biomass activity in terms of cumulative COD removal was 1.47 mg COD mg VSS^{-1} d^{-1}. A higher COD utilization rate in S1 assay suggested maximum electron flow by fermentative and acetogenic bacteria due to the abundant availability of electron donor and the absence of competition from SRB. In S2 and S3 assays, the biomass activity in terms of cumulative sulfate removal were 0.76 and 0.61 mg SO_4^{2-} mg VSS^{-1} d^{-1}, respectively (Fig. 5.9). This implied that COD utilization was mostly by SRB. Biomass activity with different carbon sources, as obtained from previous chapter 3, is shown in Table 5.4.

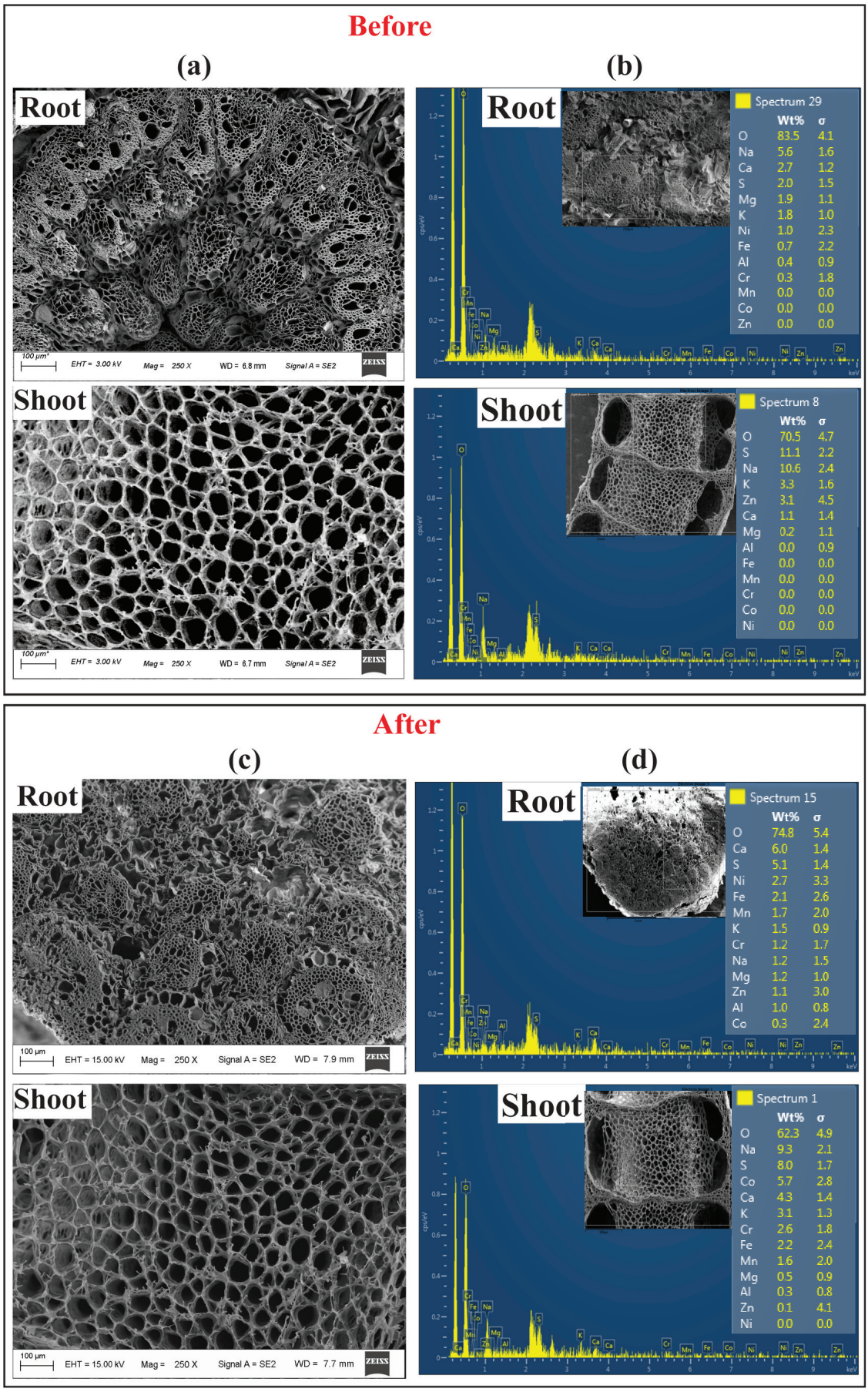

Fig. 5.7 Morphological characteristics (a and c) and metal composition (b and d) of *Typha latifolia* before (top box) and after treatment (bottom box).

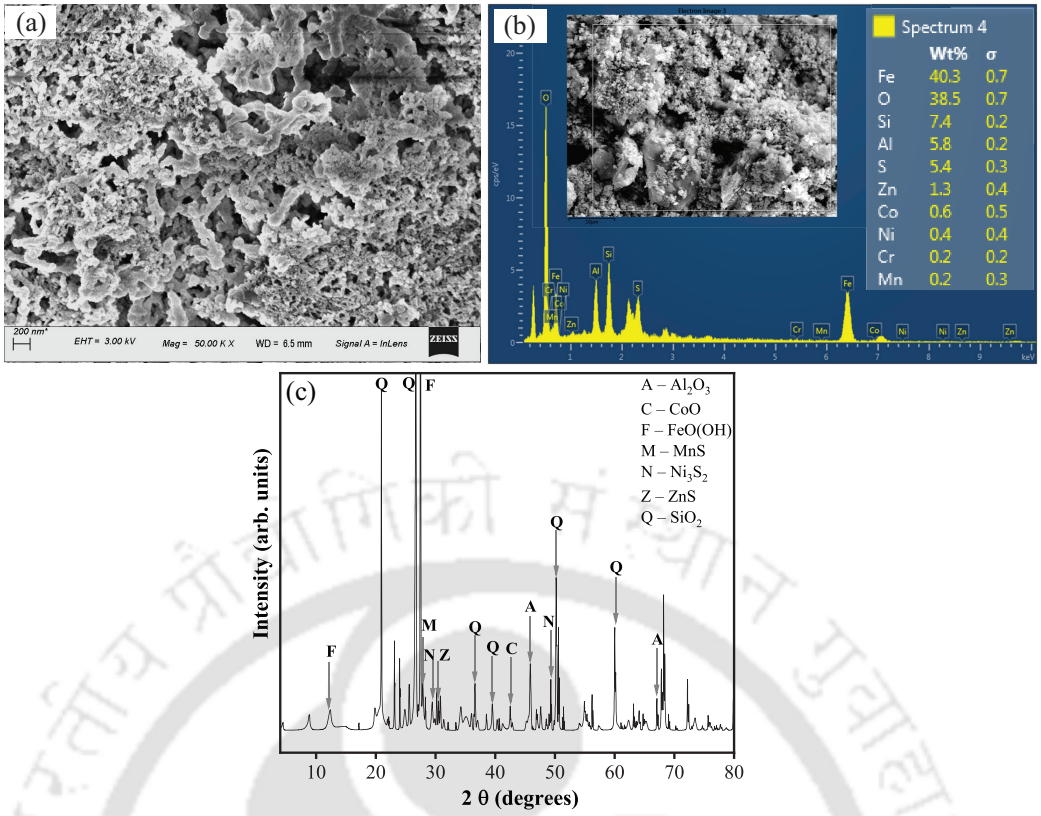

Fig. 5.8 Characteristic illustration of (a) surface morphology by SEM, (b) elemental composition and (c) XRD spectra for solid precipitate from HSSF-CW (B).

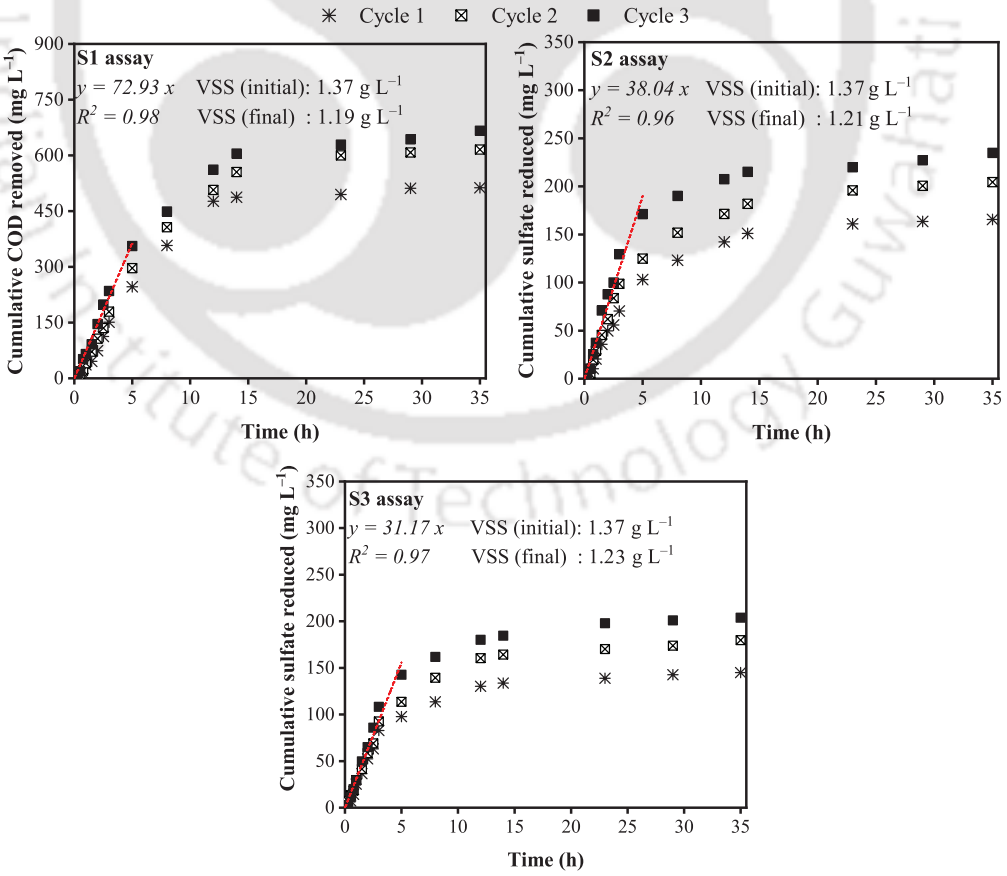

Fig. 5.9 Cumulative COD removal (mg L^{-1}) and sulfate reduction (mg L^{-1}) for different assays (S1, S2 and S3) up to three feed cycles.

Table 5.4 Comparison of biomass activity using different carbon sources in the treatment phase.

Carbon source	Biomass activity in the treatment phase	
	COD utilization rate* (mg COD removed mg TVS^{-1} d^{-1})	Specific sulfidogenic activity* (mg SO_4^{2-} reduced mg TVS^{-1} d^{-1})
Cow manure in HSSF-CW (A)	1.43	0.60
Goat manure in HSSF-CW (C)	1.05	0.79
Lactate in HSSF-CW (B)	1.47	0.61–0.76

*COD utilization rate and specific sulfidogenic activity are expressed as mg COD removed mg VSS^{-1} d^{-1} and mg SO_4^{2-} reduced mg VSS^{-1} d^{-1}, respectively in HSSF-CW (B).

The microbial diversity detected in HSSF-CW (B) mainly represented an enriched population of obligate anaerobes. The bacterial distribution and relative abundance of microbial communities at the phylum level mainly consisted of Firmicutes (37.38%), Proteobacteria (27.92%), Bacteroidetes (14.77%), OD1 (8.15%), Spirochaetes (3.62%), Planctomycetes (2.88%), OP11 (1.24%), Deferribacteres (1.06%), Actinobacteria (0.67%) and several other phyla (< 0.50%) such as Euryarchaeota, TM7, Chloroflexi, Lentisphaerae, Verrucomicrobia, Acidobacteria, Fusobacteria, OP3, GN02, Elusimicrobia, OP8, WS6, TM6, Thermotogae and Caldiserica were also identified (Fig. 5.10). Many researchers have reported similar microbial diversity at low pH environments in bioreactors and natural wetlands treating AMD (Hallberg and Johnson, 2005; Sánchez-Andrea et al., 2014; Sun et al., 2020). The most dominated phylum Firmicutes comprised of classes – Clostridia (29.50%), Bacilli (7.86%) and Erysipelotrichi (0.02%), which play a significant role in the degradation of complex carbon for SRB utilization (Burns et al., 2012). Proteobacteria consists of important classes – Epsilonproteobacteria (11.47%), Betaproteobacteria (7.59%), Deltaproteobacteria (3.78%), Alphaproteobacteria (3.76%) and Gammaproteobacteria (1.33%), which are primarily involved in the pollutant removal by controlling the cycling of organic (C and N) and inorganic (S and metals like iron) compounds (Sánchez-Andrea et al., 2014). Bacteroidetes constituted major abundance after Proteobacteria, a fermentative group of bacteria and widely found in the bio-treatment systems involved in AMD remediation and natural acidic habitat (Sánchez-Andrea et al., 2014). The bacterial groups from OD1 and OP11 are strict anaerobes related to C, S and H cycling via glycolytic pathway, in particular, the species from OD1 phyla are capable of reducing sulfur using archaeal-type hydrogenases (Wrighton et al., 2012). The presence of other phyla such as Spirochaetes, Planctomycetes, Verrucomicrobia and Chloroflexi indicates their ability to co-exist and thrive in metal stressed environments impacted by AMD, as these groups were also consistently present in organic-amended CWs.

The most abundant genera (>1%) identified were *Anaeromusa*, *Sulfuricurvum*, *Desulfosporosinus*, *Leuconostoc*, *Odoribacter*, *Treponema*, *KD1-23*, *Clostridium*, *Desulfovibrio*, *AF12*, *Lactobacillus*, *Prevotella*, *Mucispirillum* and *Geobacter* (Fig. 5.10). *Clostridium* spp. are anaerobic heterotrophs, which are probably responsible for lactate fermentation (Falagán

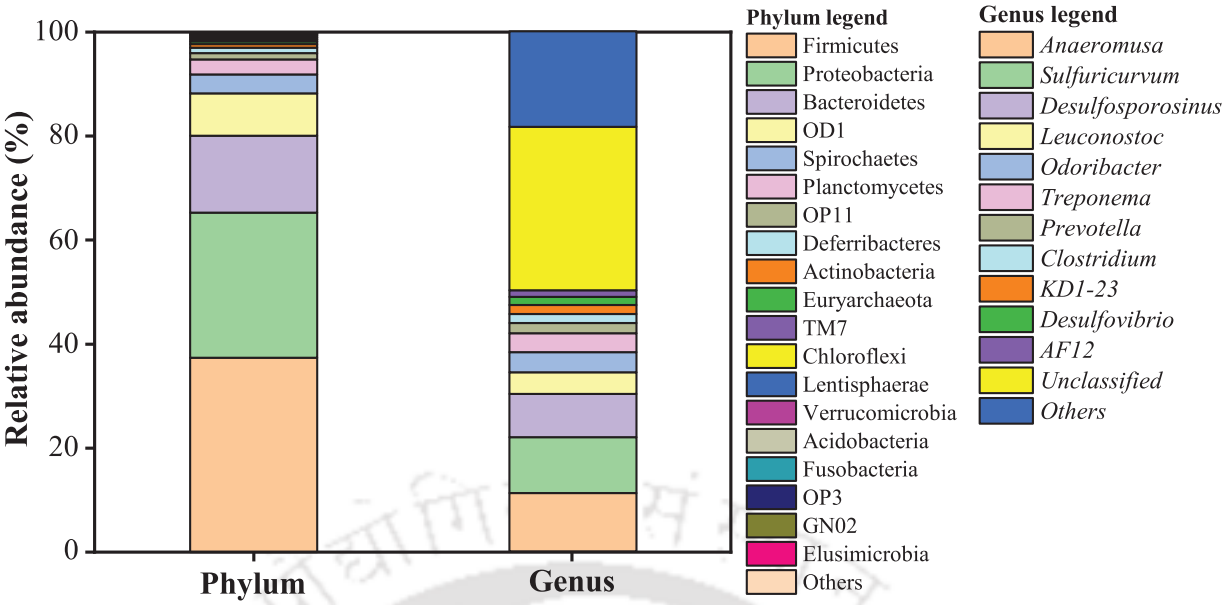

Fig. 5.10 Relative abundance (%) of bacterial communities at phylum and genus level from HSSF-CW (B).

et al., 2017), whereas *Cellulomonas* sp. are aerobic or facultative anaerobes, known for degrading organic matter (cellulosic substances) and facilitating the precipitation of metals (Chen et al., 2021). In addition, some of the species from *Bacteroides* and *Prevotella* genera are anaerobic fermenters, assist in the breakdown of large molecular weight organics and provide carbon and energy sources for SRB. The existence of genera (*Geobacter lovleyi*, *Acidiphilium* and *Halothiobacillus*) involved in iron metabolism was revealed from the phylum Proteobacteria. *Geobacter lovleyi* is identified as the prominent iron-reducing anaerobe capable of organic degradation via dissimilatory iron reduction. *Acidiphilium* sp. is an iron-reducing acidophilic bacteria, whereas *Halothiobacillus* sp. play important role in the oxidation of ferrous iron (Hallberg and Johnson, 2005). The emergence of moderately acidophilic facultative chemolithoautotrophs such as *Thiomonas* sp., capable of deriving energy from the oxidation of reduced sulfur compounds and ferrous iron, was also detected in low abundance (Hallberg and Johnson, 2005). Interestingly, the appearance of aerobic groups like *Acinetobacter* spp. (*Acinetobacter rhizosphaerae* and *Acinetobacter johnsonii*) involved in the transformation of organic nitrogen directly to nitrate and phosphorus accumulation was recognized at very low abundance. Further, Villegas-Plazas et al. (2019) and Chen et al. (2021) also identified denitrifiers (*Dechloromonas* and *Halomonas*) responsible for the nitrate removal via complete nitrate respiration even at low pH and high concentrations of ferric iron.

The assimilation of sulfate in the form of organic-S by plants and microorganisms in CWs is very limited (< 3%) (Chen et al., 2016). Therefore, dissimilatory sulfate reduction is anticipated as the major sulfate removal route, which was evident by the dominance of SRB genera (0.01–8.34%). SRB are diverse strict anaerobes, primarily identified from the phylum Firmicutes within the family Peptococcaceae (*Desulfosporosinus meridiei* and *Desulfotomaculum* sp.) and other genera from the class Deltaproteobacteria

and Epsilonproteobacteria of phylum Proteobacteria (*Desulfovibrio*, *Desulfobulbus* and sulfur-reducing, *Sulfurospirillum*). *Desulfosporosinus* are spore-forming and moderately acidophilic SRB that can maintain relatively high sulfate reduction activity (Sánchez-Andrea et al., 2014; Sun et al., 2020), whereas *Desulfovibrio* and *Desulfobulbus* are non-acetate oxidizers that could efficiently utilize lactate as an electron donor for sulfate reduction (Chen et al., 2016). Additionally, *Sulfuricurvum kujiense* and *Thiobacillus* (0.01–10.73%) were the major facultative chemolithoautotrophic sulfur-oxidizing (SOB) genera present.

5.3.8 AMD remediation mechanisms

Fig. 5.11 illustrates the major biochemical processes involved in the AMD remediation and metal retention inside HSSF-CW (B). Dissimilatory sulfate reduction was identified as the major biological pathway assisting in sulfate removal, bicarbonate alkalinity generation and metal sulfide precipitation. Various biochemical reactions occurring inside the CW were sustained by the continuous supply of lactate as the principal electron donor. The emergence of major iron metabolizing microbial groups controlled the biochemical cycling of iron (oxidation or reduction) and its availability. However, pH dictated the removal mechanisms for most of the metals through precipitation and adsorption (Sheoran et al., 2010). The removal of iron and aluminium occurred as oxides and hydroxides when the effluent pH was more than 6.0, as observed in batch adsorption and precipitation experiments. Despite good retention by precipitation mechanism in the treatment phase, a high concentration of iron and aluminium was found in the effluent (about 19.54–35.75 mg L^{-1} Fe and 3.62–6.55 mg L^{-1} Al in the outflow), explaining the possible remobilization of iron and other adsorbed elements due to the reduction of (oxy-)hydroxide species at lower pH (pH < 6.0) (Wu et al., 2019). Metals accounted for about 32.30–75.68% removal via precipitation and co-precipitation route alone, while manganese accounted the least (9.29%). The poor removal of manganese ions is attributed to the slower rate of oxidation at acidic to neutral pH and thus, precipitation of manganese accounted quite less than the adsorption (Table 3.4 and Table 5.2). At low pH as in phase VI, the manganese bearing (oxy-)hydroxides would likely undergo reductive dissolution and therefore, minimal or no removal was found (Neculita and Rosa, 2019). Zinc and nickel are rather weakly adsorbed and tend to be more bioavailable with the fluctuation in pH. Zinc is readily precipitated and possesses a strong affinity for co-precipitation in iron oxides, which may re-dissolve, being redox-sensitive and thus, this process may not be considerable (Matagi et al., 1998). However, zinc and nickel can form stable insoluble sulfide compounds, which could be the long-term dominant process for metal retention. Cobalt exhibited inferior removal and even lesser retention by precipitation (32.30%) (Table 3.4), mostly reported to be co-precipitated by hydrous oxides. Cr^{3+} being less soluble than Cr^{6+}, is rapidly bound to iron oxides and microbial surfaces (or biofilm) on wetland media via sorption and co-precipitation mechanisms, either by physical-chemical process or biological activity (Dotro et al., 2011).

Plant uptake and sequestration of metals by microbial metabolism involving bioaccumulation (an energy-dependent active process by living cells) and biosorption (an

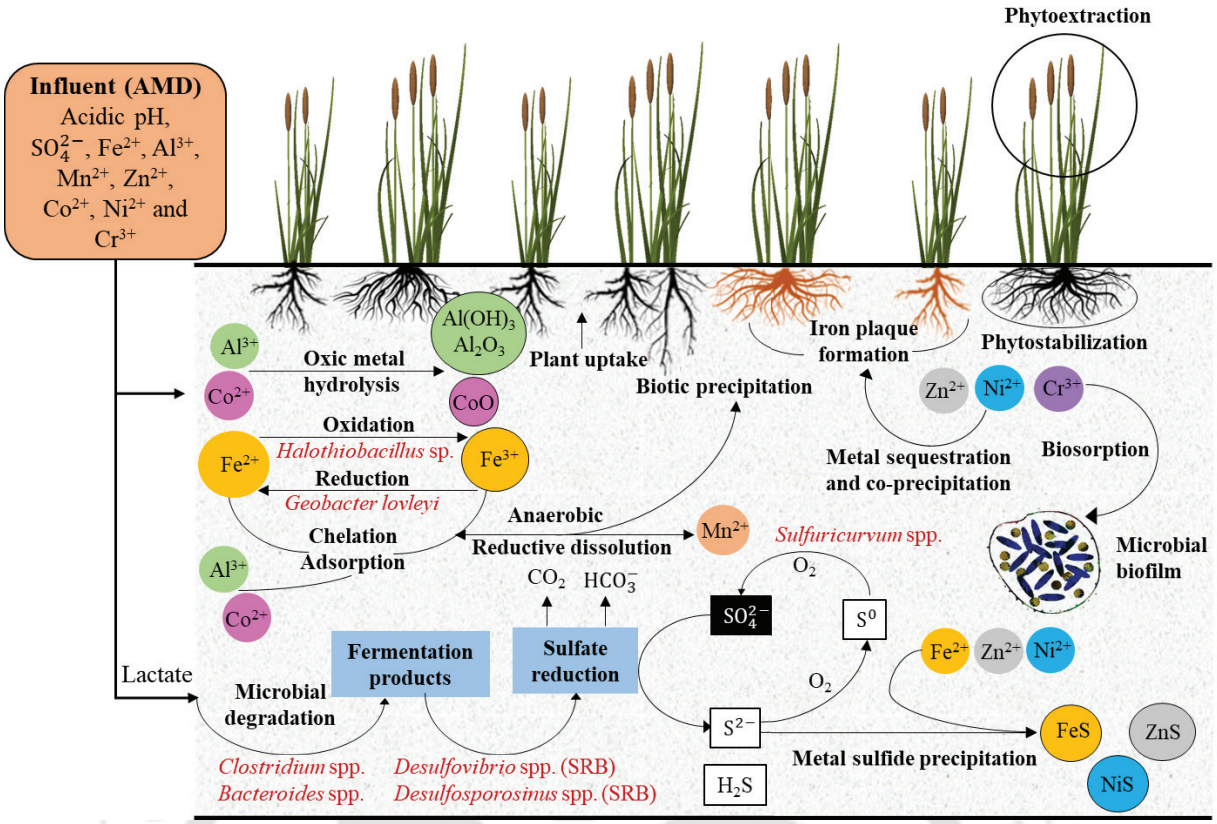

Fig. 5.11 Biochemical processes involved in the AMD remediation mechanism.

energy-independent passive process by live or dead cells) constitute important biological processes for metal removal in CWs (Matagi et al., 1998). The unaccounted metal mass removal is possibly retained through biological processes. The metal uptake by *Typha latifolia* is well documented (Manios et al., 2003) and from our previous results of Chapter 3, it was found that 0.31–3% of the influent metal is taken up by the plants, mostly in the roots (phytostabilization) with hyperaccumulator ability for Mn (Fig. 5.7). Further, previous findings accounted about 5.68–73.22% of the total plant metal uptake in the aboveground shoot tissues, suggesting minimal metal translocation (phytoextraction). Biosorption of Zn^{2+}, Ni^{2+} and Cr^{3+} is an important mechanism, which however, is quite insignificant at pH < 3.0 due to strong competition of protons for metal-binding sites on the microbial cell surface (Sheoran et al., 2010).

5.4 Summary

This study demonstrated moderate alkalinity generation and pH improvement of AMD from 2.2 to 5.6. COD/SO_4^{2-} ratio was the major governing parameter that controlled the treatment efficacy of HSSF-CW (B) supplied with lactate as an electron donor. As COD/SO_4^{2-} reduced from 0.67 (phase V) to 0.33 (phase VI), sulfate reduction decreased significantly from 74% to 44% and metal removal efficiency subsided. Metal precipitation accounted for about 32.30–75.68% of metal removal and it was recognized as the dominant long-term metal retention mechanism subject to change with pH. Possible remobilization of iron and other adsorbed elements occurred due to the reduction of (oxy-)hydroxide species at

lower pH (< 6.0) in phase VI. Therefore, desired COD/SO_4^{2-} ratio should be considered depending on the sulfate concentration present in AMD for effective metal removal. Microbial diversity represented enriched obligate anaerobes, particularly anaerobic lactate fermenters (*Clostridium* spp. and *Bacteroidetes* sp.), moderately acidophilic SRB (*Desulfosporosinus meridiei*) and SOB (*Sulfuricurvum kujiense*). This study highlighted the use of simple organic carbon to address the long-term operational sustainability issues encountered in CWs receiving acidic mine wastewater.

References

APHA (2012). *Standard Methods for the Examination of Water and Wastewater*. American Public Health Association, Washington, DC.

Bekmezci, O. K., Ucar, D., Kaksonen, A. H., and Sahinkaya, E. (2011). Sulfidogenic biotreatment of synthetic acid mine drainage and sulfide oxidation in anaerobic baffled reactor. *Journal of Hazardous Materials*, 189(3):670–676.

Burns, A. S., Pugh, C. W., Segid, Y. T., Behum, P. T., Lefticariu, L., and Bender, K. S. (2012). Performance and microbial community dynamics of a sulfate-reducing bioreactor treating coal generated acid mine drainage. *Biodegradation*, 23(3):415–429.

Chen, J., Li, X., Jia, W., Shen, S., Deng, S., Ji, B., and Chang, J. (2021). Promotion of bioremediation performance in constructed wetland microcosms for acid mine drainage treatment by using organic substrates and supplementing domestic wastewater and plant litter broth. *Journal of Hazardous Materials*, 404:124125.

Chen, Y., Wen, Y., Zhou, Q., Huang, J., Vymazal, J., and Kuschk, P. (2016). Sulfate removal and sulfur transformation in constructed wetlands: The roles of filling material and plant biomass. *Water Research*, 102:572–581.

CPCB (1993). *General Standards for Discharge of Environmental Pollutants Part-A: Effluents, Schedule - VI (Rule 3A)*. Central Pollution Control Board, New Delhi, India.

Dann, A. L., Cooper, R. S., and Bowman, J. P. (2009). Investigation and optimization of a passively operated compost-based system for remediation of acidic, highly iron-and sulfate-rich industrial waste water. *Water Research*, 43(8):2302–2316.

Dar, S. A., Kleerebezem, R., Stams, A. J. M., Kuenen, J. G., and Muyzer, G. (2008). Competition and coexistence of sulfate-reducing bacteria, acetogens and methanogens in a lab-scale anaerobic bioreactor as affected by changing substrate to sulfate ratio. *Applied Microbiology and Biotechnology*, 78:1045–1055.

Dotro, G., Larsen, D., and Palazolo, P. (2011). Preliminary evaluation of biological and physical-chemical chromium removal mechanisms in gravel media used in constructed wetlands. *Water Air and Soil Pollution*, 215(1-4):507–515.

EPA (2002). *Standards for Effluent Discharge Regulations. General Notice No. 44. of 2003*. Environmental Protection Agency. (accessed on 17.04.19).

Falagán, C., Yusta, I., Sánchez-España, J., and Johnson, D. B. (2017). Biologically-induced precipitation of aluminium in synthetic acid mine water. *Minerals Engineering*, 106:79–85.

Hallberg, K. B. and Johnson, D. B. (2005). Microbiology of a wetland ecosystem constructed to remediate mine drainage from a heavy metal mine. *Science of the Total Environment*, 338(1-2):53–66.

Hedrich, S. and Johnson, D. B. (2014). Remediation and selective recovery of metals from acidic mine waters using novel modular bioreactors. *Environmental Science & Technology*, 48(20):12206–12212.

Hörtensteiner, S. (2006). Chlorophyll degradation during senescence. *Annual Review of Plant Biology*, 57:55–77.

Johnson, D. B. and Hallberg, K. B. (2002). Pitfalls of passive mine water treatment. *Reviews in Environmental Science and Biotechnology*, 1:335–343.

Kaksonen, A. H. and Puhakka, J. A. (2007). Sulfate reduction based bioprocesses for the treatment of acid mine drainage and the recovery of metals. *Engineering in Life Sciences*, 7(6):541–564.

Lesage, E. (2006). *Behaviour of heavy metals in constructed treatment wetlands*. PhD Thesis, Faculty of Bioscience Engineering, Ghent University, Ghent, Belgium.

Lyew, D. and Sheppard, J. (2001). Use of conductivity to monitor the treatment of acid mine drainage by sulphate-reducing bacteria. *Water Research*, 35(8):2081–2086.

Manios, T., Stentiford, E. I., and Millner, P. A. (2003). The effect of heavy metals accumulation on the chlorophyll concentration of *Typha latifolia* plants, growing in a substrate containing sewage sludge compost and watered with metaliferus water. *Ecological Engineering*, 20(1):65–74.

Matagi, S. V., Swai, D., and Mugabe, R. (1998). A review of heavy metal removal mechanisms in wetlands. *African Journal for Tropical Hydrobiology and Fisheries*, 8:23–35.

Mufarrege, M. M., Hadad, H. R., Di Luca, G. A., and Maine, M. A. (2014). Metal dynamics and tolerance of *Typha domingensis* exposed to high concentrations of Cr, Ni and Zn. *Ecotoxicology and Environmental Safety*, 105:90–96.

Neculita, C. M. and Rosa, E. (2019). A review of the implications and challenges of manganese removal from mine drainage. *Chemosphere*, 214:491–510.

Neculita, C. M., Yim, G.-J., Lee, G., Ji, S.-W., Jung, J. W., Park, H.-S., and Song, H. (2011). Comparative effectiveness of mixed organic substrates to mushroom compost for treatment of mine drainage in passive bioreactors. *Chemosphere*, 83(1):76–82.

Nevatalo, L. M., Mäkinen, A. E., Kaksonen, A. H., and Puhakka, J. A. (2010). Biological hydrogen sulfide production in an ethanol–lactate fed fluidized-bed bioreactor. *Bioresource Technology*, 101(1):276–284.

Oyekola, O. O., Van Hille, R. P., and Harrison, S. T. L. (2009). Study of anaerobic lactate metabolism under biosulfidogenic conditions. *Water Research*, 43(14):3345–3354.

Probst, A., Liu, H., Fanjul, M., Liao, B., and Hollande, E. (2009). Response of *Vicia faba* L. to metal toxicity on mine tailing substrate: Geochemical and morphological changes in leaf and root. *Environmental and Experimental Botany*, 66(2):297–308.

Rai, R., Agrawal, M., and Agrawal, S. B. (2016). Impact of heavy metals on physiological processes of plants: With special reference to photosynthetic system. In *Plant Responses to Xenobiotics*, pages 127–140. Springer, Singapore.

Sahinkaya, E., Yurtsever, A., Isler, E., Coban, I., and Aktaş, Ö. (2018). Sulfate reduction and filtration performances of an anaerobic membrane bioreactor (AnMBR). *Chemical Engineering Journal*, 349:47–55.

Sánchez-Andrea, I., Sanz, J. L., Bijmans, M. F. M., and Stams, A. J. M. (2014). Sulfate reduction at low pH to remediate acid mine drainage. *Journal of Hazardous Materials*, 269:98–109.

Santos, A. M. d., Costa, J. M., Braga, J. K., Flynn, T. M., Brucha, G., Sancinetti, G. P., and Rodriguez, R. P. (2021). Lactate as an effective electron donor in the sulfate reduction: Impacts on the microbial diversity. *Environmental Technology*, pages 1–12.

Sheoran, A. S., Sheoran, V., and Choudhary, R. P. (2010). Bioremediation of acid-rock drainage by sulphate-reducing prokaryotes: A review. *Minerals Engineering*, 23(14):1073–1100.

Sizirici, B., Yildiz, I., AlYammahi, A., Obaidalla, F., AlMehairbi, M., AlKhajeh, S., and AlHammadi, T. A. (2018). Adsorptive removal capacity of gravel for metal cations in the absence/presence of competitive adsorption. *Environmental Science and Pollution Research*, 25(8):7530–7540.

Song, Y.-C., Piak, B.-C., Shin, H.-S., and La, S.-J. (1998). Influence of electron donor and toxic materials on the activity of sulfate reducing bacteria for the treatment of electroplating wastewater. *Water Science & Technology*, 38(4-5):187–194.

Sridhar, B. B. M., Diehl, S. V., Han, F. X., Monts, D. L., and Su, Y. (2005). Anatomical changes due to uptake and accumulation of Zn and Cd in Indian mustard (*Brassica juncea*). *Environmental and Experimental Botany*, 54(2):131–141.

Sun, R., Zhang, L., Wang, X., Ou, C., Lin, N., Xu, S., Qiu, Y.-Y., and Jiang, F. (2020). Elemental sulfur-driven sulfidogenic process under highly acidic conditions for sulfate-rich acid mine drainage treatment: Performance and microbial community analysis. *Water Research*, 185:116230.

Villegas-Plazas, M., Sanabria, J., and Junca, H. (2019). A composite taxonomical and functional framework of microbiomes under acid mine drainage bioremediation systems. *Journal of Environmental Management*, 251:109581.

Wrighton, K. C., Thomas, B. C., Sharon, I., Miller, C. S., Castelle, C. J., VerBerkmoes, N. C., Wilkins, M. J., Hettich, R. L., Lipton, M. S., Williams, K. H., Long, P. E., and Banfield, J. F. (2012). Fermentation, hydrogen, and sulfur metabolism in multiple uncultivated bacterial phyla. *Science*, 337(6102):1661–1665.

Wu, S. B., Vymazal, J., and Brix, H. (2019). Critical review: Biogeochemical networking of iron in constructed wetlands for wastewater treatment. *Environmental Science & Technology*, 53(14):7930–7944.

Zhao, Y., Ren, N., and Wang, A. (2008). Contributions of fermentative acidogenic bacteria and sulfate-reducing bacteria to lactate degradation and sulfate reduction. *Chemosphere*, 72:233–242.

6

Conclusions and Future Scope

This chapter summarizes the major findings of the research work along with the limitations of the study and provides recommendations for future research.

6.1 Major findings

The primary aim of the research study was the passive treatment of simulated acid mine drainage containing pollutants (such as acidity, sulfate and metals) from North Eastern Coalfield in lab-scale CWs. Seasonal characterization of the AMD from various collieries of NEC was carried out to understand the hydrochemistry of the AMD formation. CWs amended with different organic media were utilized to compare the performance efficacy and metal retention or mobilization was accounted. The prospects of resource recovery (metals) following post-treatment from the media deposits were contemplated. The role of plants, the effect of COD/SO_4^{2-} ratio, impacts of environmental and operational factors on the long-term treatment of AMD were studied. The key takeaways from the study are enlisted below:

1. The chemistry of AMD formation due to the oxidative leaching of sulfide minerals at NEC was strongly influenced by the local climatic conditions. Active collieries (Tirap and Tikak) produced highly acidic metallic discharge, particularly during the monsoon season followed by the post-monsoon season, compared to inactive or abandoned collieries (Ledo and Tipong). Severe soil contamination and metal enrichment were directly associated with overburden spoil leachate.

2. HSSF-CWs utilizing organic media exhibited excellent pH raising ability (6.3–7.4), metal removal efficiency (Fe: 91–100%, Al: 61–87%, Zn: 94–98%, Co: 92–98%, Ni: 96–98% and Cr: 99–100%) and sulfate reduction (57–62%). The effluent concentration of metals such as Fe, Al, Mn and Co exceeded the permissible discharge limit in HSSF-CW (A) amended with cow manure and bamboo chips. However, HSSF-CW (C) with goat manure and areca husk showed remarkably better treatment performance in terms of metal removal and the concentration of all metals in the effluent remained within

the discharge limit, except for Mn. Removal of manganese was most difficult and CWs demonstrated poor to negative removal.

3. Media appeared as the major metal retention sink (58–95%), whereas metal uptake in plants accounted merely 0.31–3% of the initial influent metal concentration, implying that metal uptake by plant biomass was negligible. *Typha latifolia* presented higher metal accumulation in roots than shoots (except for Mn and Co), indicating potential phytostabilization ability. The uptake of toxic metals like Cr and Ni was the least. The highest BCF (2.4) for iron and highest TF (> 2.5) for manganese revealed excellent iron extraction and manganese hyperaccumulation capability of the plant. Most metals, such as Mn, Al, Co and Ni, were presented in the weakly bound fractions of media matrix and could potentially become bioavailable under extreme environmental state.
4. CCW (unplanted) and PCW (planted) showed significant differences ($p < 0.05$) between metal removal efficiencies at varying HLRs and effluent water quality deteriorated drastically on increasing HLR. CCW presented higher sulfate removal efficiency (92–42%) than PCW (85–30%), indicating impairment of microbial sulfate reduction in the presence of plants. HLR has a stronger role in passive AMD remediation than the presence of plants in CWs. Higher heterotrophic activity and specific sulfidogenic activity were observed in CCW than in PCW, which further decreased with the increase in HLRs. Good metal extraction and recovery efficiencies were achieved from wetland media retaining metals using EDTA and organic acids; however, acetic acid is recommended, as it is quite cheap and readily biodegradable.
5. The effect of seasonality relevant to Indian subtropical climatic conditions on the AMD treatment efficacy of CW microcosms exposed to rainfall was considered. SCW (sheltered) and UCW (unsheltered) exhibited comparable treatment performance in the dry season. However, with the onset of heavy rainfall in the wet season, the effluent water quality of UCW deteriorated and significant differences were observed in the pollutant removal efficacy of SCW and UCW. UCW revealed inferior removal for all metals due to possible shortening of HRT in UCW with minimal or insignificant dilution effect. Furthermore, rainfall instigated a negative influence on the heterotrophic and sulfidogenic activity of UCW. However, because large-scale systems are insensitive to rainfall due to considerable dilution over a large area, organic-amended CWs are suggested for field-scale applications.
6. The long-term treatment performance of HSSF-CW (B) in response to different COD/SO_4^{2-} ratios using lactate was evaluated. Higher feed COD/SO_4^{2-} ratio of 0.67 promoted high sulfate reduction (74%) and metal removal with incomplete lactate oxidation (75%). When COD/SO_4^{2-} ratio decreased to 0.33, sulfate reduction decreased considerably to 44% as COD became the limiting factor. High average metal removal efficiency was achieved for Fe (73%), Al (79%), Zn (98%), Co (95%), Ni (99%) and Cr (100%), but Mn (21%).

7. The prominence of the SRB community (*Thermodesulfobium*, *Desulfotomaculum*, *Desulfovibrio* and *Desulfosporosinus*) in all CWs suggests dissimilatory sulfate reduction coupled with carbon (lactate/cow manure/goat manure) oxidation by SRB, which generated alkalinity and facilitated the metal removal by precipitation (as oxides, hydroxides and sulfides) and co-precipitation routes. Further, iron-metabolizing microbial groups (*Geobacter lovleyi*, *Acidiphilium* and *Halothiobacillus*) controlled the biochemical cycling of iron (oxidation or reduction) and its availability.

6.2 Limitations

Some of the major limitations identified from the research work are addressed below:

1. Due to the logistical constraints, the present study was conducted with synthetic AMD similar to the characteristics of AMD generated in the coal mines of NEC, Assam. However, the composition and flow rate of AMD from different collieries varies greatly with season and mining operations. Therefore, pilot-scale and field-scale applications of CWs receiving direct mine discharge from these collieries would provide a realistic treatment approach.
2. Anaerobic CWs exhibited poor to negative removal of manganese and thus, it was most challenging to remove. Therefore, additional post-treatment measures such as aeration, mixing, and, if necessary, lime addition (pH $>$ 9.0) may be provided to ensure the complete removal of iron and manganese.
3. Although organic media demonstrated excellent utilization as wetland media in the bioremediation of AMD, it is quite certain that such wetland media will have a limited lifetime. Therefore, consistent replacement of exhausted bed and thereby disposal of metal-laden media would be further required.
4. The availability of organic media differs with the location and may not be feasible to obtain in large quantities for field-scale applications.
5. The metal accumulation in plants acts as a minor metal retention sink and possibly, over time, plant litter also participates in metal accumulation due to cation adsorption. Therefore, the decomposition of plant biomass may likely re-release metals into the environment. In addition, in the case of plant harvesting, further treatment of polluted plant biomass (such as composting, pyrolysis, incineration, compaction and leaching) would be indispensable for safe disposal.
6. Following the metal extraction and recovery process from wetland media, the recovered metal precipitate might contain a heterogeneous mixture of various metals and would result in low purity. Therefore, it could be further refined and recycled to add economic value.

6.3 Scope for future work

The limitations mentioned in the previous section provide the scope for future research work. Further, the following recommendations are suggested based on the findings of the present study:

1. Treatment of real coal mine wastewater containing an elevated concentration of pollutants as observed in monsoon and post-monsoon season by CWs.
2. Isolation, culture and bio-augmentation of SRB and metal-mobilizing bacteria for the long-term enhancement of the rate of pollutant elimination in CWs.
3. Application of shock loading of pollutants and its effect on the treatment response.
4. Provisions to increase the residence time of the pollutants inside CW may be implemented to counteract the impacts under high rainfall intensity in the rainfall-prone region.
5. Long-term supply of efficient, low-cost carbon source and optimization of COD/SO_4^{2-} ratio depending on the sulfate concentration should be considered for effective metal removal.

Appendix–I

Table AI.1 List of instruments used in the present study.

Instruments	Parameters tested/ measured	Model/manufacturer/ specification
Atomic Absorption Spectrometer (FAAS)*	Metal concentration	Thermo Scientific™ iCE™ 3000 Series, USA
Block digestion unit	Sample digestion	Kelplus-Kelvac, Pelican, India
Centrifuge	Separation of suspended solids	Remi CM-8 plus, India
CHNS elemental analyzer	For elemental composition	Thermo Finnigan, USA
COD digester	COD	HACH, USA
Digital conductivity meter	Electrical conductivity	VSI 04 Deluxe, VSI electronics, India
Digital nephelo-turbidity meter	Turbidity	Systronics, India
Digital pH meter	pH	Systronics 361, India
Electronic balance	Weight of chemicals	Citizen CX 220, India
Energy Dispersive X-ray Spectrometer (EDX)	For elemental composition	Sigma, Ziess, Germany
Field Emission Scanning Electron Microscope (FESEM)	For microscopic images	Gemini 300, Zeiss, Germany
Flame Photometer	Na^+, K^+ and Ca^{2+} measurement	Systronics 128, India
Fourier Transform Infrared (FTIR) Spectroscopy	For characterization of basic classes of chemical groups	PerkinElmer, Spectrum Two, Waltham, MA
Horizontal shaker	For mixing of samples	Reico, India
Hot air oven	Solids analysis and drying	ICT, India
Ion Chromatography	Nitrate determination	792 Basic IC, Metrohm, Switzerland
Muffle furnace	Volatile solids	Multispan, India
Multiparameter water quality analysis kit	For on-site analysis of water samples	HI98194, Hanna Instruments, Romania
Peristaltic pumps	For continuous feeding	Miclins, India
Refrigerator	Sample storage	Labocon LMR-102, India
Rotatory shaker	For end-to-end mixing	GE Motors India Ltd., India
Visible spectrophotometer	NH_4^+–N, NO_2^-–N	Systronics, India
Water purification system	Millipore and milli-Q water	Merck, Germany
X-ray powder diffraction (XRD)	For phase identification	Rigaku SmartLab X-ray Diffractometer
Weather station	For recording weather data	Davis Vantage Pro, USA

*The detection limits for elements in flame AAS (in mg L^{-1}): Al (0.028), Cd (0.0028), Cr (0.0054), Co (0.01), Cu (0.0045), Fe (0.0043), Mg (0.0022), Mn (0.0016), Ni (0.008), Pb (0.016) and Zn (0.0033).

Appendix–II

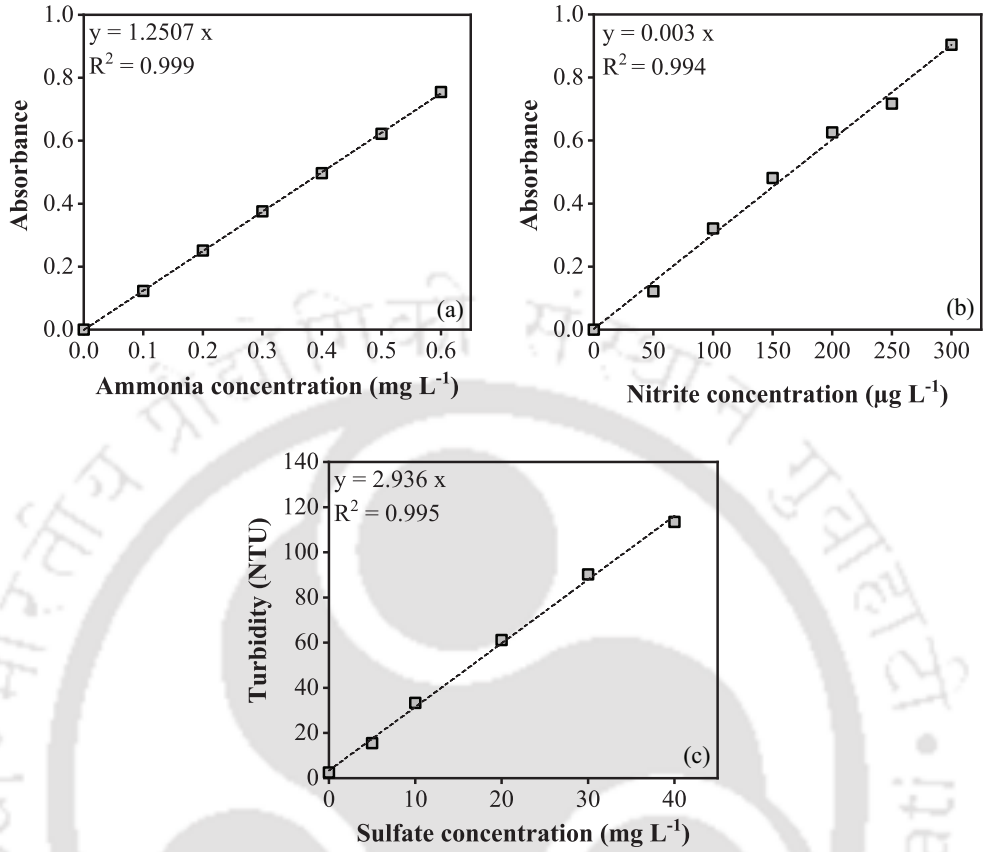

Fig. AII.1 Standard calibration curve for (a) ammonia, (b) nitrite and (c) sulfate.

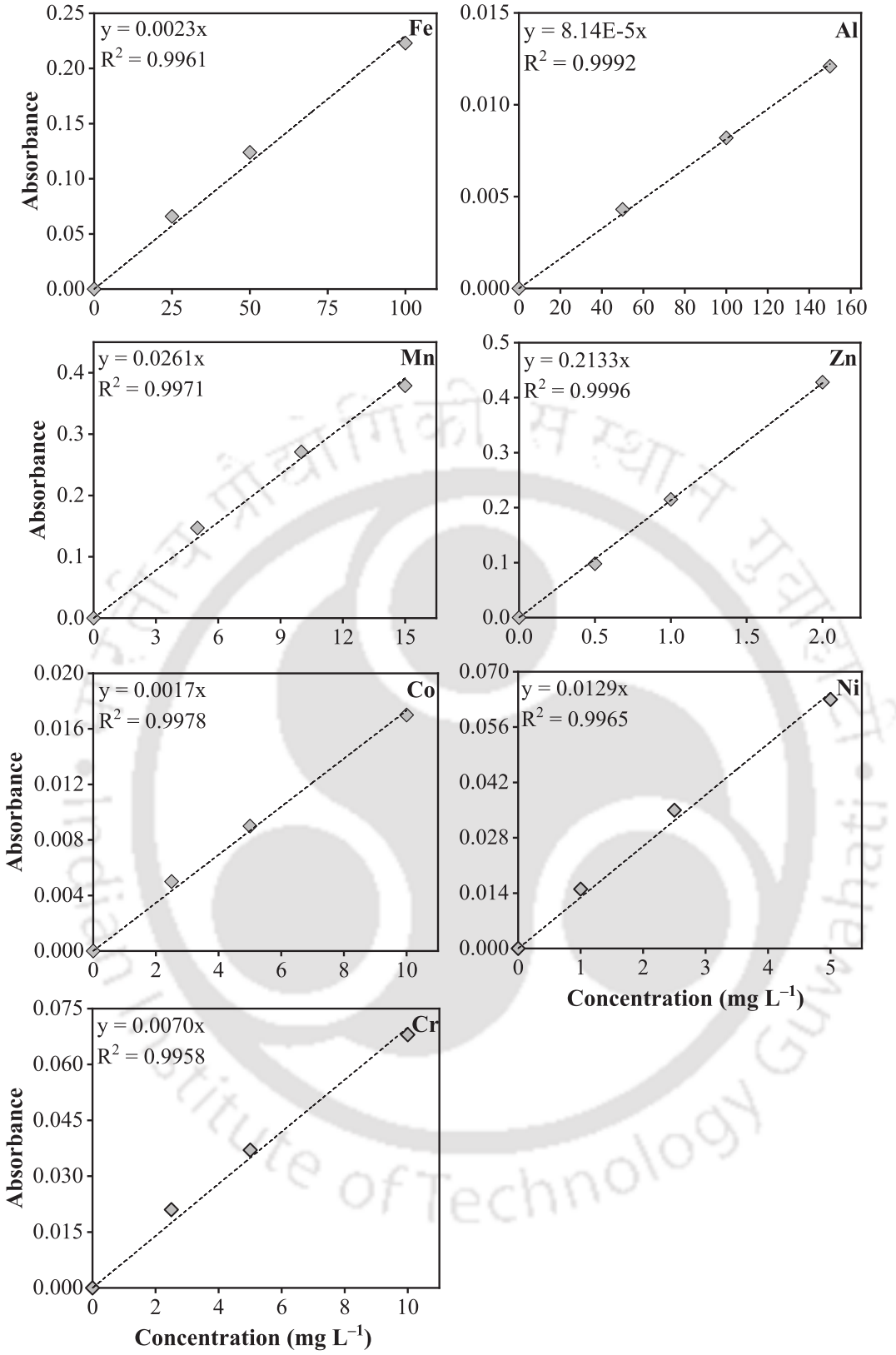

Fig. AII.2 Standard calibration curve for different metals in FAAS.

Appendix–III

Table AIII.1 Characteristics of tap water used for feed preparation.

Parameter	Unit	Mean value
pH	–	7.47 ± 0.07
Electrical conductivity	mS m^{-1}	30 ± 0.02
Total solids	mg L^{-1}	237 ± 14
Total dissolved solids	mg L^{-1}	210 ± 15
Sulfate	mg L^{-1}	29 ± 1.60
Chemical oxygen demand	mg L^{-1}	16.50 ± 3.40
Ammonia	mg L^{-1}	0.05 ± 0.01
Nitrite	mg L^{-1}	BDL
Nitrate	mg L^{-1}	0.82 ± 0.16
Alkalinity	mg L^{-1} as $CaCO_3$	53 ± 7.50
Iron	mg L^{-1}	0.56 ± 0.04
Manganese	mg L^{-1}	0.10 ± 0.02
Aluminium	mg L^{-1}	0.37 ± 0.04
Cobalt	mg L^{-1}	BDL
Nickel	mg L^{-1}	BDL
Total chromium	mg L^{-1}	BDL
Zinc	mg L^{-1}	0.07 ± 0.01

Appendix–IV

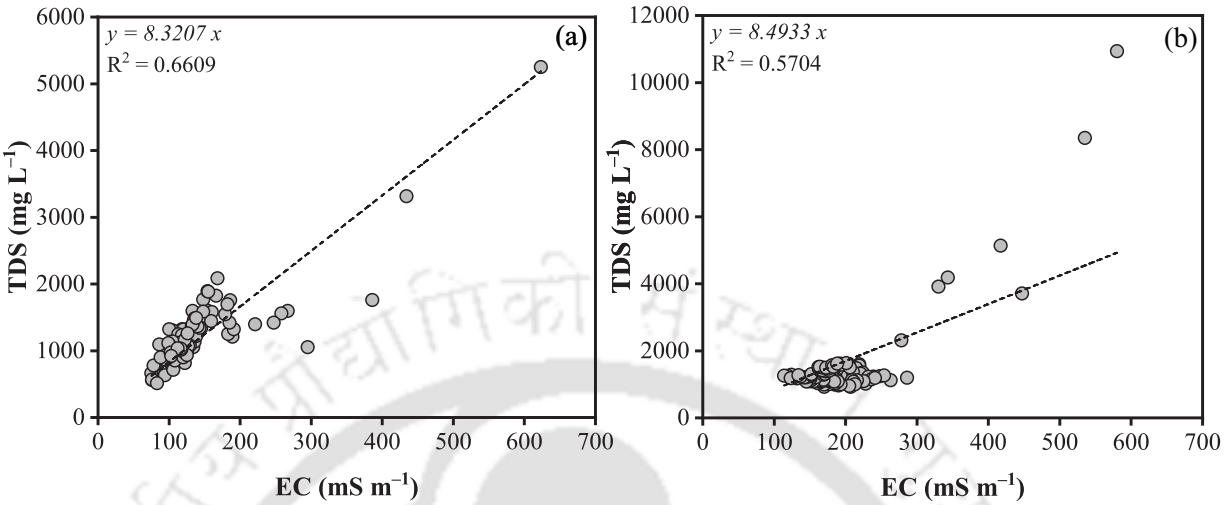

Fig. AIV.1 Relationship between EC and TDS in (a) HSSF-CW (A) and (b) HSSF-CW (C).

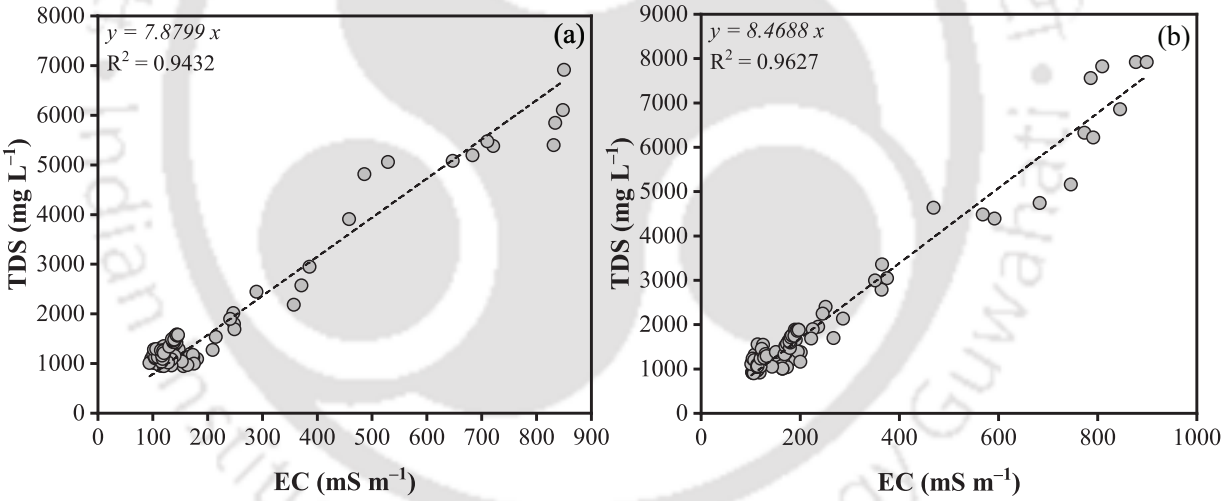

Fig. AIV.2 Relationship between EC and TDS in (a) CCW and (b) PCW.

List of Publications

Published articles

1. **Singh, S.**, and Chakraborty, S.† (2022). Impact of seasonal variation on the treatment response of constructed wetlands receiving acid mine drainage in a subtropical region. *Journal of Water Process Engineering*, 49, 103182.
2. **Singh, S.**, and Chakraborty, S.† (2022). Biochemical treatment of coal mine drainage in constructed wetlands: Influence of electron donor, biotic–abiotic pathways and microbial diversity. *Chemical Engineering Journal*, 440, 135986.
3. **Singh, S.**, and Chakraborty, S.† (2021). Zinc removal from highly acidic and sulfate-rich wastewater in horizontal sub-surface constructed wetland. *Water Science & Technology*, 84 (10–11): 3403–3414.
4. **Singh, S.**, and Chakraborty, S.† (2021). Bioremediation of acid mine drainage in constructed wetlands: Aspect of vegetation (*Typha latifolia*), loading rate and metal recovery. *Minerals Engineering*, 171, 107083.
5. **Singh, S.**, and Chakraborty, S.† (2020). Performance of organic substrate amended constructed wetland treating acid mine drainage (AMD) of North-Eastern India. *Journal of Hazardous Materials*, 397, 122719.

Articles (awaiting submission)

1. **Singh, S.**, and Chakraborty, S. Investigation on treatment performance and reformations of microbial community structure in a constructed wetland treating acid mine drainage.
2. **Singh, S.**, and Chakraborty, S. Hydrochemistry of acid mine drainage at North Eastern Coalfield, Assam, India.

Book chapters

1. **Singh, S.**†, Benny, C. K., and Chakraborty, S. (2022). An overview on the application of constructed wetlands for the treatment of metallic wastewater. In *Biodegradation and Detoxification of Micropollutants in Industrial Wastewater*, pages 103–130, Elsevier.
2. **Singh, S.**, and Chakraborty, S.† (2022). Yeast waste utilization for the treatment of acidic metallic wastewater. In *Environmental Degradation: Monitoring, Assessment and Treatment Technologies*, Springer International Publishing, Capital Publishing Company, New Delhi, India.

†represents corresponding author.

List of Conferences

1. **Singh, S.**[††], and Chakraborty, S. (2020). Zinc removal from highly acidic wastewater in horizontal sub-surface constructed wetland. *2nd International Conference on Bioprocess for Sustainable Environment and Energy (ICBSEE–2020)*, March 05–07, National Institute of Technology Rourkela, Orissa, India. (Poster)
2. **Singh, S.**[††], and Chakraborty, S. (2020). Batch study for the removal of heavy metals from acid mine drainage using yeast waste. *Recycle 2020 3rd International Conference on Waste Management*, February 13–14, Indian Institute of Technology Guwahati, Assam, India. (Oral)
3. **Singh, S.**[††], and Chakraborty, S. (2019). Screening of substrates for the removal of heavy metals from acid mine drainage (AMD), *International Conference on Innovative Trends in Civil Engineering for Sustainable Development (ITCSD–2019)*, September 13–15, National Institute of Technology Warangal, Telangana, India. (Oral)
4. **Singh, S.**[††], and Chakraborty, S. (2019). A study on the applicability of alum sludge for the treatment of acid mine drainage (AMD), *Research Conclave'19*, March 14–17, Indian Institute of Technology Guwahati, Assam, India. (Poster)
5. **Singh, S.**[††], and Chakraborty, S. (2018). An assessment on the characteristics of acid mine drainage (AMD) in Northeastern parts of India, *3rd International Conference on Sustainable Energy and Environmental Challenges (SEEC–2018)*, December 18–21, Indian Institute of Technology Roorkee, Uttarakhand, India. (Oral)
6. **Singh, S.**[††], and Chakraborty, S. (2018). A perspective on constructed wetlands: passive energy system for wastewater treatment, *Recycle 2018 2nd International Conference on Waste Management*, February 22–24, Indian Institute of Technology Guwahati, Assam, India. (Poster)

[††]represents presenting author.

Vitae

Shweta Singh *was born on 19th June 1992 in Jamshedpur, Jharkhand, India. She passed the All India Secondary School Examination (AISSE) conducted by the Central Board of Secondary Education (CBSE), Delhi in 2008 with distinction. She qualified the All India Senior School Certificate Examination (AISSCE) conducted by the CBSE, Delhi in 2010 with distinction. She completed her B. Tech in Civil Engineering from University of Calicut, Kerala, India and she was placed in first class with honours in 2014. She qualified Graduate Aptitude Test in Engineering (GATE) conducted by Indian Institute of Technology Kharagpur, West Bengal, India in 2014. She pursued M. Tech in Civil Engineering with specialization in Environmental Engineering from National Institute of Technology Agartala (NITA), Tripura, India in 2016 and secured a Cumulative Grade Points Average (CGPA) of 9.65/10.*

The author joined the Ph.D. Programme in July 2016 at the Department of Civil Engineering, Indian Institute of Technology Guwahati, Assam, India. She received research scholarship from the Ministry of Education (MoE), Govt. of India. She successfully completed the course work with 9.23/10 Cumulative Point Index (CPI). She gave the Open (Ph.D. Synopsis) Seminar on 19th May 2022 and presented her thesis work before the Doctoral Committee and her performance was satisfactory. She presented her final Viva-Voce Seminar on 10th November 2022.